

MAGYAR ÁLLAMI
EÖTVÖS LORÁND
GEOFIZIKAI INTÉZET

GEOFIZIKAI
KÖZLEMÉNYEK

ВЕНГЕРСКИЙ
ГЕОФИЗИЧЕСКИЙ
ИНСТИТУТ
ИМ Л. ЭТВЕША

ГЕОФИЗИЧЕСКИЙ
БЮЛЛЕТЕНЬ



BUDAPEST

EÖTVÖS LORÁND
GEOPHYSICAL INSTITUTE
OF HUNGARY

GEOPHYSICAL TRANSACTIONS

CONTENTS

Large-scale Tertiary strike-slip displacements recorded in the structure of the Transdanubian Range	Z. Balla A. Dudko	3
Deep reflection seismic Profile 598 in the southeastern part of the Transcarpathian depression	L. Vejmělek Č. Tomek	65
Neogene volcanism of the Nyir region (NE Hungary) as revealed by integrated interpretation of the latest geophysical data	É. Kilényi I. Polcz Z. Szabó	77
Fault system dynamics and seismic activity — examples from the Bohemian Massif and the Western Carpathians	V. Schenk Z. Schenková L. Pospíšil	101
A compilation of palaeomagnetic results from Hungary	E. Márton P. Márton	117
Filtered gravity anomaly map of Hungary	Z. Szabó	135

VOL. 35. NO. 1-2. NOV. 1989. (ISSN 0016-7177)

TARTALOMJEGYZÉK

Nagymértékű harmadidőszaki eltolódások a Dunántúli-középhegység szerkezetében	<i>Balla Z. Dudko A.</i>	63
Kéregkutató szeizmikus reflexiós szelvény a kelet-szlovákiai medence délnyugati részén	<i>L. Vejmělek Č. Tomek</i>	76
A Nyírség neogén vulkanizmusa a legújabb geofizikai adatok tükrében	<i>Kilényi É. Polcz I. Szabó Z.</i>	99
Vetőrendszerek dinamikája és a szeizmicitás összefüggése – Példák a Cseh masszívum és a Nyugati-Kárpátok területéről	<i>V. Schenk Z. Schenková L. Pospíšil</i>	116
Magyarországi paleomágneses mérések eredményei	<i>Márton E. Márton P.</i>	133
Magyarország szűrt gravitációs anomália térképe	<i>Szabó Z.</i>	142

СОДЕРЖАНИЕ

Третичные сдвиги большой амплитуды в структуре Задунайского среднегорья (Венгрия)	<i>З. Балла А. Дудко</i>	63
Профиль сейсморазведки методом отраженных волн земной коры юго-западной части Закарпатского прогиба	<i>Л. Веймелек Ч. Томек</i>	76
Неогеновый вулканизм Ньирского региона (Восточная Венгрия) в свете последних геофизических данных	<i>Э. Киленьи И. Польц З. Сабо</i>	99
Взаимосвязь между динамикой систем разрывов и сейсмичностью – примеры из Чешского массива и Западных Карпат	<i>В. Шенк З. Шенкова Л. Постшилл</i>	116
Результаты палеомагнитных измерений в Венгрии	<i>Э. Мартон П. Мартон</i>	133
Карта отфильтрованных гравитационных аномалий Венгрии	<i>З. Сабо</i>	142

LARGE-SCALE TERTIARY STRIKE-SLIP DISPLACEMENTS RECORDED IN THE STRUCTURE OF THE TRANSDANUBIAN RANGE

Zoltán BALLA* and Antonina DUDKO**

Two main epochs of intensive tectonism have been distinguished in the Transdanubian Range. The first of them occurred in the Middle Cretaceous and resulted in a synclinal structure bent in the northeast together with accompanying thrust slices. This old structural pattern has been used as a marker system in the analysis of the tectonism of the second epoch which took place in the Oligocene–Miocene. Three stages of this young tectonism have been established as follows: 1) dextral shear of the southeastern margin of the Transdanubian Range domain in the Oligocene (appr. 30–22 Ma B.P.); 2) S-shaped bending of all structures in the Early–Middle Miocene (appr. 22–14 Ma); 3) sinistral shear and compression in the Middle Miocene (appr. 14–12 Ma).

These features have been correlated with synchronous kinematic processes of the Alpine–Carpathian–Pannonian realm as follows: '1' with the removal of the northwestern Carpatho-Pannonian domains from the Alpine realm; '2' with the collision of the clockwise rotating southeastern Carpatho-Pannonian domains with the northwestern Carpatho-Pannonian domains, and with the push of the latter towards the north; '3' with the clockwise rotation of the southeastern Carpatho-Pannonian domains resulting in the sinistral shear of the contact zone with the northwestern Carpatho-Pannonian domains, and with the partial drag of the northwestern Carpatho-Pannonian domains resulting in the sinistral shear of their interiors. A check of the consequences of the regional kinematic modelling in the Transdanubian Range, i.e. in a well-studied area, has revealed consistency of local tectonic features with the regional model

Keywords: Transdanubia, Oligocene, Miocene, bending, strike-slip faults, shear, syncline, models, kinematics

1. Introduction

The Oligocene–Miocene development of the Alpine–Carpathian–Pannonian region has recently been studied by kinematic modelling [BALLA 1985, 1986, 1987]. It would be of interest to test the consequences in a well-studied area like the Transdanubian Range. The goal of this work comprises (1) selection of important and reliable tectonic data with their primary interpretation, (2) synthesis of the data selected in geological maps and in a uniform picture of kinematic features and (3) correlation of the picture obtained with the kinematics of the Alpine–Carpathian–Pannonian realm.

2. Selection and primary interpretation of data

All data on the tectonics of the Transdanubian Range (for review, see *Table 1*) can be gathered into two groups: data on the tectonics of the whole Range (regional tectonics); data of its parts (local tectonics).

* Eötvös Loránd Geophysical Institute of Hungary, Budapest, POB 35, H-1440, Hungary

** Hungarian Geological Survey, Budapest Népstadion út 14, H-1142, Hungary

2.1. Regional tectonics of the Transdanubian Range

Three main features will be discussed here (see Table I, A): the synclinal structure, the bending of all structures, and the Tertiary tectonism.

The synclinal structure of the Transdanubian Range is expressed in the general arrangement of pre-Cenozoic formations. The Palaeozoic basement with its Permian cover crops out in the southeast. Here and in the northwest it has been drilled in two continuous strips which border the Mesozoic formations from both sides. The axial zone of the syncline is marked by Jurassic and Cretaceous sediments while the limbs consist of Triassic rocks which predominate in the Range (*Fig. 1*). This picture is well-known in the Bakony Mts. and in the Vértes Hills. Further continuation of the syncline in the Grecse Hills, however, has only been suspected, and that in the Pilis Mts. and Buda Hills has never been assumed.

When we turn to the question of the age of the Bakony syncline we should mention the following facts: Permian–Neocomian sediments form a continuous sequence; the first disconformity appears at the base of the Aptian, and the second, more expressed discontinuity is observable at the base of the Albian (*Fig. 2*); the Senonian complex lies as a posttectonic cover. Consequently, the Bakony syncline started forming in the Aptian and terminated in the Turonian.

The bending of all structures in the northeast was established by SZENTES [1934], although marks of the structural deviation had already been observed previously [SCHAFARZIK 1884; FERENCZI 1926]. Instead of gradual bending (*Fig. 3*), WEIN [1976] assumed a sharp change in strikes (*Fig. 4*) which occurred in the Middle Cretaceous. The similar direction of the Senonian dykes discovered in the last few years on both the straight (Velence Hills) and rotated (Buda Hills) sections (*Fig. 3*) confirms WEIN's views on the age of the change in strikes while abundant field observations on the position and drilling data on the arrangement of Triassic beds (*Fig. 5*) support SZENTES's opinion on the gradual bending. There are no data on separating folding and bending in time. It is important to point out, however, that in the northeast the thrust structures are bent as well, therefore, they should also be regarded as Middle Cretaceous in age and cannot be separated from the fold structures in a genetic sense.

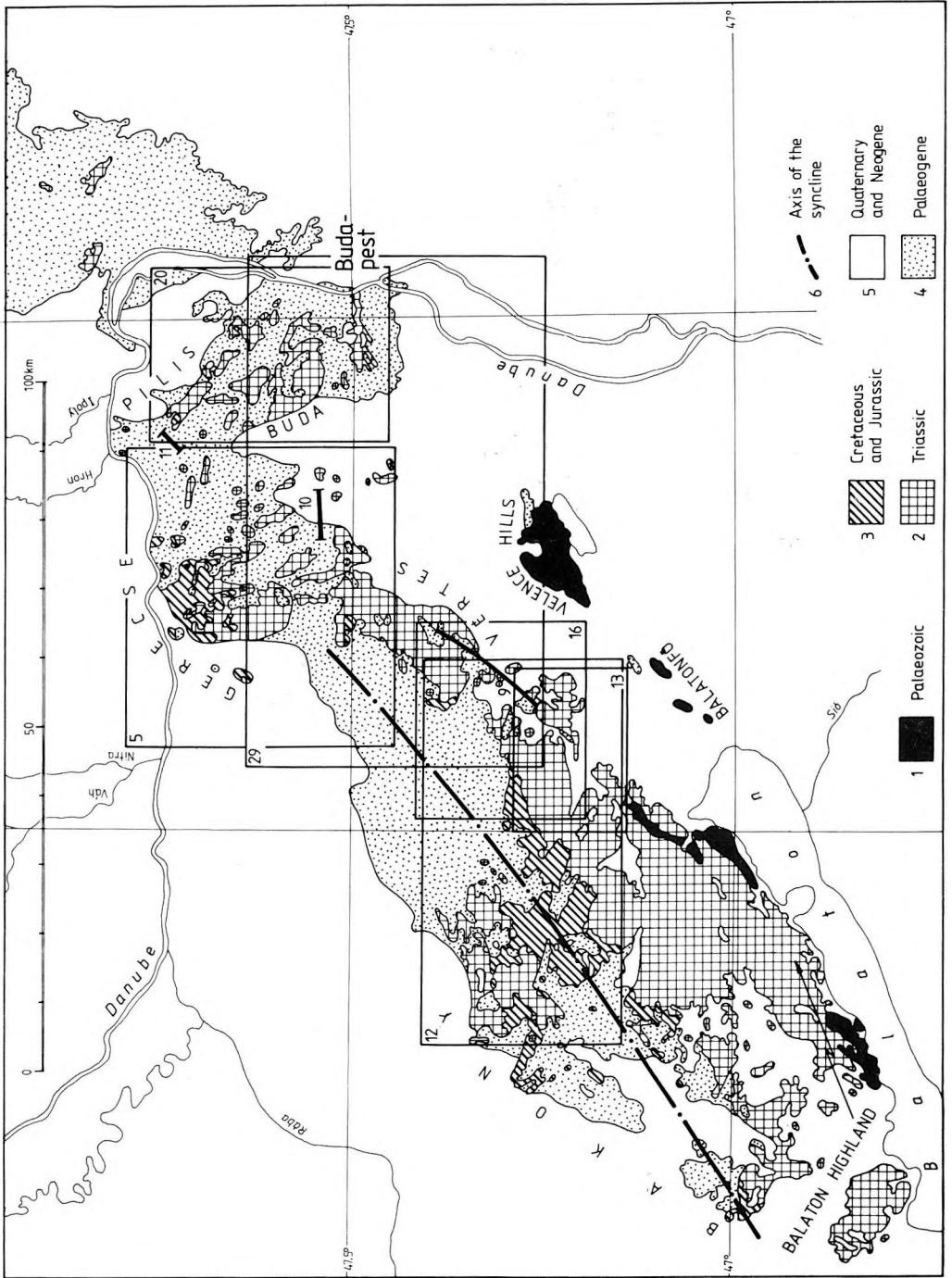
Two aspects of the Tertiary tectonism will be discussed here: (i) the arrangement of sediments and (ii) the displacements along the faults. The *general arrangement of sediments* of Eocene (*Fig. 6*) and Oligocene (*Fig. 7*) age is almost the same

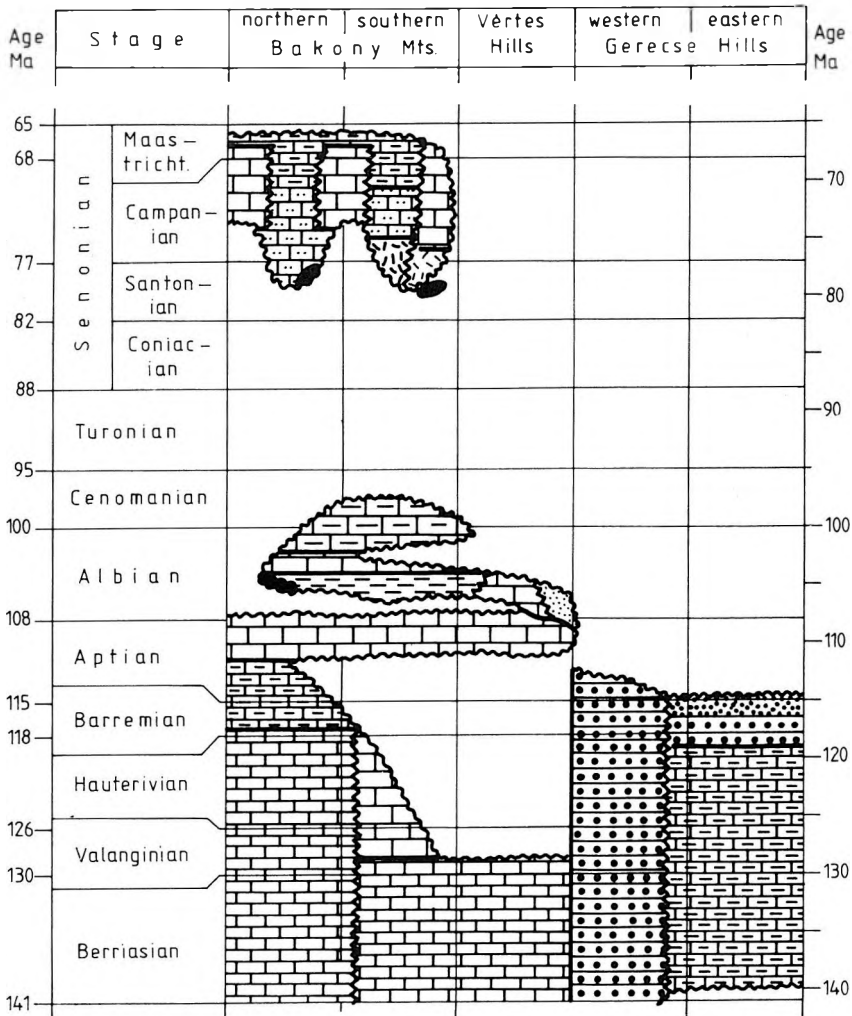
Fig. 1. Geological sketch of the Transdanubian Range. Base map: FÜLÖP [1984] (simplified). Frames of Figs. 5, 12, 13, 16, 20 and 29 as well as profiles of Figs. 9, 10 and 11 indicated

1. ábra. A Dunántúli-középhegység földtani vázlatja. Alaptérkép: FÜLÖP [1984], egyszerűsítve. Feltüntetjük az 5., 12., 13., 16., 20. és 29. ábra körvonalát, valamint a 9., 10. és 11. ábra szelvényvonalát.
1 — paleozoikum; 2 — triász; 3 — jura és kréta; 4 — paleogén; 5 — neogén és kvarter;
6 — a szinklinális tengelye

Рис. 1. Схематическая геологическая карта Задунайского среднегорья, по Фюльпу [FÜLÖP 1984], с упрощениями. Обозначены контуры рис. 5, 12, 13, 16, 20 и 29, а также профили рис. 9, 10 и 11

1 — палеозой; 2 — триас; 3 — юра и мел; 4 — палеозой; 5 — неоген и четвертичный отдел; 6 — ось синклинали





CONTINUOUS PERMIAN-JURASSIC SEQUENCE

- | | | | | | | | | |
|---|--|--------------------------|---|--|----------------------------|----|--|--|
| 1 | | Pelagic limestone | 5 | | Shallow-marine marl | 9 | | Shallow-marine sandstone |
| 2 | | Pelagic marl | 6 | | Lagoonal argillaceous marl | 10 | | Brackish and fresh-water coal measures |
| 3 | | Neritic marl | 7 | | Flysch | 11 | | Fresh-water sandstone |
| 4 | | Shallow-marine limestone | 8 | | Pelagic siltstone | 12 | | Bauxite |
- 13 ——— Conformity 14 ~~~~~ Unconformity 15 } Facial transition 16 | Uncertain relationships

Fig. 2. Stratigraphic sketch of the Cretaceous of the Transdanubian Range, after CSÁSZÁR and HAAS [1983]

2. ábra. A Dunántúli-középhegység vázlatos kréta rétegsora, CSÁSZÁR – HAAS [1983] nyomán.
 1 — nyílttengeri mészkő; 2 — nyílttengeri márga; 3 — partközeli márga; 4 — sekélytengeri mészkő;
 5 — sekélytengeri márga; 6 — lagunális agyagos márga; 7 — flis; 8 — nyílttengeri iszapkő;
 9 — sekélytengeri homokkő; 10 — csökkent sósvízi és édesvízi széntelepek; 11 — édesvízi homokkő;
 12 — bauxit; 13 — konkordancia; 14 — diszkordancia; 15 — fácies átmenet; 16 — bizonytalan kapcsolat

Рис. 2. Схематическая стратиграфическая колонка Задунайского среднегорья, по Часару и Хасу [CSÁSZÁR - HAAS 1983]

1 — пелагические известняки; 2 — пелагические мергели; 3 — прибрежные мергели; 4 — мелководные известняки; 5 — мелководные мергели; 6 — лагунные глинистые мергели; 7 — флиш; 8 — пелагические аргиллиты; 9 — мелководные песчаники; 10 — залежи солонатоводных и пресноводных углей; 11 — пресноводные песчаники; 12 — бокситы; 13 — согласное залегание; 14 — несогласие; 15 — фациальный переход; 16 — неясная связь

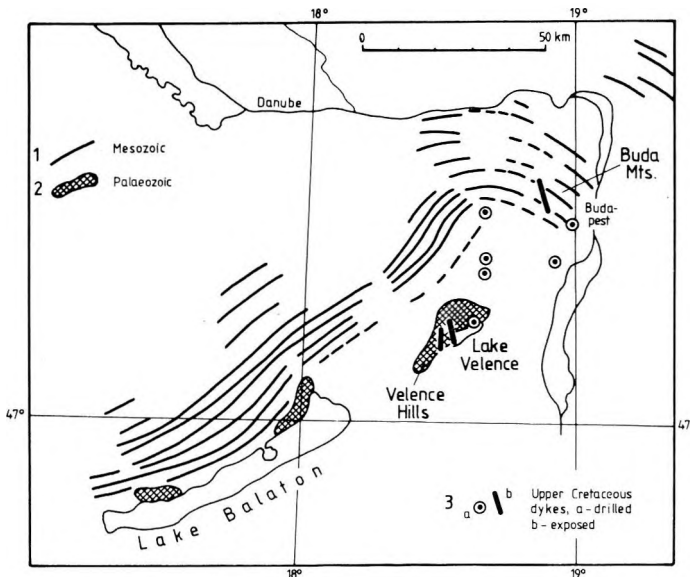


Fig. 3. Bending of the Transdanubian Range structures, after SZENTES [in VIGH and SZENTES 1952.], with Senonian dykes, after DUDKO [1984], HORVÁTH and ODOR [1984], HORVÁTH et al. [1985]. Dykes shown out of scale but in the correct position

3. ábra. A Dunántúli-középhegység szerkezeti hajlata, Szentes [VIGH – SZENTES 1952] nyomán, szenon közztelérekkel, DUDKO [1984], HORVÁTH–ODOR [1984], HORVÁTH et al. [1985] nyomán.
 A teléreket méretén kívül, de helyes csapással tüntettük fel. 1 — mezozoikum; 2 — paleozoikum;
 3 — felsőkréta telérek: a — megfúrt, b — feltárt

Рис. 3. Структурный изгиб Задунайского среднегорья, по Сентешу [VIGH–SZENTES 1952], с сенонскими дайками, по Дудко [DUDKO 1984], Хорвату и Одору [HORVÁTH–ODOR 1984], Хорвату и др. [HORVÁTH et al. 1985]. Дайки нанесены вне масштаба, но с сохранением простирааний

1 — мезозой; 2 — палеозой; 3 — верхнемеловые дайки, а — по скважинам, б — на поверхности

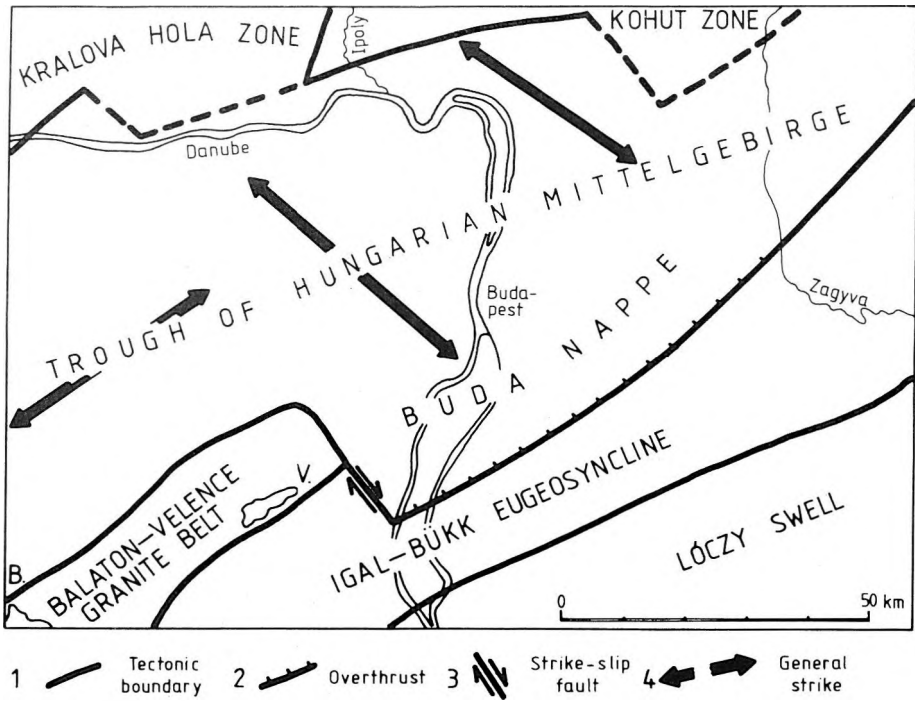


Fig. 4. Break in the structural strikes of the Transdanubian Range, modified after WEIN [1977]

4. ábra. A Dunántúli-középhegység szerkezeti csapástörése, WEIN [1977] nyomán, módosítva.
1 — tektonikus határ; 2 — feltolódás; 3 — eltolódás; 4 — általános csapásirány

Рис. 4. Структурный излом Задунайского среднегорья, по Вейну [WEIN 1977], с изменениями

1 — тектонический контакт; 2 — взброс; 3 — сдвиг; 4 — общее простирание

in spite of an erosional event between them. On the other hand, the Miocene sediments display a completely different picture (Fig. 8). The *displacements along faults* have been analysed by restoring the base of Oligocene or Miocene sequences in three geological sections (Figs. 9–11). In the situation restored, i.e. after the compensation of post-Oligocene or even post-Miocene (?) displacements, the pre-Miocene movements seem to have played a subordinate role. Based on this the Palaeogene tectonism can be regarded insignificant in both aspects: the first re-arrangement of sediments and the first significant displacements only occurred in the Miocene.

Consequently, two main revolutions took place in the tectonic development of the Transdanubian Range: 1 — folding+thrusting and bending in the *Middle Cretaceous*; 2 — structural re-arrangement in the *Neogene*. In the further discussion Middle Cretaceous structures will only be used as markers in the analysis of the young Tertiary tectonism.

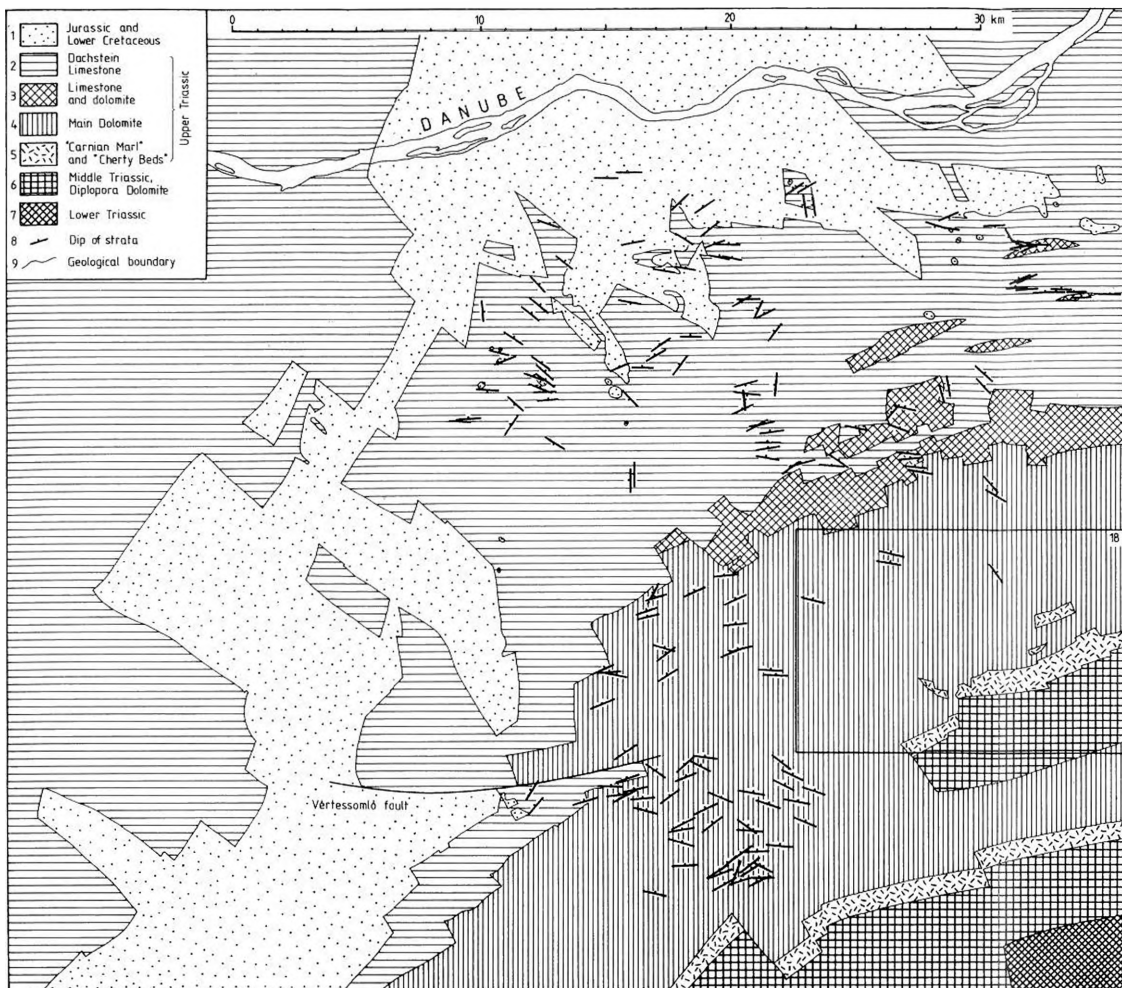


Fig. 5. Subsurface geological map of the northeastern Transdanubian Range. Base maps: CSÁSZÁR et al. [1978], GIDAI et al. [1980], SZABÓ et al. [1982]. Dips taken from FÜLÖP [1958], GIDAI et al. [1980], JASKÓ [1957b, 1957c], SÓLYOM [1953], VÉGH-NEUBRANDT [1960]. For location, see Fig. 1. Frame of Fig. 18 indicated.

5. ábra. A Dunántúli-középhegység ÉK-i részének aljzattérképe. Alaptérképek: CSÁSZÁR et al. [1978], GIDAI et al. [1980], SZABÓ et al. [1982]. Dőlés adatok: FÜLÖP [1958], GIDAI et al. [1980], JASKÓ [1957b, 1957c], SÓLYOM [1953], VÉGH-NEUBRANDT [1960] térképéről. Helyzetét l. az 1. ábrán. Feltüntetjük a 18. ábra körvonalát. 1 — júra és alsókréta; 2–5 — felsőtriász: 2 — dachsteini mészkő, 3 — mészkő és dolomit, 4 — fődolomit, 5 — karni márga és kovás rétegek; 6 — középsőtriász diplogorás dolomit; 7 — alsótriász; 8 — rétegdőlés; 9 — képződményhatár

1 — тектонический контакт; 2 — взброс; 3 — сдвиг; 4 — общее простирание

Рис. 5. Геологическая карта фундамента СВ части Задунайского среднегорья, по Часару и др. [CSÁSZÁR et al. 1978], Гидаи и др. [GIDAI et al. 1980], Сабо и др. [SZABÓ et al. 1982]. Элементы залегания взяты из работ Фюльпа [FÜLÖP 1958], Гидаи и др. [GIDAI et al. 1980], Яшко [JASKÓ 1957b, 1957c], Шойома [SÓLYOM 1953], Вегне [VÉGH-NEUBRANDT 1960]. Положение см. на рис. 1. Обозначен контур рис. 18

1 — юра и нижний мсл; 2–5 — верхний триас: 2 — дахштейнский известняк, 3 — известняки и доломиты, 4 — главный доломит, 5 — карнийские мергели и кремнистые породы; 6 — средний триас: диплопоровый доломит; 7 — нижний триас; 8 — падение слоев; 9 — геологический контакт

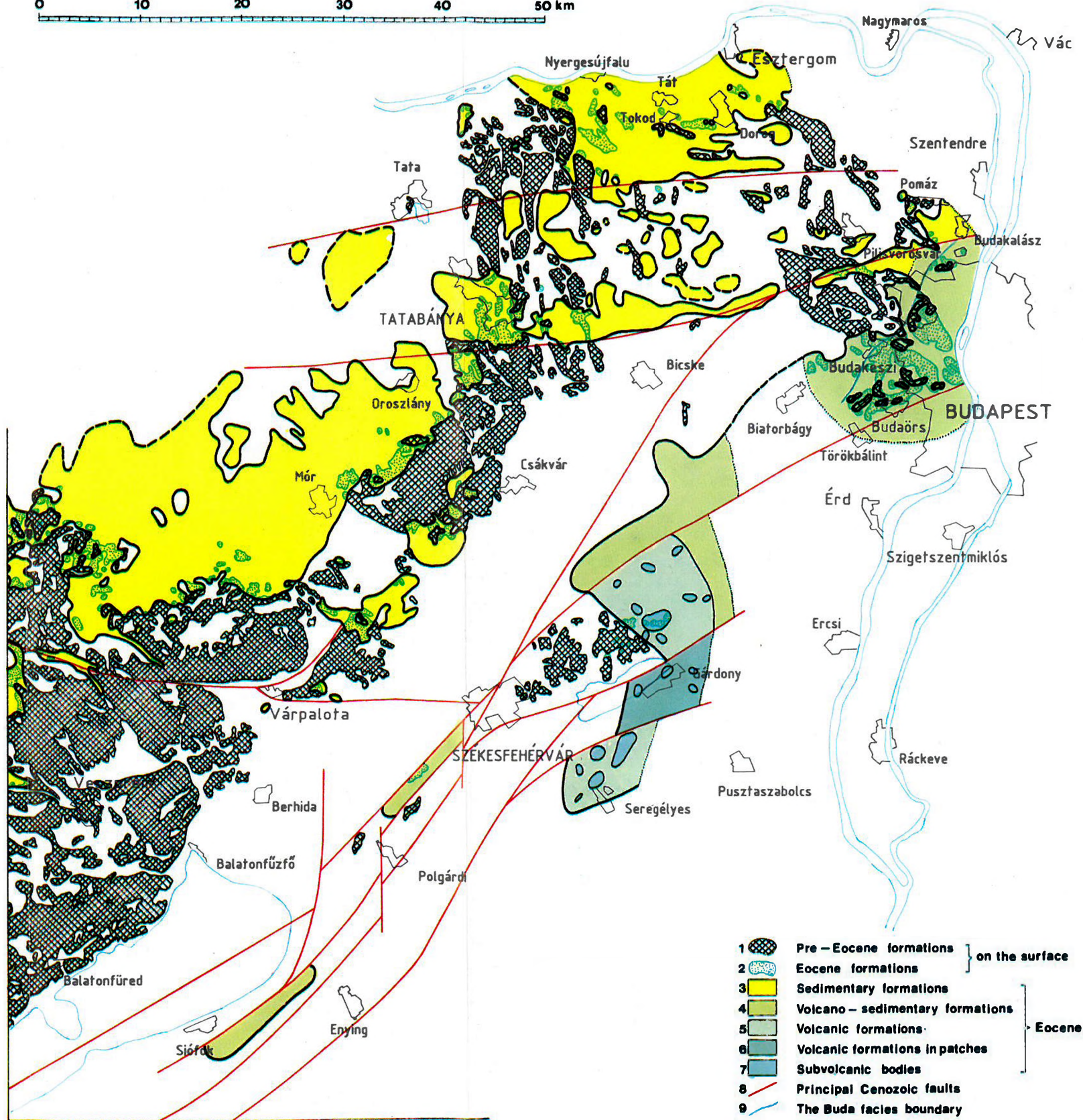
Fig. 6. Arrangement of the Eocene formations of the eastern Transdanubian Range area. Outcrops taken from FRANYÓ [1968], JÁMBOR et al. [1966], SZENTES [1969], SZENTES and BÖJTÖS-VARRÓK [1964], SZENTES and RÓNAI [1966]. Boundaries of Eocene formations modified from BERNHARDT and LANTOS [1982] and DUDKO et al. [1988] using drilling data

6. ábra. Eocén képződmények elterjedése a Dunántúli-középhegység K-i részén. Kibúvások: FRANYÓ [1968] JÁMBOR et al. [1966], SZENTES [1969], SZENTES – BÖJTÖSNÉ [1964], SZENTES – RÓNAI [1966] nyomán. Eocén képződmények határai: BERNHARDT – LANTOS [1982] és DUDKO et al. [1988] nyomán, fúrási adatok alapján módosítva. 1–2 — a felszínen: 1 — eocénnál idősebb, 2 — eocén képződmények; 3–7 — eocén: 3 — üledékes kőzetek, 4 — vulkáni-üledékes kőzetek, 5 — vulkanitok, 6 — vulkanitok foltokban, 7 — szubvulkáni testek; 8 — főbb kainozoos törések; 9 — a budai fácieshatár

Рис. 6. Распространение эоценовых образований в В части Задунайского среднего орья. Контуры выходов по Франьо [FRANYÓ 1968], Ямбору и др. [JÁMBOR et al. 1966], Сентешу [SZENTES 1969], Сентешу и Бейтёшне [SZENTES–BÖJTÖSNÉ 1964], Сентешу и Ронаи [SZENTES–RÓNAI 1966]. Контуры эоценовых образований по Бернхардту и Лантошу [BERNHARDT–LANTOS 1982] и Дудко и др. [DUDKO et al. 1988], с уточнениями по буровым данным

1–2 — на поверхности: 1 — доэоценовые образования, 2 — эоцен; 3–7 — эоцен: 3 — осадочные породы, 4 — вулканогенно-осадочные породы, 5 — вулканические породы, 6 — вулканиты в пятнах, 7 — субвулканические тела; 8 — главные кайнозойские разломы; 9 — Будайская фациальная граница

0 10 20 30 40 50 km



- | | | | |
|---|--|----------------------------------|------------------|
| 1 | | Pre - Eocene formations | } on the surface |
| 2 | | Eocene formations | |
| 3 | | Sedimentary formations | } Eocene |
| 4 | | Volcano - sedimentary formations | |
| 5 | | Volcanic formations | |
| 6 | | Volcanic formations in patches | |
| 7 | | Subvolcanic bodies | |
| 8 | | Principal Cenozoic faults | |
| 9 | | The Buda facies boundary | |

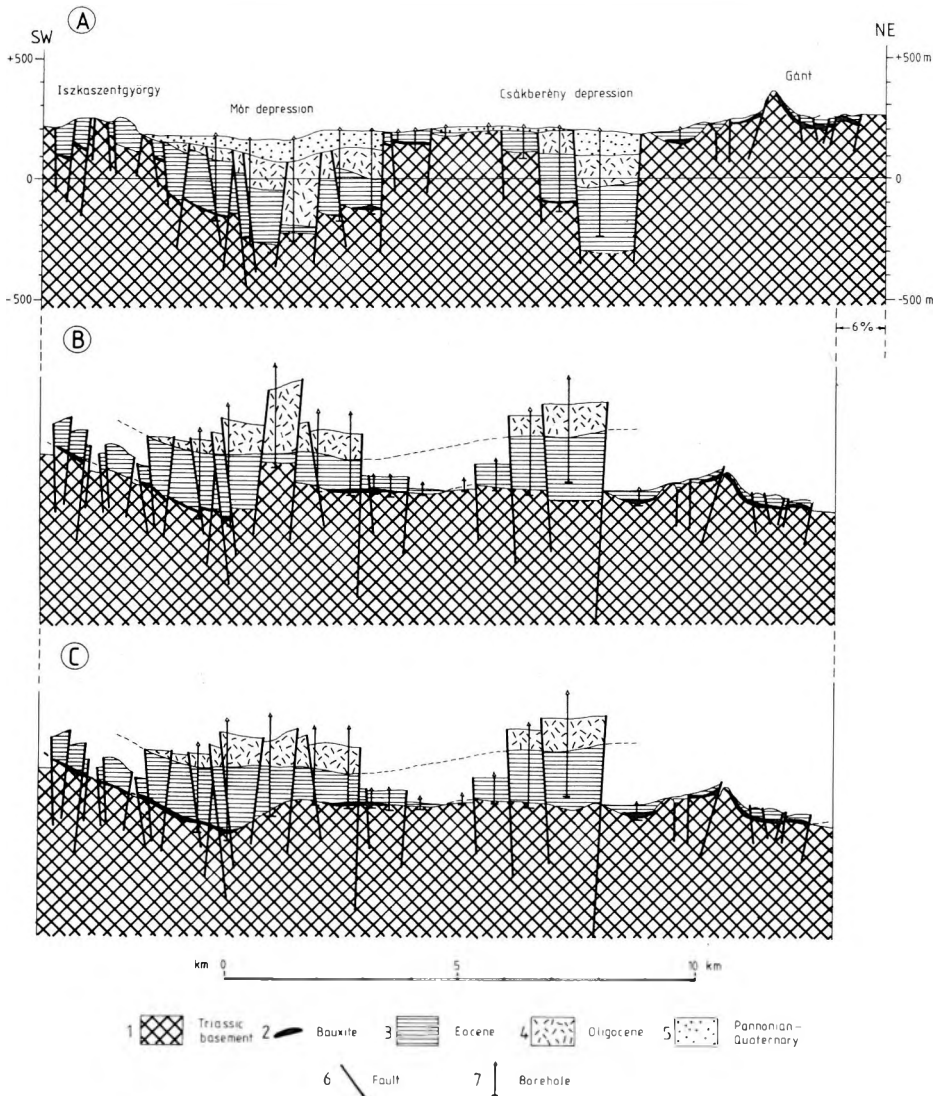


Fig. 9. Geological cross-section of the Iszkaszentgyörgy bauxite deposit (A), after SZANTNER [1982], and restoration of the Oligocene/Eocene boundary (B) with minor adjustment (C). For location, see Fig. 1.

9. ábra. Az Iszkaszentgyörgyi bauxitelőfordulás földtani szelvénye, SZANTNER [1982] nyomán (A), az oligocén/eocén határ visszaállításával (B) és apró igazításokkal (C). Helyzetét l. az 1. ábrán
1 — triász aljzat; 2 — bauxit; 3 — eocén; 4 — oligocén; 5 — pannóniai-kvarter; 6 — törés; 7 — mélyfúrás

Рис. 9. Геологический разрез по бокситовому месторождению Искасентльёрдь, по Сантнеру [SZANTNER 1982] (A), с восстановлением границы олигоцена с эоценом (B) и с мелкими поправками (C). Положение см. на рис. 1

1 — триасовый фундамент; 2 — бокситы; 3 — эоцен; 4 — олигоцен; 5 — паннонско-четвертичные отложения; 6 — разлом; 7 — буровая скважина

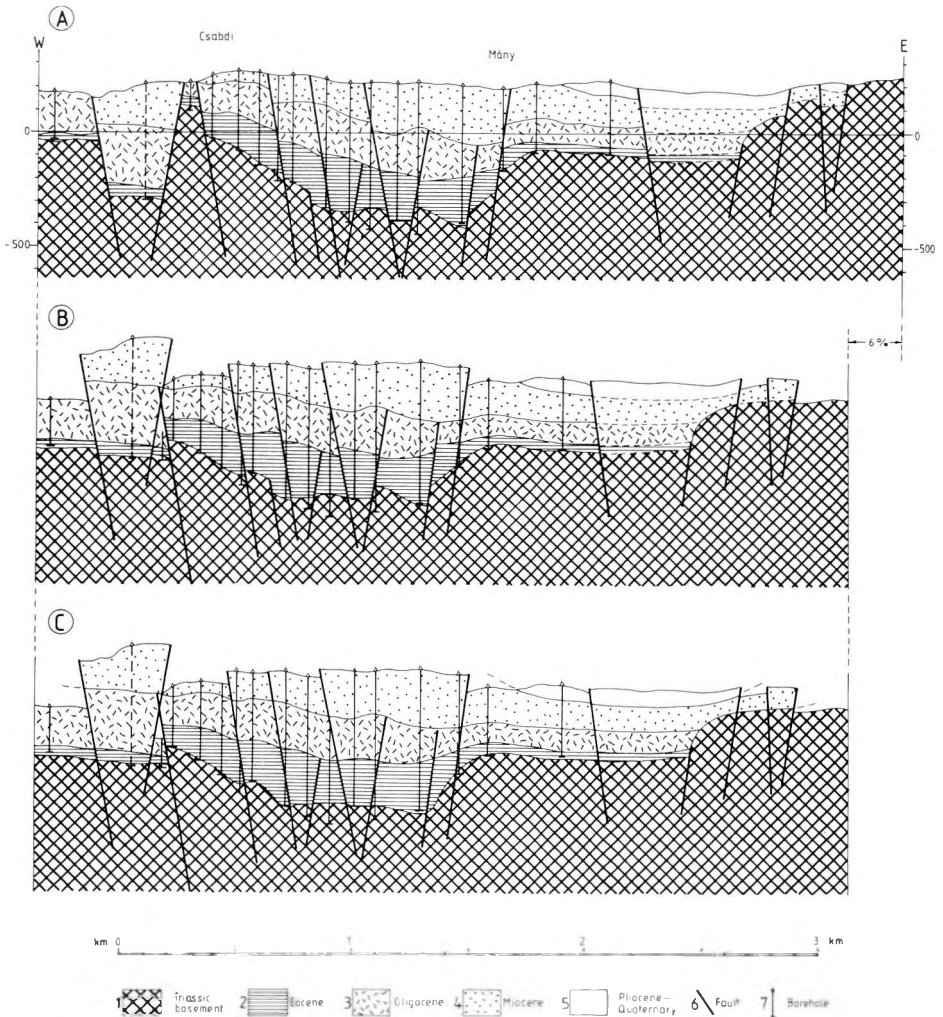


Fig. 10. Geological cross-section of the Mány coal deposit (A), after SAS et al. [1977] and restoration of the Miocene/Oligocene boundary (B) with minor adjustment (C). For location, see Fig. 1

10. ábra A Mányi kőszénélőfordulás földtani szelvénye, SAS et al. [1977] nyomán (A) a miocén/oligocén határ visszaállításával (B) és apró igazításokkal (C). Helyzetét l. az 1. ábrán. 1 — triász aljzat; 2 — eocén; 3 — oligocén; 4 — miocén; 5 — pliocén-kvarter; 6 — törés; 7 — mélyfúrás

Рис. 10. Геологический разрез по угольному месторождению Мань, по Шаш и др. [SAS et al. 1977] (A), с восстановлением границы миоцена с олигоценом (B) и с мелкими поправками (C). Положение см. на рис. 1

1 — триасовый фундамент; 2 — эоцен; 3 — олигоцен; 4 — миоцен; 5 — плиоцен-четвертичные отложения; 6 — разлом; 7 — буровая скважина

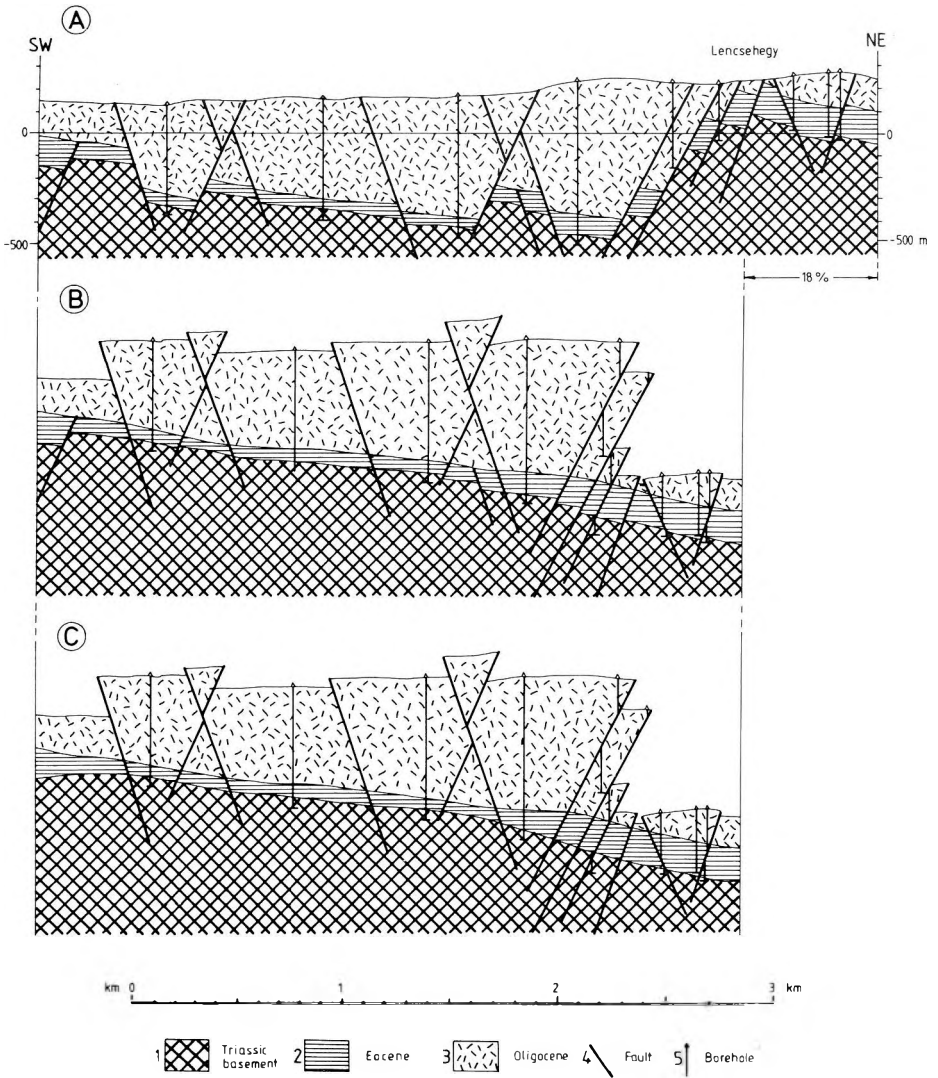


Fig. 11. Geological cross-section of the Dorog coal deposit (A), after BÁLINT et al. [1984] and restoration of the Oligocene/Eocene boundary (B) with minor adjustment (C). For location, see Fig. 1

11. ábra A Dorogi kőszénelőfordulás földtani szelvénye, BÁLINT et al. [1984] nyomán (A), az oligocén/eocén határ visszaállításával (B) és apró igazításokkal (C). Helyzetét l. az 1. ábrán
1 – triász aljzat; 2 – eocén; 3 – oligocén; 4 – törés; 5 – mélyfúrás

Рис. 11. Геологический разрез по угольному месторождению Дорог, по Балинт и др. [BÁLINT et al. 1984] (A), с восстановлением границы олигоцена с эоценом (B) и с мелкими поправками (C). Положение см. на рис. 1

1 – триасовый фундамент; 2 – эоцен; 3 – олигоцен; 4 – разлом; 5 – буровая скважина

A. REGIONAL TECTONICS			
TECTONIC FEATURES		OBJECTS OR EVENTS	AGE
Synclinal structure		Bakony Mts., Vértes Hills	Aptian-Turonian
Bending of Mesozoic structures		Gerecse Hills, Pilis Mts., Buda Hills	pre-Senonian
Tertiary tectonism		sediment re-arrangement main faults	Miocene Neogene
B. LOCAL TECTONICS			
AREAS	OBJECTS	PECULIARITIES	AGE
Bakony Mts.	syncline axis	250–70°	
	Litér thrust	SW–NE, southeast-vergent	Aptian-Turonian
	Telegdi-Roth line	W–E, dextral strike slip, 4–6 km	Aptian-Turonian?
	Várpalota depression	W–E, asymmetric trough	Lower–Middle Miocene
Vértes Hills	Bánta line	W–E, no horizontal offset?	Aptian-Turonian
		listric fault	Lower–Middle Miocene
		overthrust	Middle Miocene
	Inota line	W–E, dextral strike slip	Aptian-Turonian
		listric fault	Lower–Middle Miocene
		overthrust	Middle Miocene
		wedge-like unit	
		SW–NE, southeast-vergent	Aptian-Turonian
		N–S, asymmetric trough	Lower–Middle Miocene
		230–50°	
Gerecse Hills	thrust continuation	in the SE foreground	
	Vértessomló fault	W–E, sinistral strike slip, 6 km	
	Triassic strips	W–E, gentle arc	Aptian-Turonian
	Jurassic-Cretaceous syncline axis	complex structure	Aptian-Turonian
	Csúcs Hill	W–E, gentle arc	Aptian-Turonian
	Csúcs Hill area	Ladinian Diplopora Dolomite	
	Palaeogene in the NE	W–E faults, sequence repetitions	
Pilis Mts.		W–E faults, strike slips	Tertiary
		concentric extension, rejuvenated bending	Tertiary
		NW–SE, further bending	Aptian-Turonian
Buda Hills		elevation towards the SE	Tertiary
	Lower Carnian syncline axis	strip towards the Csúcs Hill	
		NW–SE	Aptian-Turonian
		elevation towards the SE	pre-Eocene
Balatonfővelence area	Buda line	facies boundary	Palaeogene
		no horizontal offset	
	Palaeogene beds	dislocations (compression?)	Neogene
	Nagykovácsi fault	W–E, dextral strike slip, 14 km	
	granite massif	core of a pericline structure	
	granite belt	NE–SW, S-shaped strip	
	Eocene volcanites	W–E, dextral strike slips	
	Polgárdi depression	SW–NE, asymmetric trough	Lower–Middle Miocene
		overthrust along the NW margin	Middle Miocene

Table 1. Selected data on the tectonics of the Transdanubian Range

I. táblázat. Válogatott tektonikai adatok a Dunántúli-középhegységből

Таблица I. выборочные данные по тектонике задунайского среднегорья

2.2. Local tectonic features in the Transdanubian Range

Local tectonic features will be discussed (see Table I, B) separately for orographical units (= Mts. or Hills). In the Bakony Mts. the axis of the syncline strikes in a 250–70° direction (Fig. 1). Along the southern limb of the whole Bakony syncline or, more exactly, along the Balaton Highlands, a thrust-slice structure is traceable.

Recently MÉSZÁROS [1980a, 1980b, 1982, 1983, 1985; MÉSZÁROS and TÓTH 1981] called attention to transverse strike-slip faults in the Bakony Mts. The most important fault of this type is, undoubtedly, that first described by TELEGDİ ROTH [1935: the Bakonybél–Várpalota line] and now known as the 'Telegdi-Roth line' (Fig. 12). It is traceable from the west over a distance of 40 km up to the Várpalota depression — which is the best studied Miocene depression in Hungary.

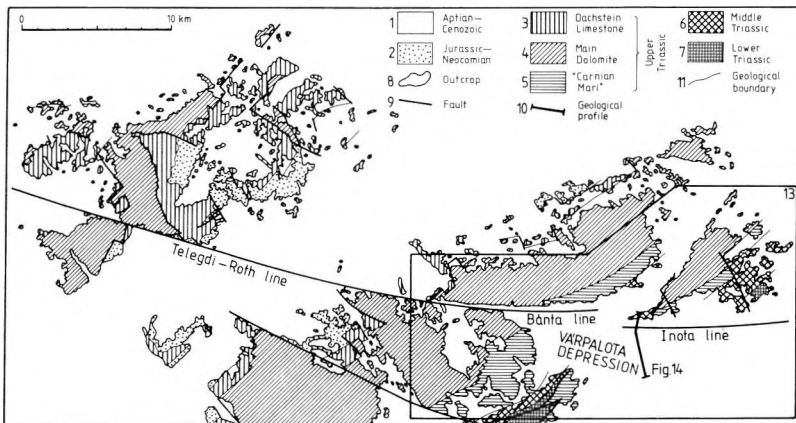


Fig.12. A fragment of the geological map of the Bakony Mts., after CSÁSZÁR et al. [1985], with the Telegdi-Roth line, subdivision of the Aptian-Cenozoic omitted. For location, see Fig. 1. Frames of Fig. 13. and profile of Fig. 14. indicated

12. ábra. Részlet a Bakony-hegység földtani térképéből, Császár et al. [1985] nyomán, a Telegdi-Roth vonallal; elhagytuk az apti-kainozoos képződmények felosztását. Helyzetét l. az 1. ábrán. Feltüntetjük a 13. ábra körvonalát és a 14. ábra szelvényvonalát. 1 — apti-kainozoikum; 2 — jura-neokom;

3–5 — felsőtriász: 3 — dachsteini mészkő, 4 — fődolomit, 5 — karni márga; 6 — középsőtriász; 7 — alsótriász; 8 — kibúvás; 9 — törés; 10 — földtani szelvény; 11 — képződményhatár

Рис. 12. Фрагмент геологической карты Баконьских гор, по Часару и др. [Császár et al. 1985], с обозначением линии Телегди-Рота; расчленение аптско-кайнозойских отложений упущено. Положение см. на рис. 1. Обозначены контур рис. 13 и профиль рис. 14

1 — апт-кайнозой; 2 — юра-неоком; 3–5 — верхний триас: 3 — дахштейнский известняк. 4 — главный доломит, 5 — карнийские мергели; 6 — средний триас; 7 — нижний триас; 8 — выходы на поверхность; 9 — разлом; 10 — геологический разрез; 11 — геологический контакт

While in the Bakony Mts. proper the straight shape of the Telegdi-Roth line implies strike-slip origin and the dextral offset can be estimated to be 4–6 km (see Fig. 12), in the western Várpalota depression no offset is suspectable along the Bánta line which continues the Telegdi-Roth line towards the east. Further in this direction the Inota line appears somewhat southerly. Along it, the arrangement of pre-Cenozoic formations implies a dextral offset of about 3 km (Fig. 13A). Alignment of the Bánta and Inota lines, however, is impossible without assuming significant displacements or deformations in the zone between them. Just here ends the wedge-like Iszka block which seems to be rotated anti-clockwise relative to the surroundings. Compensation of this rotation and of the dextral offset along the Inota line (Fig. 13B) results in the alignment of the Balaton Highlands thrust structure with that at the back of the Iszka block [RAINCSÁK 1980], i.e. in the absence of any strike-slip displacement along the Bánta line. In the resulting picture the Inota line is not the continuation of the Bánta line, and these lines are divided by the western end of the Iszka wedge.

The situation restored (Fig. 13B) means that the 4–6 km dextral offset along the Telegdi-Roth line *s.s.* (see Fig. 12) disappears in the western Várpalota depression, most probably merging in thrust structures which accompany the Litér-Bakonykúti thrust zone from the northwest. In other words, this remaining (after the restoration) strike-slip displacement is synchronous with the overthrusts along the southern limb of the Bakony syncline and it most probably occurred in the Middle Cretaceous. The Inota line situated beyond (i.e. east of) the thrust-slice structure seems to have arisen much later than the Telegdi-Roth–Bánta line, in connection with the removal of the Iszka wedge.

Fig. 13. The Várpalota depression and its surroundings. For location, see Figs. 1 or 12

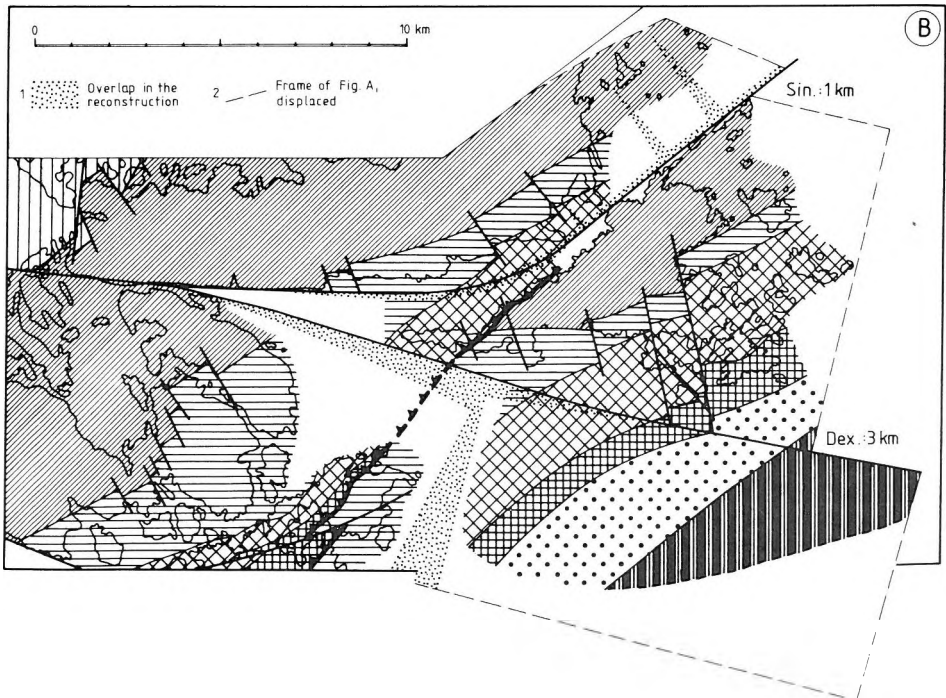
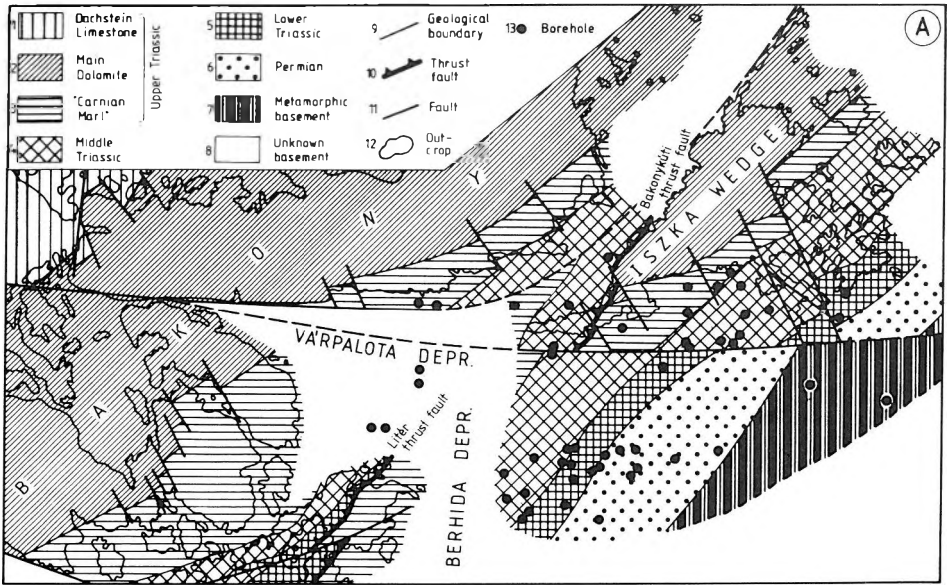
- A) Subsurface geological map of pre-Tertiary complexes. Base maps: for exposed areas, CSÁSZÁR et al. [1985], for covered areas, RAINCSÁK [1980]
- B) Situation after the restoration of the Iszka wedge. Northeastern Bakony Mts. left undeformed, and insignificant sinistral offsets not compensated

13. ábra. A Várpalotai-medence és környezete. Helyzetét l. az 1. vagy 12. b ábrán

- A) A harmadidőszak-előtti képződmények felszínének földtani térképe. Alaptérképek: kibúvási körzetekre – CSÁSZÁR et al. [1985], fedett területekre – RAINCSÁK [1980]. 1–3 — felsőtriász: 1 — dachsteini mészkő, 2 — fődolomit, 3 — karni márga; 4 — középsőtriász; 5 — alsótriász; 6 — perm; 7 — metamorf aljzat; 8 — ismeretlen aljzat; 9 — képződményhatár; 10 — feltolódás; 11 — törés; 12 — kibúvás; 13 — mélyfúrás;
- B) Az Iszkahegyi-ék visszaállítása utáni állapot. A Bakony EK-i részét nem deformáltuk s a kisméretű balos elmozdulásokat nem kompenzáltuk. 1 — átfedés a rekonstrukcióban; 2 — az A ábra kerete, eltelve

Рис. 13. Варпалотанская впадина и ее окрестности. Положение см. на рис. 1 или 12б

- A) Геологическая карта поверхности до третичных образований, по Часару и др. [CSÁSZÁR et al. 1985] для обнаженных районов и по Райнчаку [RAINCSÁK 1980] — для перекрытых
- 1–3 — верхний триас: 1 — дахштейнский известняк, 2 — главный доломит, 3 — карнийские мергели; 4 — средний триас; 5 — нижний триас; 6 — пермь; 7 — метаморфический фундамент; 8 — неизвестный фундамент; 9 — геологический контакт; 10 — взброс; 11 — разлом; 12 — область выходов; 13 — буровая скважина
- B) Ситуация после восстановления Искайского клина. СВ часть Баконьских гор оставлена без деформаций, мелкие левосторонние смещения не скомпенсированы
- 1 — перекрытие в реконструкции; 2 — контур рис. А в смещенном положении



Along both the Bánta and Inota lines subsidence and overthrust in the Miocene occurred [KÓKAY 1956, 1968, 1976, 1985]. KÓKAY [1976] related the Miocene subsidence to the „downthrust” (Fig. 14) but the same factual material allows us to connect subsidence with lystric faults and to relate overthrust to its termination (Fig. 15). Overlaps in the situation restored (Fig. 13B) indicate that the extension and subsidence in the Várpalota depression were due to the removal of the Iszka

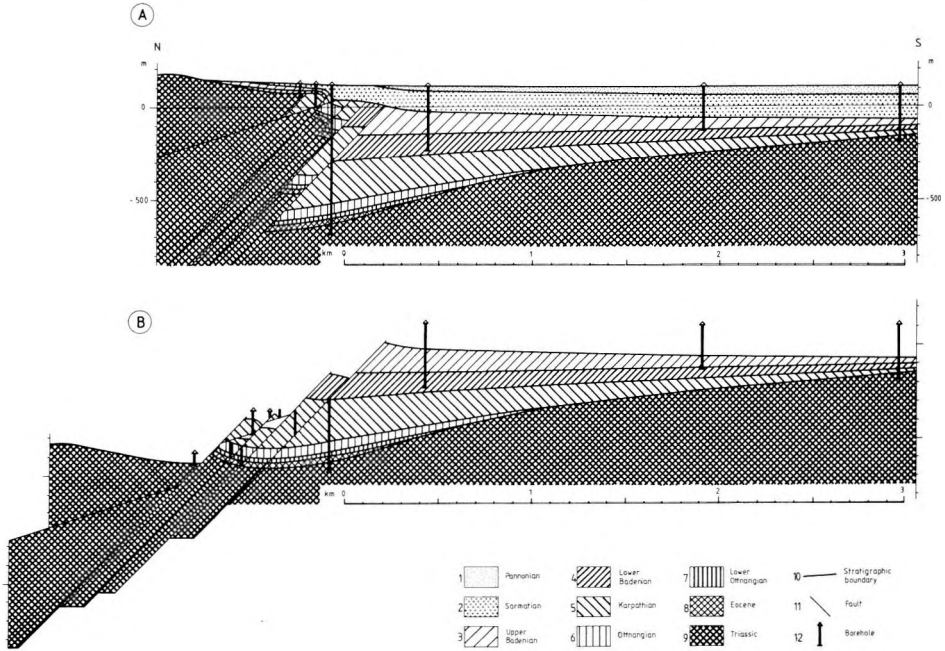


Fig. 14. Geological section across the Inota line, first version. For location, see Fig. 12

A) Present situation, after KÓKAY [1976]

B) Situation after the rigid compensation of thrusts; Badenian deposits on elevated block as well as Sarmatian and Pannonian sediments omitted

14. ábra. Földtani szelvény az Inotai-vonalon át, első változat. Helyzetét l. a 12. ábrán

A) Mai állapot KÓKAY [1976] nyomán

B) A rátolódások merev visszaállítását utáni állapot; elhagytuk a szarmata és a pannon, valamint – a kiemelkedésekről – a bádeni üledékeket. 1 – pannon; 2 – szarmata; 3 – felsőbádeni; 4 – alsóbádeni; 5 – kárpáti; 6 – ottngangi; 7 – alsóottngangi; 8 – eocén; 9 – triász; 10 – sztratigráfiai határ; 11 – törés; 12 – mélyfúrás

Рис. 14. Геологический разрез через Инотайскую линию, вариант первый. Положение см. на рис. 12

A) Современная ситуация, по Кокаи [КÓKAY 1976]

B) Ситуация после жесткого восстановления взбросов; сарматские и паннонские, а с поднятия и баденские отложения упущены

1 – паннонские отложения; 2 – сарматские отложения; 3 – верхнебаденские отложения; 4 – нижнебаденские отложения; 5 – карпатские отложения; 6 – оттнганские отложения; 7 – нижнеоттнганские отложения; 8 – эоцен; 9 – триас; 10 – стратиграфический контакт; 11 – разлом; 12 – буровая скважина

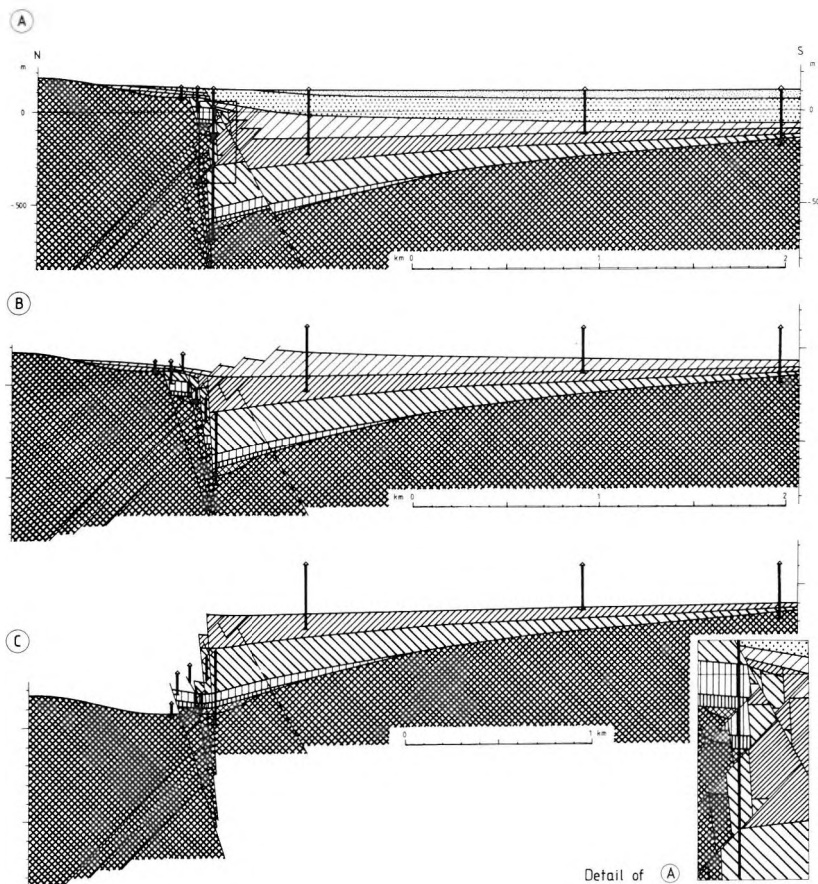


Fig 15. Geological section across the Inota line, second version. For legend, see Fig. 14

- A) Present situation in our interpretation. All data are the same as in Fig. 14. Insert in the bottom right angle of C indicated
- B) Situation after the rigid compensation of thrusts; Sarmatian and Pannonian sediments omitted
- C) Situation after the rigid compensation of the subsidence along listric faults; Lower Badenian deposits on elevated blocks as well as Upper Badenian sediments omitted. Insert demonstrates the style of the present complex structure of the tectonic zone

15. ábra. Földtani szelvény az Inotai-vonalon át, második változat. Jelkulcs a 14. ábrán

- A) Mai állapot saját értelmezésünkben. Minden adat ugyanaz, mint a 14. ábrán. Feltüntetettük a C jobb alsó sarkában levő kivágat körvonalát
- B) A rátolódások merev visszaállítására utáni állapot; elhagytuk a szarmata és pannon üledékeket
- C) A lisztrikus törések menti besüllyedés merev visszaállítására utáni állapot; elhagytuk a felsőbadeni, valamint — a kiemelkedésekről — az alsóbadeni üledékeket. A kivágat a tektonikus öv mai bonyolult szerkezeti jellegét mutatja be

Рис. 15. Геологический разрез через Инотайскую линию, вариант второй. Условные обозначения см. на рис. 14

- A) Современная ситуация в нашей интерпретации. Все данные те же, что и на рис. 4. Обозначен контур врезки в правом нижнем углу C
- B) Ситуация после жесткого восстановления взбросов; сарматские и паннонские отложения упущены
- C) Ситуация после жесткого восстановления опусканий вдоль листрических сбросов; верхнебаденские, а с поднятий и нижнебаденские отложения упущены. Врезкой демонстрируется сложность современной структуры зоны разломов

wedge. The Berhida depression south of the Várpalota depression may have been generated during the same process due to the deformation of the areas situated south of the Iszka block (see overlaps here in Fig. 13B).

In the Vértes Hills the axis of the syncline strikes in a 230–50° direction (Fig. 1) manifesting 20° anticlockwise rotation relative to the Bakony Mts. We link this rotation with that of the Iszka Block (see Fig. 13B) and conclude that the rotation boundary between the Bakony Mts. and Vértes Hills separates the Iszka block from the Bakony Mts.

Restoration of the Iszka–Vértes block relative to the Bakony Mts. (Fig. 16) requires gradual deviation of the eastern ending of the latter and compensation for the extension within young wedge-like depressions. This allows us to connect the generation of these depressions with the Vértes rotation. In the situation restored the Litér–Bakonykúti thrust continues towards the east. Its further continuation is to be expected beneath the southern foreland of the Vértes Hills towards the northeast.

The geological boundary of the Gerecse Hills with the Vértes Hills is traceable along the Vértessomló fault which manifests sinistral displacement of about 6 km (Fig. 5). The general picture of the strata dips as well as the arrangement of Triassic lithological units outlines a gentle structural bend while the distribution of Jurassic and Lower Cretaceous formations displays a complex picture (Fig. 5) as in the Bakony Mts. As yet there is no tectonic interpretation. In the first approximation,

Fig. 16. Bakony–Vértes junction area and its surroundings. For location, see Fig. 1. Frame of Fig. 13 indicated

- A) Subsurface geological map of pre-Tertiary complexes. Base maps: for exposed areas, CSÁSZÁR et al. [1985], for covered areas, RAINCÁSÁK [1980]. 'Csákberény depr.' = Csákberény depression
 B) Situation after the restoration of the Vértes Hills. Northeastern Bakony Mts. deformed and even insignificant sinistral offsets compensated

16. ábra. A Bakony és a Vértes csatlakozási öve és annak környezete. Helyzetét l. az 1. ábrán. Feltüntetjük a 13. ábra körvonalát

A) A harmadidőszak előtti képződmények felszínének földtani térképe. Alaptérképek: kibúvási körzetekre – CSÁSZÁR et al. [1985], fedett területekre – RAINCÁSÁK [1980].

1 — júra-neokom; 2–4 — felsőtriász; 2 — dachsteini mészkő, 3 — földolomit, 4 — karni márga; 5 — középsőtriász; 6 — alsótriász; 7 — perm; 8 — metamorf aljzat; 9 — ismeretlen aljzat; 10 — kibúvás; 11 — bauxittelep; 12 — képződményhatár; 13 — feltolódás; 14 — törés; 15 — mélyfúrás.

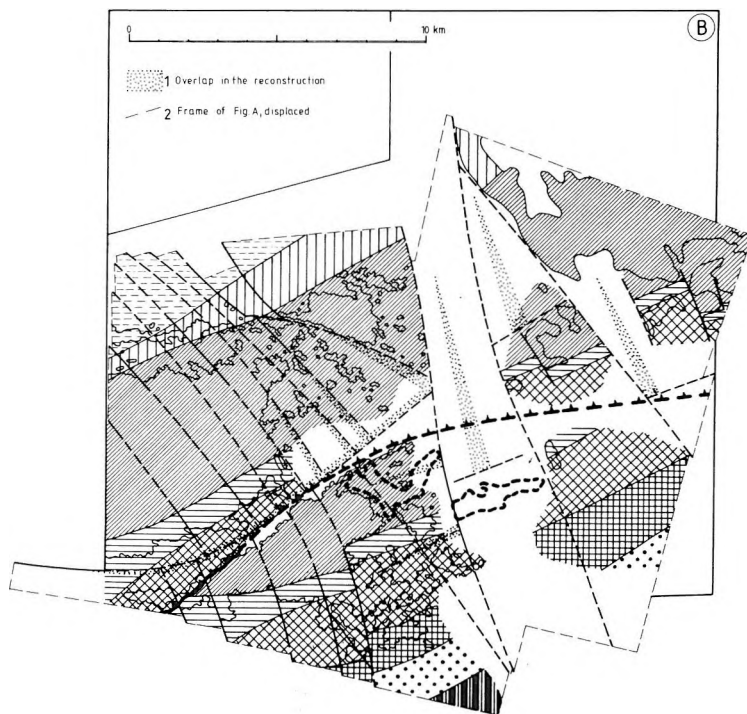
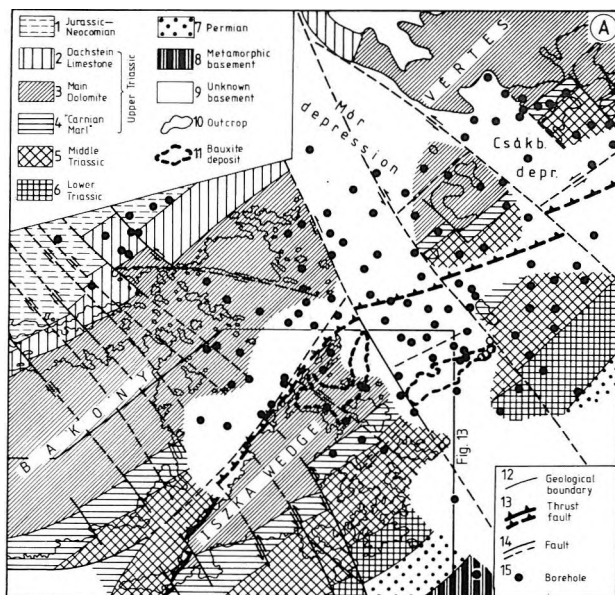
B) A Vértes visszaállítása utáni állapot. A Bakony ÉK-i részét deformáltuk s még a kisméretű balos elmozdulásokat is kompenzáltuk. 1 — átfedés a rekonstrukcióban; 2 — az A ábra kerete, eltolva

Рис. 16. Сочленение Баконьских и Вертешских гор и его окрестности. Положение см. на рис. 1. Обозначен контур рис. 13

A) Геологическая карта поверхности дотретичных образований, по Часару и др. [CSÁSZÁR et al. 1985], для обнаженных районов и по Райнчаку [RAINCÁSÁK 1980] — для перекрытых

1 — юра-неоком; 2–4 — верхний триас; 2 — дахштейнский известняк, 3 — главный доломит, 4 — карнийские мергели; 5 — средний триас; 6 — нижний триас; 7 — перм; 8 — метаморфический фундамент; 9 — неизвестный фундамент; 10 — область выходов; 11 — бокситовая залежь; 12 — геологический контакт; 13 — взброс; 14 — разлом; 15 — буровая скважина

B) Ситуация после восстановления Вертешских гор. СВ часть Баконьских гор деформирована, и даже небольшие левосторонние смещения скомпенсированы 1 — перекрытие в реконструкции; 2 — контур рис. А в смещенном положении



Jurassic and Lower Cretaceous turn towards the north apart from the gentle Triassic bend indicating an S-shaped bend of the axis of the syncline. This would be explainable by assuming sinistral strike slips (Fig. 17). Because of the complexity of the superimposed young structure and absence of any structural markers the W–E directed strike-slip faults can only be suspected in an indirect way (see below).

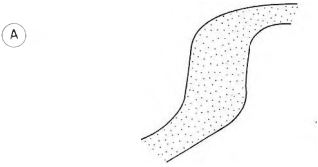


Fig. 17. Sketch to illustrate origin of the situation in the western Gerecse Hills

17. ábra. A nyugatgerecsei rajzolat keletkezési vázlata

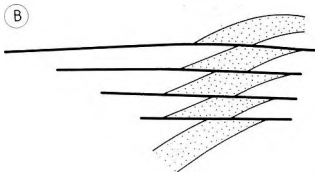
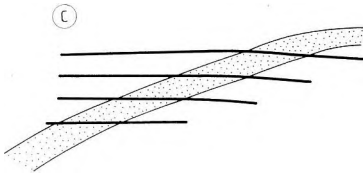


Рис. 17. Схема возникновения структурного рисунка в 3 части Геречейских гор



In the southeast, Csúcs Hill (Fig. 18A) is built up of dolomite which has been regarded as Ladinian *Diplopora* Dolomite on the basis of all direct investigations [ORAVECZ 1961; VÉGH-NEUBRANDT 1981] but assumed to be Carnian Main Dolomite on the basis of regional considerations (CSÁSZÁR et al. 1978; SZABÓ et al. 1982). West of Csúcs Hill, Góré Hill is built up of Main Dolomite with Carnian fauna [VIGH 1914]. Bituminous limestone debris on the southern slope has been thought to have originated from the base of the Carnian [ORAVECZ 1961]. The sparse network of the boreholes west and north of Csúcs Hill allows us to assume the continuation of the Lower Carnian horizon in this direction, i.e. between Góré Hill and Csúcs Hill as is expected on the basis of stratigraphic considerations if the dolomite of Csúcs Hill is really Ladinian in age (Fig. 18B). Configuration of the strips composed of Lower Carnian beds south of Csúcs Hill (Fig. 18A) would be explainable by assuming large offsets (Fig. 18B) which may equally be due to sinistral displacements, south-dipping normal faults or south-vergent overthrusts. Similar displacements would serve as an explanation for the appearance of Ladinian beds again in the north, on csúcs Hill (Fig. 18B). Finally, Lower Carnian beds are traceable towards the west along the southern marginal fault in boreholes and do not wedge out in this direction.

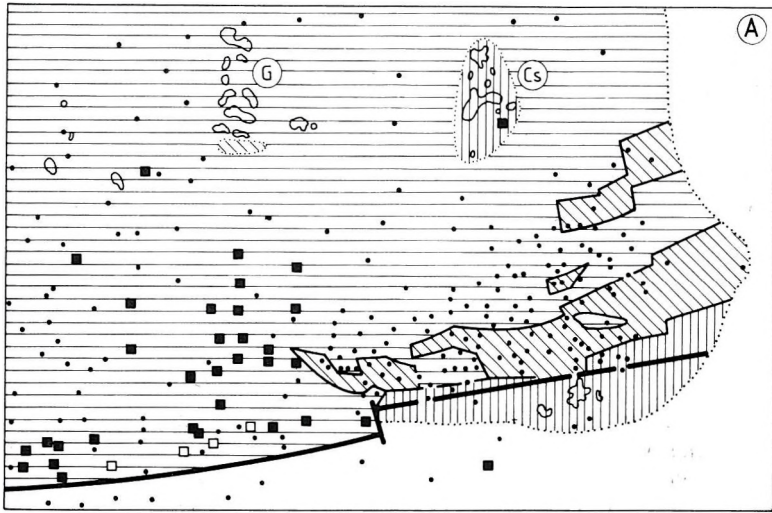
In the northeast, mostly Palaeogene sediments of increased thickness are developed while Triassic and Jurassic crop out in small ranges striking in a W–E

direction. The whole area transitional to the Pilis Mts. is mostly covered by Palaeogene sediments. This may be due to the concentric extension along the external zone of the structural bend (Fig. 19). Hence, the curvature of the bend of Mesozoic structures, which arose in the Middle Cretaceous (see 2.1.), in the area discussed probably increased in the Cenozoic, and this resulted in the break-up of the Transdanubian Range between the Gerecse Hills and Pilis Mts. In the Pilis Mts. further bending of all structures is observable (Fig. 20). North of the wide Norian (partly Rhaetian?) Dachstein Limestone strip, older (Carnian) sediments crop out. They possibly form the opposite limb of a syncline. Jurassic in the core of the syncline only occurs in the northwest probably indicating uplift of the axis in a SE direction. In the south, beyond the strip of the Carnian (partly Norian)? Main Dolomite, a deeper — in a stratigraphic sense — horizon of bituminous limestone (lowermost Carnian: WEIN 1977) crops out in small exposures. In the west-northwest direction the Lower Carnian strip may be continued just towards the northern foreland of Csúcs Hill.

In the Buda Hills the structural rotation relative to the Bakony Mts. extends 90° clockwise (Fig. 20). In a SW–NE direction, across the whole Buda Hills a sharp Palaeogene facies boundary (see in Fig. 6) is traceable. Northwest of this have developed continental, lagoonal and shallow-marine deposits while southeast of it there are basinal sediments. This is a facies boundary that has long since been well-known. HORUSITZKY [1943] explained it in terms of a southvergent Palaeogene overthrust which divides different facies types of the Triassic. SZENTES [1958] and WEIN [1976, 1977] presented geological maps for the Buda Hills which differ only in detail and agree in the absence of indications of significant displacement of the Triassic along the Palaeogene facies boundary. Moreover, Wein interpreted boundaries of the latter as facial transitions with no tectonics along them. Nevertheless, a large strike-slip along this boundary ('Buda line') is supposed [BÁLDI 1982; BÁLDI and BÁLDI-BEKE 1985]. This concept, however, lacking new geological maps and ideas concerning the structure of the Triassic is not convincing.

The arrangement of Middle and Upper Triassic sediments points to the existence here of a large syncline with an axis which strikes in the NW–SE direction and elevates towards the southeast (Fig. 20). This elevation is recorded in the arrangement of Triassic beds in the bottom of the Palaeogene depressions (fragments of Palaeogene sediments have often been preserved here at high altitudes), i.e. it is pre-Eocene in age. In the same SE direction the Palaeogene beds become more disturbed, their dips frequently achieving 30–40° which sharply contrast with the usual 3–5° dips in the northwestern foothills of the Bakony Mts., Vértes and Gerecse Hills and even east of the latter. Disturbance of Palaeogene beds reflects, perhaps, post-Palaeogene compression which was responsible for the rejuvenated elevation of the area.

Along the northern margin of the Nagykovácsi basin in the north, a west–east striking fault borders these structures. Along this Nagykovácsi fault, the Norian Dachstein Limestone in the core of the Buda syncline contacts with the Ladinian Diplopora Dolomite. Various contours of the Ladinian dolomite have been presented (Fig. 21) but when regarding the spatial distribution of Diplopora (see Figs. 21B and D) and the general structural situation, one finds Szentes's version



- | | | | | | |
|---|------------------------------------|---|--|----|-----------------------------------|
| 1 | Carnian to Norian
Main Dolomite | 2 | Lower Carnian
limestone, marl,
cherty dolomite | 3 | Ladinian
Diplopora
Dolomite |
| 4 | Outcrop | 5 | Constructed
boundary (A) | 6 | Stratigraphic
boundary (B) |
| 7 | Principal
fault | 8 | Boreholes used in
constructing boundaries (A) | 9 | Dolomite |
| | | | | 10 | Limestone or marl |

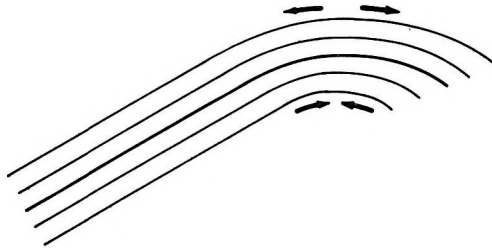


Fig. 19. Sketch to illustrate concentric extension in the northeastern Transdanubian Range

19. ábra. A Dunántúli-középhegység ÉK-i részén fellépő koncentrikus tágulás vázlatja

Рис. 19. Схема возникновения концентрического растяжения в СВ части Задунайского среднегорья

Fig. 18. Geological structure of the southeastern foreground of the Gerecse Hills. For location, see Fig. 5
 A) Subsurface geological map, after SZABÓ et al. [1982], simplified (the network of faults omitted) and completed by drilling data not used in constructing the map and by indication of Ladinian dolomite of Csúcs Hill (Cs in circle in the map) and of Lower Carnian beds on the southern slope of Góré Hill (G in circle in the map), both after ORAVECZ [1961]

B) Structural interpretation of data presented. Note: In most cases Main Dolomite (Carnian) and Diplopora Dolomite (Ladinian) have not correctly been distinguished in boreholes

18. ábra. A Gerecse DK-i előterének földtani szerkezete. Helyzetét l. az 5. ábrán

A) Aljzattérkép SZABÓ et al. [1982] nyomán, egyszerűsítve (a törésháló elhagyva) és az eredeti térkép szerkesztésében nem használt fúrásokkal, valamint a Csúcs-hegy (a térképen Cs körben) ladiniai dolomitjával és a Góré-hegy (a térképen G körben) D-i lejtőjének alsókarni képződményeivel (mindkettő ORAVECZ [1961] nyomán) kiegészítve

B) A bemutatott adatok szerkezeti értelmezése. Megjegyzés: az esetek többségében bizonytalan a (karni) földolomit és a (ladini) diploporás dolomit elkülönítése a fúrásokban. 1 — karni–nóri: földolomit;

2 — alsókarni: mészkő, márga, kovás dolomit; 3 — ladiniai: diploporás dolomit; 4 — kibúvás; 5 — szerkesztett határ (A); 6 — sztratigráfiai határ (B); 7 — fővető;

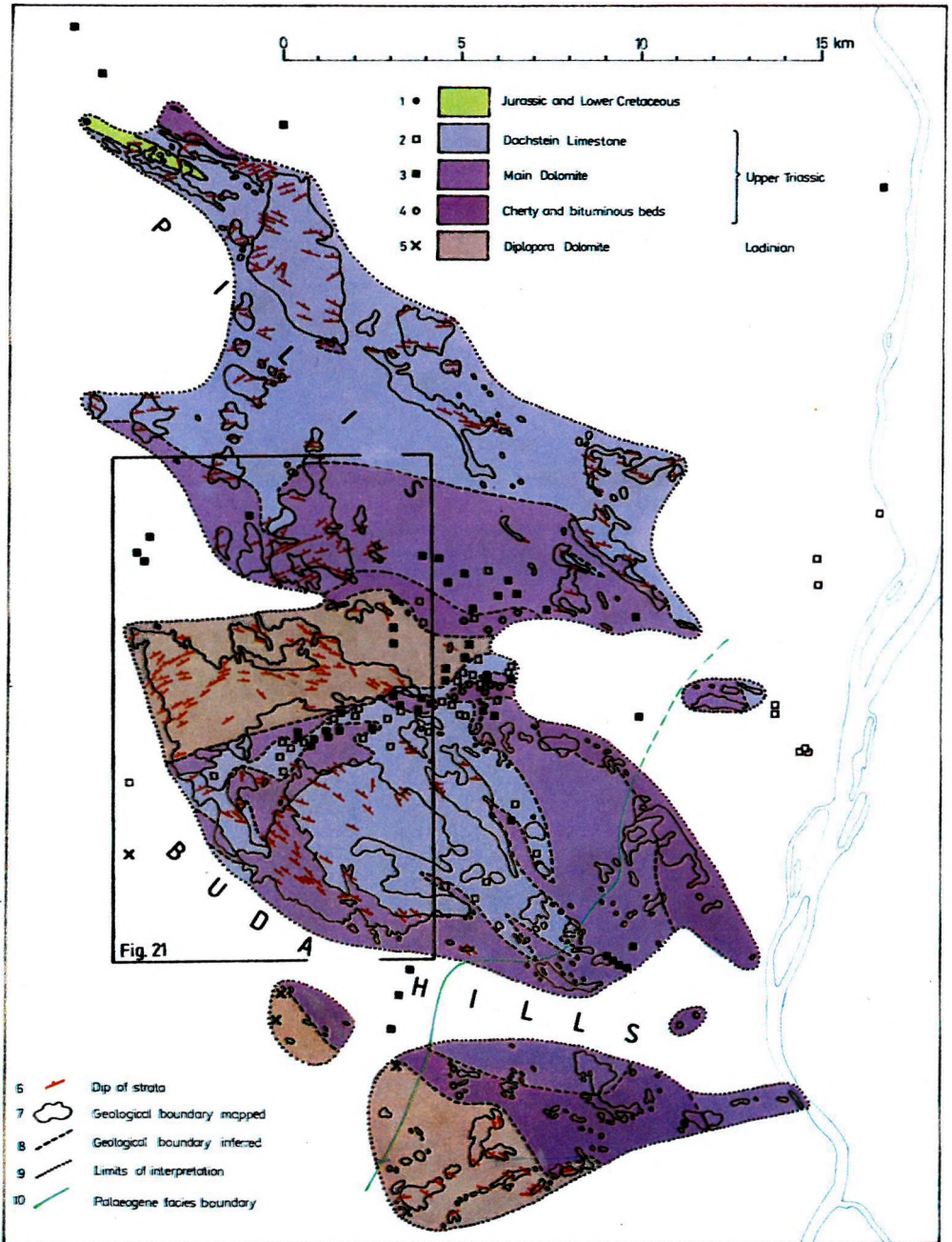
8 — az A térkép határainak szerkesztéséhez felhasznált mélyfúrások; 9–10 — további, dolomitot (9), ill. mészkövet vagy márgát (10) harántolt fúrások

Рис. 18. Геологическая структура ЮВ форланда Геречейских гор. Положение см. на рис. 5

A) Геологическая карта фундамента, по Сабо и др. [SZABÓ et al. 1982], с упрощениями (сеть разломов упущена), дополненная скважинами, не использованными при составлении первичной карты, а также доломитами ладинского яруса на горе Чуч (на карте — Cs в кружочке) и породами нижнекарнийского подъяруса на южном склоне горы Горе (на карте G в кружочке), в обоих случаях, по данным Оравеца [ORAVECZ 1961]

B) Структурная интерпретация представленных данных. Примечание: разделение доломитов на диплопоровые (ладинские) и главные (карнийские) по скважинам в большинстве случаев не надежно

1 — карнийский и норийский яруса: главный доломит; 2 — нижнекарнийский подъярус: известняки, мергели, кремнистые доломиты; 3 — ладинский ярус: диплопоровый доломит; 4 — область выходов; 5 — отстроенный геологический контакт (A); 6 — стратиграфический контакт (B); 7 — главный сброс; 8 — буровые скважины, использованные в составлении карты A; 9–10 — дальнейшие скважины, вскрывшие доломиты (9) или мергели (10)



(Fig. 21C) most acceptable (see Fig. 20). The sharp stratigraphic change is accompanied by a sharp change in the general strike direction (Fig. 20), both of them suggesting large-scale dextral displacement along the Nagykovácsi fault (Fig. 22). The offset along it is estimated to be 14 km, and the axis of the Buda syncline seems to be the westerly displaced continuation of the axis of the Pilis syncline.

The Balatonfő–Velence area in the south is the only area with fundamentally new factual material [DUDKO 1988a, 1988b]. Carboniferous granites exposed in the Velence Hills are limited in the east and form the core of a periclinal structure (Fig. 23) which involves Palaeozoic, Permian, Lower and Middle Triassic formations. At the same time, granites are traceable in boreholes a long way towards the southwest forming a continuous belt which is of characteristic S-shape on the map (Fig. 23). Gentle bending even of the granite body of the Velence Hills is presumably based on the change of the Late Eocene (to Early Oligocene?) palaeomagnetic directions (Fig. 24).

The Eocene volcano-sedimentary formation east and south of the Velence Hills is displaced by west–east directed dextral strike-slip faults (Fig. 23). North, west and southwest of the Velence Hills, occurrences of this formation are restricted to narrow and deep depressions whose stratigraphic columns are easy to correlate (Fig. 25); therefore, they may have been separated due to later movements.

Miocene sediments fill in the deep and narrow Polgárdi depression which follows the rotated section of the Balaton–Velence granite belt. The reflexion seismic profile across it and the borehole columns (Fig. 26) reveal structure and stratigraphy close to those of the Várpalota depression (Fig. 15A). Consequently, the history of the basin formation was probably the same (see Figs. 15B–C). On the basis of this similarity uniform kinematics (Fig. 27) can be supposed for the whole Balatonfő–Iszka area in which all Cenozoic basins are related to the Vértes rota-

Fig. 20. Subsurface geological map of the Pilis Mts. and Buda Hills constructed using BALOGH's [1961], FERENCZ's [1953], HEGEDŰS's [1951], SIKABONYI's [1952], SZENTES's [1958] and WEIN's [1977] maps and drilling data. For location, see Fig. 1. Frame of Fig. 21 indicated

20. ábra. A Pilis- és a Budai-hegység aljzattérképe BALOGH [1961], FERENCZ [1953], HEGEDŰS [1951], SIKABONYI [1952], SZENTES [1958] és WEIN [1977] térképei nyomán, fúrési adatok felhasználásával szerkesztve. Helyzetét l. az 1. ábrán. Feltüntetjük a 21. ábra körvonalát. 1 — júra és alsókréta; 2–4 — felsőtriász: 2 — dachsteini mészkő, 3 — földolomit, 4 — kovás és bitumenes rétegek; 5 — diplopórási dolomit (ladini); 6 — rétegdőlés; 7 — térképezett képződményhatár; 8 — következtetett képződményhatár; 9 — az értelmezés határa; 10 — paleogén fációs határ

Рис. 20. Геологическая карта фундамента Будайских и Пилишских гор, по данным Балога [BALOGH 1961], Ференца [FERENCZ 1953], Хегедюша [HEGEDŰS 1951], Шикабоньи [SIKABONYI 1952], Сентеша [SZENTES 1958] и Вейна [WEIN 1977] и с использованием буровых данных. Положение см. на рис. 1. Обозначен контур рис. 21
1 — юра и нижний мел; 2–4 — верхний триас: 2 — дахштейнский известняк, 3 — главный доломит, 4 — кремнистые и битуминозные породы; 5 — диплопоровый доломит (ладинский); 6 — падение слоев; 7 — откартированный геологический контакт; 8 — предполагаемый геологический контакт; 9 — контур интерпретации; 10 — фациальная граница палеогенового возраста

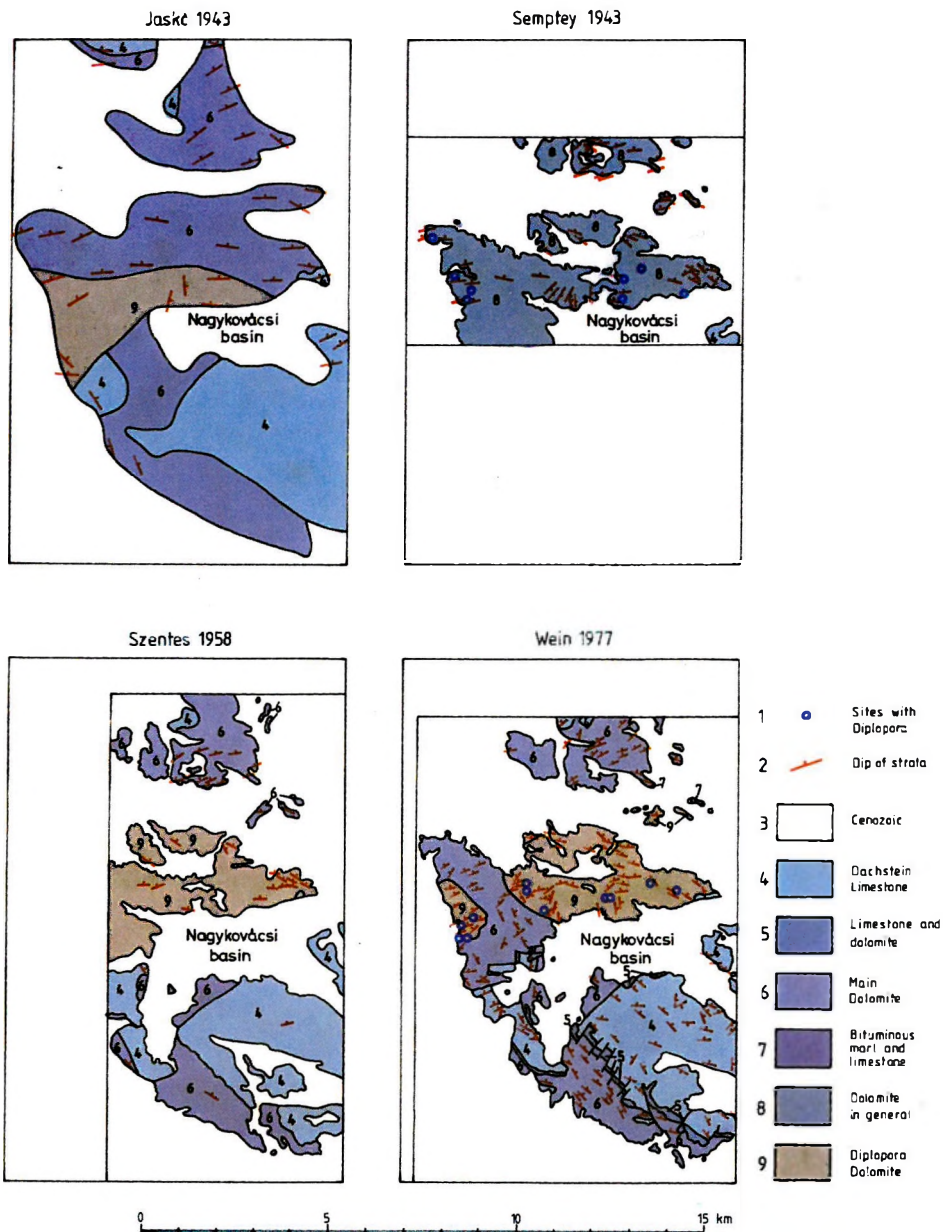


Fig. 21. Versions of the geological map of the north-western Buda Hills. For location, see Fig. 20

21. ábra. Változatok a Budai-hegység ÉNy-i részének földtani térképére. Helyzetét l. a 20. ábrán. 1 — diplopóra leletek; 2 — rétegdőlés; 3 — kainozoikum; 4 — dachsteini mészkő; 5 — mészkő és dolomit; 6 — fődolomit; 7 — bitumenes márga; 8 — dolomit általában; 9 — diplopóras dolomit

Рис. 21. Варианты геологической карты СЗ части Будаийских гор. Положение см. на рис. 20

1 — пункты находок диплопор; 2 — падение слоев; 3 — кайнозой; 4 — дахштейнский известняки; 5 — известняки и доломиты; 6 — главный доломит; 7 — битуминозные мергели; 8 — доломиты вообще; 9 — диплопоровый доломит

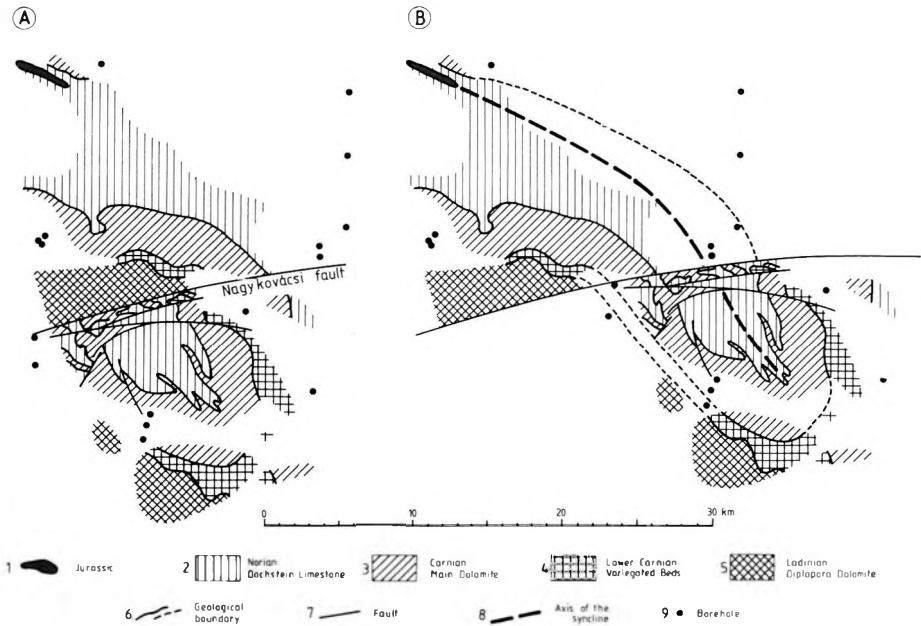


Fig. 22. The Nagykovácsi fault. Schematic subsurface geological map. Simplified from Fig. 20

22. ábra. A Nagykovácsi-törés. Vázlatos aljzatterkép: a 20. ábra egyszerűsített változata.

- 1 — júra; 2 — nóri dachsteini mészkő; 3 — karni fődolomit; 4 — alsókarni kovás és bitumenes rétegek;
5 — ladini diplopórási dolomit; 6 — képződményhatár; 7 — törés; 8 — a szinklinális tengelye;
9 — mélyfúrás

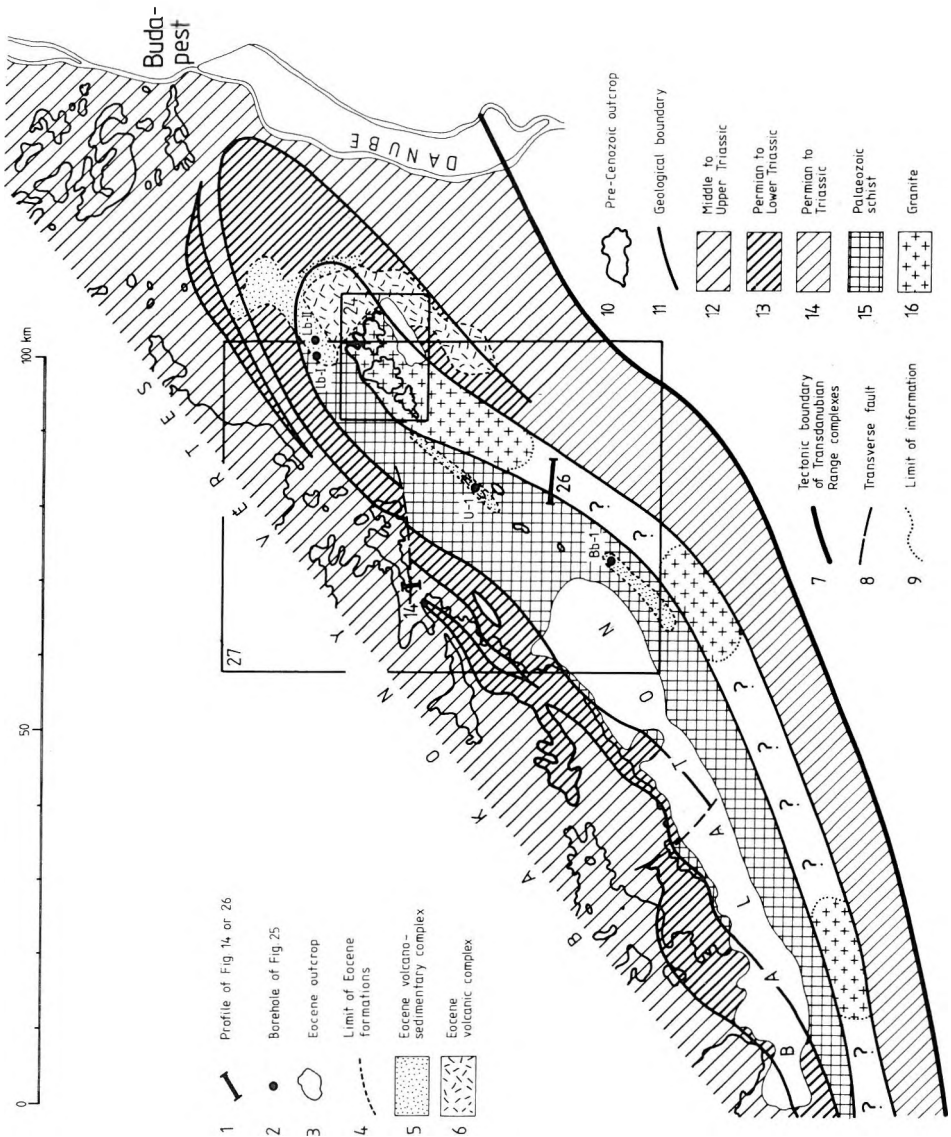
Рис. 22. Надьковачинский разлом. Схематическая геологическая карта фундамента: упрощенный вариант рис. 20

- 1 — юра; 2 — норийский ярус: дахштейнский известняк; 3 — карнийский ярус: главный доломит; 4 — нижнекарнийский подъярус: кремнистые и битуминозные отложения; 5 — ладинский ярус: диплопоровый доломит; 6 — геологический контакт; 7 — разлом; 8 — ось синклинали; 9 — буровая скважина

tion. The filling of the Mór and Csákberény depressions is of Late Oligocene or Early Miocene age, and the subsidence was of subsequent type (see Fig. 26). The filling of the Várpalota, Berhida and, probably, Polgárdi depressions is of Ottnangien–Badenian age, and the subsidence was of synchronous type (see Fig. 15). Compression, as a later event, was probably independent of the rotation.

2.3. Summary of the tectonics

Previously, the old (Middle Cretaceous) synclinal structure of the Transdanubian Range was only clear in the west (Bakony Mts. and Vértes Hills). On the basis of the arrangement and position of Triassic and Jurassic beds, this syncline has been traced through the Gerecse Hills and Pilis Mts. into the Buda Hills, and the bending of this syncline together with associated thrust structures has been cleared up in accordance with SZENTES's [1934] ideas [VIGH and SZENTES



1952]. Analysis of the disturbances in the general picture has led to the discovery of young rotations and large-scale strike-slip displacements in both directions. The Tertiary age of these movements is supported by considerations on the regional tectonics of the Transdanubian Range and by direct observations in the Balatonfővelence area.

Formerly, faults of NW–SE and SW–NE directions were regarded most important, and N–S striking faults were assumed to play an additional role in the Gerecse

Fig. 23. Subsurface geological map of pre-Miocene formations of the Balatonfő–Velenca area, after DUDKO et al. [1988], modified and completed. Frames of Figs. 24 and 27, boreholes in Fig. 25 and profile of Fig. 26 indicated

23. ábra. A Balatonfő–Velenca körzet miocén előtti képződményeinek térképe, DUDKO et al. [1988] nyomán, módosítva és kiegészítve. Feltüntetjük a 24. és 27. ábra körvonalát, a 25. ábra fúrásait és a 26. ábra szelvényvonalát. 1 — a 14. ill. 26. ábra szelvényének helyzete; 2 — mélyfúrás; 3 — eocén kibúvás; 4 — az eocén elterjedési határa; 5 — eocén vulkáni-üledékes összlet; 6 — eocén vulkáni összlet; 7 — a Dunántúli-középhegység összeleteinek tektonikai határa; 8 — eltolódás; 9 — információhatár; 10 — harmadkorinál idősebb kibúvás; 11 — képződményhatár; 12 — középső-felsőtriász; 13 — perm-alsótriász; 14 — perm-triász; 15 — paleozoos palák; 16 — gránit

Рис. 23. Карта домиоценовых образований района Балатонфё–Веленце, по Дудко и др. [DUDKO et al. 1988] с изменениями и дополнениями. Обозначены контуры рис. 24 и 27, скважины рис. 25 и профиль рис. 26

1 — линии профилей рис. 14 и 16; 2 — буровая скважина; 3 — выходы эоцена; 4 — контур распространения эоцена; 5 — вулканогенно-осадочный комплекс эоцена; 6 — вулканогенный комплекс эоцена; 7 — тектоническая граница распространения комплексов, слагающих Задунайское среднегорье; 8 — сдвиг; 9 — контур наличия информации; 10 — выходы дотретичных образований; 11 — геологический контакт; 12 — средний–верхний триас; 13 — перм–нижний триас; 14 — пермь–триас; 15 — палеозойские сланцы; 16 — граниты

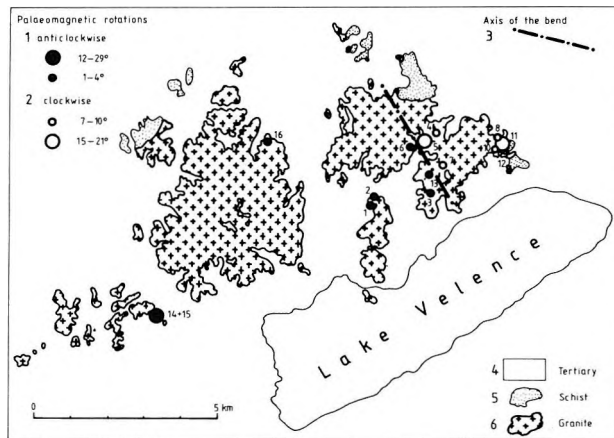


Fig. 24. Late Eocene palaeomagnetic directions of the granite body in the Velenca Hills, after MÁRTON E. [1986]. Figures indicate serial numbers of sites. All rotations given relative to the 328–148° direction (site No. 12). For location see Fig. 23

24. ábra A velencai gránittest felsőeocén paleomágneses irányai MÁRTON E. [1986] nyomán. Feltüntetjük a mintavételi helyek sorszámait. Minden elfordulást a 328–148° irányhoz (12. sz. mintavételi hely) viszonyítottunk. Helyzetét l. a 23. ábrán. 1–2 — paleomágneses elfordulások: 1 — óramutató járásával ellentétes, 2 — óramutató járásával egyező; 3 — a hajlat tengelye; 4 — harmadidőszaki képződmények; 5 — pala; 6 — gránit

Рис. 24. Позднеэоценовые палеомагнитные направления веленцейских гранитов, по Мартон [MÁRTON E. 1986]. Обозначены номера пунктов отбора проб. Все повороты отнесены к направлению 328–128° (пункт I. 12). Положение см. на рис. 23

1–2 — палеомагнитные повороты: 1 — против часовой стрелки, 2 — по часовой стрелке; 3 — ось изгиба; 4 — третичные отложения; 5 — сланцы; 6 — граниты

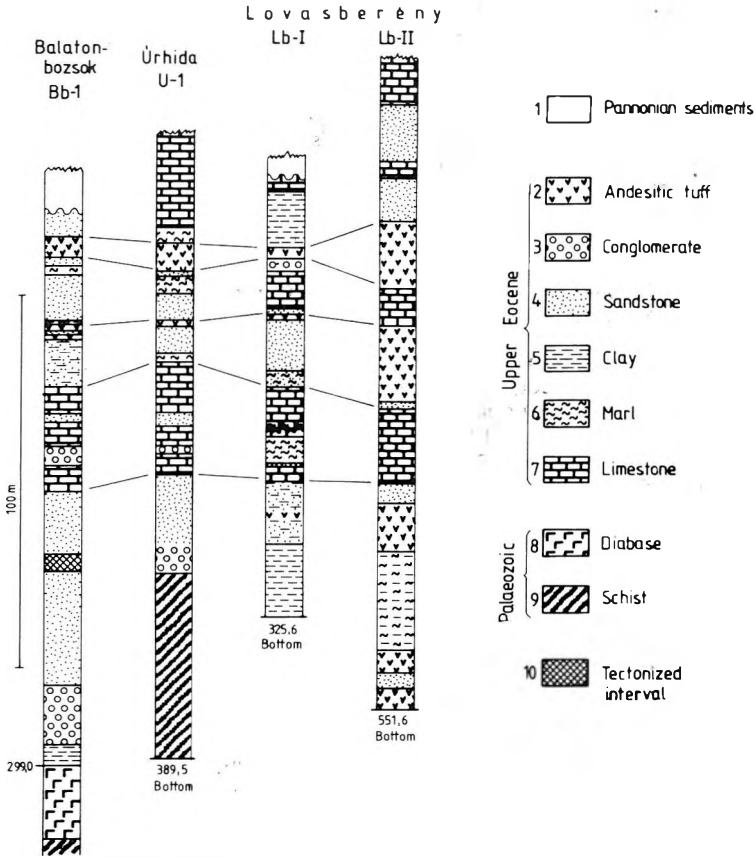


Fig. 25. Correlation of the Eocene sequences in the grabens of the Balatonfő–Velece area after DUDKO [1988b]. For location of the boreholes, see Fig. 23

25. ábra. Eocén rétegsorok párhuzamosítása a Balatonfő–Velece körzetben DUDKO [1988b] nyomán. A fúrásponatok a 23. ábrán láthatók. 1 — pannóniai üledékek; 2–7 — felsőeocén: 2 — andezit tufa, 3 — konglomerátum, 4 — homokkő, 5 — agyag, 6 — márga, 7 — mészkő; 8–9 — paleozoikum: 8 — diabáz, 9 — pala; 10 — tektonikusan igénybevett szakasz

Рис. 25. Корреляция эоценовых разрезов в районе Балатонфő–Велеце, по Дудко [Дудко 1988b]. Положение скважин см. на рис. 23

1 — паннонские отложения; 2–7 — верхний эоцен: 2 — андезитовые туфы, 3 — конгломераты, 4 — песчаники, 5 — глины, 6 — мергели, 7 — известняки; 8–9 — палеозой: 8 — диабазы, 9 — сланцы; 10 — зона тектонических нарушений

area, all of them with prevailing vertical offsets. Newly established faults of the Gerecse–Pilis area, probably with large-scale strike-slip movements, are of nearly W–E direction. So, both the old (Middle Cretaceous) and young (Tertiary) structures have been put in a new light, and this requires a new synthesis of the facts revealed.

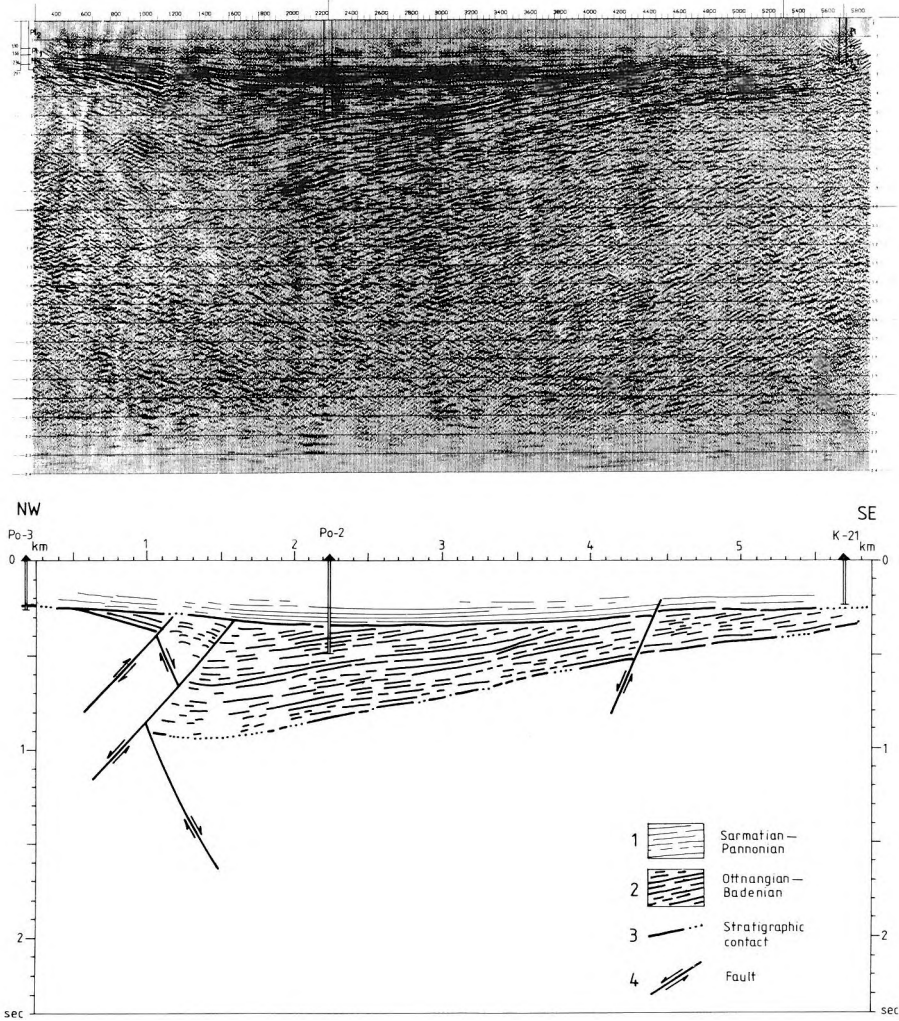


Fig. 26. Geological section across the Polgárdi depression. For location, see Fig. 23

26. ábra. A Polgárdi-medence földtani szelvénye. Helyzetét l. a 23. ábrán

A) Migrált reflexiós szeizmikus szelvény, MAJKUTH [1985] nyomán

B) Földtani értelmezés, DUDKO [1988b] nyomán, módosítva és kiegészítve.

1 — szarmata–pannóniai; 2 — ottngangi–bádeni; 3 — sztratigráfiai határ; 4 — törés

Рис. 26. Геологический разрез Польгардинской впадины. Положение см. на рис. 23

A) Сейсмический профиль МОВ с миграцией, по Майкуту [Майкутн 1985]

B) Геологическая интерпретация, по Дудко [Дудко 1988b], с изменениями и дополнениями

1 — сарматский и паннонский яруса; 2 — оттнангский и баденский яруса; 3 — стратиграфический контакт; 4 — разлом

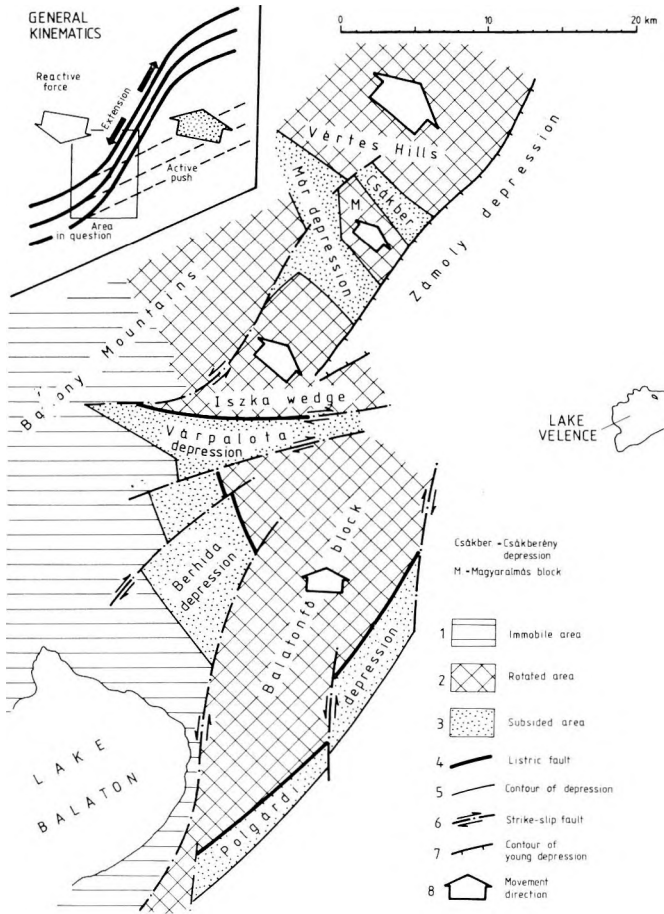


Fig. 27. Movement pattern and subsidence processes connected with the Vértés rotation in the Balatonfő area (see also Figs. 13 and 16). For location, see Fig. 23

27. ábra. A Balatonfő mozgásai és süllyedései a Vértés elfordulásával kapcsolatban (l. még a 13. és 16. ábrát). Helyzetét l. a 23. ábrán. 1 — mozdulatlan terület; 2 — elfordult terület; 3 — lesüllyedt terület; 4 — lisztikus vető; 5 — süllyedékhatar; 6 — eltolódás; 7 — fiatal süllyedék határa; 8 — mozgásirány

Рис. 27. Смещения и опускания в районе Балатонфё в связи с поворотом Вертешских гор (см. также рис. 13 и 16). Положение см. на рис. 23

1 — неподвижная область; 2 — повернутая область; 3 — опущенная область; 4 — листрический сброс; 5 — контур впадины; 6 — сдвиг; 7 — контур молодой впадины; 8 — направление смещения

3. Synthesis of data

On the basis of the selection and primary interpretation of data two kinds of syntheses will be carried out: (i) construction of a static picture, i.e. of a geological map, and (ii) elaboration of a dynamic picture, i.e. estimation of the main kinematic events and of their succession. Based on these two kinds of synthesis we will restore the situation before each main kinematic event. The results of this kinematic modelling are expected to influence the geological map.

3.1. The geological map

In constructing the geological map we used the most recent materials (see *Table II*) and as many drilling data as possible. Our working scale was 1:200,000 but the publication scale is 1:500,000; this does not allow us to display the boreholes. Our map has been constructed for the area with exposed pre-Miocene formations and with a comparatively dense network of boreholes. Except for the southwest where the western Bakony Mts. have been omitted we stopped constructing the map in the areas with insufficient drilling data. Furthermore, we have omitted all formations above the first disconformity (i.e. beginning with the Aptian, see Fig. 2) and displayed first of all the old, Middle Cretaceous, fold-thrust structure dismembered by young, Tertiary faults. In tracing these faults, we have taken into account the arrangement and the shape of the exposures of pre-Cenozoic complexes, furthermore, the topography of the earth's surface and of the pre-Cenozoic basement and, finally, the arrangement and the thickness variations of Eocene (Fig. 6), Oligocene (Fig. 7) and Miocene (Fig. 8) formations.

In the Bakony Mts. and Balaton Highlands, which are much better exposed and much better studied than other areas, we constructed a new picture of the fault network in order to display the real character of the structure. In all other areas we neglected as many transversal faults as possible because of uncertainties in their mapping. Hence, the geological map is a simplified reflection of existing structures which are probably of the same character as in the west but cannot be displayed in the same way because of insufficient data.

On the subject of the Vértes Hills, our map is a simplified version of previous maps. In a tectonic sense, the only principal problem arises with the continuation of the double-sliced structure of the Balaton Highlands ('Litér thrust') in the Vértes Hills area. As for the Gerecse Hills, Pilis Mts. and Buda Hills our map gives a completely new interpretation of available data. Our map for the Velence-Balatonfő area is a developed version of that recently constructed [DUDKO et al. 1988].

The most problematic is the area situated within the Vértes-Gerecse-Pilis-Buda arc. On the basis of the arrangement of the Eocene sediments (Fig. 6), the Vértessomló fault seems to be continuously traceable into the Nagykovácsi fault (Fig. 28A). Consequently, the two ends of the same fault exhibit strike-slip displacements of opposite sense: sinistral in the west (Vértessomló) and dextral in the east (Nagykovácsi). This fact necessitates the assumption of a new tectonic phenomenon which compensates the difference between the offsets, i.e. 20 km. Although there are various ways of solving this problem (Fig. 28B), the most convenient is the assumption of a 20 km dextral displacement along a SW-NE striking fault located

TRANSDANUBIAN RANGE

CSÁSZÁR et al.	1978	1:100,000		
KORPÁS	1981	1:200,000		
<i>BAKONY</i>				
CSÁSZÁR et al.	1985	1: 50,000		
FRANYÓ	1968	1:200,000		
RAINCSÁK	1980	1: 50,000		
SZENTES	1969	1:200,000		
SZENTES and RÓNAI	1966	1:200,000	+	Vértes
<i>VÉRTES</i>				
JASKÓ	1939	1: 80,000	+	Gerecse
SÖLYOM	1953	1: 50,000	+	Gerecse
SZENTES and BÓJTÓS-VARRÓK	1964	1:200,000	+	Gerecse-Pilis-Buda
SZENTES and RÓNAI	1966	1:200,000	+	Bakony
<i>GERECSE</i>				
FÜLÖP	1958	1: 50,000		
GIDAI et al.	1980	1: 25,000	+	Pilis
JASKÓ	1939	1: 80,000	+	Vértes
JASKÓ	1943	1:150,000	+	Pilis-Buda
JASKÓ	1957b	1: 38,000	+	Pilis
JASKÓ	1957c	1: 33,000		
ORAVECZ	1961	1:140,000	+	Pilis-Buda
SÖLYOM	1953	1: 50,000	+	Vértes
SZENTES and BÓJTÓS-VARRÓK	1964	1:200,000	+	Vértes-Pilis-Buda
SZABÓ et al.	1982	1: 25,000		
<i>PILIS</i>				
BALOGH	1961	1: 10,000		
FERENCZ	1953	1: 20,000		
GIDAI et al.	1980	1: 25,000	+	Gerecse
HEGEDŰS	1951	1: 33,000		
JÁMBOR et al.	1966	1:200,000	+	Buda
JASKÓ	1943	1:150,000	+	Gerecse-Buda
JASKÓ	1957a	1: 3,800		
JASKÓ	1957b	1: 38,000	+	Gerecse
ORAVECZ	1961	1:140,000	+	Gerecse-Buda
SIKABONYI	1952	1: 60,000		
SZENTES	1958	1: 50,000	+	Buda
SZENTES and BÓJTÓS-VARRÓK	1964	1:200,000	+	Vértes-Gerecse-Buda
WEIN	1977	1: 25,000	+	Buda
<i>BUDA</i>				
JÁMBOR et al.	1966	1:200,000	+	Pilis
JASKÓ	1943	1:150,000	+	Gerecse-Pilis
ORAVECZ	1961	1:140,000	+	Gerecse-Pilis
SZENTES	1958	1: 50,000	+	Pilis
SZENTES and BÓJTÓS-VARRÓK	1964	1:200,000	+	Vértes-Gerecse-Pilis
WEIN	1977	1: 25,000	+	Pilis

Table II. List of materials used in construction of the geological map

II. táblázat. A földtani térkép szerkesztéséhez felhasznált anyagok jegyzéke

Таблица II. Список материалов, использованных при составлении геологической карты

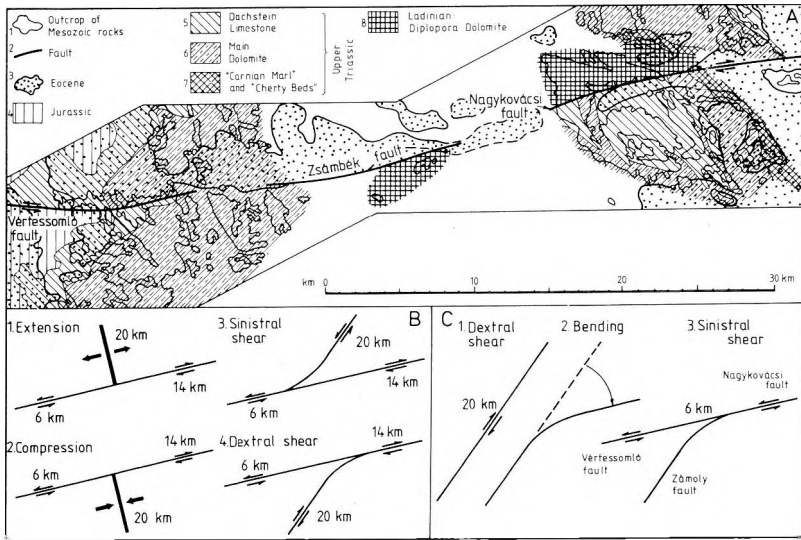


Fig. 28. The Vértessomlyó–Nagykovácsi fault. For location, see Fig. 29
 A) The geological basis. Outcrops taken from JÁMBOR et al. [1966], SZENTES and BOJTOS-VARRÓK [1964]; subsurface geology after CSÁSZÁR et al. [1978], see also Figs. 5, 18 and 22
 B) Some models for interpretation. Offsets taken from the geological map (A)
 C) Origin of the present situation in the frame of the dextral shear model in B.

28. ábra. A Vértessomlyó–Nagykovácsi törés. Helyzetét l. a 29. ábrán.

- A) A földtani alap. Kibúvások: JÁMBOR et al. [1966], SZENTES–BOJTOSNÉ [1964] nyomán; mélyföldtan: CSÁSZÁR et al. [1978] nyomán, l. még az 5., 18. és 22. ábrát. 1 – kibúvás; 2 – törés; 3 – eocén; 4 – júra; 5–7 – felsőtriász: 5 – dachsteini mészkő, 6 – fődolomit, 7 – karni márga és kovás rétegek; 8 – ladinai diplopórási dolomit
- B) Néhány értelmezési modell. Elmozdulások: a földtani térképről (A). 1 – tágulás; 2 – összenyomás; 3 – balos nyírás; 4 – jobbos nyírás.
- C) A mai állapot létrejötte a B jobbos eltolódási modelljének keretében. 1 – jobbos nyírás; 2 – meghajlás; 3 – balos nyírás

Рис. 28. Вертешшомлойско-Надьковачинский разлом. Положение см. на рис. 29

- A) Геологическая основа. Контуры выходов – по Ямбору и др. [JÁMBOR et al. 1966], Сентешу и Бейтешне [SZENTES–BOJTOSNÉ 1964]; глубинная геология – по Часару и др. [CSÁSZÁR et al. 1978], см. также рис. 5, 18 и 22
- 1 – область выходов; 2 – разлом; 3 – зоцен; 4 – юра; 5–7 – верхний триас: 5 – дахштейнский известняк, 6 – главный доломит, 7 – карнийские мергели и битуминозные отложения; 8 – ладинский диплопоровый доломит
- B) Некоторые варианты интерпретации. Смещения – по геологической карте (A)
 1 – растяжение; 2 – сжатие; 3 – левое скальвание; 4 – правое скальвание
- C) Возникновение современной ситуации в рамках варианта с правосторонним смещением в B: 1 – правый сдвиг; 2 – изгиб; 3 – левый сдвиг

somewhere between the Vértes and Velence Hills and turned into the Nagykovácsi fault. The situation obtained can be understood in terms of three successive events (Fig. 28C).

The compensating dextral strike-slip fault is traceable from the northwestern rim of the Buda Hills into the north-western foreland of the Velence Hills. In the area situated between this Zámoly fault and the Buda Hills, drilling data display at least two repetitions of the north-dipping Triassic stratigraphic sequence which can be interpreted in terms of two south-vergent overthrusts (Fig. 29). The more southerly one is correlatable with the continuation of the Litér–Bakonykúti thrust

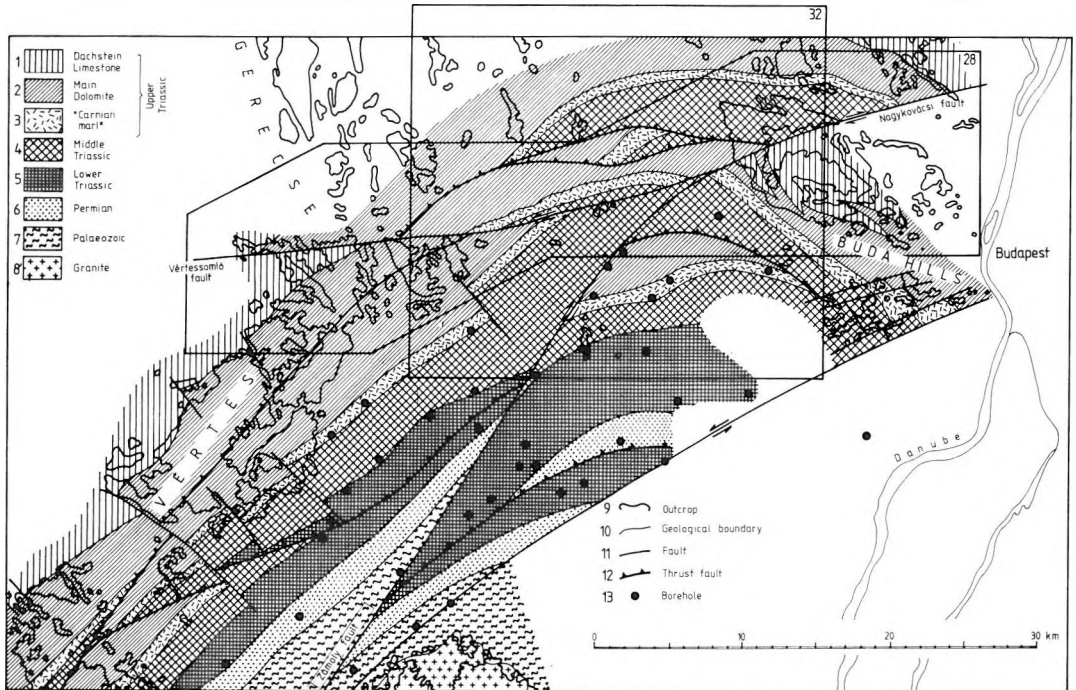


Fig. 29. The geology of the Zámoly fault. Subsurface geology constructed on the basis of drilling data. Geological boundaries corrected by restoring the strike-slip displacements. For location, see Fig. 1. Frames of Figs. 28 and 32 indicated

29. ábra. A Zámolyi-törés geológiája. Az aljzattérkép fúrési adatok alapján készült. A földtani határokat az eltolódások visszaállításával korrigáltuk. Helyzetét 1. az 1. ábrán. Feltüntetjük a 28. és 32. ábra körvonalát. 1–3 – felsőtriász: 1 – dachsteini mészkő, 2 – fődolomit, 3 – karni márga; 4 – középsőtriász; 5 – alsótriász; 6 – perm; 7 – paleozoikum; 8 – gránit; 9 – kibúvás; 10 – képződményhatár; 11 – törés; 12 – feltolódás; 13 – mélyfúrás

Рис. 29. Геология Замойского разлома. Карта фундамента составлена по буровым данным. Геологические границы скорректированы в соответствии с восстановлением сдвигов. Положение см. на рис. 1. Обозначены контуры рис. 28 и 32
1–3 – верхний триас: 1 – дахштейнский известняк, 2 – главный доломит, 3 – карнийские мергели; 4 – средний триас; 5 – нижний триас; 6 – пермь; 7 – палеозой; 8 – граниты; 9 – область выходов; 10 – геологический контакт; 11 – разлом; 12 – взброс; 13 – буровая скважина

while the northern overthrust is expected to continue west of the Nagykovácsi basin, then, in the southern foreland of the Gerecse Hills. That is why here (see Fig. 18A) south-vergent overthrusts are chosen to explain the arrangement of Triassic formations. Continuation of this overthrust is to be expected within the unusually wide strip of the Main Dolomite in the southern Gerecse Hills and in the Vértes Hills. The simplest graphic solution of the problem with the further continuation of the intra-Vértes overthrust is its joining the bend of the Bakonykúti overthrust north of the Iszka block (Fig. 29).

The resulting geological map (Fig. 30) reflects all tectonic features selected in the previous section (Table I). In tracing strike-slip faults and geological contours in the areas covered by young sediments and poorly elucidated by drilling data we use kinematic modelling results (see in section 3.3.)

3.2. Kinematic features

Five kinds of kinematic features have been established: dextral shear, sinistral shear, extension, compression and bending of structures formed previously (Table III).

Some kinematic features of different type are synchronous: (1) Sinistral strike slip along the Bánta line, dextral strike slip along the Inota line, extension in the Várpalota depression and rotation of the Iszka block reflect general bending of structures (see Fig. 27). (2) Extension in the Dorog area was generated by the bending (Fig. 19). The latter may be complementary with that in the Iszka area but not necessarily. Independently of this problem, using the model for the concentric (parallel) folds in a horizontal plane (Fig. 19) we can suppose compression in the core of the bend. Uplift of the Velence Hills area perhaps reflects this compression.

In other cases a certain succession of kinematic features is observable: (1) The history of the Zámoly, Nagykovácsi and Vértessomló faults (see Fig. 28C) outlines

FEATURE	OBJECT	DIRECT AGE	DEDUCED AGE
dextral shear	Telegdi-Roth line	Middle Cretaceous?	-
	Inota line	Early-Middle Miocene	22-14 Ma
	Nagykovácsi fault	Oligocene-Miocene	30-22 Ma
	Zámoly fault	Oligocene-Miocene	30-22 Ma
	Balatonfő-Velence Eocene	Oligocene-Miocene	30-14 Ma
sinistral shear	Bánta line	Early-Middle Miocene	22-14 Ma
	Vértessomló fault	Oligocene-Miocene	14-12 Ma
extension	Várpalota depression	Early-Middle Miocene	22-14 Ma
	Berhida depression	Early-Middle Miocene	22-14 Ma
	Polgárdi depression	Early-Middle Miocene	22-14 Ma
	Mór depression	Miocene	22-14 Ma
	Csákerényi depression	Miocene	22-14 Ma
	Dorog coal basin	Miocene	22-12 Ma
compression	Várpalota depression	Middle Miocene	14-12 Ma
	Polgárdi depression	Middle Miocene	14-12 Ma
	southern Buda Hills	Miocene	22-12 Ma
bending	Zámoly fault	Early-Middle Miocene	22-14 Ma
	Vértes-Iszkahegy rotation	Early-Middle Miocene	22-14 Ma

Note: 'Direct age' inferred from local data (1.2.) and 'deduced age' from the regional analysis (2.2.)

Table III. Kinematic features and their ages

III. táblázat. A kinematikai jelenségek és koruk

Таблица III. Кинематические явления и их возраст

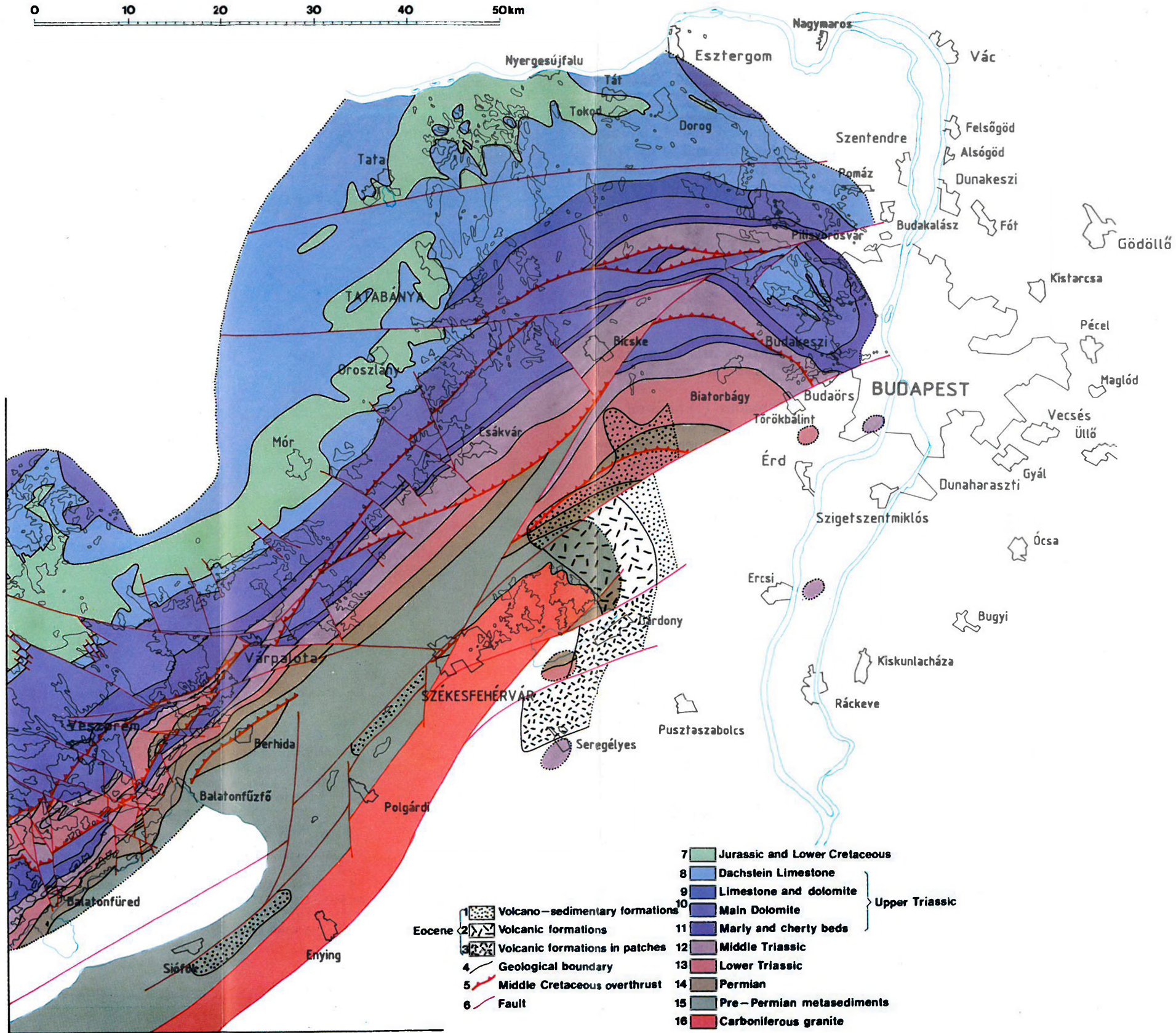
Fig. 30. Geological map of the eastern Transdanubian Range area. I. Present situation. Materials used in the construction listed in Table II

30. ábra. A Dunántúli-középhegység K-i részének földtani térképe. I. Mai állapot. A szerkesztéshez felhasznált anyagokat a II. táblázatban soroltuk fel. 1–3 — eocén: 1 — vulkáni-üledékes összlet, 2 — vulkanitok, 3 — vulkanitok foltokban; 4 — képződményhatár; 5 — középsőkréta feltolódás; 6 — törés; 7 — júra és alsókréta; 8–11 — felsőtriász: 8 — dachsteini mészkő, 9 — mészkő és dolomit, 10 — földolomit, 11 — márgás és kovás rétegek; 12 — középsőtriász; 13 — alsótriász; 14 — perm; 15 — permnél idősebb metaszedimentek; 16 — karbon gránit

Рис. 30. Геологическая карта восточной части Задунайского среднегорья.

I. Современная ситуация. Материалы для составления перечислены в табл. II
1–3 — эоцен: 1 — вулканогенно-осадочный комплекс, 2 — вулканиты в пятнах; 4 — геологический контакт; 5 — среднемеровой взброс; 6 — разлом; 7 — юра и нижний мел; 8–11 — верхний триас: 8 — дахштейнский известняк, 9 — известняки и доломиты, 10 — главный доломит, 11 — мергелистые и кремнистые отложения; 12 — средний триас; 14 — перм; 15 — допермские метаморфизованные отложения; 16 — каменноугольные граниты

0 10 20 30 40 50km



- | | | | |
|---|--------------------------------|----|-------------------------------|
| 1 | Volcano-sedimentary formations | 7 | Jurassic and Lower Cretaceous |
| 2 | Volcanic formations | 8 | Dachstein Limestone |
| 3 | Volcanic formations in patches | 9 | Limestone and dolomite |
| 4 | Geological boundary | 10 | Main Dolomite |
| 5 | Middle Cretaceous overthrust | 11 | Marly and cherty beds |
| 6 | Fault | 12 | Middle Triassic |
| | | 13 | Lower Triassic |
| | | 14 | Permian |
| | | 15 | Pre-Permian metasediments |
| | | 16 | Carboniferous granite |
- } Upper Triassic

the following succession: dextral shear — bending — sinistral shear. (2) The structure and position of the Várpalota and Polgárdi depressions (see Figs. 13, 15, 26 and 27) implies the following succession: bending-related extension — compression.

When using bending as a marker to correlate these two successions we can regard 'dextral shear — bending+extension' as the beginning of the entire succession. In this case the temporal relationships between the sinistral shear and compression at the end of the succession remain unclear. Because of insufficiency in information on relationships between various kinematic features we should take into account the possibility of their unrevealed combinations.

The age of kinematic features cannot, in general, be established in a direct way. We consider the filling of depressions to be the most reliable indicator of the age of the movements. There are two general possibilities (Fig. 31): (A) The subsidence

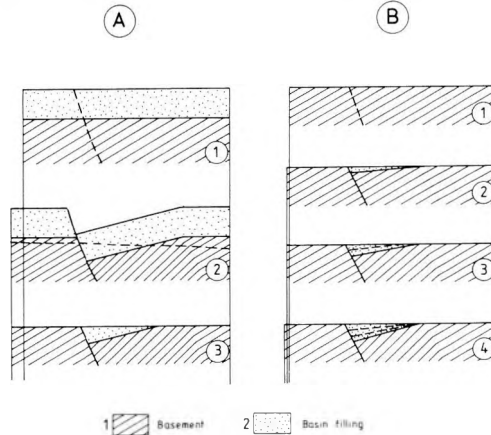


Fig. 31. Depressions as indicators of displacements

A) Subsidence after sedimentation

B) Subsidence coeval with sedimentation

Numeration = successive events; in A: 1 — initial situation after sedimentation, 2 — situation after subsidence, 3 — situation after erosion; in B: 1 — initial situation before sedimentation, 2, 3, 4 — successive stages of sedimentation and subsidence. Broken line: in A.1 and B.1 — future normal fault, in A.2 — future erosion surface, in B.3 and B.4 — previous accumulation surface

31. ábra. Süllyedékek mint elmozdulások indikátorai

A) Üledékfelhalmozódás utáni süllyedés

B) Üledékfelhalmozódással egyidejű süllyedés

Sorszámozás = egymásutáni események; az A-n: 1 — kiindulási állapot az üledékfelhalmozódás után, 2 — besüllyedés utáni állapot, 3 — lepusztulás utáni állapot; a B-n: 1 — kiindulási állapot az üledékfelhalmozódás előtt, 2, 3, 4 — a süllyedés és üledékfelhalmozódás egymás után következő szakaszai. Szaggatott vonal: az A.1-en és B.1-en — leendő vetődés, az A.2-n — leendő lepusztulási felszín, a B.3-on és B.4-en — korábbi felhalmozódási térszín. 1 — aljzat; 2 — medenceüledék

Рис. 31. Впадины в качестве индикаторов смещений

A) Опускания после осадконакопления

B) Опускания одновременно с осадконакоплением

Нумерация — последовательные события; в А: 1 — исходная ситуация после накопления осадков, 2 — ситуация после опусканий, 3 — ситуация после денудации; в В: 1 — исходная ситуация перед накоплением осадков, 2, 3, 4 — последовательные стадии опусканий и осадконакопления. Прерывистая линия: в А.1 и В.1 — будущий сброс, в А.2 — будущая денудационная поверхность в В.3 и В.4 — прежняя аккумуляционная поверхность

1 — фундамент; 2 — отложения впадин

took place after the sedimentation, and the filling is the result of the preservation of sediments during the later erosion. In this case the palaeogeography recorded in sediments is independent of the shape of the depression. (B) The subsidence was accompanied by sedimentation, and the filling arose synchronously. In this case the facies and thickness arrangement is controlled by the shape of the depression. Keeping in mind the necessity of distinguishing between these alternatives we start analysis with the youngest depressions and then pass over to older and older.

The *Budajenő depression* clearly postdates both dextral and sinistral displacements (Fig. 32). Strike-slip faults are not reflected in its isoline pattern while the same faults are recognizable east and west of the Budajenő depression. Its stratigraphic sequence comprises Oligocene, Miocene and Pliocene sediments. Oligocene beds are certainly older than the subsidence [KORPÁS 1981] while Middle Miocene to Pliocene (Sarmatian–Pannonian) sediments are synchronous with it [JASKÓ 1943]. There are no data on the Middle Miocene (Badenian) palaeogeographic pattern of the Budajenő depression but it is clear that strike-slip displacements ended in the Miocene.

The *Várpalota*, *Berhida* and *Polgárdi depressions* have been related to the Vértes rotation (Fig. 27). In their stratigraphic sequences the subsidence is recorded in Lower (Ottungian) and Middle (Karpethian to Badenian) Miocene facies pattern; accordingly, these basins are of synchronous type (see Fig. 31B), i.e. the Lower and

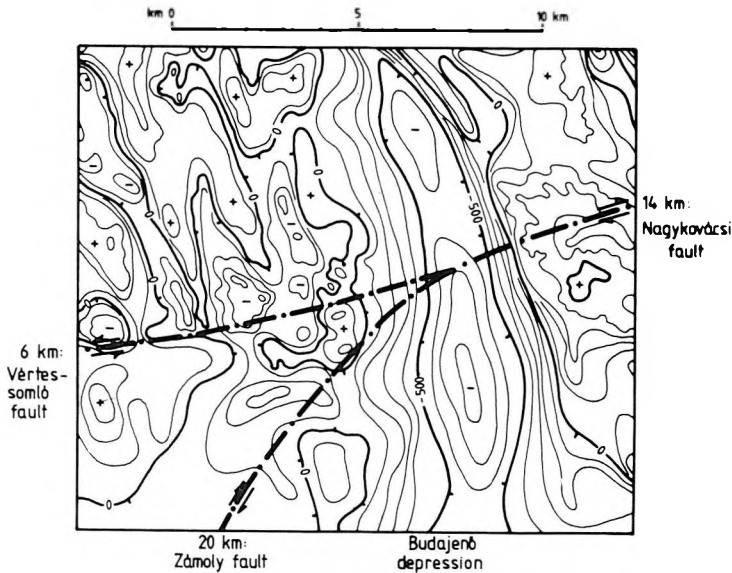


Fig. 32. The Budajenő depression presented in isolines of the topography of the pre-Cenozoic basement. Fragment of CSÁSZÁR et al.'s [1978] map. For location, see Fig. 29

32. ábra. A Budajenői-medence a kainozoikumnál idősebb képződmények domborzatában. CSÁSZÁR et al. [1978] térképének részlete. (Helyzetét l. a 29. ábrán)

Рис. 32. Будаёнёйская впадина в рельефе поверхности докайнозойских образований. Фрагмент карты Часара и др. [CSÁSZÁR et al. 1978]. Положение см. на рис. 29

Middle Miocene beds accumulated during the subsidence. In the Late Badenian (?) and Early Sarmatian a compressional event took place in all three depressions in question probably indicating a change in the kinematics. Upper Sarmatian and Pannonian sediments clearly postdate this compression (see Fig. 15A). Consequently, the Vértes rotation, i.e. the bending, could have taken place in the Early–Middle Miocene and ended before the Early Sarmatian (Late Badenian?).

The *Mór* and *Csákberény* depressions may also be related to the extension that took place during the Vértes rotation (see Fig. 27). Their filling comprises Eocene and Oligocene sediments with no record of the present shape of the depression. Consequently, these depressions are of subsequent type (see Fig. 31A), and the only statement concerning the age of the basin forming is that the subsidence took place after the Oligocene.

The *Palaeogene depressions of the Gerecse area* probably reflect further bending of Mesozoic structures (see Fig. 19). It is an old question whether they are of subsequent or synchronous type; recently, however, more and more scientists accept the idea of their subsequent origin [KORPÁS 1981; KÁZMÉR 1984]. Accordingly, the secondary bending could have taken place in the Miocene (latest Oligocene?).

The *Eocene formations of the Balatonfő–Velenca area* were affected by dextral strike slips (Fig. 33), and the basins are most probably of subsequent type (see Fig. 24 and note constant thicknesses of correlated sequences in random borehole columns).

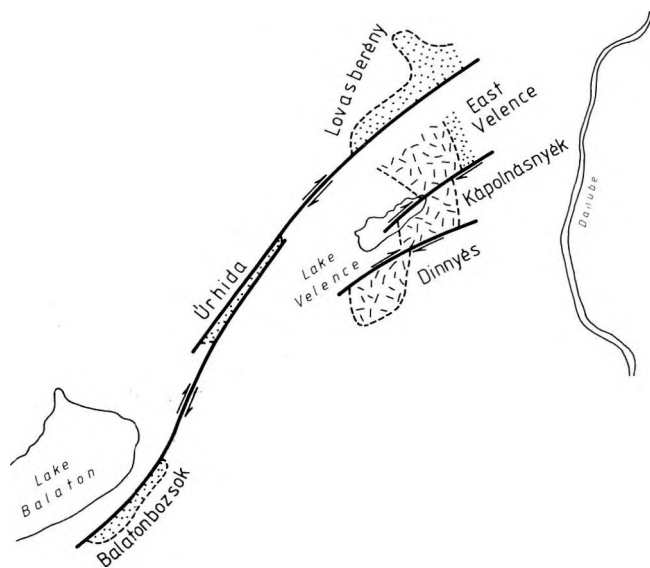


Fig. 33. Dextral shear recorded in the arrangement of the Eocene depressions in the Balatonfő–Velenca area. Simplified from DUDKO'S [1988b] map

33. ábra. Jobbos eltolódás tükröződése a Balatonfő–Velenca körzet eocén medencéinek elrendeződésében. DUDKO [1988b] térképe nyomán, egyszerűsítve

Рис. 33. Отражение правых сдвигов в размещении эоценовых впадин района Балатонфő–Веленце. По карте Лудко [Дудко 1988b] с упрощениями

From these data, it can be concluded that *compression* took place in the Late Badenian (?) to Early Sarmatian (appr. 14–12 Ma B.P.) while *bending* took place in the Early–Middle Miocene (appr. 22–14 Ma B.P.). Judging from its lower and upper age limits (lower = Eocene formations, see Figs. 23 and 33; upper = bending, see Fig. 28), *dextral displacements* seem to have occurred in the Oligocene (and in the earliest Miocene?). Lower and upper age limits for the *sinistral shear* (lower = bending, see Fig. 28; upper = the Budajenő depression, see Fig. 32) put it in the same time span as the compression in question, i.e. these features were nearly synchronous. Consequently, at least three kinematic events can be distinguished: dextral shear, bending and sinistral shear + compression. Based on the succession and age of principal kinematic events we pass over to the modelling of former situations.

3.3. Kinematic modelling

The aim of modelling is to restore situations before each of three kinematic events. The restoration results in transformed geological maps. Since the amount of erosion during the time spans modelled cannot accurately be determined there is no other way than extrapolating the present erosion level into the past. In other words, all transformed geological maps display the present surface, and this obviously results in contouring errors. Errors in areas covered by Palaeogene sediments are due solely to insufficiency in data. Areas without Palaeogene sediments where errors due to erosion may appear are of various types. In the Buda Hills and Pilis Mts. Palaeogene sediments in spots are wide-spread even at high altitudes demonstrating that the structural pattern at the base of the Palaeogene almost equals that in present geological maps. A similar situation can be assumed for the Gerecse and even the Vértes Hills. Notable erosional errors may appear in areas inside the Vértes–Gerecse–Pilis–Buda arc where the contouring is least exact owing to insufficiency in drilling data. We therefore hope that the use of the erosion surface of pre-Cenozoic formations in its present form will not result in additional errors.

In the first step, the situation before the sinistral shear and compression will be restored. It may be related to the Middle Miocene (appr. 14 Ma B.P.).

The only fault with a confirmed and considerable sinistral offset is the Vértessomló line along the Vértes/Gerecse boundary (see Fig. 8). On the basis of the arrangement of Eocene sediments it is traceable far to the east (see Fig. 28). A similar configuration of Eocene sediments (see Fig. 6) is observable some 15 km to the north. In view of this analogy as well as of the pre-Cenozoic outcrop configuration (Fig. 30) and of the pre-Cenozoic basement topography another strike-slip fault is located along this northern strip. It follows the southern boundary of the Dorog Eocene and, further west, is expected south of Tata. The eastern continuation can be assumed towards Szentendre. The general arrangement of Eocene sediments in this area arose before Oligocene although the strike slips along controlling faults may have occurred later. No other faults of this type required in the model (see Fig. 17) are traceable. It is possible that north of the Vértessomló–Zsámbék fault one or more strike slips of the same direction are present but because of the lack in tracing criteria they are not displayed on the map.

While the offset along the Vértessomló fault is directly determinable from the map there is no basis for exact determination of the offset along the northern fault. We consider the difference in position of the western limit of the Kiscellian Clay (Early–Middle Oligocene) north and south of the line (Fig. 7) to reflect a post-Oligocene sinistral strike slip of about 10 km along the line and we accept this value in the restoration.

Compression is directly recorded in the overthrusts along the northern rim of the Várpalota and along the NW rim of the Polgárdi depressions. A zone of Badenian compression has recently been established along Lake Balaton and further on towards the northeast [BALLA et al. 1988]. The magnitude of the compression, however, cannot be estimated although it could hardly be significant in view of the absence of highly disturbed Miocene beds in the whole area.

Taking into account all the above considerations we can only regard the situation restored (Fig. 34) as a first approximation. In the reconstruction the Bakony Mts. together with the geographical elements have been kept immobile, and all restorations have been carried out relative to them. No constraints exist for moving the northernmost unit towards the east during the restoration. Its position has been chosen on the basis of general alignment (i) of Jurassic–Cretaceous strips in accordance with the model (Fig. 17) and (ii) of the western boundaries of the Kiscellian (Middle Oligocene) clays [see in KÖRÖSI 1981] north and south of the fault. There is no information on the position of the Velence–Balaton granite belt before displacements, that is why it is not shifted. The uncertainties adversely affect further reconstructions.

In the second step the situation before the bending will be restored. It may be related to Early Miocene (appr. 22 Ma B.P.). Based on the S-shape of the structures two bends should be straightened: the 'lower' in the southwest and the 'upper' in the northeast.

The *lower bend* is directly reflected by the deviation of the granite belt along Lake Balaton towards the northeast around the eastern end of the lake. As the Vértessomló rotation reflects the same bend (see Fig. 27) the straightening of the lower bend should be extended from the Bakony–Vértessomló junction (see Figs. 13B and 16B) to the Balatonföld–Velence area on the basis of the general movement pattern (Fig. 27).

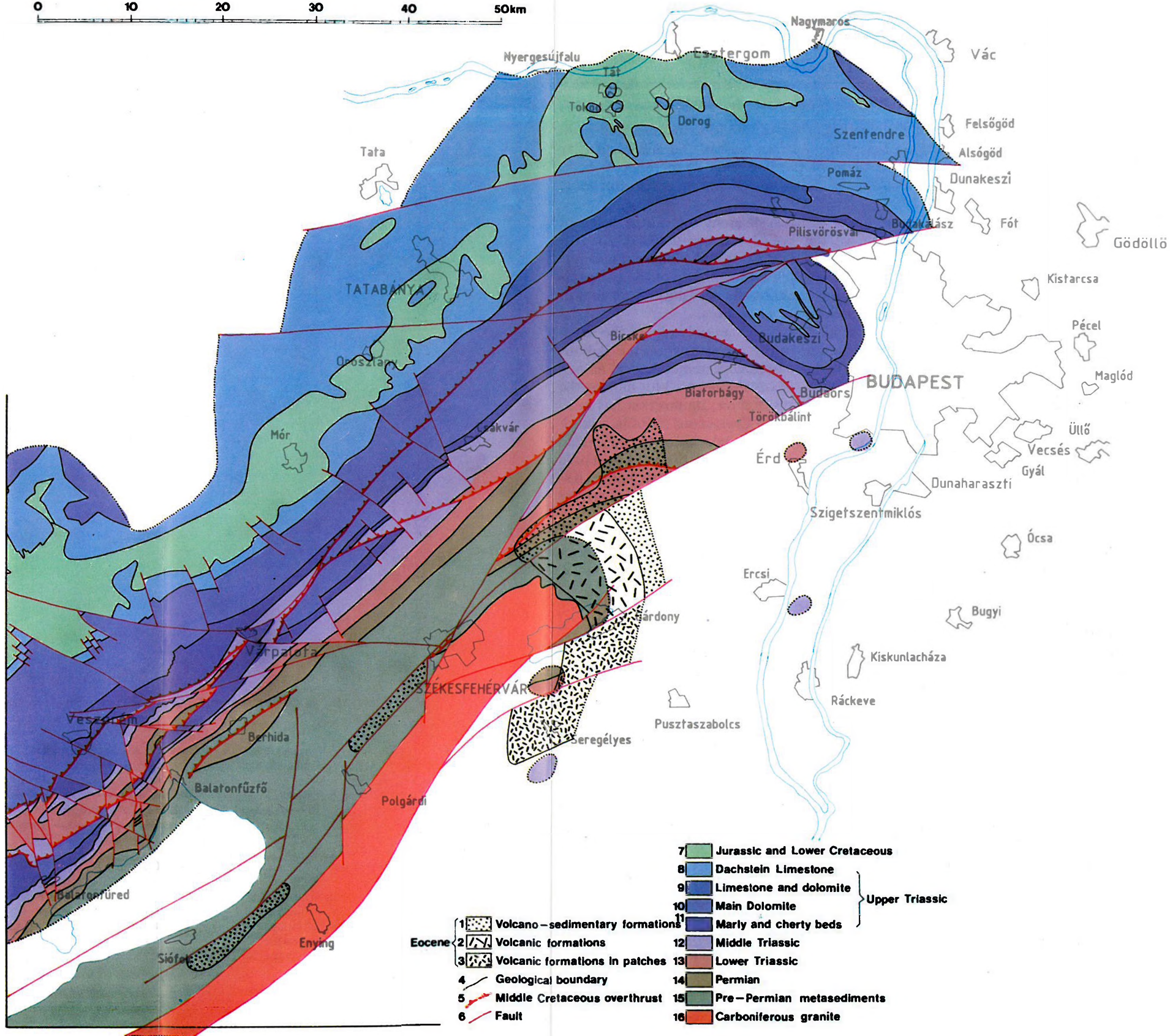
The *upper bend* is clearly expressed in the Zámoly–Nagykovácsi arc (see Fig. 28) and is suspected in both the configuration of the ending of the granite belt in the Velence Hills (see Fig. 23) and in the Eocene palaeomagnetic directions (see Fig. 24). The Zámoly line approaches the granite belt in the Velence area and, straightening the granite belt, on the one hand and the Bakony–Vértessomló and Zámoly–Nagykovácsi bends on the other, separately results in a gap between them which wedges out towards the southwest. A corresponding compression is improbable in the Miocene, therefore, additional deformations or displacements are needed to close the gap.

In this relation it is of importance that the Velence granite body has only suffered slight arching since the Eocene and it has not rotated significantly relative to the Bakony Mts. — as can be concluded from palaeomagnetic data [MÁRTON E. 1986, MÁRTON E. and MÁRTON P. 1983]. Accordingly, the Velence granite together with the Buda Hills and areas situated between them on the southeastern flank of

Fig. 34. Geological map of the eastern Transdanubian Range area. II. Situation before the sinistral shear. Restored by kinematic modelling

34. ábra. A Dunántúli-középhegység K-i részének földtani térképe. II. Balos nyírás előtti állapot. Kinematikai modellezéssel szerkesztve. 1–3 — eocén: 1 — vulkáni-üledékes összlet, 2 — vulkanitok, 3 — vulkanitok foltokban; 4 — képződményhatár; 5 — középsőkréta feltolódás; 6 — törés; 7 — júra és alsókréta; 8–11 — felsőtriász: 8 — dachsteini mészkő, 9 — mészkő és dolomit, 10 — földolomit, 11 — márgás és kovás rétegek; 12 — középsőtriász; 13 — alsótriász; 14 — perm; 15 — permnél idősebb metaszedimentek; 16 — karbon gránit.

Рис. 34. Геологическая карта восточной части Задунайского среднегорья. II. Ситуация до левых сдвигов. Составлена путем кинематического моделирования 1–3 — эоцен: 1 — вулканогенно-осадочный комплекс, 2 — вулканиты, 3 — вулканиты в пятнах; 4 — геологическая граница; 5 — среднемиоценовый взброс; 6 — разлом; 7 — юра и нижний мел; 8–11 — верхний триас: 8 — дахштейнский известняк, 9 — известняки и доломиты, 10 — главный доломит, 11 — мергелистые и кремнистые отложения; 12 — средний триас; 13 — нижний триас; 14 — пермь; 15 — допермские метаморфизованные отложения; 16 — каменноугольные граниты



the Zámoly fault can be regarded as a tectonic wedge which moved as a rigid body during the bending. Lower Triassic beds drilled within the granite belt on the western shore of the Lake Velence may mark a west-east directed southern boundary of the wedge. Because of lack of data on the internal structure of the granite belt south of this boundary the behaviour of this belt can only be described in terms of ductile deformation although the real process obviously involved relative displacements of rigid blocks along faults.

In modelling the situation before the bending of the granite belt, three constraints have been taken into account. First, the southeastern boundary of the granite belt has been located in the straight continuation of the Balaton section of the same boundary; second, it has been accepted that the stretching of the granite belt took place along its northwestern boundary which acted as the southwestern continuation of the Zámoly fault, and, third, the Velence granite has been kept with no rotation on the head of the granite body. Restoration of the shape of the granite body resulted in nearly north-south oriented eastern boundary of the granites and in the elimination of dextral offsets between the Lovasberény and East Velence as well as between the East Velence and Kápolnásnyék Eocene (see Fig. 33). These dextral strike slips appeared to be connected with the removal of the Velence-Buda wedge towards the northeast along the Zámoly line which acted as a sinistral strike slip on the other side of the wedge. An analogous process can be supposed along the fault between the Kápolnásnyék and Dinnyés Eocene.

Straightening of the Zámoly-Nagykovácsi fault (see Fig. 28) requires compensation of the extension in the areas north of the Vértessomló-Zsámbék line and especially in the Dorog area. This extension is well recorded in the thickness arrangement of the Oligocene sediments (see Fig. 7). Equivalent compression in the core of the bend (see Fig. 19), i.e. in the Velence-Balatonfő area, may serve as an explanation for the total absence of Palaeogene sediments in the southeastern foreground of the Bakony Mts. and Vértes Hills (see Figs. 6 and 7) due to uplift and erosion in the Early Miocene. On the basis of above considerations the synthetic map (Fig. 35) has been constructed.

In the third step, the situation before the dextral displacements will be restored. It can be related to the Early Oligocene (appr. 30Ma B.P.). The alignment of Triassic formations across the Nagykovácsi fault was the basis of the restoration. Because of various deformations required in the previous steps of modelling significant changes in tracing the assumed geological boundaries have been made, always in harmony with available drilling and superficial data. That is why contours in some places differ from those in partial studies (Figs. 13, 16, 18, 22, 27, 28 and 29).

In the situation restored there is no alignment between the axes of the Buda and Pilis synclines. This may be due to the existence of an unrevealed strike slip of NW-SE direction along the SW border of the northwestern Pilis Mts. Because of the absence of any convincing information on the structure of the surrounding basinal areas we see no possibilities for tracing this fault.

It is worth mentioning that the simple rigid restoration of the Eocene volcano-sedimentary complex of the Balatonfő-Velence area (Fig. 36A) was carried out in the previous step of modelling. Taking into account the possibility of internal shear for the areas south of Lake Velence (Fig. 36B) and the uncertainties in determining the primary arrangement of the Balatonbozsok, Urhida and Lovasberény depres-

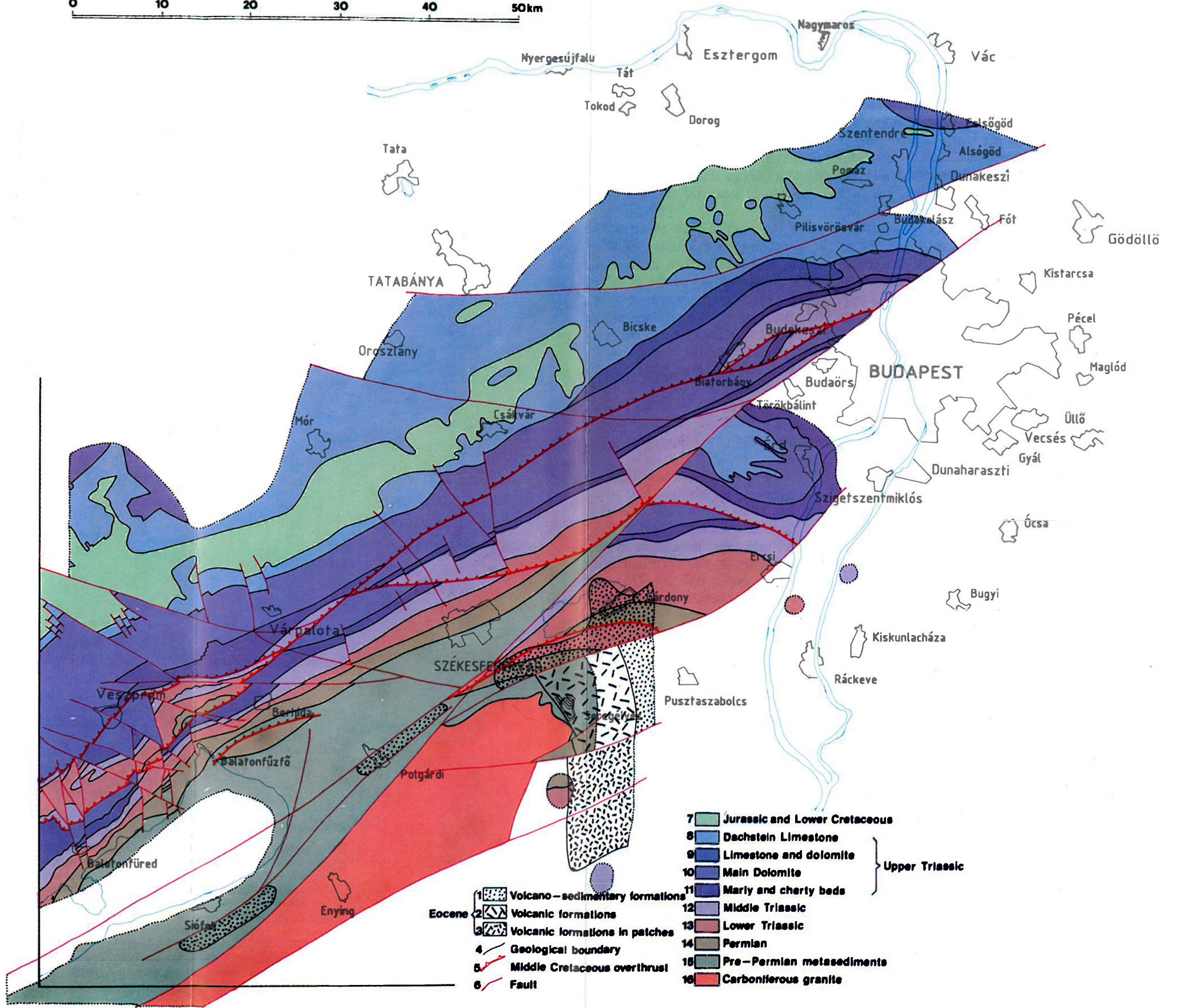
Fig. 35. Geological map of the eastern Transdanubian Range area. III. Situation before the bending. Restored by kinematic modelling

35. ábra. A Dunántúli-középhegység K-i részének földtani térképe. III. Meghajlás előtti állapot. Kinematikai modellezéssel szerkesztve

1–3 — eocén: 1 — vulkáni-üledékes öszlet, 2 — vulkanitok, 3 — vulkanitok foltokban;
4 — képződményhatár; 5 — középsőkréta feltolódás; 6 — törés; 7 — júra és alsókréta; 8–11 — felső-triász: 8 — dachsteini mészkő, 9 — mészkő és dolomit, 10 — fődolomit, 11 — márgás és kovás rétegek;
12 — középsőtriász; 13 — alsótriász; 14 — perm; 15 — permnél idősebb metaszedimentek;
16 — karbon gránit

Рис. 35. Геологическая карта восточной части Задунайского среднегорья. III. Ситуация до изгиба. Составлена путем кинематического моделирования

1–3 — эоцен: 1 — вулканогенно-осадочный комплекс, 2 — вулканиты, 3 — вулканиты в пятнах; 4 — геологическая граница; 5 — среднемиоценовый взброс; 6 — разлом; 7 — юра и нижний мел; 8–11 — верхний триас: 8 — дахштейнский известняк, 9 — известняк и доломиты, 10 — главный доломит, 11 — мергелистые и кремнистые отложения; 12 — средний триас; 13 — нижний триас; 14 — пермь; 15 — допермские метаморфизованные отложения; 16 — каменноугольные граниты



sions (Fig. 36C) and of the East-Velence Eocene field (Fig. 36D) we can conclude that no convincing criteria for the correct reconstruction exist. The same is true for the granites. That is why this whole area has been left with no changes in the synthetic map (Fig. 37) and possibilities for its restoration will be discussed in a regional frame.

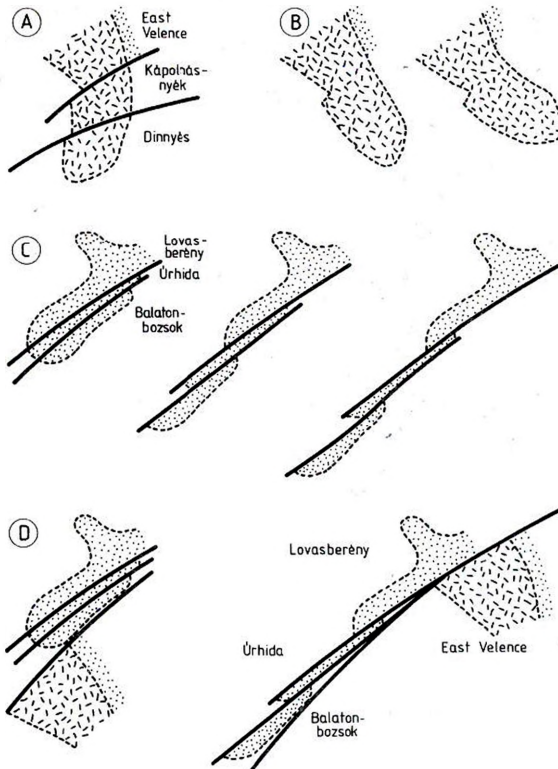


Fig. 36. Versions of the restoration of dextral strike slips in the Balatonfő-Velence area

- A) Rigid restoration of the Eocene volcano-sedimentary formation
- B) Versions of plastic restoration of the Eocene volcano-sedimentary formation
- C) Versions of fitting the Balatonbozsok, Úrhida and Lovasberény depressions
- D) Versions of fitting the depressions (C) and the East-Velence Eocene field

36. ábra. Változatok a Balatonfő-Velence körzet jobbos elmozdulásainak visszaállítására

- A) Az eocén vulkáni-üledékes összlet merev visszaállítására
- B) Változatok az eocén vulkáni-üledékes összlet képlékeny visszaállítására
- C) Változatok a Balatonbozsoki-, Úrhidai- és Lovasberényi-medence illesztésére
- D) Változatok a medencék (C) és a keletvelencei eocén mező illesztésére

Рис. 36. Варианты восстановления правых сдвигов района Балатонфő-Веленце.

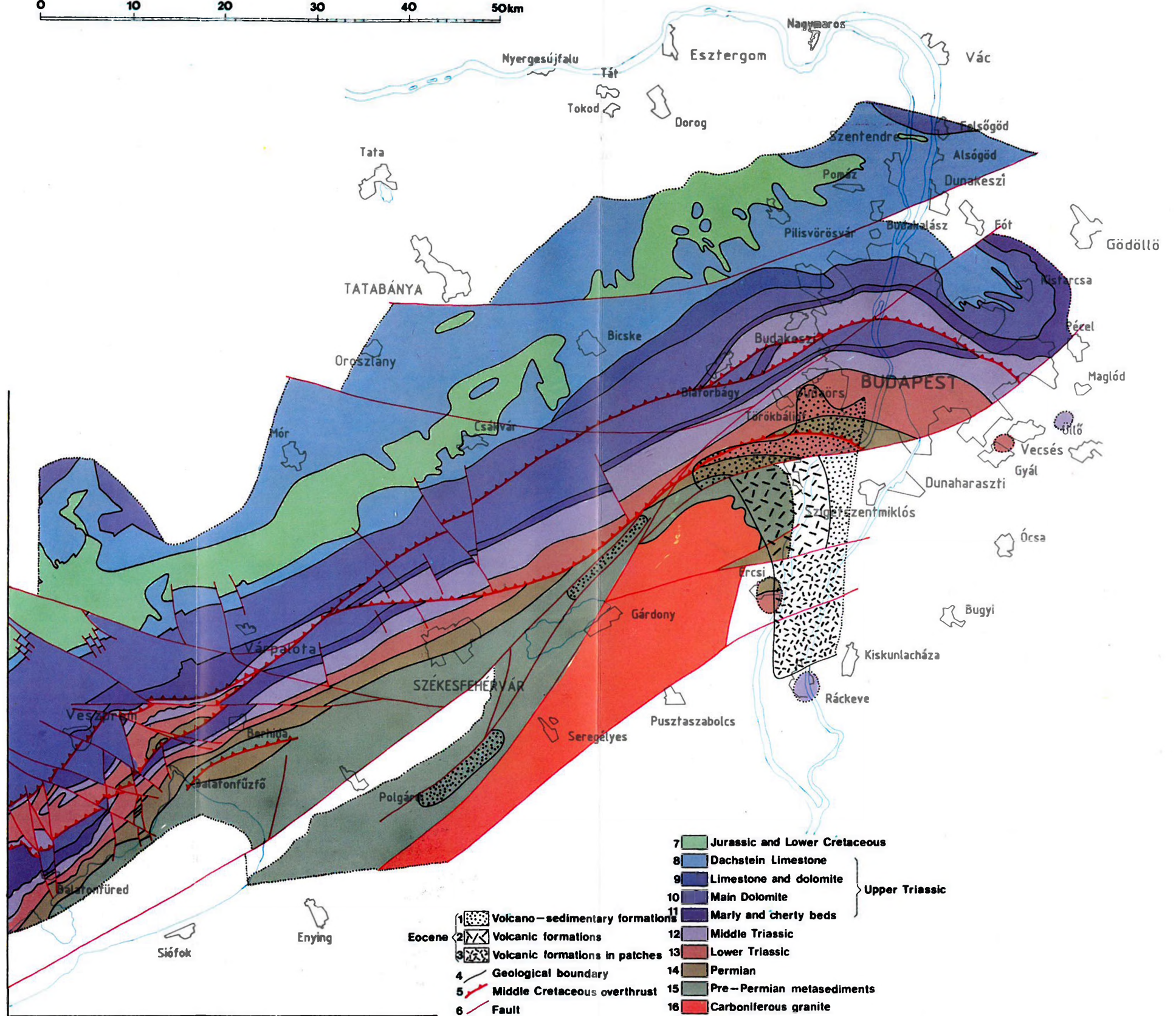
- A) Жесткое восстановление эоценовой вулканогенно-осадочной толщи
- B) Варианты пластичного восстановления эоценовой вулканогенно-осадочной толщи
- C) Варианты стыковки Балатонбожской, Урхидайской и Ловашбереньской впадин
- D) Варианты стыковки впадин (C) и восточновеленцеиского эоценового поля

Fig. 37. Geological map of the eastern Transdanubian Range area. IV. Situation before the dextral shear. Restored by kinematic modelling

37. ábra. A Dunántúli-középhegység K-i részének földtani térképe. IV. Jobbos nyírás előtti állapot. Kinematikai modellezéssel szerkesztve. 1–3—eocén: 1 — vulkáni-üledékes öszlet, 2 — vulkanitok, 3 — vulkanitok foltokban; 4 — képződményhatár; 5 — középsőkréta feltolódás; 6 — törés; 7 — júra és alsókréta; 8–11 — felsőtriász: 8 — dachsteini mészkő, 9 — mészkő és dolomit, 10 — földolomit, 11 — márgás és kovás rétegek; 12 — középsőtriász; 13 — alsótriász; 14 — perm; 15 — permnél idősebb metaszedimentek; 16 — karbon gránit

Рис. 37. Геологическая карта восточной части Задунайского среднегорья. IV. Ситуация до правых сдвигов. Составлена путем кинематического моделирования

1–3 — эоцен: 1 — вулканогенно-осадочный комплекс, 2 — вулканиты, 3 — вулканиты в пятнах; 4 — геологическая граница; 5 — средне меловой взброс; 6 — разлом; 7 — юра и нижний мел; 8–11 — верхний триас: 8 — дахштейнский известняк, 9 — известняки и доломиты, 10 — главный доломит, 11 — мергелистые и кремнистые отложения; 12 — средний триас; 13 — нижний триас; 14 — перм; 15 — допермские метаморфизованные отложения; 16 — каменноугольные граниты



- 1 [Symbol] Volcano-sedimentary formations
- 2 [Symbol] Volcanic formations
- 3 [Symbol] Volcanic formations in patches
- 4 [Symbol] Geological boundary
- 5 [Symbol] Middle Cretaceous overthrust
- 6 [Symbol] Fault

- 7 [Color] Jurassic and Lower Cretaceous
- 8 [Color] Dachstein Limestone
- 9 [Color] Limestone and dolomite
- 10 [Color] Main Dolomite
- 11 [Color] Marly and cherty beds
- 12 [Color] Middle Triassic
- 13 [Color] Lower Triassic
- 14 [Color] Permian
- 15 [Color] Pre-Permian metasediments
- 16 [Color] Carboniferous granite

Upper Triassic

Eocene

4. Correlation with the Oligocene–Miocene kinematics of the Alpine–Carpathian–Pannonian realm

Three stages of the Oligocene–Miocene tectonic history of the Transdanubian Range have been revealed: 1) dextral shear of the southeastern margin in the Oligocene (and Early Miocene?), 2) S-shaped bending of all structures in the area between Lake Balaton and the Danube River in the Early–Middle Miocene, 3) sinistral shear in the Middle Miocene. They can be correlated with kinematic features in the wide surroundings by means of comparison with synchronous events.

4.1. Dextral shear in the Oligocene

The Oligocene is the time of the removal of the Transdanubian Range domain from the Alpine realm [KÁZMÉR and KOVÁCS 1985.]. This removal requires dextral displacement of the Bakony domain relative to the Southern Alps [KÁZMÉR 1984] and serves as a general explanation for the dextral shear of the southeastern margin and foreland of the Transdanubian Range. The question is, however, which is the trace of this displacement. According to KOVÁCS's [1983] and KÁZMÉR's [1984] primary ideas [see also in KÁZMÉR and KOVÁCS 1985, furthermore, in KÁZMÉR 1986] the Balaton line bears the total dextral offset of about 450–500 km. The eastern continuation of this line is, however, ambiguous, and this sole fact is sufficient to create doubts.

The problem of the eastern continuation of the unit removed from the Alpine realm has been left open [KÁZMÉR and KOVÁCS 1985] although it is not less important than the problem of the western end. There are two principal possibilities for the eastern end of the moving unit (*Fig. 38*).

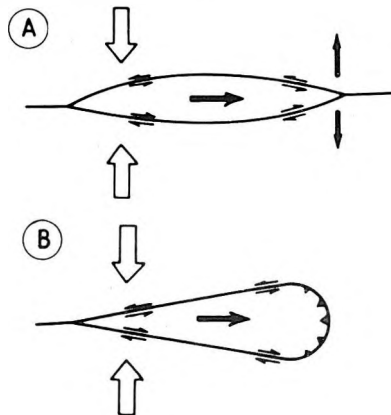


Fig. 38. Models for an escaping domain

38. ábra. Egy kinyomódó egység modelljei

Рис. 38. Модели выжимающегося блока

When regarding the Rába and Balaton lines to be rigid boundaries of the moving unit one can only find the wedge model to be acceptable. East or northeast of the Buda Hills, however, there are no proofs of large-scale (several hundreds of km) Oligocene displacements or of a wedge which progresses towards the east and necessarily suffers deformations along the strike. Hence, the blunt-body model seems to be more probable even in the first approximation.

In this case the convergent boundary in the east can only be located in the Magura zone of the West Carpathians. Since the Pieniny Klippen belt cannot be crossed by any Oligocene kinematic boundary, the Magura convergent boundary is only traceable into the intra-Carpathian area through „gates”: along the Botiza nappes (Maramureş) in the east and through the Vienna basin in the west (Fig. 39A). This means that the southern boundary of the moving unit should be located within the Maramureş–Szolnok flysch belt and the northern boundary should be assumed somewhere in the Alpine/Carpathian junction area (Fig. 39A). Consequently, both the Rába and the Balaton lines are situated inside the moving unit and not on its boundaries.

The problem of the Rába line and of the northern transcurrent boundary has been discussed elsewhere [BALLA 1988b] and is beyond the topic of this work though a discussion of the southern transcurrent boundary would be important as a means of understanding the role of the Balaton line and the structural pattern of the southeastern margin and foreland of the Transdanubian Range.

According to the structural pattern and to the abundant Permian–Mesozoic palaeomagnetic data [MÁRTON E. and MÁRTON P. 1983; MÁRTON E. and ELSTON 1985], in the Bakony Mts. and in the Balaton Highlands there are no significant deformations which could have resulted in relative rotations of different blocks. This whole area can be regarded almost or totally rigid during the Tertiary tectonism, and the total offset of the dextral displacement relative to the Alpine real can be measured between this Bakony–Balaton domain and the Southern Alps. When considering the shape of all domains in the northeastern continuation of the Bakony–Balaton domain (Fig. 39) we can state that all of them have southwestern tails, the same being true for the Bakony–Balaton domain. Based on the general tendencies we assume the Buzsák Permian–Triassic to continue the Seregélyes tail of the Buda domain [BALLA et al. 1988].

We restored the pre-Cenozoic image of the Alpine–Carpathian realm (Fig. 39C) on the basis of Senonian palaeomagnetic directions keeping all domains in their present contours and fixing the DAV line to the Northern Calcareous Alps, the Rába and Balaton lines to the Bakony Mts. and the Pusteria–Gailtal (= Periadriatic = PA) line to the Southern Alps. Between these lines wedge-like gaps (= hatched areas) appeared which reflect a pressing out of the East Alpine/West Carpathian and South Alpine/Middle Transdanubian (= south of the Bakony Mts.) domains. The system of southwestern tails of all North Pannonian domains is possibly related to the pressing out of the Alpine realm accompanied by dextral shear in the Oligocene. In the hypothetical situation restored the formations, now forming the tails, should be gathered into the southern continuations of the corresponding domains.

This conclusion gives the basic idea for the restoration of the southeastern margin and foreland of the Transdanubian Range. This basic idea comprises gathering

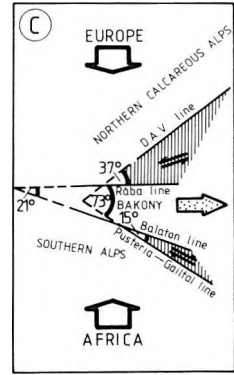
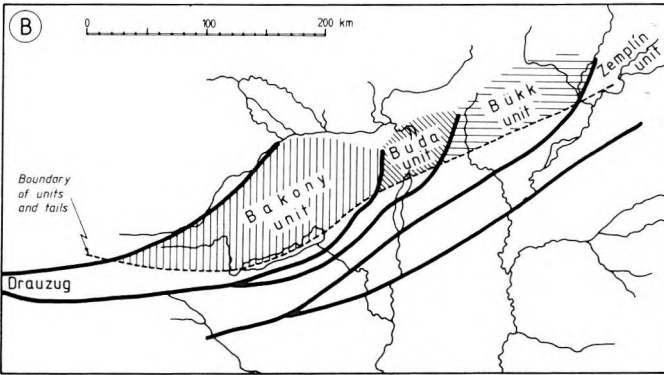
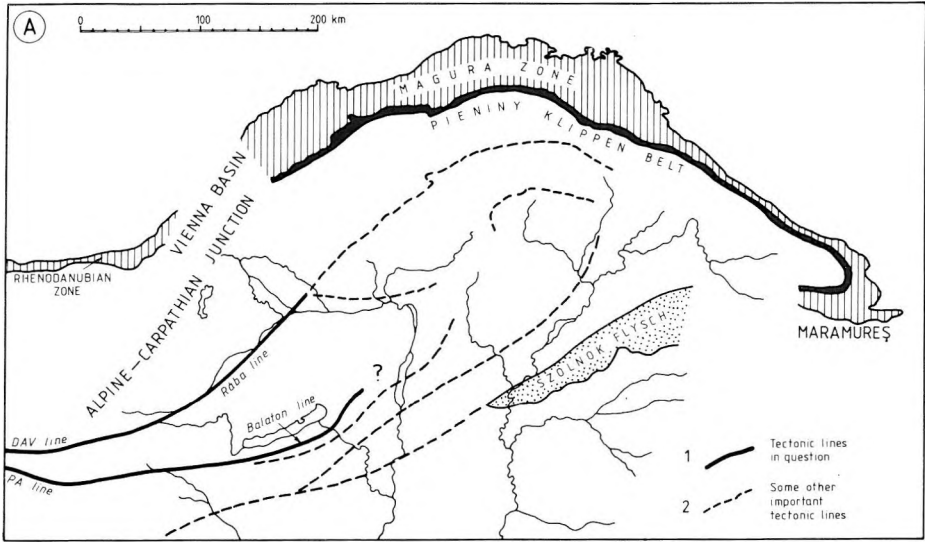


Fig. 39. Kinematics of the blunt-body model

- A) Sketch to illustrate the position of the Pieniny Klippen belt and of the DAV–Rába and Periadriatic (PA) – Balaton lines
- B) The system of southwestern tails
- C) Sketch to illustrate the situation before the removal of the Bakony unit from the Alpine realm, simplified after BALLA [1988a]

39. ábra. A tompatest-modell kinematikája

- A) A Pieniny Szirtöv, valamint a DAV–Rába- és a Periadriai (PA) – Balaton-vonal helyzete (vázlat).
1 — a tárgyalt tektonikai vonalak; 2 — más fontos tektonikai vonalak
- B) A DNY-i nyúlványok rendszere
- C) A Bakonyi-egység alpi területéről való kinyomódását megelőző állapot (vázlat, BALLA [1988a] nyomán, egyszerűsítve)

Рис. 39. Кинематика тупого тела

- A) Положение Пьенинской Утесовой зоны, а также ДАВ–Рабской и Периадриатическо (РА)–Балатонской линий
- B) Система югозападных хвостов
- C) Ситуация до выжатия Баконьской единицы из Альпийской области; схема по Балла [BALLA 1988a], с упрощениями

all granites up to the Buzsák area into a simple body of elliptic shape and all Permian-Mesozoic complexes of the Seregélyes-Buzsák zone into the southeastern continuation of the Buda syncline, i.e. east of the granite body restored (Fig. 40). In the reconstruction Lake Balaton and the Danube River have been kept in rigid connection with the Bakony domain.

Consequently the East Velence pericline [DUDKO 1988a], implying that granites of the Balaton-Velence zone mark the core of an anticline which corresponds to the Bakony-Vértes syncline, probably arose in two distinct deformation stages as follows: 1 — during the clockwise bending of the Pilis-Buda structures relative to the Bakony-Vértes structures in the Middle Cretaceous; 2 — in the course of the dextral shear of the southern margin of the Velence-Buda formations in the Oligocene. Discussion of the problem, that in the Middle Cretaceous the previously formed syncline was bent or the bending occurred synchronously with the folding and thrusting, is beyond the scope of this work. Notwithstanding, the situation restored (Fig. 40) approximately corresponds to that which existed during the Senonian, Palaeocene and Eocene when the Transdanubian Range domain was still inside the Alpine realm, before the removal towards the east but after the Middle

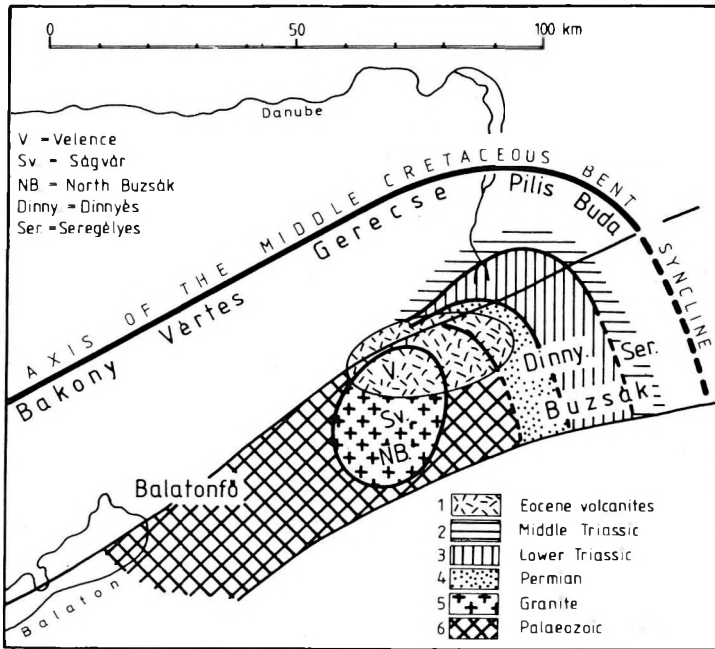


Fig. 40. Sketch of the Velence-Buda area at the Oligocene/Eocene boundary

40. ábra. A Velencei- és a Budai-hegység körzetének vázlata az oligocén/eocén határ környékén.
1 — eocén vulkanitok; 2 — középsőtriász; 3 — alsótriász; 4 — perm; 5 — gránit; 6 — paleozoikum.

Рис. 40. Схема окрестностей Веленцевских и Будаевских гор примерно на границе олигоцена с эоценом
1 — эоценовые вулканиты; 2 — средний триас; 3 — нижний триас; 4 — перм; 5 — граниты; 6 — палеозой

Cretaceous tectonism. The Velence–Dinnyés volcanic formations of Late Eocene (to Early Oligocene?) age primarily formed a west–east elongated area; the present NNE–SSW elongation of this area arose solely because of dextral shear and corresponding clockwise rotation around the Velence granite body in the Oligocene.

It can be supposed that the east-directed motion of the Bakony–Buda unit resulted in the compression along its strike and in an increase of the curvature of the Vértes–Gerecse–Pilis–Buda arc (see Fig. 19) generated in the Middle Cretaceous (see. 2.1.). This process cannot be separated from the later bending of the same type (see in 4.2.) that is why the whole effect has been related to the latter.

4.2. Bending in the Early–Middle Miocene

The Early–Middle Miocene (appr. 22–14 Ma B.P.) is the time of the collision of the South Pannonian domain with the North Pannonian domain and of the anti-clockwise rotation of the North Pannonian domain because of its push by the clockwise rotating South Pannonian domain from the south [BALLA 1985]. The anti-clockwise rotation of the whole North Pannonian domain has been recorded in its palaeomagnetic directions [MÁRTON E. and MÁRTON P. 1983] and in the synchronous folding and thrusting of the Outer West Carpathians [KRS and ROTH 1979; KRS et al. 1979]. The collision and push would serve as a general explanation for the compression during the time span in question. The bending, however, requires something more than a simple compression, viz. transversal sinistral shear (Fig. 41A). Conditions for such a shear existed in the early stages of the collision when the imaginary continuation of what was then the western but is now the northwestern boundary of the South Pannonian domain (Fig. 41B) could have lain somewhere between Lake Balaton and the Danube River being fixed to the Bakony–Balaton area in the situation restored. Compression could have occurred first of all east of this imaginary line (see Fig. 41A). The well-known dislocations of the Buda Palaeogene disappearing towards the northwest, i.e. further from the active compression, may be related to this process although the angular unconformity between the Miocene and Palaeogene has not been ascertained.

West of the line above, viz. south of Lake Balaton, convergence between the North and South Pannonian domains took place from the earliest Miocene, however, its traces have only been established for the Badenian — although earlier Miocene compressive structures are probable in the areas situated somewhat further south [BALLA et al. 1988]. In an eastern direction these structures cease east of the Danube River [BALLA 1988b].

Summarizing, the kinematic model elaborated for the whole Carpatho–Pannonian realm [BALLA 1985], offers a plausible explanation for the young bending of the Transdanubian structures including bending of the Balaton–Velence granite belt and of the Vértes–Buda area. The direction of movement of the blocks in the Bakony–Vértes junction area (Fig. 27), furthermore, the direction of the shear of the granite belt required for its stretching during the bending and, lastly, the removal direction of the Velence–Buda wedge are in harmony with the direction of the Early–Middle Miocene push in the rotation history of the Carpatho–Pannonian realm [BALLA 1985].

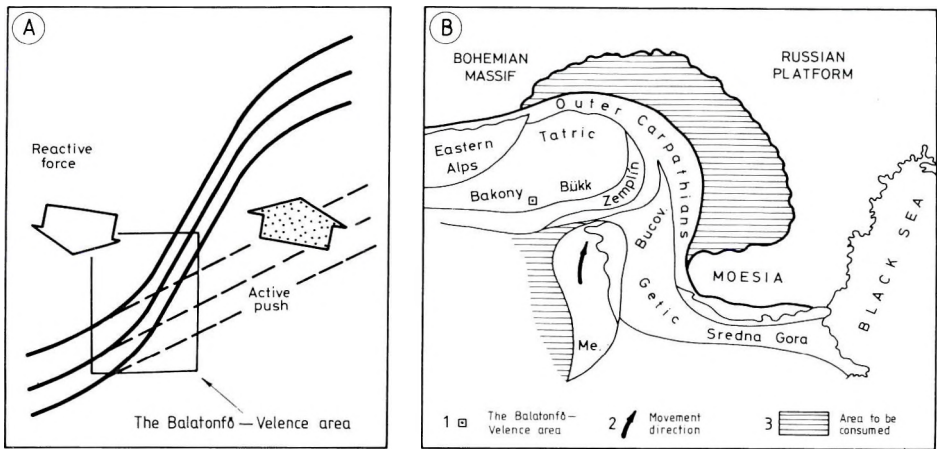


Fig. 41. The origin of the S-shaped bends

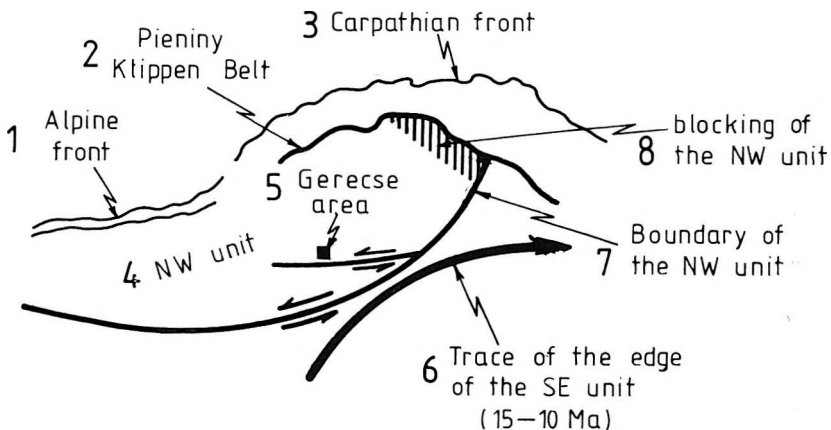
- A) Sketch of the transversal shear
 B) Regional kinematics at 20 Ma B.P., simplified and completed after BALLA [1985]

41. ábra. Az S-alakú hajlatok eredete

- A) A harántnyírás vázlata
 B) Regionális kinematika 20 millió évvel ezelőtt, BALLA [1985] nyomán, egyszerűsítve és módosítva
 1 — a Balatonfő-Velence terület; 2 — mozgási irány; 3 — a későbbiekben felemészített terület

Рис. 41. Происхождение S-образных изгибов

- A) Схема поперечного скалывания
 B) Региональная кинематика 20 млн. лет назад. По Балла [BALLA 1985], с упрощениями и изменениями
 1 — район Балатонфё-Веленце; 2 — направление смещения; 3 — область, исчезающая в дальнейшем



4.3. Sinistral shear in the Middle Miocene

The Middle Miocene (appr. 14–12 Ma B.P.) is the time of the continuing clockwise rotation of the South Pannonian domain. The North Pannonian domain had finished its anticlockwise rotation while the convergence between the South and North Pannonian domains west of the Danube River was in progress. Gradually sinistral shift became the dominant process. This provides a plausible explanation for the sinistral shear of the Transdanubian Range as recorded in strike-slip displacements of W–E direction in the Gerecse–Pilis area (Fig. 42). The blocking of the northwestern unit (= North Pannonian + Inner+Central West Carpathian domains) in the northeast is an important condition of this process.

5. Conclusions

The tracing of an old (Middle Cretaceous) bent syncline together with accompanying longitudinal overthrusts along the whole Transdanubian Range appears to be a fruitful method of structural investigation. Analysis of the position of Tertiary depressions has resulted in the dating of the main tectonic events. Kinematic modelling, i.e. restoration of the situations before these events and the corresponding corrections in the interpretation of data has led to the construction of a new geological map and to a new concept of the tectonic history of the Transdanubian Range. This tectonic history has been correlated in detail with the Oligocene–Miocene kinematics of the Alpine–Carpathian–Pannonian realm, and the essence of the Oligocene and Early Miocene history of the southeastern foreland of the Transdanubian Range has been revealed on the basis of the regional kinematics.

The dismembering of the Transdanubian Range due to subvertical displacements along the faults, which strike in the N–S to NW–SE direction, has been connected with processes which postdate all large-scale strike-slip displacements within the Transdanubian Range. A kinematic interpretation of these movements could be given in a special work.



Fig. 42. Sketch to illustrate the origin of the sinistral shear in the Gerecse area. Modified after BALLA [1987]



42. ábra. A Gerecse-vidéki balos nyírás eredete (vázlat). BALLA [1987] nyomán, módosítva
1 — alpi front; 2 — Pieniny Szirtöv; 3 — kárpáti front; 4 — ÉNy-i szerkezeti egység; 5 — Gerecse;
6 — a DK-i szerkezeti egység szélének útja (15–10 millió év között); 7 — az ÉNy-i szerkezeti egység
határa; 8 — az ÉNy-i egység mozgását blokkoló terület



Рис. 42. Происхождение левого скальвания в районе Геречейских гор (схема), по Балла [BALLA 1987], с изменениями.

1 — фронт Альп; 2 — Пьенинская Утесовая зона; 3 — фронт Карпат; 4 — Северо-западная структурная единица; 5 — Герече; 6 — след перемещения края Юго-восточной структурной единицы; 7 — контур Северо-западной структурной единицы; 8 — область, блокировавшая движение Северо-западной единицы

REFERENCES

- BÁLDI T. 1982: Mid-Tertiary tectonic and palaeogeographic evolution of the Carpathian–East Alpine–Pannonian system (in Hungarian with English summary). *Öslénytani Viták* **28**, pp. 79–155
- BÁLDI T. and BÁLDI-BEKE M. 1985: The evaluation of the Hungarian Palaeogene basins. *Acta Geol. Hung.* **28**, 1–2, pp. 5–28
- BÁLINT CS., BERNHARDT B., LANTOS M. and KOVÁCS G. 1984: Preliminary prospecting project for the perspective Eocene coal area of Lencsehegy South (in Hungarian). Manuscript. Hung. Geol. Surv., Budapest
- BALLA Z. 1985: The Carpathian loop and the Pannonian basin: A kinematic analysis. *Geophys. Trans.* **30**, 4, pp. 313–353
- BALLA Z. 1986: Palaeotectonic reconstruction of the central Alpine–Mediterranean belt for the Neogene. In: L.P. Zonenshain (Ed.), *Tectonics of the Eurasian fold belts*. *Tectonophysics* **127**, 3/4, pp. 213–243
- BALLA Z. 1987: Tertiary palaeomagnetic data for the Carpatho Pannonian region in the light of the Miocene rotation kinematics. In: D. V. Kent and M. Krs (Eds.), *Laurasian palaeomagnetism and tectonics*. *Tectonophysics* **139**, 1/2, pp. 67–98
- BALLA Z. 1988a: Clockwise palaeomagnetic rotations of the Alps in the light of the structural pattern of the Transdanubian Range. *Tectonophysics* **145**, 3/4, pp. 277–292
- BALLA Z. 1988b: On the origin of the structural pattern of Hungary. *Acta Geol. Hung.* **31**, 1–2, pp. 53–63
- BALLA Z., R. TÁTRAI M. and DUDKO A. 1988. The young tectonics of Middle Transdanubia (in Hungarian with English summary). *Ann. Rep. Eötvös L. Geophys. Inst.* for 1986, pp. 74–94
- BALOGH K. 1961: Problems of Triassic in the Buda–Pilis Mountains (in Hungarian). Manuscript, Hung. Geol. Surv., Budapest
- BENHARDT B. and LANTOS M., 1982: Report on the compiling the Eocene coal assessment for the Transdanubian Range (in Hungarian). Manuscript, Hung. Geol. Surv., Budapest
- BIHARI D., DARIDA-TICHY M., DUDKO A., HORVÁTH I. and ÓDOR L. 1978: Hydrocarbon assessment for the Transdanubian Range (in Hungarian). Hung. Geol. Surv., Budapest
- CSÁSZÁR G., HAAS J. and JOCHA-EDELÉNYI E. 1978: Bauxite-geological map of the Transdanubian Range (superficial deposits omitted), scale 1:100,000. Hung. Geol. Surv., Budapest
- CSÁSZÁR G. and HAAS J. 1983: Lithostratigraphic formations of Hungary (in Hungarian). Hung. Geol. Surv., Budapest
- CSÁSZÁR G., CSEREKLEI E. and GYALOG L. 1985: Geological map of the Bakony Mountains (scale 1:50,000). Hung. Geol. Surv. Budapest
- DUDKO A. 1984. Exploration of magmatic rocks by means of magnetometry near the village of Nagykovácsi, Buda Hills (in Hungarian with Russian summary). *Ann. Rep. Hung. Geol. Inst.* for 1982, pp. 263–269
- DUDKO A. 1988a: The East-Velence pericline (in Hungarian with English summary). *Földt. Közl.* **117**, 3, pp. 255–260
- DUDKO A. 1988b: The structural history of the Balatonfő–Velence area (in Hungarian with English summary). *Földt. Közl.* **118** (in press)
- DUDKO A., HORVÁTH I. and ÓDOR L. 1988: Structural-geological map of the Velence Hills and the Balatonfő, Pannonian sediments omitted, scale 1:50,000. Hung. Geol. Surv. (in prep.)
- FERENCZ K. 1953: Conditions géologiques du mont Pilis et du territoire situé au S de celui-ci (in Hungarian with French summary). *Ann. Rep. Hung. Geol. Inst.* for 1943, Final part, pp. 7–38
- FERENCZI I. 1926: Data on the geology of the Buda–Kovácsi Hills (in Hungarian). *Földt. Közl.* **55**, pp. 196–211
- FRANYÓ F. 1968: Geological map of Hungary, scale 1:200,000, sheet L–33–VI Győr. Hung. Geol. Surv., Budapest
- FÜLÖP J. 1958: Die kretazeischen Bildungen des Gerecse-Gebirges. *Geol. Hung.*, ser. *Geol.* **11**, pp. 57–88
- FÜLÖP J. (Ed) 1984: Geological map of Hungary, scale 1:500,000 (in Hungarian). Hung. Geol. Surv., Budapest
- GIDAI L., NAGY G. and SIPOSS Z.. 1980: Geological map of the Dörg coal basin (scale 1:25,000). Hung. Geol. Surv., Budapest
- HEGEDŰS GY. 1951: Daten zur geologischen Kenntnis des Pilis-Gebirges (in Hungarian with German summary). *Ann. Rep. Hung. Geol. Inst.* for 1945–47, part II. pp. 173–190
- HORUSITZKY F. 1943: Principal tectonics units of the Buda Hills (in Hungarian). *Beszámoló a Földtani Intézet Vitaüléseinek Munkálatairól.* **5**, 5, pp. 238–251

- HORVÁTH I. and ÓDOR L. 1984: Alkaline ultrabasic rocks and associated silicocarbonatites in the NE part of the Transdanubian Mountains (Hungary). *Miner. Slovaca* **6**, 1, pp 115–119
- HORVÁTH I., ÓDOR L. and DUDKO A. 1985: Investigation of alkaline ultramafics of the northeastern Transdanubian Range (in Hungarian). Manuscript, Hung. Geol. Surv., Budapest
- JÁMBOR A., MOLDVAY L., RÓNAI A., SZENTES F. and WEIN Gy. 1966: Geological map of Hungary, scale 1:200,000, sheet L-33-II Budapest. Hung. Geol. Surv., Budapest
- JASKÓ S. 1939: Geologische Beschreibung der Hügellandschaft von Alcsut–Etyek (in Hungarian with German summary). *Földt. Közl.* **69**, 4–6, pp. 109–130
- JASKÓ S. 1943: Geological history, tectonics and boreholes of the Bicske bay (in Hungarian). *Beszámoló a Földtani Intézet Vitaüléseinek Munkálatairól*, **5**, 5, pp. 254–302
- JASKÓ S. 1957a: Der Bauxit von Pilisszántó (in Hungarian with German summary). *Annals Hung. Geol. Inst.* **46**, 3, pp. 489–494
- JASKÓ S. 1957b: Beiträge zur Geologie des Gebietes zwischen den Gebirgen Gerecse und Pilis (in Hungarian with German summary). *Annals Hung. Geol. Inst.* **46**, 3, pp. 495–504
- JASKÓ S. 1957c: Bauxitgeologische Beschreibung des zwischen Bicske, Szár, Tatabánya und Tarján gelegenen Gebietes (in Hungarian with German summary). *Annals Hung. Geol. Inst.* **46**, 3, 505–523
- KÁZMÉR M. 1984: Continental escape of the Bakony–Drauzug unit in the Palaeogene (in Hungarian with English summary). *Általános Földt. Sz.* **20**, pp. 53–101
- KÁZMÉR M. 1986: Tectonic units of Hungary: Their boundaries and stratigraphy (A bibliographic guide). *Ann. Univ. Sci. Budapest., sect. Geol.* **26**, pp. 45–120
- KÁZMÉR M. and KOVÁCS S. 1985: Permian–Palaeogene palaeogeography along the eastern part of the Insubric–Periadriatic lineament system: Evidence for continental escape of the Bakony–Drauzug unit. *Acta Geol. Hung.* **28**, 1–2, pp. 71–84
- KÓKAY J. 1956: Tektonische Bewegungsverhältnisse in der Umgebung von Várpalota (in Hungarian with German summary). *Földt. Közl.* **86**, 1, pp. 17–29
- KÓKAY J. 1968: Tectonic theories in the light of Bakony Mountains evidence (in Hungarian with English summary). *Földt. Közl.* **98**, 3–4, pp. 381–393
- KÓKAY J. 1976: Geomechanical investigation of the southern margin of the Bakony Mountains and the age of the Litér fault line. *Acta Geol. Acad. Sci. Hung.* **20**, 3–4, pp. 245–257
- KÓKAY J. 1985: Tectonic and geomechanical studies in the Bántapuszta basin (Várpalota, Bakony Mountains) (in Hungarian with English summary). *Ann. Rep. Hung. Geol. Inst. for 1983*, pp. 43–50
- KORPÁS L. 1981: Oligocene–Lower Miocene formations of the Transdanubian Central Mountains in Hungary (in Hungarian with an extended English summary). *Annals Hung. Geol. Inst.* **64**, 140 p.
- KOVÁCS S. 1983: Major tectonic outline of the Alps (in Hungarian with English summary). *Általános Földt. Sz.* **18**, pp. 77–155
- KRS M. and ROTH Z. 1979: The Insubric–Carpathian block system: its origin and disintegration. *Geol. Sb., Geol. Carp.* **30**, 1, pp. 3–18
- KRS M., PRUNER P. and ROTH Z. 1979: Palaeotectonics and palaeomagnetism of Cretaceous rocks of the Outer West Carpathians of Czechoslovakia. *Geophys. Sb.* 1978, **26**, 512, pp. 269–291
- MAJKUTH T. 1985: Supply of data on geophysical measurements in the Velence Hills area in 1984 (in Hungarian). Manuscript, Eötvös L. Geophys. Inst., Budapest
- MÁRTON E. 1986: Palaeomagnetism of igneous rocks from the Velence Hills and Mecsek Mountains. *Geophys. Trans.* **32**, 2, pp. 83–145
- MÁRTON E. and MÁRTON P. 1983: A refined polar wander curve for the Transdanubian Central Mountains and its bearing on the Mediterranean history. *Tectonophysics* **98**, 1–2, pp. 43–57
- MÁRTON E. and ELSTON D. P. 1985: Structural rotations from palaeomagnetic directions of some Permian–Triassic red beds, Hungary. *Geophys. Trans.* **31**, 1–3, pp. 217–230
- MÉSZÁROS J. 1980a: Structural geology in the service of bauxite prospecting (the Halimba–Herend–Csehbánya area) (in Hungarian). *Földt. Kutatás* **23**, 4, pp. 9–12
- MÉSZÁROS J. 1980b: Prospecting for manganese ore by structural geological and geophysical methods (in Hungarian). *Földt. Kutatás* **23**, 4, pp. 13–16
- MÉSZÁROS J. 1982: Major horizontal tectonic dislocations as a guide to mineral prospecting in the western Bakony Mountains in Hungary (with English summary). *Ann. Rep. Hung. Geol. Inst. for 1980*, pp. 517–526
- MÉSZÁROS J. 1983: Structural and economic-geological significance of strike-slip faults in the Bakony Mountains (in Hungarian with English summary). *Ann. Rep. Hung. Geol. Inst. for 1981*, pp. 485–502

- MÉSZÁROS J. 1985: Methodological guide to the construction of strike-slip displacements. Bakony Mountains, I. Neogene strike slips (in Hungarian). In: Gyakorlati szerkezetföldtani vizsgálatok. Budapest, pp. 59–88
- MÉSZÁROS J. and TÓTH I. 1981: Horizontal dislocations in the surroundings of Ajka and their practical importance (in Hungarian with English summary). *Általános Földt. Sz.* **16**, pp. 25–34
- ORAVECZ J. 1961: Die Triasbildungen des Schollengebietes zwischen den Gerecse- und Buda-Piliser Gebirgen (in Hungarian with German summary). *Földt. Közl.* **91**, 2, pp. 173–185
- RAINCSÁK GY. 1980: Geological makeup and structure of a Triassic range between Várpalota and Iszkaszentgyörgy (in Hungarian with English Ann. Rep. Hung. Geol. Inst. for 1978, pp. 187–196
- SAS E., GERBER P., SCHMIEDER A., SZANTNER F., VÉGH S.-né and PAPP J. 1977: Final summary report on the Mány prospecting area (in Hungarian). Manuscript, Hung. Geol. Surv., Budapest
- SCHAFARZIK F. 1984: Report on the geological mapping in the Pilis Mountains in summer 1883 (in Hungarian). *Földt. Közl.* **14**, 4–8, pp. 249–272 or *Ann. Rep. Hung. Geol. Inst. for 1883*, pp. 91–114
- SEMPTEY F. 1943: Geological conditions of the Szénás Hills between the villages of Nagykovácsi and Pilisszentiván (in Hungarian). *Földtani Szemle Melléklete*
- SIKABONYI L. 1952: Alternance de calcaire et de dolomite dans la montagne Buda-Pilis (in Hungarian with French summary). *Földt. Közl.* **82**, 1-3, pp. 76–80
- SÓLYOM F. 1953: Le levé géologique du Vértes septentrional et du Gerecse méridional (in Hungarian with French summary). *Ann. Rep. Hung. Geol. Inst. for 1950*, pp. 221–230
- SZABÓ N., SZÜCS J., MUNTYÁN I., PUCHNER F., LAPOS J., VÉGH S.-né, BAROSS G., SASS E., REZESSY G. and MAJKUTH T. 1982: Report on the complex geological and mineral explorations in the southeastern Gerecse Hills; final explanatory note (in Hungarian). Manuscript, Hung. Geol. Surv., Budapest
- SZANTNER F. 1982: Tectonic conditions and geological history of bauxite deposits in Hungary (in Hungarian). Manuscript, Hung. Geol. Surv., Budapest
- SZENTES F. 1934: Beiträge zur tektonischen Entwicklung der Umgebung des Nagykevély-Gebirgszuges bei Budapest (in Hungarian with German summary). *Földt. Közl.* **64**, 10–12, pp. 283–296
- SZENTES F. 1958: Geological map of the Buda Hills, scale 1:50,000. In: Pécsi M. (Ed.), *The image of nature in Budapest* (in Hungarian), Akadémiai Kiadó, Budapest, Encl. or in: SCHAFARZIK F., VENDL A. and PAPP F. 1964: Geological excursions in the surroundings of Budapest (in Hungarian). *Műszaki Könyvkiadó*, Budapest, Encl.
- SZENTES F. 1969: Geological map of Hungary, scale 1:200,000, sheet L-33-XII Veszprém. Hung. Geol. Surv., Budapest
- SZENTES F. and BÖJTÖS-VARRÓK K. 1964: Geological map of Hungary, scale 1:200,000, sheet L-34-I Tatabánya. Hung. Geol. Surv., Budapest
- SZENTES F. and RÓNAI A. 1966: Geological map of Hungary, scale 1:200,000, sheet L-34-VII Székesfehérvár. Hung. Geol. Surv., Budapest
- TELEGGI ROTH K. 1935: Daten aus dem Nördlichen Bakony-Gebirge zur jungmesozoischen Entwicklungsgeschichte der „Ungarischen Zwischenmasse“ (in Hungarian with German summary). *Matematikai és Természettudományi Értesítő* **52**, p. 205–252
- VÉGH-NEUBRANDT E. 1960: Petrologische Untersuchung der Obertrias-Bildungen des Gerecsegebirges in Ungarn. *Geol. Hung., ser. Geol.* **12**, pp. 75–125
- VÉGH-NEUBRANDT E. 1981: Report on the investigation of the basement in the Gerecse foreground (in Hungarian). Manuscript, Hung. Geol. Surv., Budapest
- VIGH F. and SZENTES F. 1952: Structural and protection layer conditions in the Dorog coal basin with special reference to the prevention of cavern water afflux (in Hungarian with English summary). *Bányász. Lapok* **85**, 11, pp. 588–600
- VIGH GY. 1914: Contributions to the knowledge on the Triassic of the surroundings of Esztergom (in Hungarian). *Földt. Közl.* **44**, 10–12, pp. 572–577
- WEIN GY. 1976: Die Entwicklungsgeschichte des Budaer Gebirges. *Acta Geol. Acad. Sci. Hung.* **20**, 1–2, pp. 135–160
- WEIN Gy. 1977: The tectonics of the Buda Hills (in Hungarian with English summary) Hung. Geol. Surv., Budapest., 76 p.

NAGYMÉRETŰ HARMADIDŐSZAKI ELTOLÓDÁSOK A DUNÁNTŰLI-KÖZÉPHEGYSÉG SZERKEZETÉBEN

BALLA Zoltán és DUDKO Antonina

A Dunántúli-középhegységben két fő időszakban léptek fel erőteljes tektonikai mozgások. Az első a középsőkréta, amikor a szinklinális szerkezet kialakult és ÉK-i részén meghajlott a kísérő rátolódásokkal együtt. Ezt az idős szerkezeti képet markerként használtuk a második, oligocén-miocén korú tektonizmus elemzésében. Ezen utóbbin belül az alábbi három szakaszt különböztettük meg: 1) a Dunántúli-középhegységi egység DK-i peremének jobbos nyírása az oligocénben (kb. 30–22 m. éve), 2) valamennyi szerkezet S-alakú meghajlása az alsó-középsőmiocénben (kb. 22–14 m. éve) és 3) balos nyírás és összenyomódás a középsőmiocénben (14–12 m. éve).

Ezeket a jelenségeket az alábbi módon korreláltuk az Alp–Kárpát–Pannon régió azonos korú kinematikai folyamataival: az '1'-et az ÉNy-i Kárpát–Pannon egység alpi területről való kinyomódásával, a '2'-öt az óramutató járásával egyező irányban elforduló DK-i Kárpát–Pannon egység ÉNy-inak ütközésével és az utóbbi É felé nyomásával, végül a '3'-at a DK-i Kárpát–Pannon egység óramutató járásával egyező irányú elfordulásával, amely az ÉNy-i Kárpát–Pannon egység szegélyének és — részleges elvonzolás következtében — belső részeinek a balos nyírását eredményezte. A regionális kinematikai modellezéssel levont következtetések ellenőrzése a Dunántúli-középhegységben, azaz egy jól tanulmányozott körzetben, a helyi tektonikai jelenségek összhangját bizonyítja a regionális modellel.

ТРЕТИЧНЫЕ СДВИГИ БОЛЬШОЙ АМПЛИТУДЫ В СТРУКТУРЕ ЗАДУНАЙСКОГО СРЕДНЕГОРЬЯ (ВЕНГРИЯ)

Золтан БАЛЛА, Антонина ДУДКО

В Задунайском среднегорье интенсивные тектонические движения имели место в две главные эпохи. Первая из них — средний мел, когда образовалась синклиналичная структура, которая была изогнута на северо-востоке вместе с сопровождающими взбросами. Эта древняя структура использовалась в качестве маркерной системы при изучении тектонизма второй, олигоценно-миоценовой эпохи. В пределах последней выделены следующие три этапа: 1 — правое скалывание ЮВ окраины Задунайского среднегорья в олигоцене (примерно 30–22 млн. лет назад), 2 — s-образный изгиб всех структур в раннем-среднем миоцене (примерно 22–14 млн. лет назад) и 3 — левое скалывание и сжатие в среднем миоцене (примерно 14–12 млн. лет назад).

Все эти явления были скоррелированы с одновозрастными кинематическими процессами в Альпийско-Карпатско-Паннонском регионе: „1” — с выжиманием северозападной Карпато-Паннонской единицы из Альпийской области, „2” — со столкновением юговосточной Карпато-Паннонской единицы, поворачивающейся по часовой стрелке, с северозападной и с отталкиванием последней к северу, наконец, „3” — с поворотом юговосточной Карпато-Паннонской единицы по часовой стрелке, приведшим к левому скалыванию окраин северозападной единицы и — в связи с частичным увлечением последней — также и ее внутренних областей. Проверка выводов, полученных по региональному кинематическому моделированию, в Задунайском среднегорье, то-есть в хорошо изученном районе, свидетельствует о соответствии локальных тектонических явлений региональной модели.

DEEP REFLECTION SEISMIC PROFILE 598 IN THE SOUTHWESTERN PART OF THE TRANSCARPATHIAN DEPRESSION

Libor VEJMĚLEK* and Āestmír TOMEK*

The paper presents results and an interpretation of seismic reflection Profile 598, which was recorded in the same way as common industrial profiles but with an extended recording time of 12 seconds. The line is situated in Eastern Slovakia and extends across the Zemplín Hills to the Transcarpathian Depression in a SW-NE direction. The Moho was detected as a relatively sharp seismic boundary at a depth of about 26 km. NE dipping reflections, suggesting deformation of the crust-mantle boundary, are probably the consequence of crustal extension. Seismic results in the Zemplín Hills area, together with other geophysical and topographical data, allowed the position of the boundary fault to be located on the WSW side of the Zemplín Horst. A detailed interpretation of the Neogene sedimentary fill-up is not possible because of the absence of boreholes along the profile and the disturbing influences of surrounding geological structures (e.g. buried volcanic bodies). Determination of the sedimentary basin floor is also ambiguous because seismogeological conditions are unfavourable. Interpretation results are in agreement with opinions on the dextral pull-apart origin of the Transcarpathian Depression presented by ROYDEN et al. [1983]

Keywords: Transcarpathian Depression, Zemplín Horst, deep seismic profiling, geophysical data, Moho discontinuity

1. Introduction and geological setting

The results of two deep-crustal reflection profiles across the West Carpathians have recently been presented [TOMEK et al. 1987]. For greater detail, we have also recorded several shorter profiles using standard oil-exploration recording parameters, but with recording times of 12 s and greater. In this paper initial results from one of those profiles are presented, a 26 km long reflection traverse from the Zemplín Hills to the Transcarpathian Depression (line 598, *Fig. 1*).

In the Zemplín Hills area the profile passes through Late Palaeozoic rocks of Zemplín-Mecsek type, which are not encountered elsewhere in the West Carpathians [GRECULA and EGYÜD 1977]. The Transcarpathian Depression forms the promontory of the Pannonian Basin, extending northeastward into the Carpathians. Its geology was described by RUDINEC et al. [1981] as well as DURICA [1982]. The filling of the Transcarpathian Depression has been thoroughly interpreted by MOŘKOVSKÝ et al. [1986]. In its northeastern part the profile extends past the buried Malčice body formed by andesite volcanic products of the Lower Sarmatian age [SLÁVIK 1972]. The body was encountered in Malčice-1 borehole and has been mapped by aerial geophysical surveys and by measurements along adjacent seismic reflection profiles [MOŘKOVSKÝ et al. 1986].

* Geofyzika Brno, POB 62, 612 Brno, Czechoslovakia
Manuscript received (revised version): 28 November, 1988

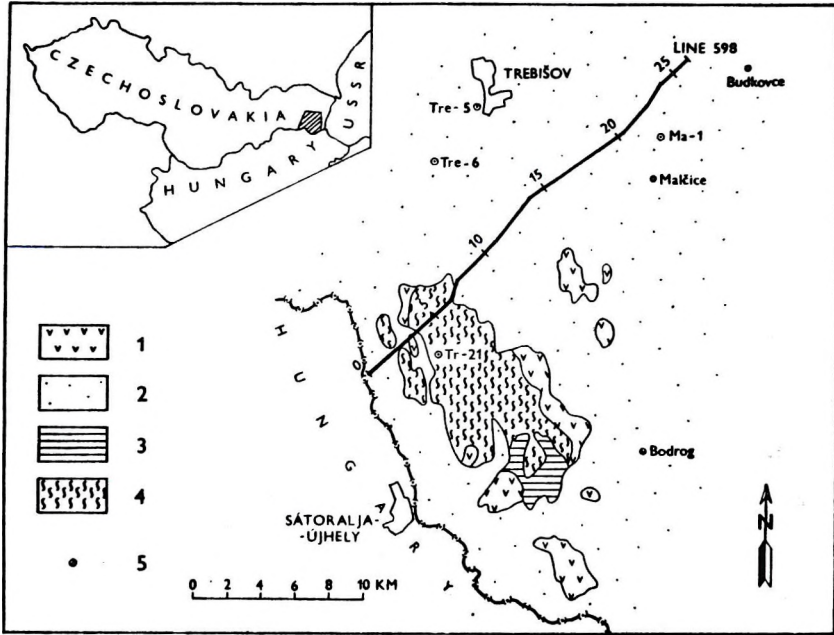


Fig. 1. Location of seismic line 598

1 — Neogene volcanites; 2 — Neogene to Recent sediments; 3 — Mesozoic (Triassic) of the Zemplín Hills; 4 — Palaeozoic (Carboniferous-Permian) of the Zemplín Hills; 5 — borehole

1. ábra. Az 598 sz. szeizmikus vonal helyszínvázlata

1 — neogén vulkanitok; 2 — üledékek neogéntól recensig; 3 — a Zempléni-hegység mezozoikuma (triász); 4 — a Zempléni-hegység paleozoikuma (karbon–perm) 5 — mélyfúrás

Рис. 1. План ситуации профиля № 598 сейсморазведки

1 — неогеновые вулканиты; 2 — неоген–четвертичные отложения; 3 — мезозой (триас) Земплинских гор; 4 — палеозой (карбон–перм) Земплинских гор; 5 — скважина

There are two different tectonic units in the territory studied: the Transcarpathian Depression and the so-called Zemplín Inselberg, formed by sediments of Late Palaeozoic and Triassic age (Fig. 1). The Transcarpathian Depression acquired its present shape during the Late Badenian to Pannonian episode of rapid subsidence, syndimentary normal faulting (with strike-slip component), and immense volcanic activity [DURICA et al. 1978]. The basement belongs to the Palaeo-Alpine and Meso-Alpine edifice of the Carpathians and its maximum depth is about 6 km. The whole depression east of the Prešov–Tokaj Mts. is characterized by high heat flow, positive regional gravity and high fluid pressure in the sediments, caused by dehydration during recent metamorphic recrystallization.

The Zemplín Horst is a significant morphologic feature on the SW side of the Transcarpathian Depression. The rocks exposed on the horst are primarily Stephanian sediments [GRECULA and EGYÜD 1977]. The sediments are of deltaic and neritic origin, containing arkoses and black shales along with coal seams.

Sedimentation continued gradually into the Permian, when continental to lagoonal facies with acid volcanites were developed. The relationship between Permian and Lower Triassic rocks (conglomerates, sandstones and quartzites) is uncertain. The geological history of the Zemplín Hills area, according to GRECULA and EGYÜD [1977], parallels the tectonic development of the Mecsek Mts. (Hungary) and the Reșița zone of the Getic nappe in Banat (Romania).

New geological mapping and boreholes revealed an imbricated thrust tectonic pattern of the Late Palaeozoic age in the Zemplín Horst area. The system of partially overthrust slices forms a nappe-like structure (the Zemplín nappe), which was thrust from the NNE to the SSW [GRECULA and EGYÜD 1977]. Geomorphologically, the Zemplín Hills are an intricate horst structure rising from the surrounding lowland [KVITKOVIČ in ČECHOVIČ et al. 1963]

2. Data

Because of the complicated terrain in the Zemplín Hills area, the slalom-line profiling method was chosen, with a dynamite source split-spread configuration, and 24-fold CDP coverage. Recording was done with a DFS-IV, 48-channel digital system. The recording time was 12 s, with a 2 ms sampling interval. The results of processing by an RDS 500 computer using the seismic software package GEOMAX is the unmigrated time section shown in Fig. 2. The two-way time of 12 s represents a

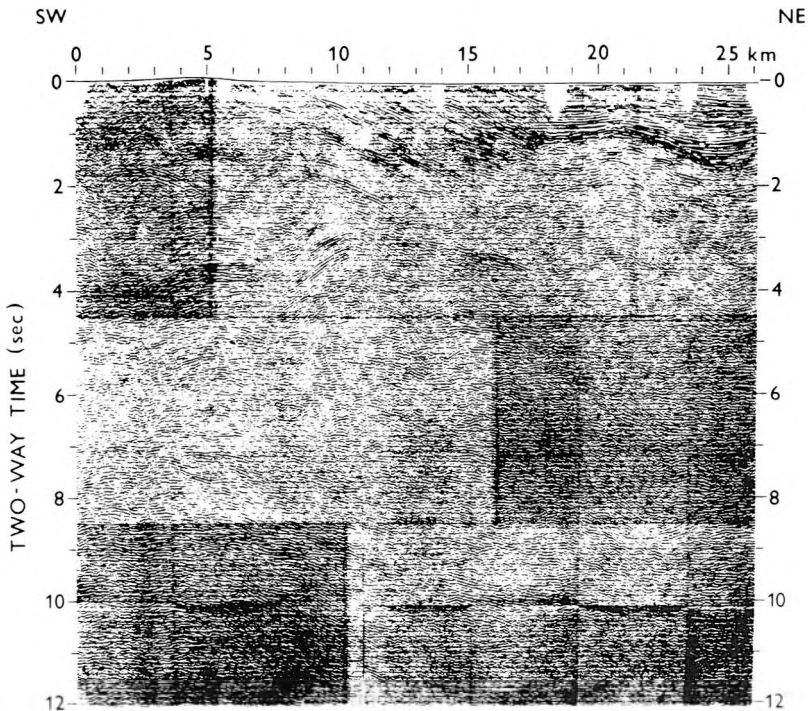


Fig. 2. Unmigrated time section of Profile 598

2. ábra. Az 598 sz. vonal időszelvénye

Рис. 2. Временной разрез вдоль профиля № 598

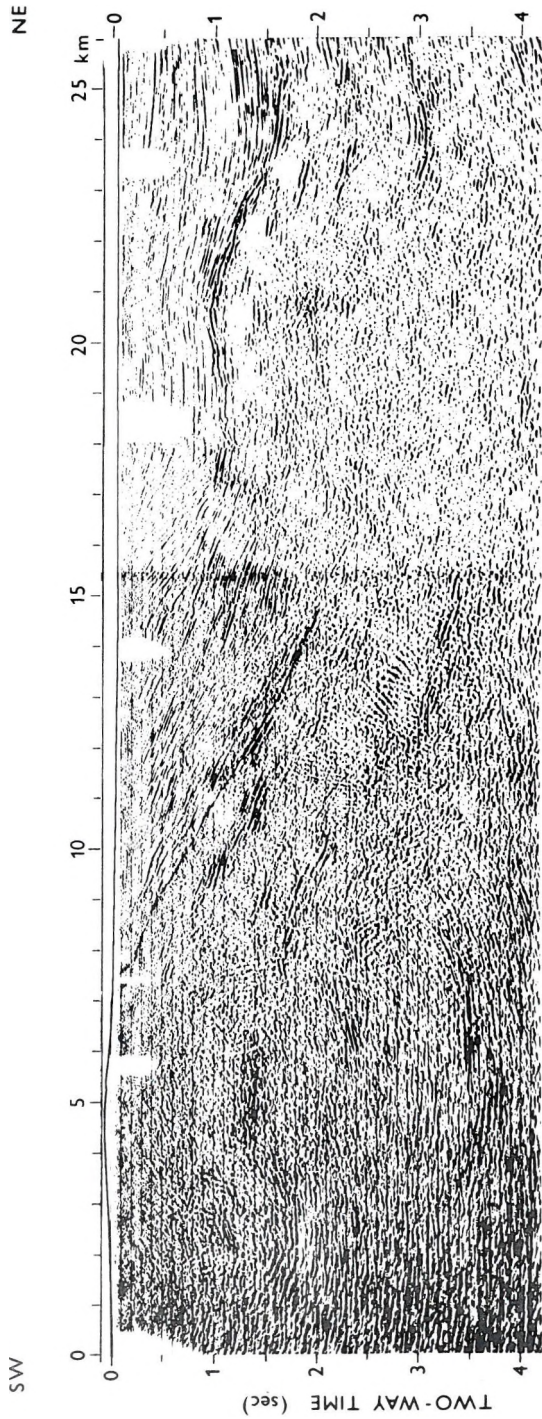


Fig. 3. Migrated time section of Profile 598

3. ábra. Az 598 sz. vonal migrált időszelvénye

Рис. 3. Временной разрез вдоль профиля № 598 с миграцией

depth of 30 to 36 km, the Moho discontinuity in the study area is assumed to be at a depth of less than 30 km [MAYEROVÁ et al. 1985]. The upper part of the section to the two-way time of 4.2 s was processed into a migrated time section (Fig. 3) suitable for interpretation of the sedimentary basin fill.

Within the upper crust (approx. to 5 s) the seismogeological conditions are most favourable in the area of Neogene sediments. Regarding the deeper structure, the conditions are better in the southwestern part of the profile owing to a thinner sedimentary cover and hence a smaller seismic attenuation. Side reflections from the slopes of the Malčice volcanic body also considerably devalue the useful signals in the northeastern part of the section (Figs. 2 and 3).

The velocity distribution was derived from well shooting from boreholes in the vicinity of the profile (Tr-21 in the Zemplín Hills area, Tre-5, Tre-6 and Ma-1 in the Neogene area, Fig. 1). For greater depths, the velocity curves derived from well shooting were consecutively extrapolated assuming a layer velocity of 6000 ms^{-1} .

Results of ground measurement of the vertical component of the magnetic field to the scale of 1:25,000, detailed gravity measurement (also 1:25,000) and topographic maps of the area of interest to the scales of 1:25,000 and 1:100,000 were used to construct the ΔZ , the Δg and the terrain relief along the profile (Fig. 4), as well as a topographic scheme of the study area (Fig. 5). On the gravity

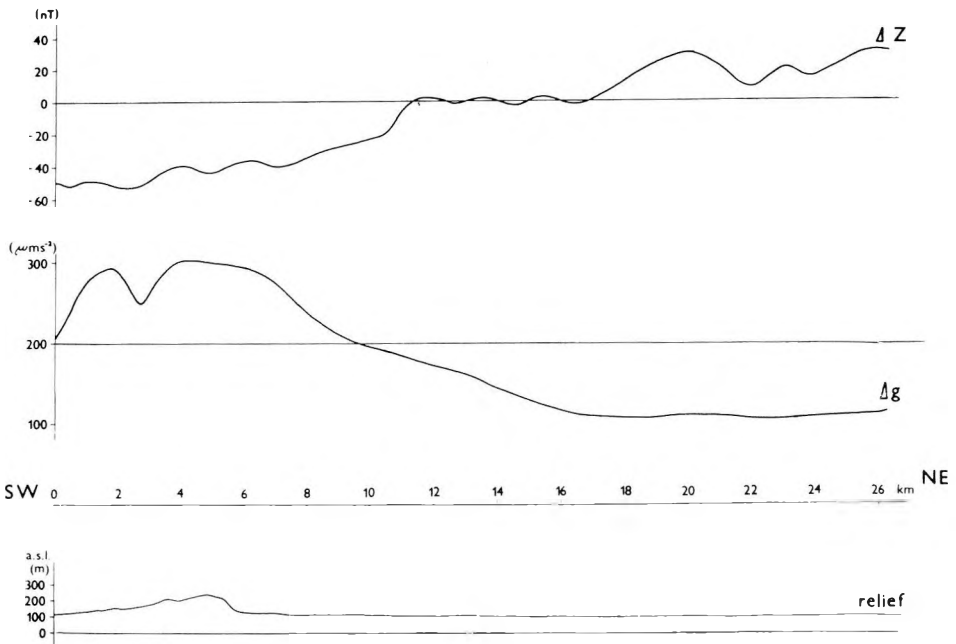


Fig. 4. Curves of ΔZ , Δg and the topography along seismic line 598

4. ábra. Az 598 sz. vonal ΔZ , és Δg görbéje, valamint topográfiája

Рис. 4. Кривые ΔZ и Δg , а также рельеф вдоль профиля № 598

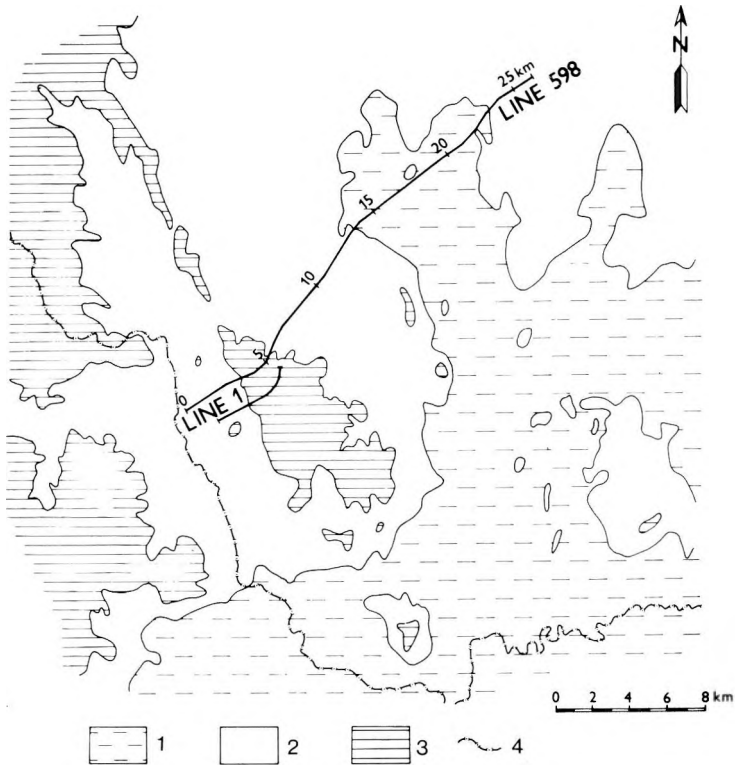


Fig. 5. Topographic scheme with the location of seismic lines 1 and 598
 1 — elevation less than 100 m a.s.l.; 2 — elevation between 100-200 m a.s.l.;
 3 — elevation more than 200 m a.s.l.; 4 — state frontier

5. ábra. Topográfiai vázlat az 1 sz. és 598 sz. szeizmikus vonallal
 1 — magasság < 100 m tsz. f.; 2 — magasság 100-200 m tsz.f. között; 3 — magasság > 200 m tsz. f.;
 4 — államhatár

Рис. 5. Топографическая схема сейсмических профилей № 1 и 598
 1 — высоты < 100 м над ур. моря; 2 — высоты 100–200 м над ур. моря; 3 — высоты > 200 м над ур. моря; 4 — государственная граница

map (Fig. 6) the Zemplín Hills are manifested by maximum gravity values, while the Neogene depression exhibit decreased gravity values. A local positive anomaly, with its centre 2 km to the SE of km 20.5, is due to the andesites of the Malčice volcanic body.

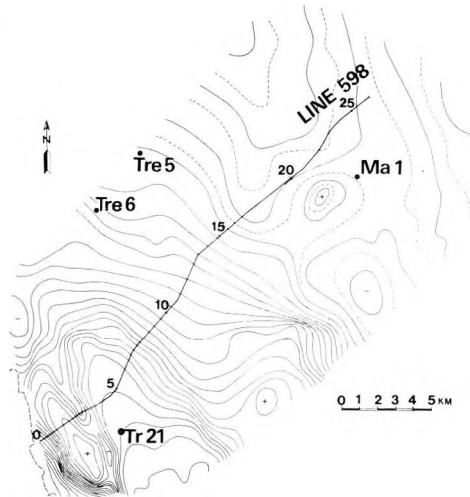


Fig. 6. Gravity map with locations of boreholes and seismic Profile 598

6. ábra Gravitációs térkép a mélyfúrások és az 598 sz. szeizmikus vonal feltüntetésével

Рис. 6. Карта гравитационных аномалий с обозначением буровых скважин и сейсмического профиля № 598

3. Discussion

The sediments of the Transcarpathian Depression occur from km 7.5 to the end of the profile. Neogene sedimentary layers are very distinct on the seismic section (Fig. 3). The division of basin fill into stratigraphic stages (Fig. 8) is only intended to show general orientation because of the absence of deep boreholes along the profile. The seismic picture of sedimentary horizons is disturbed by side reflections from the slopes of the Malčice volcanic body. Because of unfavourable seismogeological conditions (insignificant acoustic impedance contrast between basement and overlying sediments), and the lack of boreholes penetrating the whole sedimentary complex, the determination of the basin relief is ambiguous. Moreover, owing to anomalously increased heat flow values – 105 mW m^{-2} according to ČERMÁK [1968] – in the deeper parts of the basin, the Neogene sediments are metamorphosed almost into the green schist facies [DURICA et al. 1979]. That is why there is little difference in acoustic impedance at the sediment-basement contact. Our interpretation is based on an abrupt change in the character of the reflection pattern, and on data from crossing profile 585 [LUKÁŠOVÁ et al. 1985]. The depth of the basin gradually increases to approx. 3600 m at km 15 (approx 2 s in time section in Fig. 3). It cannot be followed farther as the useful signal interferes with strong side reflections from the Malčice volcanic body. At around km 24,

where the depth is assumed to be greatest, the basement may be indicated by reflections at about 3.2 s. These events can be particularly well recognized in the migrated time section (Fig. 3). The calculated depth here is approx. 5800 m.

Up to km 18 the sedimentary fill below 200 ms is characterized by the dipping of layers to the NE, presumably caused by large subsidence. The layers above 200 ms are horizontal. Considering the data from the nearest boreholes, it can be assumed that the horizontally situated sediments are Pannonian and younger. Within the sedimentary fill there are numerous minor synsedimentary faults, revealed by interruptions of reflections and by diffracted waves (Fig. 7).

In the Zemplín Hills area, Late Palaeozoic rocks rise to the surface around km 2.5 and between km 4 and 7.5 (Fig. 1). These outcrops are separated by a graben filled with Neogene sediments which are well indicated by gravity data (Figs. 4 and 6). By gravity modelling, the depth of the graben was estimated at about 500 m, which corresponds to the two-way time between 450 and 500 ms. In the time section (Fig. 2) however, the structure is not observable. At times over 600 ms diffracted

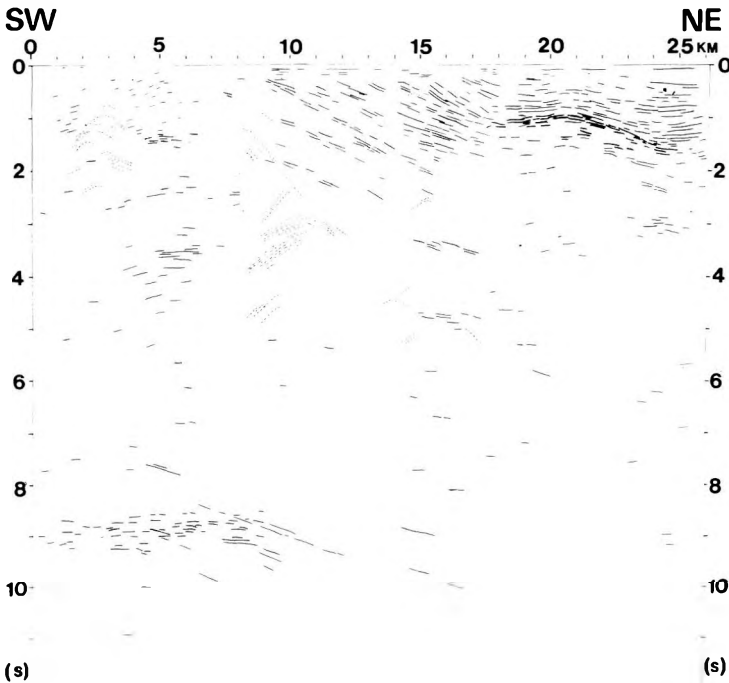


Fig. 7. Line drawing derived from the unmigrated time section of Profile 598. Diffracted waves are marked with dashed lines

7. ábra. Az 598 sz. vonal migrálatlan időszelvényéből nyert vonalrajz. A diffraktált hullámokat szaggatott vonal jelöli.

Рис. 7. Штриховой рисунок, полученный по временному разрезу профиля № 598 без миграции. Волны дифракции обозначены пунктиром

waves appear, suggesting an almost vertical discontinuity (Figs. 2 and 7). Similar but more distinct waves are observed in a corresponding position on parallel reflection line 1 (Fig. 5). The recording time used on this profile was 3 s, which corresponds to a depth of 7-8 km. A comparison with the terrain relief (Fig. 5) shows that the interpreted fault represents the main tectonic boundary of the Zemplín Horst to the SW. Regarding its linear course and nearly vertical dip, it can be assumed that it is a strike-slip fault.

The boundary between the Palaeozoic rocks and the crystalline complex encountered in borehole ZD-8 (6 km to the SE of Profile 598) at the depth of 1310 m [EGYÜD 1982] cannot be observed in the time section. Up to the time of 1.3 s (depth of approx. 3400 m), besides the diffracted waves, weak SW-dipping reflections prevail (Figs. 2 and 7). Apparently, the seismic pattern here is influenced by tectonic disturbances of rocks rather than by their lithology. However, the complex tectonics of the Zemplín Hills area in the whole range of the upper crust was confirmed, but a more detailed determination of internal structure is not possible. The prevailing SW dipping reflections in the Zemplín Inselberg do not agree with the nappe structure with thrust planes dipping ENE as interpreted by GRECULA and EGYÜD [1977]. The NE margin of the horst has a more complicated structure than the SW margin, with faults extending into the basement beneath the sedimentary basin (indicated by the groups of diffracted waves in the range from km 7.5 to 15 at times from 1 s to 5 s – Figs. 2 and 7).

The lower crust, represented by the time range from approx. 5 to 8.5 s, is manifested by numerous, medium to strong fragmentary seismic events. A remarkable feature in the seismic section is a series of rather strong reflections from the beginning of the profile up to km 9 at times between 8.6 and 9.2 s (Figs. 2 and 7). It is assumed that these are reflections from the Moho discontinuity, a relatively sharp seismic boundary with the thickness of the transition zone of about 1.5 km (Fig. 8). The interpreted depth of about 26 km and the character of the reflections are in close agreement with results of deep seismic reflection profiling on adjacent Hungarian territory [POSGAY et al. 1981]. From km 9 up to the end of the profile reflections from the Moho do not appear, presumably as a consequence of energy loss due to the greater thickness of neogene sediments.

NE-dipping reflections appear between 7.5 and 9.5 s in the time section (km 4 to 17, Fig. 7). After migration and depth conversion, these events appear to be associated with a disturbance of the Moho. The relationship of dipping events on the bottom of the crust to the tectonics of the study area can only be speculative. It is possible that these events are related to an extension which resulted in crustal thinning and basin subsidence. This thinning is evidently due to a large extension during the last 16 Ma (Badenian-Recent), with prevailing extensional deformation in the Badenian and Sarmatian.

4. Conclusion

The main result concerning the deep structure of seismic line 598 is the determination of the Moho depth of about 26 km in the Zemplín Hills area. This relatively small crustal thickness can be explained as a consequence of extension and as-

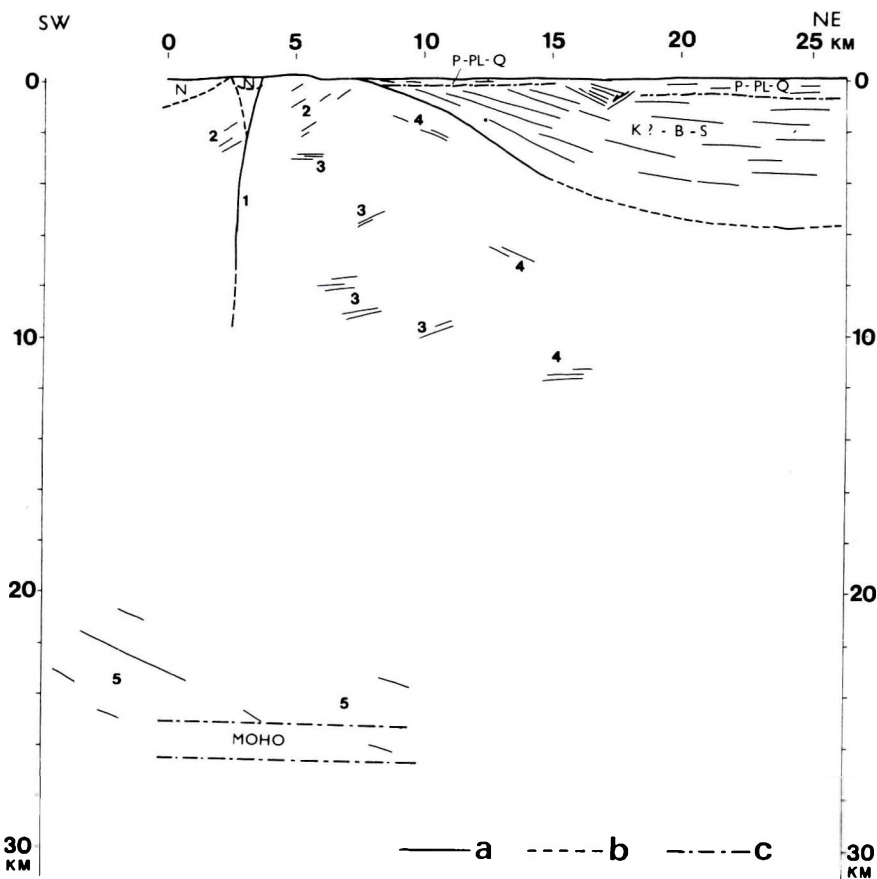


Fig. 8. Schematic depth section of Profile 598

- a — interpreted reflections; b — presumed boundaries; c — zone of the Moho discontinuity;
 N — Neogene; K — Karpathian; B — Badenian; S — Sarmatian; P — Pannonian; PL — Pliocene;
 Q — Quaternary; 1 — the WSW boundary fault of the Zemplín Horst;
 2 — dipping reflectors from the Zemplín Hills; 3 — reflectors in the upper crust in the area of the
 Zemplín Hills; 4 — reflectors in the basement of the sedimentary basin;
 5 — zone of dipping reflectors in the lower crust reaching the crust-mantle boundary

8. ábra. Az 598 sz. vonal vázlatos mélységszelvénye

- a — értelmezett reflexiók; b — feltételezett képződményhatárol; c — a Mohorovičić diszkontinuitás
 zónája; N — neogén; K — kárpáti; B — bádeni; S — szarmata; P — pannon; PL — pliocén;
 Q — negyedidőszaki üledékek; 1 — a Zempléni-sasbérc NyDNy-i határvetője; 2 — meredek dőlésű
 reflexiók a Zempléni-hegységéből; 3 — reflexiók a Zempléni-hegység felső kérgéből; 4 — reflexiók az
 üledékes medence aljzatából; 5 — a kéregköpeny határig lenyúló meredek dőlésű reflexiók

Рис. 8. Схематический разрез профиля № 598 по глубине.

- a — интерпретируемые отражения; b — предполагаемые геологические границы; c — зона
 Моховоричича; N — неоген; K — карпатский ярус; B — баденский ярус; S — сарматский
 ярус; P — паннонский ярус; PL — плиоцен; Q — четвертичные отложения; 1 — сброс,
 ограничивающий Земплинские горы с ЮЗ; 2 — крутонаклоненные отражения из
 Земплинских гор; 3 — отражения из верхней части коры Земплинских гор;
 4 — отражения из фундамента впадины, заполненной осадками; 5 — крутонаклоненные
 отражения, опускающиеся до границы кора-мантия

sociated basin subsidence, especially in the Badenian to Sarmatian ages. As for the lower crust structure, profile 598 contains no significant new information.

Results of interpretation of seismic line 598 are in agreement with contemporary views on the origin of the Transcarpathian Depression as presented by ROYDEN et al. [1983]. According to these authors this basin is a pull-apart basin and its development is associated with slip along a system of dextral faults. Movements had the greatest intensity in the Badenian to Sarmatian ages. Crustal thinning to 26 km, and possibly failure on the crust-mantle boundary, as suggested by dipping events on the seismic section, is also in agreement with this idea.

The fault restricting the Zemplín Hills in the WSW seems to belong to the fault system mentioned above. If so, it may also have been active till recent times. From that point of view, the Zemplín Hills are a horst structure formed in a transtensional tectonic regime.

REFERENCES

- ČECHOVIČ V., BOUČEK B., FRANKO O., FUSÁN O., KULLMAN E., KUTHAN M., KVIKOVIC J. and ZORKOVSKÝ V. 1963: Comments to the general geological map of Czechoslovakia 1:200,000. Sheet M-34-XXXIV Trebisov (in Slovak). Geofond Bratislava
- ČERMÁK V. 1968: Terrestrial heat flow in Eastern Slovakia. *Geofyz. Sborník*, XV, Academia, Praha, pp. 305-318
- DURICA D. 1982: Geology of East Slovakian Lowland (in Slovak). *Miner. Slovaca*, Monografia 1, pp. 3-60
- DURICA D., FALC M. and SUK M. 1979: Recent metamorphism in Neogene sediments of Eastern Slovakia. *Vestník Ústř. Úst. Geol.*, 54, pp. 207-213
- DURICA D., KALIČIAK M., KREUZER H., MÜLLER P., SLÁVIK J., TÖZSÉR J. and VASS D., 1978: Sequence of volcanic events in eastern Slovakia in the light of recent radiometric age determinations. *Vestník Ústř. Úst. Geol.*, 53, pp. 75-88
- EGYÜD K. 1982: Sedimentology of Upper Palaeozoic strata in the Zemplinské vrchy Mts. (SE Slovakia) (in Slovak). *Miner. Slovaca*, 14, 4, pp. 385-401
- GRECULA P. and EGYÜD K. 1977: Position of the Zemplin Inselberg in the tectonic frame of the Carpathians (in Slovak). *Miner. Slovaca*, 9, pp. 449-462
- LUKÁŠOVÁ R., KAŇOVÁ M., STUDENÝ J. and REJMAN P. 1985. Report on the reflection seismic measurement in the East Slovakian neogene in 1984. (in Czech). Manuscript, Geofyzika Brno
- MAYEROVÁ M., NAKLÁDALOVÁ Z., IBRMAJER I. and HERRMANN H. 1985: MOHO – discontinuity in Czechoslovakia according to results of DSS and quarry blasts (in Czech). *Sborník referátů 8. celostátní konference geofyziků, České Budějovice. Sekce S1 – seizmická*, pp. 44-53
- MORKOVSKÝ M., LUKÁŠOVÁ R. and NOVÁK J. 1986: New results of geophysical prospecting in the East Slovakian Neogene basin. *Sbor. geol. věd, Užité geofyz.*, 21, pp. 29-96
- POSGAY K., ALBU I., PETROVICS I. and RÁNER G. 1981: Character of the Earth's crust and upper mantle on the basis of seismic reflection measurements in Hungary. *Earth Evol. Sci.*, 1, 3-4, pp. 272-279
- ROYDEN L., HORVÁTH F. and RUMPLER J. 1983: Evolution of the Pannonian basin system. 1. *Tectonics*, 2, pp. 63-90
- RUDINEC R., TOMEK Č. and JIŘÍČEK R. 1981: Sedimentary and structural evolution of the Transcarpathian Depression. *Earth Evol. Sci.*, 1, 3-4, pp. 205-211
- SLÁVIK J. 1972. Buried volcanic mountains in the South of the East Slovakia (in Slovak) *Geol. Práce, Správy* 58, pp. 41-56
- TOMEK Č., DVORÁKOVÁ L., IBRMAJER I., JIŘÍČEK R. and KORÁB T. 1987: Crustal profiles of active continental collisional belt: Czechoslovak deep seismic reflection profiling in the West Carpathians. *Geophys. J. R. Astr. Soc.* 89, 1, pp. 383-388

KÉREGKUTATÓ SZEIZMIKUS REFLEXIÓS SZELVÉNY A KELET-SZLOVÁKIAI MEDENCE DÉLNYUGATI RÉSZÉN

Libor VEJMĚLEK és Čestmír TOMEK

Az 598 sz. szeizmikus reflexiós szelvényt a rutin ipari felvételezéssel azonos módon mértük, azzal a különbséggel, hogy a rögzítési időt 12 s-re terjesztettük ki. A vonal a Zemplén-hegységben indul és átszeli a kelet-szlovákiai medencét délnyugat-északkelet irányban. A Mohorovičič határfelületet viszonylag éles szeizmikus határként érzékeltük 26 km mélységben. A kéreg–köpeny határ deformációjára utaló északkeleti dőlésű reflexiók valószínűleg kéregextenzió következményei. A Zemplén-hegység területének szeizmikus adatai, valamint geofizikai és topográfiai adatok lehetővé tették a Zemplén sashérc NyDNY-i határvetőjének meghatározását. A neogén üledékes feltöltődés részletes elemzése nem lehetséges szelvény menti furólyukak hiányában. Tovább nehezíti az értelmezést a környező eltemetett vulkáni testek zavaró hatása. Az üledékes medencealjazat meghatározása szintén bizonytalan a kedvezőtlen szeizmogeológiai viszonyok miatt. Az értelmezés összhangban van ROYDEN et al. [1983] véleményével a kelet-szlovákiai medence jobbos széthúzásos eredetéről.

ПРОФИЛЬ СЕЙСМОРАЗВЕДКИ МЕТОДОМ ОТРАЖЕННЫХ ВОЛН ЗЕМНОЙ КОРЫ ЮГО-ЗАПАДНОЙ ЧАСТИ ЗАКАРПАТСКОГО ПРОГИБА

Либор ВЕЙМЕЛЕК, Честмир ТОМЕК

В работе рассматриваются результаты и интерпретация профиля I 598 сейсморазведки методом отраженных волн. Измерения вдоль профиля были проведены по системе серийных измерений, принятых на производстве, с единственным отличием, заключавшимся в том, что время записи было расширено до 12 сек. Линия профиля начинается в Земплинских горах и пересекает Восточно-Словацкую впадину в направлении с юго-запада на северо-восток. Поверхность Мохоровичича отмечалась сравнительно резкой сейсмической границей на глубине 26 км. Отражения, наклоненные к северо-востоку, свидетельствуют о деформации границы коры с мантией и, повидимому, представляют собой результат растяжения коры. Данные сейсморазведки по территории Земплинских гор, а также геофизическая и топографическая информация обеспечили возможность определения положения сброса, ограничивающего Земплинский горст с ЗЮЗ. Детальный анализ процесса заполнения впадины осадками был невозможен из-за отсутствия скважин вдоль профиля. Далее, интерпретация затруднялась вследствие помех от погрешенных вулканических тел вблизи от профиля. Фундамент впадин прослеживался также неоднозначно в связи с неблагоприятными сейсмогеологическими условиями. Интерпретация находится в согласии с точкой зрения ROYDEN et al. [1983] о том, что Восточно-Словацкая впадина возникла по схеме растяжения с правым сдвигом.

NEOGENE VOLCANISM OF THE NYÍR REGION (NE HUNGARY) AS REVEALED BY INTEGRATED INTERPRETATION OF THE LATEST GEOPHYSICAL DATA

Éva KILÉNYI*, Iván POLCZ* and Zoltán SZABÓ*

Oil exploration of the NE corner of Hungary is hindered by the buried volcanics found practically in all boreholes of the area. Determination of the type, position, age, etc. of the volcanic bodies may influence our understanding of the oil potentials of the area. The seismic survey of 1986 provided much better quality material than ever before. We could separate the volcanic tuffs from the subvolcanic bodies thus providing a basis for gravity and magnetic modelling. The anomaly maps show integrated effects making some of the small-size volcanic bodies unrecognizable. A filter test provided two map series resulting in good correlation of seismic-, gravity- and magnetic data. Starting from the known shape and position of the source, the density differences, susceptibilities and inclinations could be determined. Comparing radiometric ages and magnetostratigraphy, it was found that there were two cycles of volcanic activity separated in time by 1-2 Ma, the second marking the latest intensive tectonic events of the forming of the Pannonian Basin.

Keywords: Pannonian Basin, Neogene volcanism, reflection seismic survey, gravity modelling, magnetic modelling, radiometric age

1. Introduction

The existence of intensive palaeovolcanic activity in the Nyír region has long been known from both the geomagnetic map and boreholes. Seismic reflection prospecting, started in 1969, was hindered by the volcanic cover, energy being unable to penetrate it. To assess the hydrocarbon potentials of the area the most important question was whether any source rock could be expected below the volcanic tuffs. Geoelectric measurements, first tellurics combined with dipole equatorial soundings [NEMESI et al. 1981], and later with the magnetotelluric method [NEMESI et al. 1987], provided some information by classifying the area into three types: (i) no volcanics present, (ii) low-resistivity formation (marine sediments) below volcanic cover, and (iii) volcanics immediately on high-resistivity basement (Mesozoic carbonates or crystalline basement) [NEMESI et al. 1986].

Boreholes were always sited on the top of structural highs, finding volcanic tuff and no sign of hydrocarbons. None of the boreholes reached the basement of the volcanic series. One of the latest such boreholes was Necs-1, in the south-western corner of our present area, which penetrated nearly 3000 m of the volcanic formations and stopped in them at a depth of 4008 m. Lithological descriptions of the cores show a gradual transition of a stratovolcanic series — starting with tuffs dominating and giving way to lavas dominating — into a subvolcanic body described as diorite.

Table 1. K/Ar age of samples from northeastern Hungary [after SZÉKY-FUX et al. 1987].

1. táblázat. ÉK-Magyarországi kőzetminták K/Ar kor adatai [SZÉKYNÉ FUX et al. 1987 nyomán]

Таблица 1. Калий-аргоновые возраста горных пород Северо-восточной Венгрии [по SZÉKY-FUX et al. 1987]

No.	Locality, rock	Examined fraction	K %	$^{40}\text{Ar}/\text{rad}$	$^{40}\text{Ar}/\text{rad}$	K/Ar age (Ma)	Average age (Ma)
	Lelőhely, kőzet	Vizsgált frakció		%	(nom^3/g)	K/Ar kor (mill. év)	Átlag kor (mill. év)
	Пункт отбора, порола	Исследуемая фракция				K/Ar возраст, млн. лет	Средний возраст, млн. лет
665.	Kisújszállás ÉK-1 1664–1682 m rhyolite	biotite	6.60	0.81	$4.772 \cdot 10^{-6}$	18.5 ± 0.7	} 18.34 ± 0.47
				0.27	$4.614 \cdot 10^{-6}$	17.9 ± 1.0	
666.	Kisújszállás ÉK-1 1863–1880 m rhyolite	biotite	1.90	0.47	$1.367 \cdot 10^{-6}$	18.4 ± 0.8	} 18.13 ± 0.44
		feldspar	7.36	0.86	$5.190 \cdot 10^{-6}$	18.0 ± 0.7	
				0.47	$5.170 \cdot 10^{-6}$	18.0 ± 0.8	
		feldspar	2.04	0.60	$1.466 \cdot 10^{-6}$	18.4 ± 0.8	
497.	Kisújszállás-1 1614–1617 m rhyolite tuff	biotite	4.83	0.10	$2.746 \cdot 10^{-6}$	14.6 ± 2.0	} 17.8 ± 2.1
		feldspar	1.25	0.22	$6.484 \cdot 10^{-7}$	13.3 ± 0.9	
				0.31	$6.068 \cdot 10^{-7}$	12.4 ± 0.8	
496.	Kisújszállás-13 1765–1770 m rhyolite tuff	biotite	5.88	0.35	$3.603 \cdot 10^{-6}$	15.7 ± 0.8	} 17.7 ± 1.1
881.	Kisújszállás-13 1905–1909 m andesite	bulk rock	2.42	0.52	$1.280 \cdot 10^{-6}$	13.6 ± 0.6	
738.	Nyírmártonfalva-1 932–935 m andesite	bulk rock	2.63	0.57	$1.391 \cdot 10^{-6}$	13.5 ± 0.8	} 13.7 ± 0.6
				0.64	$1.432 \cdot 10^{-6}$	13.9 ± 0.6	
		biotite	6.91	0.39	$4.571 \cdot 10^{-6}$	16.9 ± 0.8	} 17.1 ± 0.5
				0.56	$4.651 \cdot 10^{-6}$	17.2 ± 0.7	
834.	Nádudvar-13 1605.5–1607.0 m rhyolite tuff	biotite	5.62	0.26	$4.201 \cdot 10^{-6}$	19.1 ± 1.2	} 17.8 ± 2.1
				0.16	$3.970 \cdot 10^{-6}$	18.1 ± 1.4	
		biotite	5.54	0.15	$3.294 \cdot 10^{-6}$	15.2 ± 1.3	
		feldspar	0.65	0.09	$3.153 \cdot 10^{-7}$	12.5 ± 1.5	
662.	Nádudvar-9 1612–1617.1 m rhyolite tuff	biotite	5.74	0.26	$3.972 \cdot 10^{-6}$	17.7 ± 1.1	} 17.4 ± 0.8
				0.24	$3.844 \cdot 10^{-6}$	17.1 ± 1.1	
		feldspar	0.47	0.15	$2.921 \cdot 10^{-7}$	16.0 ± 1.3	} 16.5 ± 0.9
736.	Józsa-2. 1633–1637 m rhyodacite	biotite	6.05	0.14	$3.823 \cdot 10^{-6}$	16.2 ± 1.6	
				0.27	$3.938 \cdot 10^{-6}$	16.7 ± 1.0	} 15.8 ± 0.5
676.	Nyírmártonfalva-1 716–721 m rhyolite	biotite	6.98	0.79	$4.342 \cdot 10^{-8}$	15.9 ± 0.7	
				0.80	$4.278 \cdot 10^{-6}$	15.7 ± 0.7	} 16.0 ± 0.6
		feldspar	0.71	0.12	$4.183 \cdot 10^{-7}$	15.2 ± 1.8	
348.	Nyírmártonfalva-1 2183–2184 m rhyolite	bulk rock	5.31	0.57	$3.303 \cdot 10^{-6}$	15.9 ± 0.8	} 16.0 ± 0.6
				0.51	$3.318 \cdot 10^{-6}$	16.0 ± 0.8	
836.	Józsa-3 1326–1331 m rhyodacite tuff	biotite	6.29	0.24	$3.596 \cdot 10^{-6}$	14.6 ± 0.9	} 14.3 ± 1.8
1130.	Penészlek-3 1272.5–1290.5 m rhyolite tuff	biotite	6.27	0.11	$3.492 \cdot 10^{-6}$	14.3 ± 1.8	
1131.	Penészlek-3 1255.0–1272.5 m rhyolite tuff	biotite	6.26	0.39	$3.666 \cdot 10^{-6}$	15.0 ± 0.7	} 14.6 ± 0.9
1132.	Penészlek-3 1332.0–1342.0 m rhyolite tuff	biotite	6.00	0.26	$3.417 \cdot 10^{-6}$	14.6 ± 0.9	
1092.	Penészlek-7 1276.0–1285.0 m rhyolite tuff	biotite	5.79	0.14	$3.038 \cdot 10^{-6}$	13.4 ± 1.4	} 13.8 ± 0.9
1091.	Penészlek-15 1303.0–1306.0 m rhyolite tuff	plagioclase	0.51	0.26	$2.728 \cdot 10^{-7}$	13.8 ± 0.9	

No.	Locality, rock	Examined fraction	K %	$^{40}\text{Ar}/\text{rad}$ %	$^{40}\text{Ar}/\text{rad}$ (nom ³ /g)	K/Ar age (Ma)	Average age (Ma)
	Leőhely, kőzet	Vizsgált frakció				K/Ar kor (mill.év)	Átlag kor (mill.év)
	Пункт отбора, порода	Исследуемая фракция				K/Ar возраст, млн. лет	Средний возраст, млн. лет
1135.	Penészlek-18 1734.0–1737.0 m rhyolite tuff	biotite	3.11	0.34	$1.941 \cdot 10^{-11}$	15.9 ± 0.9	
1126.	Nyirábrány-1 1435.0–1440.0 m rhyolite tuff	biotite	5.60	0.31	$3.285 \cdot 10^{-6}$	15.0 ± 0.8	
537.	Kaba É-4 1520–1525 m rhyolite tuff	biotite	6.41	0.39	$3.423 \cdot 10^{-6}$	13.7 ± 0.8	} 13.7 ± 0.7
		biotite	6.11	0.32	$3.412 \cdot 10^{-6}$	13.6 ± 1.1	
		biotite		0.15	$3.573 \cdot 10^{-6}$	15.0 ± 0.9	} 15.0 ± 0.7
		biotite		0.23	$3.599 \cdot 10^{-6}$	15.1 ± 1.0	
		feldspar	0.52	0.21	$2.431 \cdot 10^{-7}$	12.0 ± 0.7	} 14.4 ± 0.8
495	Hajdúszoboszló-9 1375.0–1377.5 m rhyolite tuff	biotite	4.62	0.13	$2.691 \cdot 10^{-6}$	14.9 ± 1.4	
		biotite	0.18		$2.527 \cdot 10^{-6}$	14.0 ± 1.0	} 14.4 ± 0.8
		biotite	4.84	0.10	$3.042 \cdot 10^{-6}$	16.1 ± 1.8	
		feldspar	0.59	0.41	$4.3161 \cdot 10^{-7}$	18.7 ± 1.1	
542.	Hajdúszoboszló-22 1448–1450 m rhyolite tuff	biotite	5.76	0.23	$3.056 \cdot 10^{-6}$	13.6 ± 0.9	
		feldspar	0.49	0.19	$2.303 \cdot 10^{-7}$	12.0 ± 0.9	
733.	Balmazújváros-3 1216–1219 m propylitized amphibole andesite	bulk rock	2.87	0.26	$1.659 \cdot 10^{-6}$	14.8 ± 1.0	
349.	Balmazújváros-5 1415–1418 m andesite	bulk rock	2.67	0.66	$1.684 \cdot 10^{-6}$	15.5 ± 0.9	} 15.8 ± 0.6
		bulk rock		0.77	$1.746 \cdot 10^{-6}$	16.1 ± 0.8	
817.	Hajdúböszörmény-2 1526,5–1527.5 m andesite	bulk rock	2.75	0.56	$1.624 \cdot 10^{-6}$	15.1 ± 0.7	
1133.	Penészlek-17 1745.0–1750.0 m andesite	bulk rock	2.52	0.28	$1.231 \cdot 10^{-6}$	12.6 ± 0.7	
		bulk rock	2.39	0.51	$1.179 \cdot 10^{-6}$	12.6 ± 0.6	
		biotite	2.31	0.60	$1.110 \cdot 10^{-6}$	12.3 ± 0.5	
506.	Balmazújváros-4 1227–1231 m rhyolite tuff	biotite	5.64	0.28	$2.548 \cdot 10^{-6}$	11.5 ± 0.6	} 12.1 ± 0.5
		biotite	5.58	0.50	$2.720 \cdot 10^{-6}$	12.5 ± 0.7	
		feldspar	2.63	0.44	$1.251 \cdot 10^{-6}$	12.2 ± 0.6	
		feldspar	3.78	0.70	$1.839 \cdot 10^{-6}$	12.5 ± 0.6	
816.	Hajdúböszörmény-1 1000.0–1001.7 m rhyolite tuff	biotite	3.91	0.21	$1.801 \cdot 10^{-6}$	11.0 ± 0.7	
		feldspar	0.50	0.35	$2.157 \cdot 10^{-7}$	11.0 ± 0.5	
508.	Nádudvar-5 1930–1932 m propylitized andesite	bulk rock	2.60	0.33	$1.029 \cdot 10^{-6}$	10.4 ± 0.6	} 9.9 ± 0.5
		bulk rock		0.41	$0.962 \cdot 10^{-6}$	9.7 ± 0.5	
		bulk rock		0.52	$0.982 \cdot 10^{-6}$	9.7 ± 0.5	
835.	Nádudvar-7 1875.0–1875.5 m andesite	bulk rock	3.05	0.43	$1.102 \cdot 10^{-6}$	9.2 ± 0.5	
669.	Nádudvar-2 1725–1730 m baked rhyolite tuff	biotite	4.33	0.12	$1.818 \cdot 10^{-6}$	11.1 ± 1.3	
578.	Gelénés-1 631 m tuff	biotite	5.65	0.09	$2.583 \cdot 10^{-6}$	11.6 ± 1.8	} 11.0 ± 0.6
		biotite		0.13	$2.499 \cdot 10^{-6}$	11.3 ± 1.2	
		biotite		0.12	$2.229 \cdot 10^{-6}$	10.1 ± 1.2	
		biotite		0.15	$2.403 \cdot 10^{-6}$	10.9 ± 1.2	
		feldspar	0.35	0.11	$1.422 \cdot 10^{-7}$	10.5 ± 1.4	
575.	Gel-1. 942.5 m tuff	feldspar	1.08	0.43	$4.376 \cdot 10^{-7}$	10.4 ± 0.6	
565.	Gel-1. 1265 m ash tuff	bulk rock	3.50	0.39	$1.946 \cdot 10^{-6}$	14.3 ± 0.7	
569.	Gel-1. 1324 m ash tuff	bulk rock	2.69	0.30	$1.336 \cdot 10^{-6}$	12.8 ± 0.7	
568.	Gel-1. 1378 m ash tuff	bulk rock	2.20	0.36	$1.147 \cdot 10^{-6}$	13.4 ± 0.7	
570.	Gel-1. 1407 m ash tuff	bulk rock	1.40	0.20	$9.383 \cdot 10^{-7}$	17.2 ± 1.2	

No.	Locality, rock	Examined fraction	K %	$^{40}\text{Ar}/\text{rad}$ %	$^{40}\text{Ar}/\text{rad}$ (nom ³ /g)	K/Ar age (Ma)	Average age (Ma)
	Lelőhely, kőzet	Vizsgált frakció				K/Ar kor (mill. év)	Átlag kor (mill. év)
	Пункт отбора, порода	Исследуемая фракция				K/Ar возраст, млн. лет	Средний возраст, млн. лет
576.	Gel-1. 1639 m rhyolite tuff	biotite	2.35	0.17	$1.355 \cdot 10^{-6}$	14.7 ± 1.2	} 12.2 ± 1.0
		feldspar	0.44	0.20	$1.962 \cdot 10^{-7}$	11.5 ± 1.3	
		feldspar	0.70	0.50	$3.368 \cdot 10^{-7}$	12.8 ± 0.8	
577	Gel-1. 1959.2–1962.2 m obsidian	bulk rock	1.19	0.03	$3.912 \cdot 10^{-7}$	8.4 ± 3.2	} 8.4 ± 2.1
		feldspar	2.05	0.04	$3.892 \cdot 10^{-7}$	8.4 ± 3.0	
815.	Gel-1. 1955–1997 m rhyolite tuff	feldspar	2.05	0.22	$5.644 \cdot 10^{-7}$	6.9 ± 0.5	} 6.9 ± 0.4
		bulk rock	2.73	0.29	$5.457 \cdot 10^{-7}$	6.8 ± 0.5	
737.	Barabás, quarry, rhyolite	bulk rock	2.73	0.44	$1.200 \cdot 10^{-6}$	11.3 ± 0.5	}
730.	Barabás-1. B-1. 78 m, rhyolite tuff	bulk rock	2.44	0.33	$1.066 \cdot 10^{-6}$	11.2 ± 0.6	
461.	Tarpa, quarry, lower dacite	bulk rock	2.10	0.60	$8.690 \cdot 10^{-7}$	10.6 ± 0.5	} 10.5 ± 0.3
		bulk rock	2.00	0.36	$8.215 \cdot 10^{-7}$	10.4 ± 0.6	
462.	Tarpa, quarry, upper dacite	bulk rock	2.10	0.50	$8.584 \cdot 10^{-7}$	10.4 ± 0.5	}
		bulk rock	2.10	0.15	$8.529 \cdot 10^{-7}$	10.4 ± 0.8	
284.	Nagyszöllős, Feketehegy piroxenandesite	bulk rock	1.83	0.49	$7.016 \cdot 10^{-7}$	9.9 ± 0.5	}
		bulk rock	1.83	0.57	$7.182 \cdot 10^{-7}$	10.0 ± 0.5	
724.	Nyíregyháza-1 2543.5–2546.5 m rhyolitic propylite	feldspar	0.42	0.09	$2.240 \cdot 10^{-7}$	13.7 ± 1.6	} 13.5 ± 0.9
		feldspar	0.68	0.14	$3.517 \cdot 10^{-7}$	13.3 ± 1.1	
		bulk rock	2.48	0.50	$9.686 \cdot 10^{-7}$	10.0 ± 0.4	
320.	Nyíregyháza-1 2162–2164 m dacite	feldspar	0.50	0.16	$1.991 \cdot 10^{-7}$	10.2 ± 0.8	} 10.3 ± 0.6
		feldspar	0.52	0.15	$2.111 \cdot 10^{-7}$	10.4 ± 0.8	
350.	Nyíregyháza-1 2000–2005 m rhyolite	bulk rock	2.63	0.36	$1.101 \cdot 10^{-6}$	10.7 ± 0.8	} 10.8 ± 0.6
		bulk rock	2.63	0.12	$1.121 \cdot 10^{-6}$	10.9 ± 0.8	
818.	Kisvárdá (thermal well) 1152 m rhyolite	bulk rock	2.96	0.25	$1.146 \cdot 10^{-6}$	10.0 ± 0.7	}
		bulk rock	3.87	0.62	$1.641 \cdot 10^{-6}$	10.9 ± 0.8	
346.	Hajdúnánás-1 1997–2000 m rhyolite	bulk rock	3.87	0.42	$1.799 \cdot 10^{-6}$	11.9 ± 0.7	} 11.4 ± 0.7
		bulk rock	2.72	0.60	$1.273 \cdot 10^{-6}$	12.0 ± 0.5	
679.	Komoró-1 1883.72–1833.3 m andesite	bulk rock	2.72	0.50	$1.288 \cdot 10^{-6}$	12.1 ± 0.5	} 12.1 ± 0.4
		bulk rock	1.45	0.46	$6.816 \cdot 10^{-7}$	12.1 ± 0.6	
680.	Komoró-1 2395.3–2395.7 m propylitic dacite	bulk rock	1.45	0.46	$6.816 \cdot 10^{-7}$	12.1 ± 0.6	}
		bulk rock	2.81	0.69	$1.231 \cdot 10^{-6}$	11.2 ± 0.6	
678.	Komoró-1 2438.3–2438.7 m dacitic propylite	bulk rock	2.81	0.24	$1.222 \cdot 10^{-6}$	11.1 ± 0.8	} 11.2 ± 0.5
		bulk rock	1.76	0.31	$7.699 \cdot 10^{-7}$	11.1 ± 0.7	
170.	Nagyecséd-1 1109–1110.5 m andesit	bulk rock	1.76	0.31	$7.699 \cdot 10^{-7}$	11.1 ± 0.7	}
		bulk rock	1.69	0.41	$6.739 \cdot 10^{-7}$	10.2 ± 0.6	
176.	Nagyecséd-1 3017–3019 m propylitic andesite	bulk rock	1.69	0.41	$6.739 \cdot 10^{-7}$	10.2 ± 0.6	}
		bulk rock	0.33	0.11	$1.870 \cdot 10^{-7}$	14.5 ± 1.5	
971.	Nagyecséd-1 4000.0–4000.8 m epidote diorite	bulk rock	0.33	0.11	$1.870 \cdot 10^{-7}$	14.5 ± 1.5	}
		bulk rock	0.81	0.27	$4.106 \cdot 10^{-7}$	13.0 ± 0.8	
1088.	Hajdúnánás-2 1545–1546 m piroxene andesite	bulk rock	0.81	0.27	$4.106 \cdot 10^{-7}$	13.0 ± 0.8	

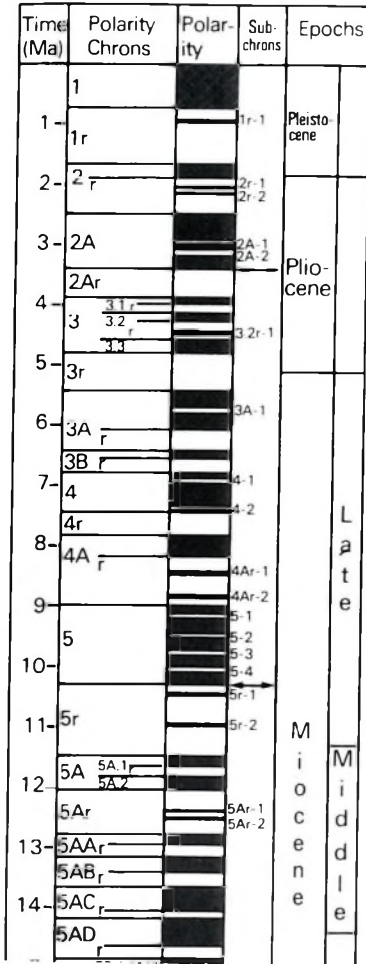


Fig. 2. Polarity–time scale [after HARLAND et al. 1982]

2. ábra. Mágneses polaritás–idő skála
[HARLAND et al. 1982 nyomán]

Рис. 2. Шкала полярность–время [по HARLAND et al. 1982]

2. Seismic data

The seismic survey of 1986 is comprised of 361 km of explosion seismics (Fig. 3). For the interpretation 185 km of former VIBROSEIS[®] profiles were reprocessed in 1987. The quality of explosion profiles was much higher, though for constructing maps the VIBROSEIS[®] profiles had to be used with equal weight. But in our paper all time sections illustrating the topic are taken from the 1986 survey.

The most striking discordance in all seismic sections is the boundary between Pannonian marine sediments and underlying volcanics consisting mainly of acidic and intermediate volcanic tuffs. Typical of these latter, is the high energy, chaotic reflection pattern (see Fig. 4). Inside the thick volcanic complex one can delineate another surface — in most cases not reflecting — separating another reflection pattern, the one which is practically reflection free. Following these characteristics in all reflection profiles a series of grotesque-shaped bodies could be delineated, fitting the ideas one forms of subvolcanic bodies.

[®] CONOCO trademark



Fig. 3. Location map of the seismic survey of 1986

3. ábra. Az 1986. évi szeizmikus mérések helyszínvázlata

Рис. 3. План ситуации сейсморазведки 1986 г.

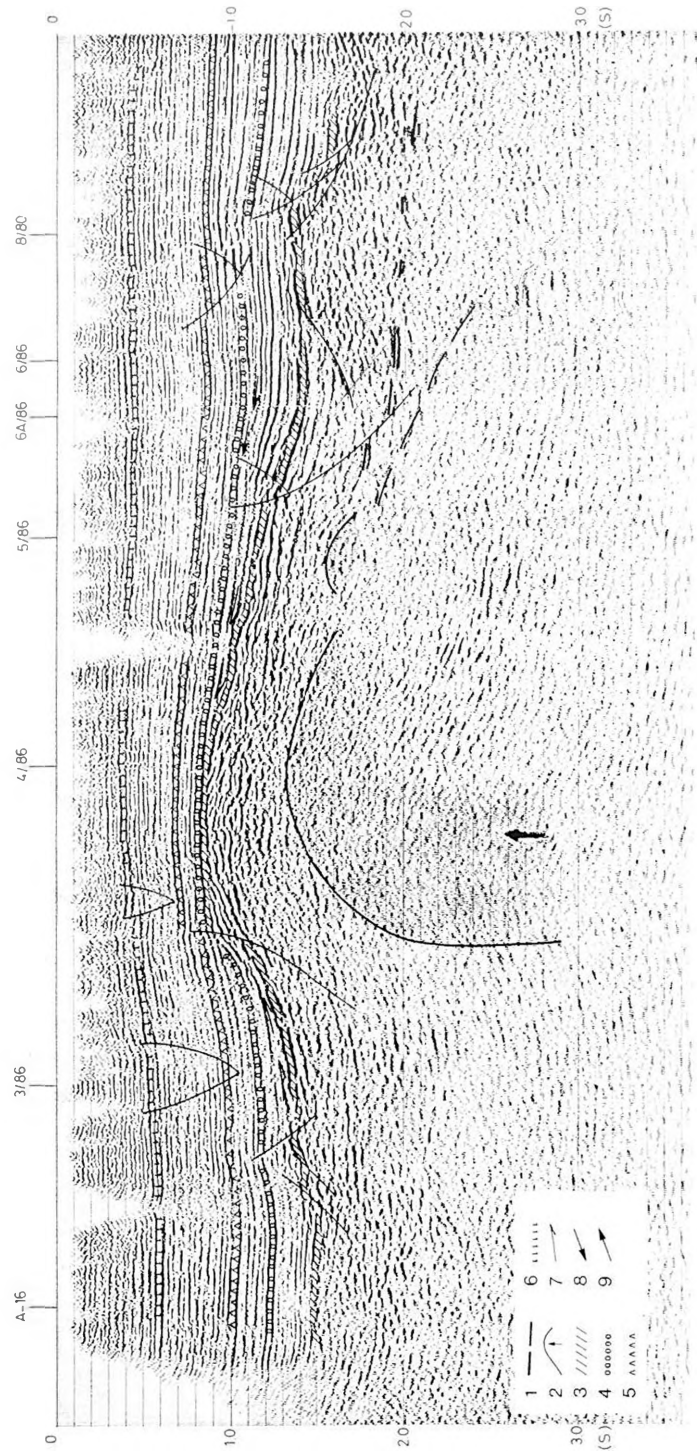


Fig. 4. Migrated time section Me-12/86

1 — basement (probably Mesozoic); 2 — subvolcanic intrusion or centre of stratovolcano;
 3 — contact of Pannonian sediments and Miocene volcanics; 4 — top of seismic sequence A;
 5 — top of seismic sequence B; 6 — top of seismic sequence C; 7 — onlap; 8 — downlap;
 9 — toplap

4. ábra. Me-12/86 migrált időszelvény. Jelmagyarázatot lásd az 5. ábrán

Рис. 4. Временной разрез Me-12/86 с миграцией; прочие обозначения см. на рис. 5

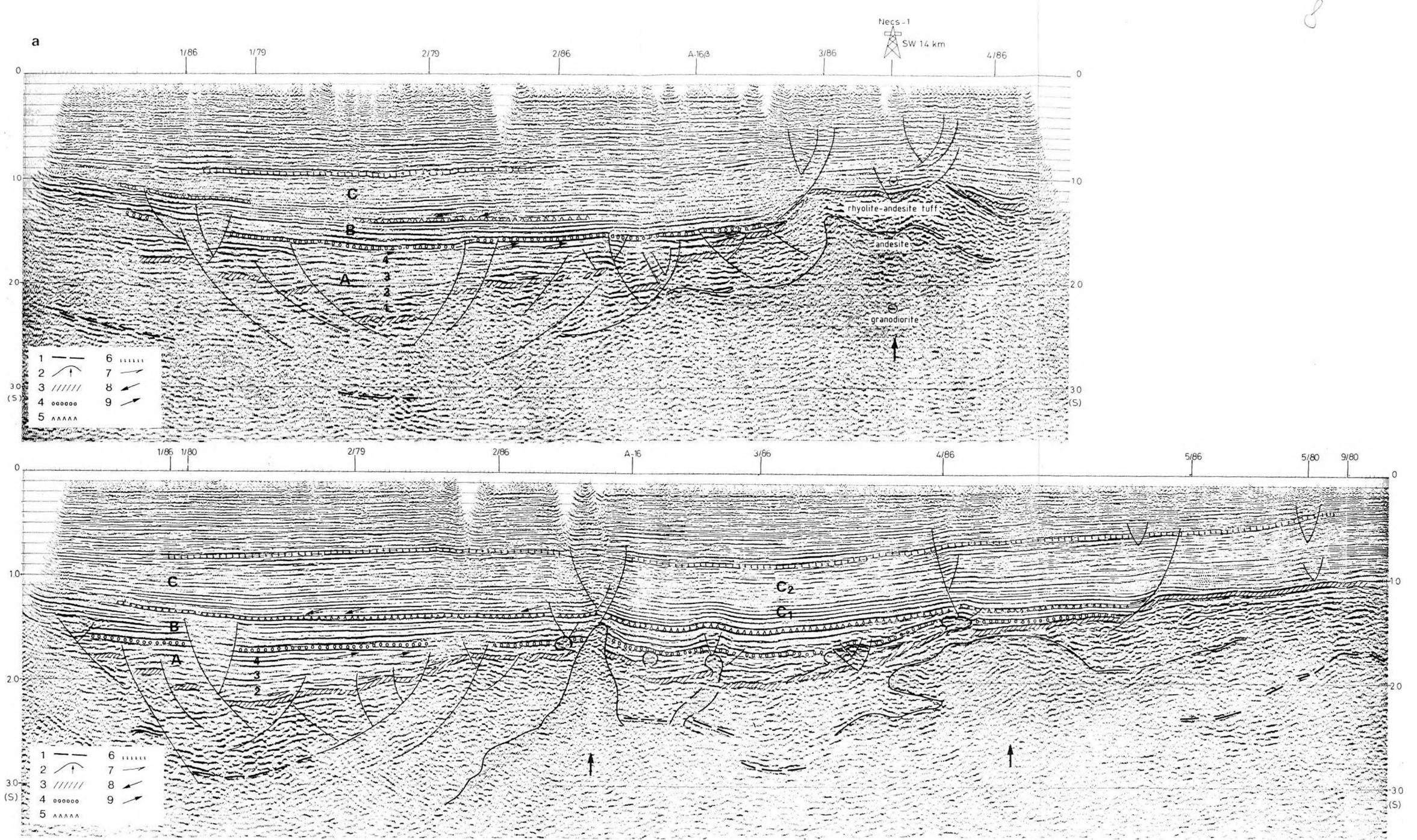


Fig. 5. Migrated time sections: a) Me-8/86, b) Me-9/86 (for legend see Fig. 4)

5. ábra. Migrált időszelvények: a) Me-8/86, b) Me-9/86
 1 — medencealjzat (mezozoos vagy idősebb); 2 — szubvulkáni intruzió, vagy vulkáni központ; 3 — pannóniai üledékek és miocén vulkanitok határa; 4 — az A szeizmikus szekvencia felső határa; 5 — a B szeizmikus szekvencia felső határa; 6 — a C szeizmikus szekvencia felső határa; 7 — rálapolódás; 8 — alsó elvégződés; 9 — felső elvégződés

Рис. 5. Временные разрезы
 а) Me-8/86, б) Me-9/86
 1 — фундамент (мезозойский или более древний); 2 — субвулканическая интрузия или вулканический центр; 3 — контакт паннонских отложений и миоценовых вулканитов; 4 — верхний контакт сейсмической единицы А; 5 — верхний контакт сейсмической единицы В; 6 — верхний контакт сейсмической единицы С; 7 — налегание с выклиниваниями; 8 — нижнее замыкание; 9 — верхнее замыкание

Most of these bodies are covered by a thick blanket of volcanic tuffs which is overlain by the Pannonian marine series. In profile Me-9/86 (*Fig. 5/b*) we can see another type of subvolcanic body emerging: the narrow steep forms intrude into the marine sediments, the main body has several branches all looking very much like dykes.

Profile Me-9/86 facilitates the estimation of the age difference between the two volcanic bodies of different origin. With this aim, let us see what can be deduced from seismic stratigraphy. The deepest marine sequence (*A*) onlaps the — probably eroded — surface of the volcanic hills. Signs of erosion are not trivial everywhere, but at some places, as in profile Me-12/86 (*Fig. 4*), it is. Sequence *A*, starts to fill up the deepest parts of the Mátészalka basin (*Fig. 6*) and gradually diminishes towards the south until the last member wedges out on the flank of the volcanic hill in the southern end of the profile. At the top of sequence *A*, signs of toplap can be seen (*Fig. 5/b*) marking a short time interval of sea-level drop. The second sequence (*B*), characterized by extremely good reflections both in energy and continuity, onlaps the elevations of sequence *A*, and the same volcanic hill on which sequence *A* wedges out. Sequence *C* — most probably a deltaic sequence, at least on the northern end of the profile — uniformly covers all former sediments. The change of character northward from the top of the volcanic intrusion refers to environmental transition from delta plain to prodelta. This suggests that the immediate surrounding of the intrusion was originally more elevated, the listric faults above it marking the collapse of a higher dome. Both from structure and stratigraphy one can deduce that the intrusion must have happened around the time marked by the boundary between sequences *B* and *C*.

The uniform cover of sequence *C* can be regarded as Upper Pannonian lake-marsh-lacustrine sediments [BÉRCZI and PHILLIPS 1985]. From seismic data two maps were constructed: a contour map of the Sarmatian-Pannonian boundary (*Fig. 6*) and a combined map showing the contours of the Mesozoic (or crystalline) basement and the top of those magmatic bodies which can be regarded either intrusive or stratovolcanic but of lavas dominating (*Fig. 7*). The deep parts of the migrated time sections suffer from increasing unreliability — caused by decreasing signal-to-noise ratio. Yet one feature seems to be quite certain: in the zones of magmatic intrusion the basement disappears, as if dissolved by the upsurging magma.

3. Gravity and magnetic data

Verification of the seismic interpretation can be expected from gravity and magnetic modelling. The schematic Bouguer anomaly map of the area (*Fig. 8*) shows a regional minimum, all local effects appearing as secondary anomalies. The geomagnetic *DZ* map (*Fig. 9*) is somewhat similar: the integrated effect of nearby volcanic bodies gives a composite anomaly map smothering the individual anomalies.

To improve on both gravity and magnetic anomaly maps, a numerical filter test was carried out with a band-pass filter and a high-pass filter [MESKÓ 1967, 1968]. The resulting maps are presented in *Figs. 10, 11, 12* and *13*. It is obvious that the high-pass filter of $k=6$ provided the best resolution by enhancing the anomalies corresponding to the narrow intrusion of profile Me-9/86 (*Fig. 5/b*).

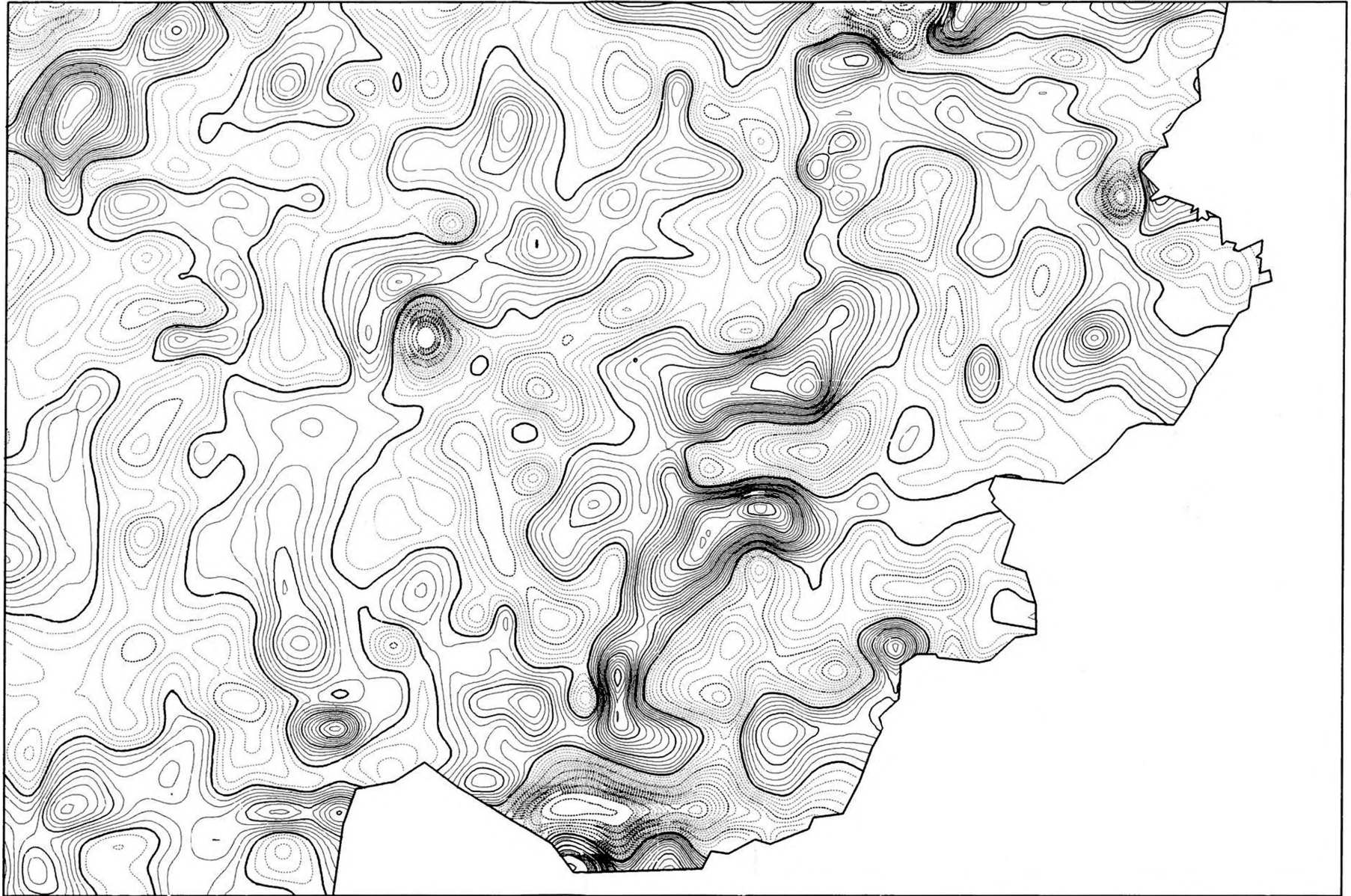


Fig. 13. Filtered ΔZ -anomaly map, $\kappa = 6$. Positive anomalies — continuous lines, negative anomalies — dashed lines. Contour interval: 2 nT

13. ábra. Szűrt ΔZ -anomália térkép, $\kappa = 6$. Pozitív anomáliák folytonos, negatív anomáliák szaggatott vonallal jelölve. Szintvonalköz: 2 nT

Рис. 13. Карта остаточных ΔZ -аномалий, $\kappa = 6$. Положительные аномалии обозначены сплошными, отрицательные — пунктирными линиями. Сечение изолиний — 2 нТ

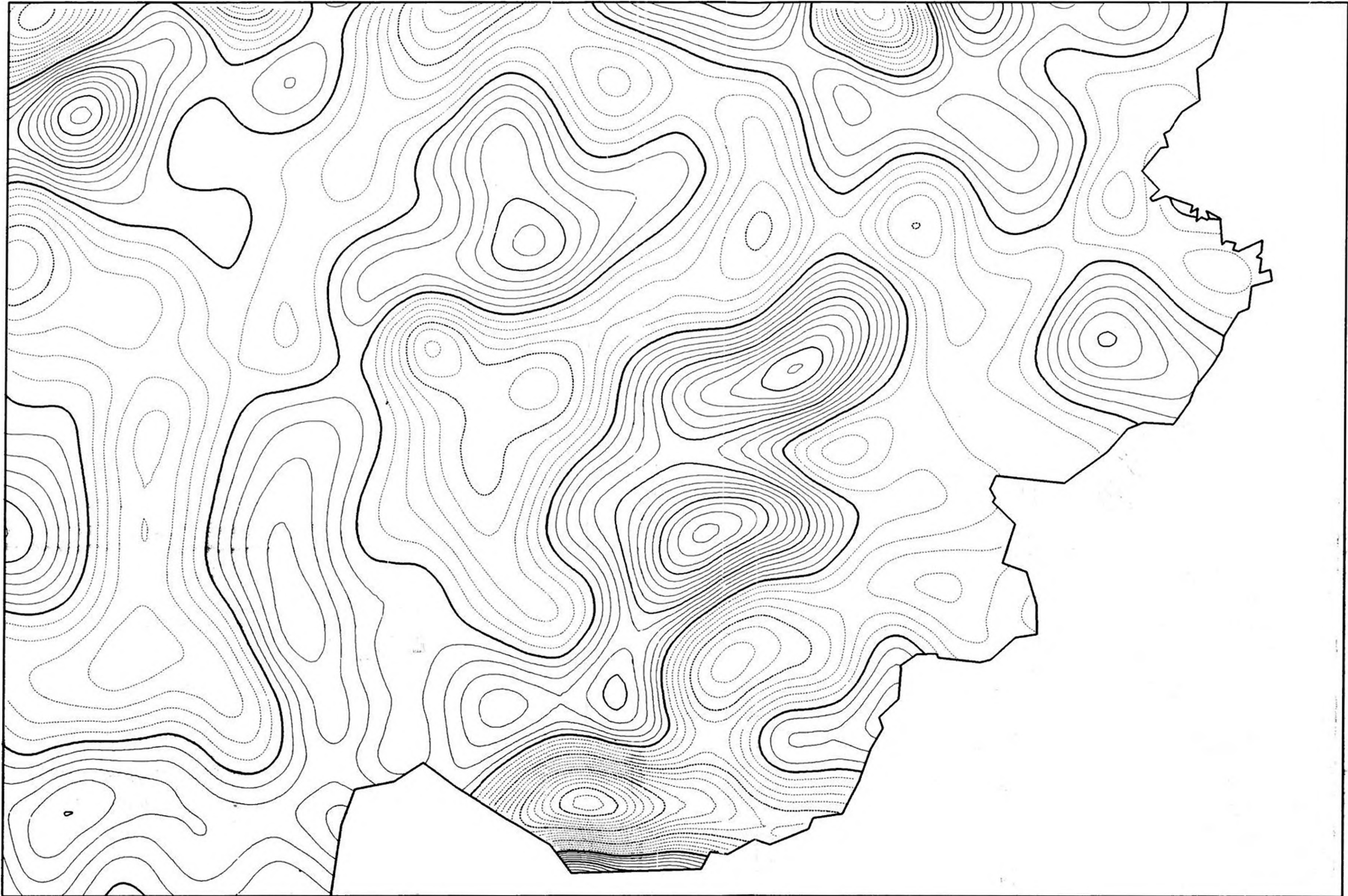


Fig. 12. Filtered ΔZ -anomaly map, $\kappa = 7-4$. Positive anomalies — continuous lines, negative anomalies — dashed lines. Contour interval: 2 nT

12. ábra. Szűrt ΔZ -anomália térkép, $\kappa = 7-4$. Pozitív anomáliák folytonos, negatív anomáliák szaggatott vonallal jelölve. Szintvonalköz: 2 nT

Рис. 12. Карта остаточных ΔZ -аномалий, $\kappa = 7-4$. Положительные аномалии обозначены сплошными, отрицательные — пунктирными линиями. Сечение изолиний — 2 нТ

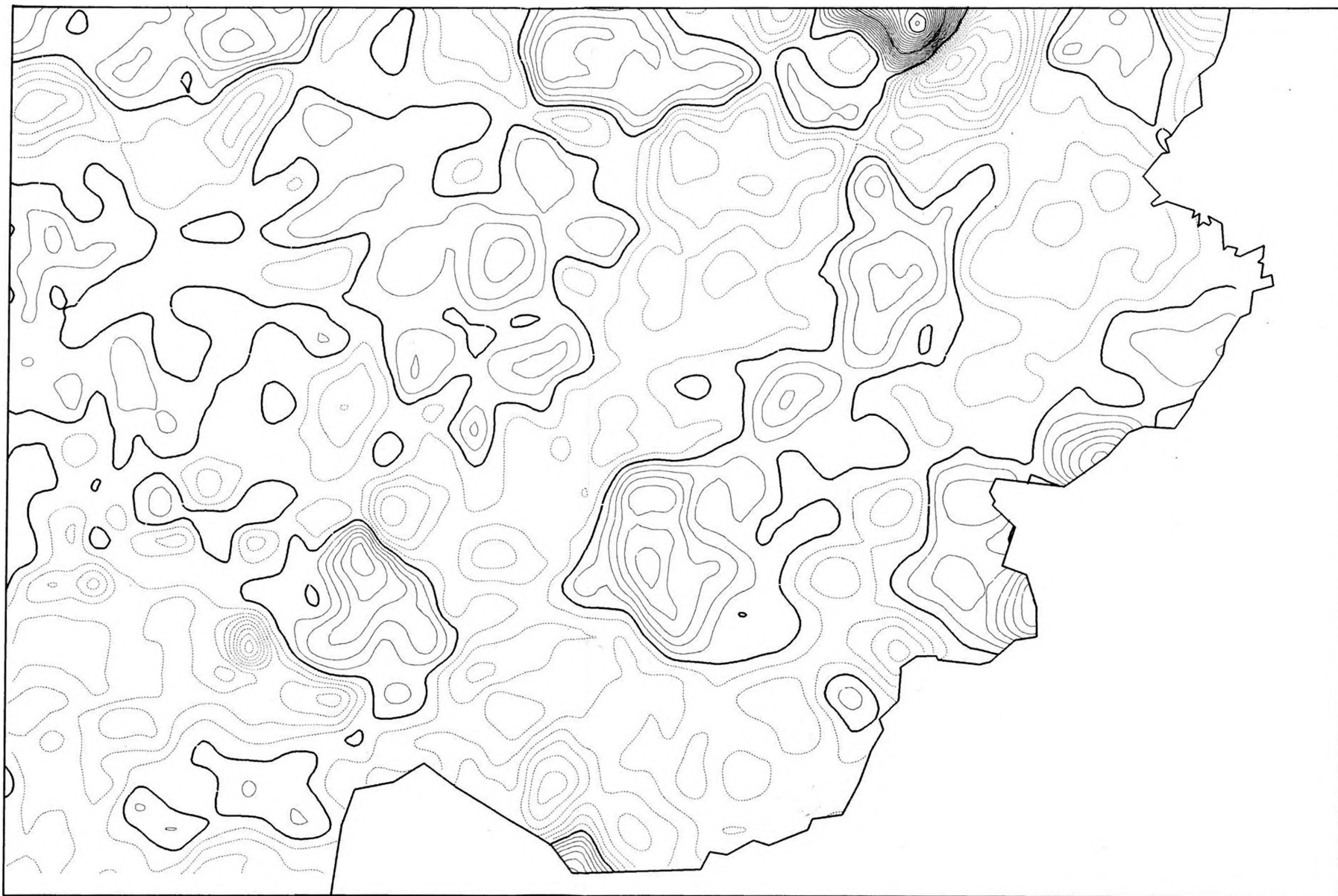


Fig. 11. Filtered gravity anomaly map, $\kappa = 6$. Positive anomalies — continuous lines, negative anomalies — dashed lines. Contour interval: 0.1 mGal

11. ábra. Szűrt gravitációs maradékanomália térkép, $\kappa = 6$. Pozitív anomáliák folytonos, negatív anomáliák szaggatott vonallal jelölve. Szintvonalköz: 0,1 mgal

Рис. 11. Карта остаточных гравитационных аномалий $\kappa = 6$. Положительные аномалии обозначены сплошными, отрицательные — пунктирными линиями. Сечение изолиний — 0,1 мгал

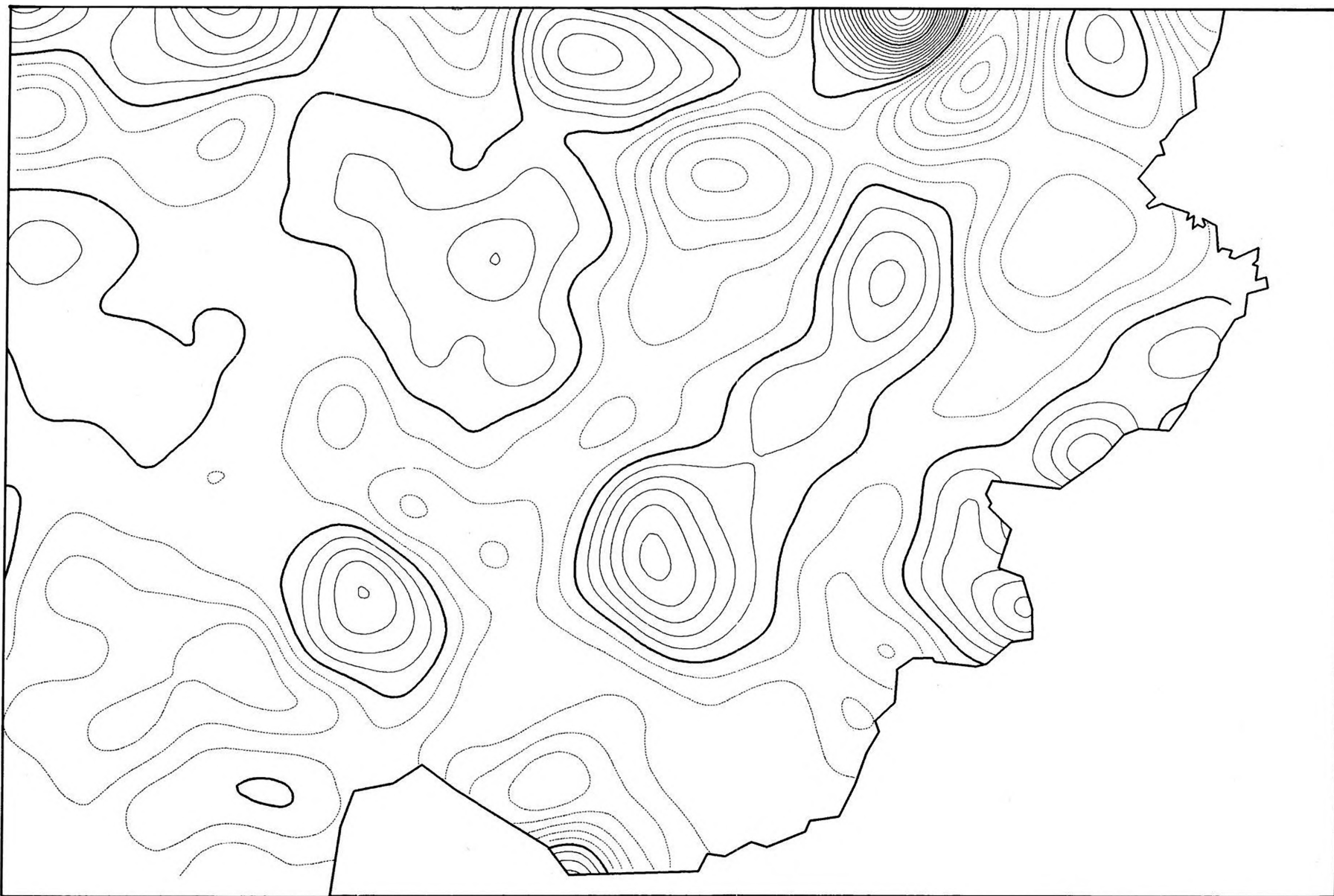


Fig. 10. Filtered gravity anomaly map, $\kappa = 7-4$. Positive anomalies — continuous lines. negative anomalies — dashed lines. Contour interval: 0.1 mGal

10. ábra. Szűrt gravitációs maradékanomália térkép, $\kappa = 7-4$. Pozitív anomáliák folytonos, negatív anomáliák szaggatott vonallal jelölve. Szintvonalköz: 0,1 mgal

Рис. 10. Карта остаточных гравитационных аномалий, $\kappa = 7-4$. Положительные аномалии обозначены сплошными, отрицательные — пунктирными линиями. Сечение изолиний — 0,1 мгал

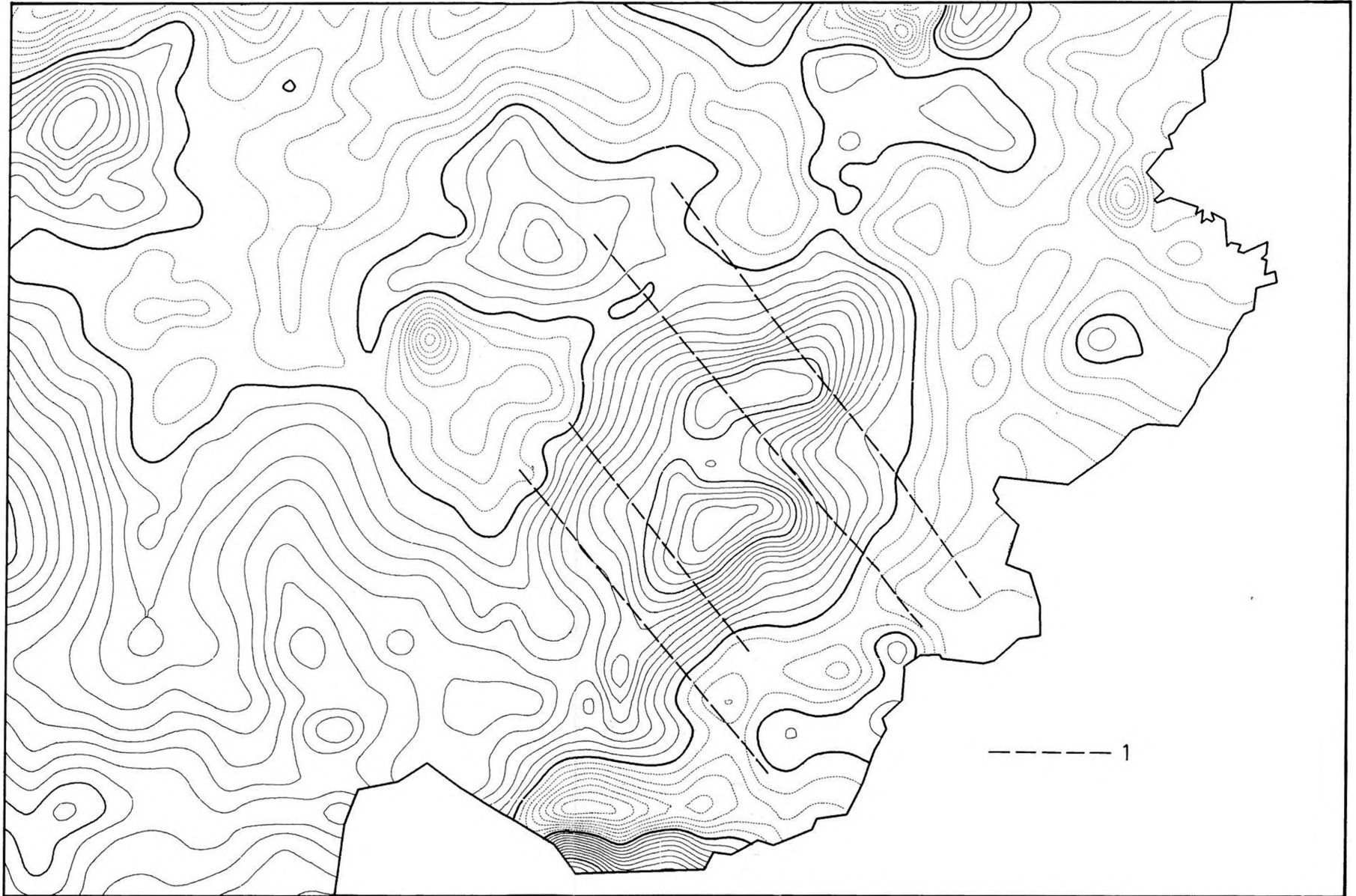


Fig. 9. ΔZ -anomaly map. Positive anomalies — continuous lines, negative anomalies — dashed lines
 . Contour interval: 10 nT. 1 — line of model calculation

9. ábra. ΔZ -anomália térkép. Pozitív anomáliák folytonos, negatív anomáliák szaggatott vonallal jelölve.
 Szintvonalköz: 10 nT. 1 — modellszámítás helye

Рис. 9. Карта аномалий ΔZ . Положительные аномалии обозначены сплошными,
 отрицательные — пунктирными линиями. Сечение изолиний — 10 нТ
 1 — профиль модельных расчетов

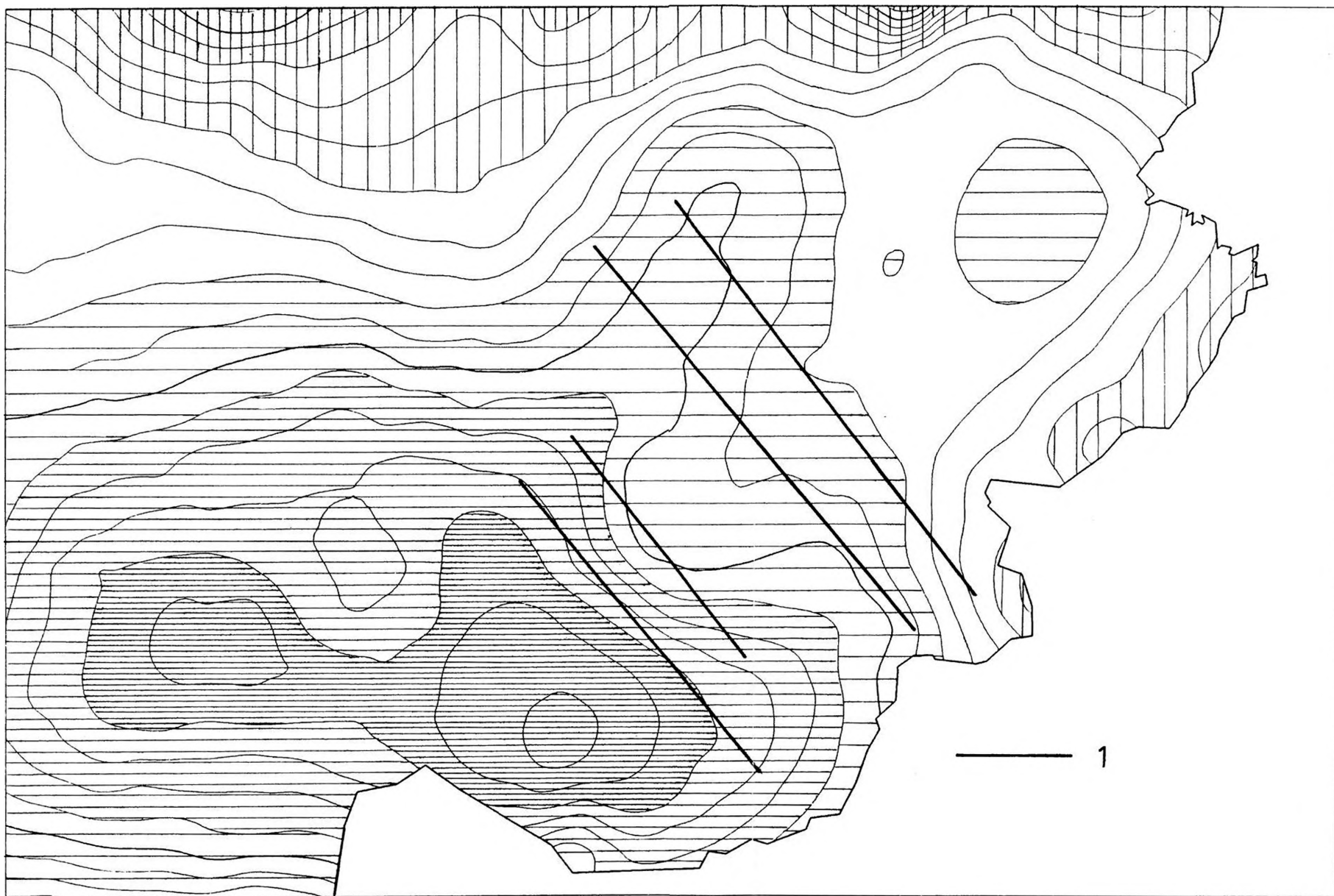


Fig. 8. Bouguer anomaly map. Horizontal shading: negative anomalies, vertical shading: positive anomalies, with growing density – increasing negative and positive values. Contour interval: 1 mGal. 1 — line of model calculation

8. ábra. Bouguer-anomália térkép. Vízszintes vonalkázás negatív, függőleges vonalkázás pozitív anomáliákat jelöl, a vonalkázás sűrűsége növekvő anomália értékekkel növekszik. Színtvonalköz: 1 mgal
1 — modellszámítás helye

Рис. 8. Карта аномалий Буге. Горизонтальной штриховкой обозначены отрицательные, вертикальной — положительные аномалии, густота штриховки возрастает с усилением аномалий. Сечение изолиний — 1 мгал
1 — профиль модельных расчетов

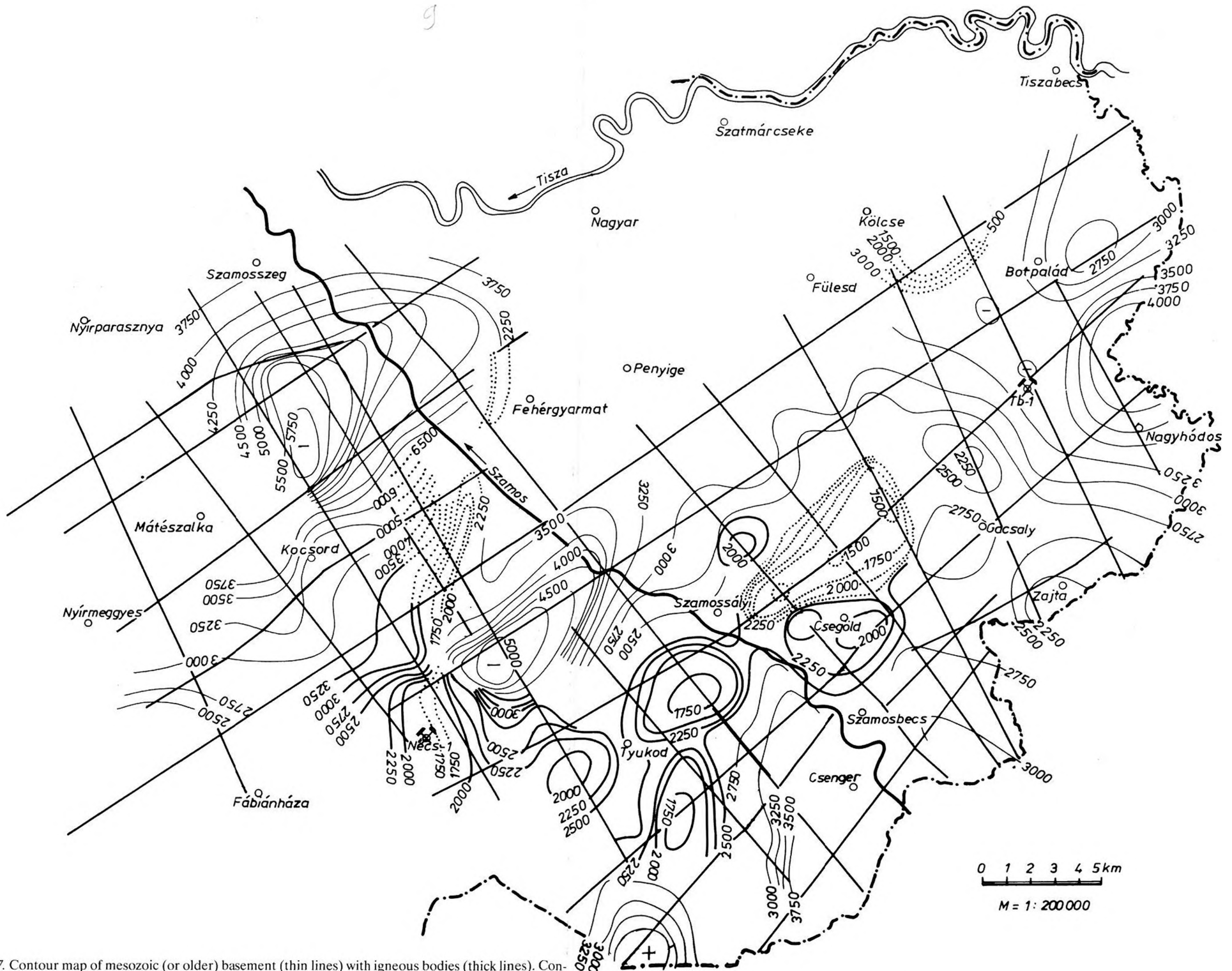


Fig. 7. Contour map of mesozoic (or older) basement (thin lines) with igneous bodies (thick lines). Contour interval: 250 m. Bodies of normal magnetization are marked by continuous lines, those of reversed magnetization by dotted lines

7. ábra. A mezozoos (vagy idősebb) aljazat szintvonalas mélységtérképe (vékony vonalak) kombinálva a vulkáni testek felszínének mélység szintvonalával (vastag vonalak). Szintvonalköz: 250 m. Normál mágnesezettségű testek folytonos vonallal, fordított mágnesezettségű testek pontozott vonallal jelölve

Рис. 7. Карта изолиний равных глубин залегания мезозойского (или более древнего) фундамента (тонкие линии) в комбинации с картой изолиний равных глубин залегания кровли вулканических тел (жирные линии). Сечение изолиний — 250 м. Прямо намагниченные тела обозначены сплошными, а отрицательно — пунктирными линиями

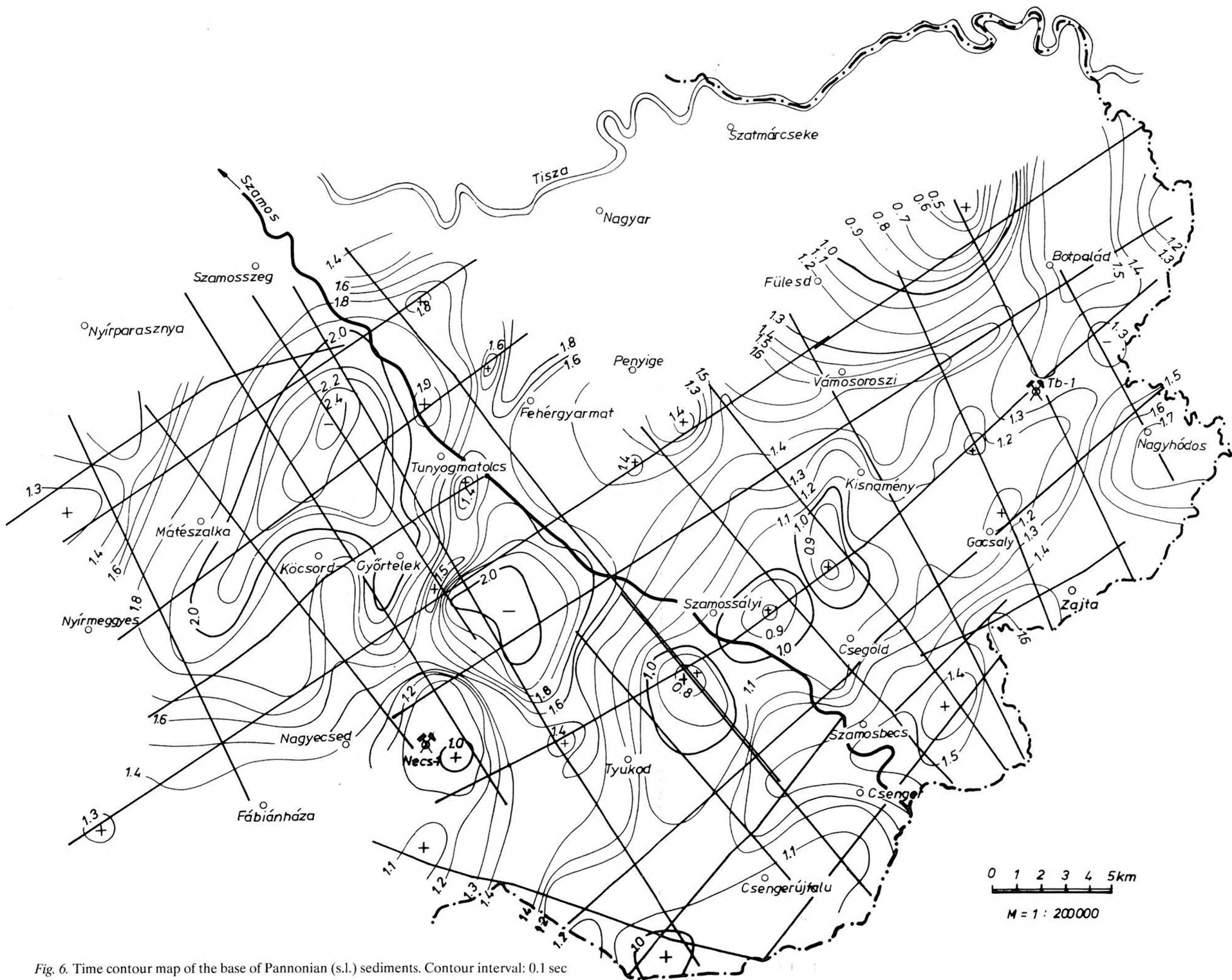


Fig. 6. Time contour map of the base of Pannonian (s.l.) sediments. Contour interval: 0.1 sec

6. ábra. A pannóniai üledékek aljzatának időszintvonalas térképe. Szintvonalköz: 0,1 s

Рис. 6. Карта подошвы паннонских (s. l.) отложений в изолиниях времени. Сечение изолиний — 0,1 сек

For forward modelling the unfiltered data had to be used. Numerical model calculations started from fixed shape and position; the variables being density differences and susceptibility and inclination, respectively. Locations of model calculations are marked on the Bouguer anomaly- and the ΔZ -anomaly map. The models providing the best fit are presented in *Figs. 14 and 15*.

The density differences resulting from the modelling are realistic: the tuff caps of the volcanic bodies provide lower density than the overburden ($\Delta\sigma = -0.1 - -0.2 \text{ t/m}^3$) except for profile Me-12, most probably because of the distorting effect of the regional anomaly. The volcanic bodies (either stratovolcanic with lavas dominating or subvolcanic intrusions) could be modelled by a positive density difference varying between 0.25 and 0.45 t/m^3 , reflecting the ratio of lavas. The basement shows the most uniform density difference of $+0.50 - +0.55 \text{ t/m}^3$.

The magnetic modelling provided susceptibility- and inclination values — both of which can be regarded as rough approximations only. Inclination influences the horizontal shift of the anomaly, while susceptibility affects its amplitude. The

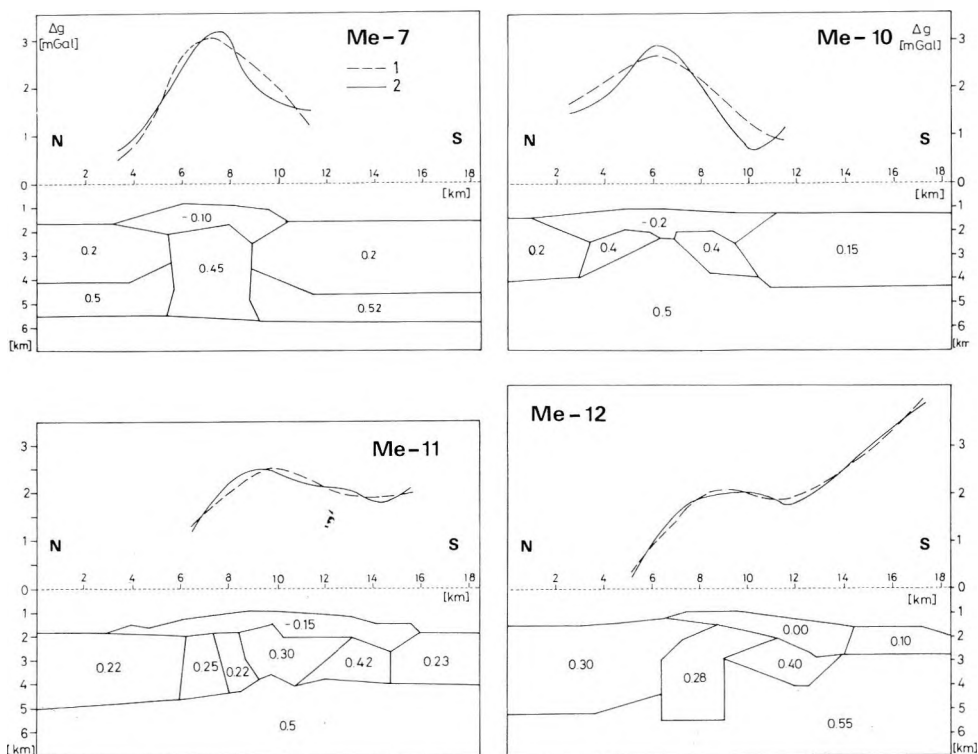


Fig. 14. Gravity model calculations, density differences in t/m^3 . 1 — observed anomaly; 2 — calculated anomaly

14. ábra. Gravitációs modellszámítások, sűrűségkülönbségek t/m^3 -ben. 1 — mért anomáliák; 2 — számított anomáliák

Рис. 14. Расчет гравитационных моделей, разности плотностей — в т/куб. м
1 — аномалии измеренные; 2 — аномалии расчетные

susceptibilities are rather low for andesitic sources ($\kappa = 0.0010 - 0.0028$ cgs = $12.6 \cdot 10^{-3} - 35.2 \cdot 10^{-3}$ SI), but not absurdly low. This seems to back the presumptions of the sources being centres of stratovolcanoes. The tuff caps are non-magnetic. For shifting the anomalies to the proper place, in most cases $I=110^\circ$ was needed, which — in the present field of 63.5° — can mean reversed polarity, although the near-lying igneous bodies disturb each other's magnetic field. In profile Me-7, where a single body is the source, $I=63.5^\circ$ provided the best shift.

The main problem of both models is the distorting effect of the regional field. The filtered anomaly maps separate the local and regional fields but the anomaly values of the residuals become distorted by the computation. Thus they are not suitable for modelling. A qualitative method of estimating both normal and reversed polarity of the magnetic source is to determine the direction of the neces-

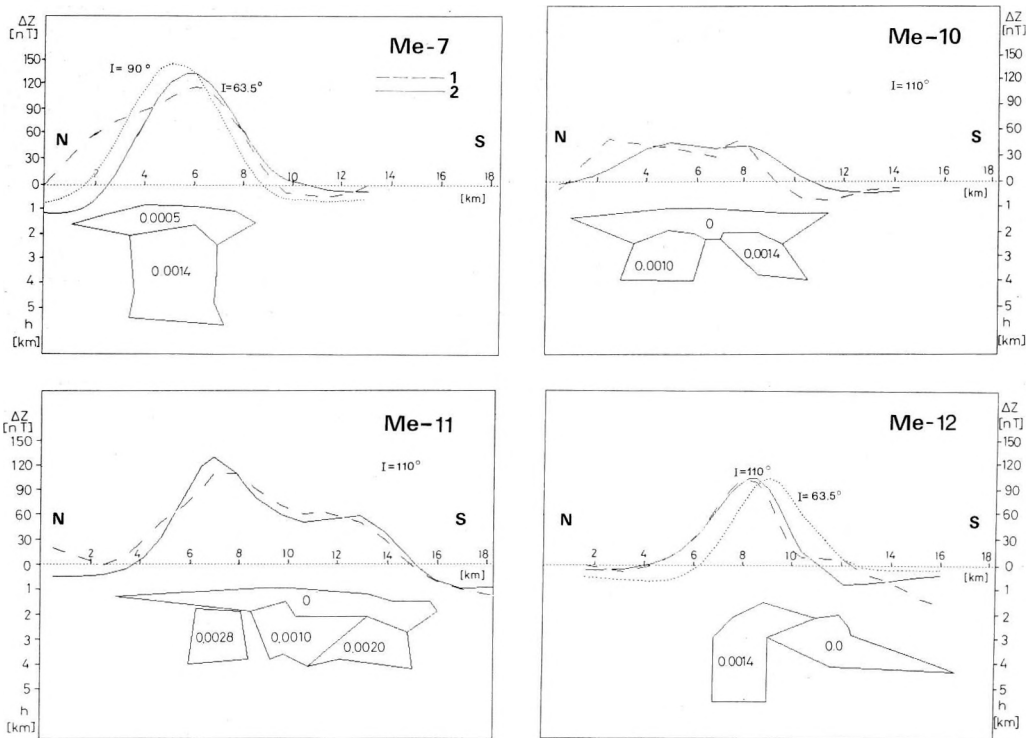


Fig. 15. Geomagnetic model calculations, susceptibilities in cgs. 1 — observed anomaly; 2 — calculated anomaly (dotted lines mark anomalies where the inclination value used for computation produced misfit)

15. ábra. Mágneses modellszámítások, szuszceptibilitás értékek cgs-ben. 1 — mért anomáliák. 2 — számított anomáliák (pontozott vonallal egy nem jó illeszkedést eredményező inklinációval számított görbét jelöltünk)

Рис. 15. Расчет геомагнитных моделей, значения восприимчивости — в CGS 1 — аномалии измеренные; 2 — аномалии расчетные (пунктирной линией обозначена кривая, рассчитанная при наклонении, не обеспечивающем удовлетворительной сходимости)

sary shift. As the shape and position of the source is known from seismics, this procedure is acceptable. The filtered anomaly maps can then be used to refine this approximation. Thus we cannot provide a definite inclination value, only a classification of the volcanic bodies according to their polarity. In this way we can classify all volcanic bodies appearing in the seismic sections and not only those where model calculations were carried out. The result is presented in Fig. 7 by drawing the contours of the normal polarity sources with continuous and the reversed polarity sources by dotted lines.

4. Interpretation

Seismic stratigraphy of Eastern Hungary has been studied by several authors [POGÁCSÁS - VÖLGYI 1982, KÉSMÁRKY et al. 1982, MATTICK et al. 1985]. Most of these studies relate to one or two deep wells; for correlation of lithostratigraphy and seismic stratigraphy, the 5842 m deep Hód-I well is generally used. The deepest part of the lithostratigraphic column is represented by Badenian argillaceous marl and aleurite. Deposits of considerable thickness of Badenian (or Sarmatian) marine sediments only appear in the deepest subbasins (in Hód-I from 5164 m till 5842 m bottom-hole depth), otherwise they form a thin (maximum 200 m) cover on the basement. The seismic character of this sequence is not uniform and is affected by tectonic events. Therefore — in the absence of any borehole penetrating Badenian marine sediments in our study area — it is extremely difficult to decide by seismic stratigraphic means whether the marine sediments of the deep Mátészalka basin belong to the Badenian or to the Pannonian. As timing of the volcanic intrusion of profile Me-9/86 (Fig. 5/b) is very important, we have to try to integrate all available information to determine the age of the sediments it intruded. The Komoro-I borehole — the only one in NE Hungary penetrating the Mesozoic basement — is far to the north from our present area (see Fig. 1). There, below 1328 m of Pannonian-Quaternary sediments and 1872 m of volcanic tuffs, a 341 m thick layer of Badenian argillaceous marl was found above Middle Triassic limestone and dolomite. Thus we cannot exclude the possible presence of Badenian sediments.

In profile Me-9/86 (Fig. 5/b), the deepest seismic sequence marked by *A*, can be followed till near the southern end, where it onlaps the elevation connected to the volcanic intrusion of Nagyecsed, which consists mainly of volcanic tuffs. K/Ar age determinations on the Nagyecsed cores provided ages around 11 Ma, which signifies upper-most Badenian or lower-most Pannonian. Thus the sediments overlying this volcanic complex cannot be older than Pannonian. If we still do not want to accept that all marine sediments belong to the Pannonian, we ought to divide seismic sequence *A* into two. In profile Me-9/86 there is no sign of a sequence boundary. In profile Me-8/86 (Fig. 5/a) which traverses the deepest part of the Mátészalka basin, there is an angular unconformity between 2.0 and 2.1 sec. The 300 ms thick sequence of partly high-energy reflections and partly a reflection-free zone, may be regarded as a separate seismic sequence and classified as older than Pannonian. If by similarity this is transferred to profile Me-9/86, it would result in transposing members 1 and 2 of sequence *A* into the Badenian. Even with this reduced thickness, the volcanic intrusion penetrated a 700 ms (~1400 m) thick Pannonian complex.

Studies of the Pannonian basin with the methods of basin analysis [HORVÁTH et al. 1986, POGÁCSÁS et al. 1988] provided rates of subsidence and sediment accumulation. Estimated values for this latter — compaction included — are 0.5–1.0 mm/year. The 1400 m thick Pannonian sediments thus indicate 1.4–2.8 Ma between the two volcanic cycles. This result is in accordance with the K/Ar age determinations (Table I and Fig. 1) which found 8–10 Ma old rocks in the boreholes of Gelénes and Kiszvárd and in the outcrops of Tarpa and Nagyszöllős along the Soviet–Hungarian border.

The overall trend of the age of volcanism becoming younger and younger towards the northeast is even backed by the change of polarity from normal to reversed (Fig. 7). The 8–10 Ma old volcanic activity not constrained to a small area proves that even in the Lower Pannonian tectonic forces were still active in the area.

Acknowledgements

The authors wish to express their thanks to the National Oil and Gas Trust for enabling them to publish this work. They appreciate the contribution of all colleagues working in seismic data processing — first of all Zoltán Timár — and Róbert Stomfai and Attila Sárhidai, who helped them with gravity and magnetic modelling, and computer graphics, respectively.

REFERENCES

- BÉRCZI I. and PHILLIPS R. L. 1985: Processes and depositional environments within Neogene deltaic-lacustrine sediments, Pannonian basin, southeast Hungary. *Geophys. Trans.*, **31**, 1–3, pp. 55–74
- HARLAND W. B., COX A. V., LLEWELLYN P. G., PICKTON C. A. G., SMITH A. G., WALTERS R. 1982: A geologic time scale. Cambridge Earth Sci. Ser., Cambridge University Press, 131 p.
- HORVÁTH F., DOVÉNYI P., VERMES M. and HARGITAY M. 1986: Reconstruction of compaction of Neogene sediments from seismic and well data (in Hungarian). ELTE Geoxp. VGMK report, Budapest, 91 p.
- KÉSMÁRKY I., POGÁCSÁS GY. and SZANYI B. 1982: Seismic stratigraphic interpretation in Neogene–Quaternary depressions of eastern Hungary (in Hungarian). *Magyar Geofizika*, **23**, 1–2, pp. 20–30
- MATTICK R., RUMPLER J. and PHILLIPS R. L. 1985: Seismic stratigraphy of the Pannonian basin in southeastern Hungary. *Geophys. Trans.*, **31**, 1–3, pp. 13–54
- MESKÓ A. 1967: Gravity interpretation and information theory II. Smoothing and computation of regionals. *Annales Univ. Sci. Bud. Sectio Geologica*, **10**, pp. 15–27
- MESKÓ A. 1968: Gravity interpretation and information theory III. The method of second derivatives. *Annales Univ. Sci. Bud. Sectio Geologica*, **11**, pp. 37–60
- NEMESI L., HOBOT J. 1981: Geoelectric investigation of the deep structures of the eastern part of the Great Hungarian Plain (in Hungarian with English abstract) *Geophys. Trans.*, **27**, pp. 7–98
- NEMESI L., POLCZ I., STOMFAI R., SZEIDOVITZ ZS. 1986: Volcanic rocks of the Nyir region as revealed by geophysics. Paper presented in Hungarian at a special meeting of the Ass. of Hung. Geophys. May 27–28, 1986, Miskolc
- NEMESI L., CSORGEI J. and LÁDA F. 1987: Geoelectric measurements in the Nyir region (in Hungarian). *Ann. Report of ELGI for 1986*, pp. 63–65
- POGÁCSÁS GY., VÖLGYI L. 1982: Seismic representation of Pannonian lithostratigraphic and lithogenetic units in eastern Hungary (in Hungarian). *Magyar Geofizika*, **23**, 3, pp. 82–93

- POGÁCSÁS GY., SZALAY Á., LAKATOS L., SZANYI B., VÁRNAI P. 1988: Backstripping based on seismic stratigraphy in the Pannonian Basin. Proceedings of the 33rd Int. Geophys. Symp. Prague, pp. 127–138
- SZÉKY-FUX V., PÉCSKAY Z., BALOGH K. 1987: Radiometric chronology of the buried Miocene volcanics of northern and central Transbiscia (in Hungarian with English and Russian abstract). Bull. of the Hung. Geol. Soc., 117, 3, pp. 223–235

A NYÍRSÉG NEOGÉN VULKANIZMUSA A LEGÚJABB GEOFIZIKAI ADATOK TÜKRÉBEN

KILÉNYI Éva, POLCZ Iván és SZABÓ Zoltán

A nyírségi kutatást hátrányosan befolyásoló neogén vulkáni testek jellegének, sztratigráfiai helyzetének megismerése segítségünkre lehet a terület köolaj- és földgáz-perspektívitásának értékelésében. Az 1986. évi szeizmikus reflexiós mérések minden korábbinál jobb minőségű szelvényeket eredményeztek. Ezeket elválaszthatók a tufák a szubvulkáni testektől, ezáltal megnyitva az utat újszerű gravitációs és mágneses modellszámításokra. Az anomália-térképeken némely kisebb ható nem ismerhető fel, ezért az összetett hatók szétválasztására szűrés kísérletet végeztünk. A két anomália-térképsorozat már lényegesen jobb korrelációt biztosít a szeizmikus szelvényekkel. A szeizmikával meghatározott ható alakzatokból és mélységekből kiindulva meghatároztuk a sűrűség-különbségeket, illetve a szuszeptibilitás- és inklináció értékeket. A radioaktív kormeghatározási és magnetosztratigráfiai adatok összevetéséből arra a következtetésre jutottunk, hogy a vulkanitokat két, egymástól 1–2 millió évvel elválasztott vulkáni ciklus hozta létre, a második a Pannon medencét kialakító legfiatalabb tektonikai mozgásokhoz kapcsolódva.

НЕОГЕНОВЫЙ ВУЛКАНИЗМ НЬИРСКОГО РЕГИОНА (ВОСТОЧНАЯ ВЕНГРИЯ) В СВЕТЕ ПОСЛЕДНИХ ГЕОФИЗИЧЕСКИХ ДАННЫХ

Эва КИЛЕНЬИ, Иван ПОЛЬЦ и Золтан САБО

Познание характера и стратиграфического положения неогеновых вулканических тел, оказывающих неблагоприятное влияние на проведение геологоразведочных работ в Ньирском регионе, может оказаться полезным при оценке нефтегазоносности. В 1986-ом году сейсморазведка методом отраженных волн дала профили лучшего, чем когда-либо прежде, качества. На них можно отделить туфы от субвулканических тел, обеспечивая возможность расчета нового типа по определению гравитационных и магнитных возмущающих тел. На картах аномалий некоторые из небольших тел уже не распознаются, поэтому проведены эксперименты по фильтрации с целью разделения сложных тел. Полученные серии карт аномалий обнаруживают сильно улучшенную корреляцию с сейсмическими профилями. Исходя из морфологических особенностей и глубины залегания возмущающих тел, по данным сейсмиоразведки, были определены разности плотностей, а также значения магнитной восприимчивости и наклона. Путем сопоставления данных по радиологическому возрасту и магнитостратиграфическим сделан вывод о том, что вулканы возникли в ходе двух циклов, разделенных перерывом длительностью в 1–2 млн. лет, причем второй из них связан с наиболее молодыми тектоническими движениями, оформившими Паннонскую впадину.

**FAULT SYSTEM DYNAMICS AND SEISMIC ACTIVITY—
EXAMPLES FROM THE BOHEMIAN MASSIF AND THE WESTERN
CARPATHIANS**

Vladimír SCHENK^{*}, Zdeňka SCHENKOVÁ^{*} and Lubomil POSPÍŠIL^{**}

Two fault systems have been investigated from the viewpoint of their long- and short-term dynamics. The following features have been studied: character of the geological development of the systems during the Late Tertiary and Quaternary, geological evidence of horizontal and vertical movements of structural blocks; crustal movements, remote sensing data (lineaments determined from satellite images), data on seismic activity, gravity and magnetic anomalies. They were found to confirm horizontal displacements along the lineaments investigated. Both their direction and position were determined.

Keywords: seismic activity, satellite images, wrench-fault tectonics, seismotectonics, geodynamics, Bohemian Massif, Western Carpathians.

1. Introduction

The mechanism of rock fracturing depends on the stress and strain conditions in the Earth's crust and Upper Mantle. In our paper attention is given to geological and geophysical features, to remote sensing data and to seismological investigations of selected areas, thus contributing to identifying new fault systems in the upper part of the Earth's crust with characteristics common in strike-slip faults. Therefore ANDERSON's [1951] and MOODY and HILL's [1956] theories on wrench-fault tectonics can be applied, in which the dominant motion of one block relatively to the other is horizontal and the fault planes are essentially vertical.

The term wrench fault is a translation of the German word *blatt*, originally used by SUESS [1885], and is synonymous with the terms strike-slip fault and transcurrent fault. Some concepts of wrench-fault dynamics have been developed by ANDERSON [1951], KENNEDY [1946], HUBBERT [1951], HAFNER [1951], BILLINGS [1954], MOODY and HILL [1956]. ANDERSON [1951] outlined the fundamental concept of rock fracturing. The planes of actual shear do not coincide with the planes of maximum shear stress, but lie closer to the axis of maximum compressive stress and far from the angle of shear. HUBBERT [1951] indicated that although this angle depends on the properties of the materials, a good average for rocks is approximately 31 ± 2 degrees. HAFNER [1951] emphasized that the orientation of the stress ellipsoid was variable. Many observations of tectonic faulting (normal-, thrust- and wrench faults) can be explained by the orientation of the stress ellipsoid. MOODY and HILL [1956] extended the works on faulting of ANDERSON [1951],

^{*} Geophysical Institute, Czechosl. Acad. Sci. Božni II/1401, 14131 Praha 4-Spořilov, Czechoslovakia

^{**} Geofyzika, Ječná 29a, 61246 Brno 12, Czechoslovakia

Manuscript received (revised version): 20 May, 1989

HAFNER [1951] and HUBBERT [1951] by developing the hypothesis that folds, thrust faults and wrench faults could be generated as a result of the movement along a large wrench fault.

A hypothetical wrench-fault system determines 1st-, 2nd- and 3rd-order wrench faults with their corresponding drag folds [MOODY and HILL 1956]. This model was applied to two sites in Czechoslovakia to explain movements of blocks. The first site belongs to a relatively old Variscan structure of the Bohemian Massif, the other to young structures of the Western Carpathians. Both structures were affected by the latest Alpine orogeny.

2. Data and method of interpretation

Some systems of lineations were distinguished in the Bohemian Massif and in the Western Carpathians on LANDSAT images [DOKTÓR and GRANICZNY 1982, POSPÍŠIL et al. 1986]. According to geophysical and geological data [MALKOVSKÝ et al. 1974, KLINEC et al. 1985], some horizontal displacements along these systems can be supposed although subsequent vertical movements mask their features. The lineations are located in seismooactive areas. Along these lineations a lot of evidence of wrench-fault tectonics can be found.

The lineaments detected in satellite images were drawn into the map of lineations and compared to the occurrences of earthquakes, geological data and results of geophysical measurements. In this way we obtained independent data for delineation and verification of the interpreted boundaries and information on their geodynamic activity. As to the geological data, we focused our attention on the pattern of the known fault systems — on the jointed crush belts, on the regions with manifestations of gravity tectonics, on the directions and orientations of axes of sedimentary basins, as well as on their development in time and space.

From the viewpoint of geomorphology we were mainly interested in the orientations of ridges and valleys, in the pattern of the river network and in the erosion forms of the tectonic systems. Gravity and magnetic maps or rather some types of their derivatives, the map of vertical density contacts [LINSSE 1967], the map of horizontal gradients as well as other types of derived maps appeared to be suitable material for geodynamic studies. A comparison of lineaments with the results of palaeomagnetic studies contributed to the definition of the types of the tectonic boundaries.

The comparison of the lineation map with the map of earthquake epicentres [SCHENKOVÁ et al. 1979, KÁRNÍK et al. 1984], i.e. the correlation of some interpreted boundaries with earthquake occurrences is presented. In order to obtain some information on the dependence of seismic energy attenuation in the broader vicinity of earthquake foci and its relationship to the geological structure, we analyzed the known macroseismic fields [Eds: PROCHÁZKOVÁ and KÁRNÍK 1978].

It is known that the asymmetry of macroseismic fields of earthquakes discloses the directions of decreased seismic energy attenuation. An anomalous decrease of seismic energy with distance can be accounted for by the structure of the area: if waves propagate parallel to structural directions, they are less attenuated than if they propagate across these directions. To enhance such directions some macroseismic fields were processed in the following way: in twelve (30 degree angles) radial

directions starting from the earthquake epicentre (*Fig. 1*) the radii R_i corresponding to the same attenuation were read. This means the distances of the isoseismal from the epicentre R_i where $i = 1, 2, \dots, 12$, were obtained and by averaging them, the mean radius, \bar{R} , of the given isoseismal was calculated. Then by a simple subtraction ($R_i - \bar{R}$) we obtained positive or negative deviations from the mean radius R . The average of the positive deviations are illustrated in circular direction diagrams and drawn in the tectonic maps. the relations between the intensity deviations and structural elements were observed in all the diagrams. The elongation of the deviations gives the direction in which a smaller attenuation of energy takes place.

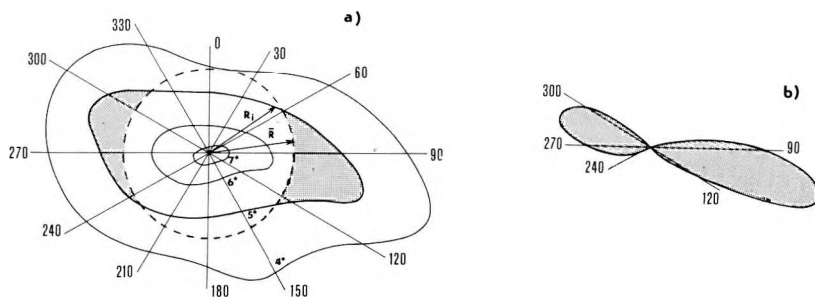


Fig. 1. Graphical determination of directions of lower seismic energy attenuations around an earthquake epicentre from the asymmetric shape of its isoseismal field

a) example for the isoseismal of 5°, b) direction is expressed by positive value $R_i - \bar{R}$

1. ábra. A földrengés epicentrumok körüli kisebb csillapítási irányok grafikus meghatározása az izoszeizták aszimmetrikus alakjából

a) az 5-ös izoszeiztára kidolgozott példa, b) a szerkezeti irányt az $(R_i - \bar{R})$ pozitív értékei tükrözik

Рис. 1. Графическое определение направлений минимального затухания вокруг эпицентров землетрясений по асимметрии изосейст.

a) Пример, разработанный для изосейсты 5, b) структурное направление отражается положительными значениями $(R_i - \bar{R})$

3. Hronov–Poříčí fault system (Bohemian Massif)

3.1 Geological characteristics

The Hronov–Poříčí tectonic system (*Fig. 2, E*) is about 20 km long and runs in the NW–SE direction and separates the Intra–Sudetic depression (*Fig. 2, c*) from the Krkonoše piedmont basin (*Fig. 2, b*). The main fault is an overthrust [MALKOVSKÝ et al. 1974; Ed.: TÁSLER 1983] and forms the NE boundary of the Hronov–Poříčí trough. The fault zone lies between two tectonic systems: the Main Sudetic fault (*Fig. 2, B*) bounds it in the north and the Lužice–Jílovice system (*Fig. 2, A*) in the south.

The Main Sudetic fault is of Variscan age and is probably connected with the Asturian movements [OBERC 1972]. It lies crosswise to the main tectonic units of that age, e.g. in relation to the axis of the flexure of the Eastern Krkonoše, to the northern edge of the Variscan intrusion of Krkonoše Granite and to the Asturian

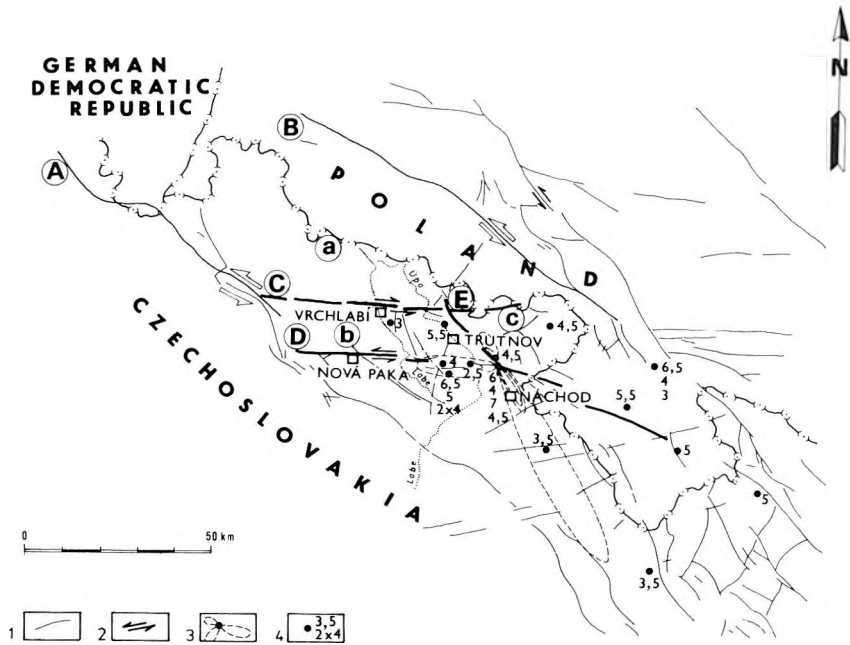


Fig. 2. Tectonic sketch and earthquakes of the Hronov-Poříčí fault system

1 — fault; 2 — horizontal displacement; 3 — direction of lower seismic energy attenuation;

4 — earthquake epicentre and its intensity; A — Lužice-Jilovice fault;

B — Main Sudetic fault; C — Vrchlabí lineament; D — Nová Paka lineament;

E — Hronov-Poříčí fault zone; a — Krkonoše Mts.;

b — the sub-Krkonoše piedmont; c — Intra-Sudetic depression

2. ábra. A Hronov-Poříčí törérendszer tektonikus vázlatja és földrendései

1 — törés; 2 — horizontális elmozdulás 3 — csökkent szeizmikus csillapítási irányok;

4 — földrendés epicentrum és intenzitás értékek; A — Lužice-Jilovice törés; B — fő Szudéta törés;

C — Vrchlabí lineamens; D — Nová Paka lineamens; E — Hronov-Poříčí töréses öv;

a — Krokonoše helység; b — szub-Krkonoše előtér; c — Intruszudéta süllyedék

Рис. 2. Тектоническая схема и землетрясения Хроновско-Поричской системы разломов.

1 — разломы; 2 — горизонтальное смещение; 3 — направления минимального

сейсмического затухания; 4 — эпицентры землетрясений и значения их интенсивности;

A — Лужицко-Йиловицкий разлом; B — Главный Судетский разлом; C — Врхлабский

линеамент; D — Нова-Пакский линеамент; E — Хроновско-Поричская зона разломов;

a — Карконошские горы; b — форланд Карконошских гор; c — Внутрисудетский прогиб

and Laramide structures in the surrounding basins. Therefore the Main Sudetic fault could be assumed to be connected with tension and in principle, to gravity tectonics. Some segments of the Main Sudetic fault probably came into existence as a result of tangential stresses parallel to it (strike-slip fault), which caused the flexural slope of the Eastern Krkonoše to be formed. OBERC [1972] proved that after the Main Sudetic fault was formed, movements took place many times along it and that the fault was accompanied by numerous smaller shifts of different age. Movements along the Main Sudetic fault were still going on in the Tertiary Age.

The Lužice–Jílovice fault zone (Fig. 2, *A*) belongs to the most significant sub-hercynian normal faults of NW–SE direction in the Bohemian Massif. In some parts, the faults have a reverse character of movements [MISAŘ et al. 1983]. Even though horizontal movements have not been geologically documented along the fault zone, some authors assume their existence [BALATKA et al. 1983, ZEMAN et al. 1983]. The evidence of these movements can be found in geophysical maps and remote sensing data. The Lužice–Jílovice fault zone is assumed to have a deep-seated character. Changes of directions in the courses of rivers and axis orientations of young anticlines show that the fault must have also been active in the Tertiary Age [ZEMAN et al. 1983]. Extensive effusions of Neogene basalts are observed in the whole zone between the Sudetic faults and the Lužice–Jílovice zone.

We presume the wrench tectonics model [MOODY and HILL 1956] to be valid for the explanation of the origin and the present mobility of the Hronov–Poříčí fault zone. In consequence of the horizontal movements on the above-mentioned pair of wrench fault systems (Main Sudetic and Lužice–Jílovice), we presume that at bifurcations, a system of transcurrent faults of the 2nd order originated (Nová Paka and Vrchlabí). These are distinctly discernible in satellite images.

3.2. Seismological data

The movement of the blocks along the Hronov–Poříčí wrench-fault system first gave rise to a flexure and later to an overthrust of the constituent blocks with respect to each other. The existence of these movements is corroborated not only by the presence of the gravity and magnetic anomalies in the places of block faults, but also by the distribution of the earthquakes in this area.

In respect to the recent seismic activity [PROCHÁZKOVÁ and KÁRNÍK 1978, SCHENKOVÁ and KÁRNÍK 1988], the Hronov–Poříčí fault zone is one of the most active in Bohemia. The last recorded shocks of November 21, 1979 ($I_0 = 5^\circ$ MSK), and of May 7, 1984 ($i = 4.5^\circ$ MSK), testify to continuous tectonic movement along this fault system. The earthquake epicentres lie south of the fault on the Nová Paka lineament (Fig. 2, *D*). They apparently involved even the strongest earthquake in Bohemia this century on January 10, 1901, the epicentre of which was between Trutnov and Náchod, and with macroseismic effects as much as 7° MSK. Another strong earthquake occurred on January 31, 1883, in the valley of the Úpa river ($I_0 = 6.5^\circ$ MSK). The origin of this can be associated with the Nová Paka tectonic zone. The macroseismic fields of earthquake shocks are mostly elongated in the direction of the Krkonoše Mts., i.e. in the NW–SE Sudetic direction. The focal depths determined by macroseismic observations vary from 5 to 15 km.

3.3 Seismotectonic and geodynamic analyses

Since no fault plane solutions that would allow the main directions of faults to be determined exist in this region, we analysed the shape of the isoseismals as described in Chapter 2, to determine the tectonic directions.

The asymmetry of the macroseismic field of the January 10, 1901 shock, exhibits two directions of decreased seismic energy attenuation with distance (Fig. 2):

- direction NW–SE corresponding to the orientation of the local structures, determined from the isoseismals of the near field;
- direction approximately E–W reflecting the structural conditions of a broader vicinity of the shock, determined from the isoseismals of the far field.

Both these directions coincide with the previously determined faults; the former coincides with the orientation of the Hronov–Poříčí fault and the latter with the orientation of the 2nd-order sinistral wrench faults (Nová Paka and Vrchlabí lineaments).

If we analyze the data from the point of view of wrench-fault tectonics [MOODY and HILL 1956], it seems that the pressure is still active, rejuvenating the faults in the Hronov–Poříčí fault zone (Fig. 3) from time to time. Since a recent movement along the Ohře rift is assumed to have a divergent character [KOPECKÝ 1979], we can suppose the pressure is acting in the E–W direction. Under such conditions the Lužice–Jílovice and the Main Sudetic faults are considered 1st-order wrench faults, and the Nová Paka and Vrchlabí lineaments can be considered as 2nd-order wrench faults. The Hronov–Poříčí fault, as an overthrust, balances the compression caused by the uplift, the movement and rotation of the Krkonoše Mts. block to the SE, and the movement of this block between the Nová Paka and Vrchlabí lineaments. In both cases, the character of the movements along these lineaments could be considered as sinistral strike slips. It is also confirmed by the deformation of river courses and by the orientation of young anticlines.

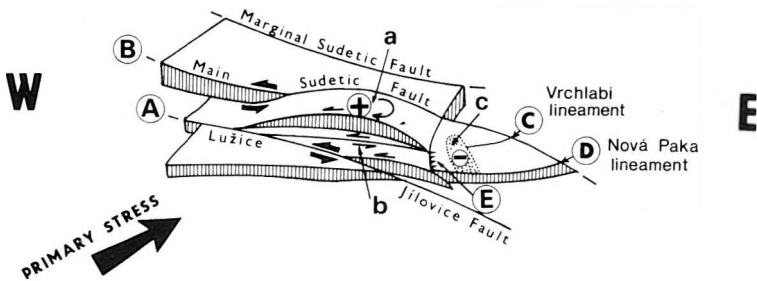


Fig. 3. Schematic block diagram of movements along and around the Hronov–Poříčí fault zone
+ : elevation; - : depression; for other symbols see Fig. 2.

3. ábra. A Hronov–Poříčí törésés öv menti és körüli mozgások vázlatos blokkdiagrammja
+ : kiemelkedés; - : süllyedék; egyéb jelöléseket lásd a 2. ábrán.

Рис. 3. Схематическая блок-диаграмма смещений вдоль Хроновско–Поричской зоны разломов и в ее окрестностях
+ : поднятие; - : прогиб; прочие обозначения см. на рис. 2

4. Revúca fault system (Western Carpathians)

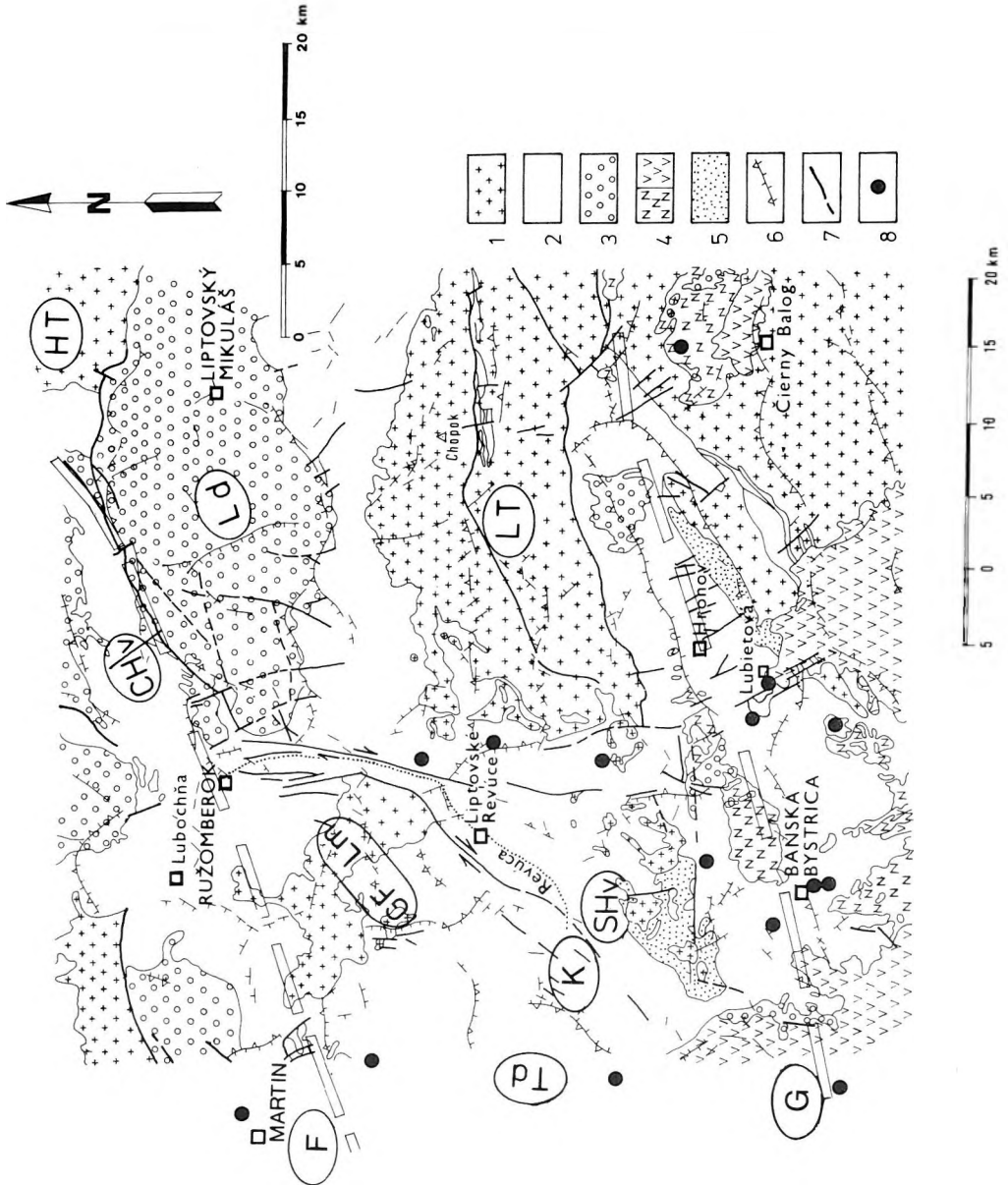
4.1 Geological characteristics

KUBÍNÝ [1962] assumed the Revúca fault system (*Fig. 4*) to be of Variscan age. According to BUJNOVSKÝ [1979] it is a dextral strike-slip fault accompanied by a system of secondary faults oriented perpendicularly to the main displacement direction, and is active from time to time even in the Quaternary. The dextral displacement of the Lubochna Crystalline Massif was inferred from its erect position on the north side, from longitudinal faults that reach as far as the Križna nappe (*K*), from the tectonic contact of the Lower Cenomanian–Neocomian complexes with the granitoid core, and from the straight line of the Revúca river valley, which is typical of large displacements. The Revúca fault system (*Fig. 5, H*) is located between two major tectonic elements; the Myjava–subTatra (*F*) [JANKŮ et al. 1984] and the Hron (*G*) tectonic zones [KLINEC et al. 1985, POSPÍŠIL et al. 1986]. These two zones are plotted in *Fig. 4.*, too, and marked by the same letters. Both are regarded as horizontal displacements.

The Myjava–subTatra tectonic zone represents a significant lineament that influences the distribution and position of the fundamental blocks in the Western Carpathians. For instance, the Klippen belt starts west of Vienna, runs NE in the basement of the Vienna basin as far as the Myjava–subTatra lineament near the town of Kúty [JIRÍČEK 1978, KOCÁK et al. 1973], then it turns into the direction of this lineament (i.e. the ENE direction) and after approximately 40 km it resumes the original direction. In this part, an intensive vertical gradient of recent crustal movements was observed (the southern block of the Vienna basin subsiding—KVÍTKOVIČ and VANKO 1980). A similar distance can be observed between elevated crystalline blocks of the Little Carpathians, the Povážský Inovec Mts., and the Little Fatra. The results of MUŠKA and VOZÁR [1984] furnished a new significant fact. They found distinct differences in the palaeomagnetic directions within Palaeozoic complexes of the Tatrídes [ANDRUSOV 1965]. These differences can be observed along both the Myjava–subTatra and the Hron lineaments (*Fig. 5*).

The Hron tectonic zone [DOKTŮR and GRANICZNY 1982, KLINEC et al. 1985] is of essential importance in the formation of the gravity nappe in the Low Tatra area (*Fig. 6*). The change of the axes of gravity anomalies accompanying Tertiary depressions (in *Fig. 5* from west to east: Piešťany bay — i, Topolčany bay–Bánovce depression — g–h, Bacúrov depression — l) and of the gradients of positive gravity anomalies of the Little Carpathians, the Tribeč Mts., and the Branisko Mts. are the main manifestations of the Myjava–subTatra and Hron tectonic zones, the latter being traced up to the flysch belt [POSPÍŠIL et al. 1986]. The earthquake occurrences along the Hron tectonic zone give evidence that the boundary is active even today. In the section between the towns of Banská Bystrica and Brezno, bounded by the Revúca and the Mýto–Tisovec faults (*Fig. 5, H and J*), the focal depths reached 10 km. Based on the fault plane solutions, the character of movements was found to be horizontal displacement [POSPÍŠIL et al. 1985], and it can be assumed that it was a right–lateral strike slip.

There is indirect evidence of the Myjava–subTatra and Hron tectonic zones in the map of the Western Carpathians [FUSÁN et al. 1971], e.g. the faults or fault zones in the Danube–Rába basin, which mainly strike NE–SW and bound the basement structural elements, turn to the ENE–WSW direction corresponding to the gravity data [IBRMAJER 1964]. Moreover, in the area between the two fault zones, the thick series of the Central Carpathian Palaeogen sediments is preserved under



Miocene sediments [FUSÁN et al. 1971, 1987]. The importance of these lineaments in the Western Carpathians is further confirmed by recent seismic activity along these lines.

4.2 Seismological data

The data on the occurrence of strong earthquakes [BOUČEK 1987, PROCHÁZKOVÁ and KÁRNÍK 1978, SCHENKOVÁ and KÁRNÍK 1988] in Central Slovakia (Fig. 4) mostly come from an earlier period so that the epicentres of some shocks around the Revúca fault system might be inaccurate. Nevertheless, it can be shown that except for the earthquakes confined to the Verona-Semmering-Vah lineament in the Western Carpathians [SCHENK et al. 1985, BUDAY et al. 1986], a large number of the earthquakes in Central Slovakia are confined to the surroundings of the Revúca fault system. The strongest earthquake in the region between the Western Carpathians and the Little Fatra occurred near Žilina (Jan. 15, 1858, $I = 7.5^{\circ} - 8^{\circ}$ MSK) at a depth of approximately 12 km. The region afflicted by this shock was elongated in the northwest direction, covered an area of 66 000 square km and reached as far as Moravia.

The earthquakes originating in Central Slovakia are bound to the area of the broader surroundings of the town of Banská Bystrica. To a certain extent, their occurrence can be correlated with the region of the intersection of the Revúca fault system and the Hron tectonic zone. The most interesting, and in fact unclarified, is the strong shock of June 5, 1443 ($8^{\circ} - 9^{\circ}$ MSK), which caused serious damage in a large area. In contemporary writings a shock felt in Hungary, Moravia, Poland, Bohemia and Austria is mentioned. From the fragmentary information available, its

Fig. 4. The Revúca tectonic system

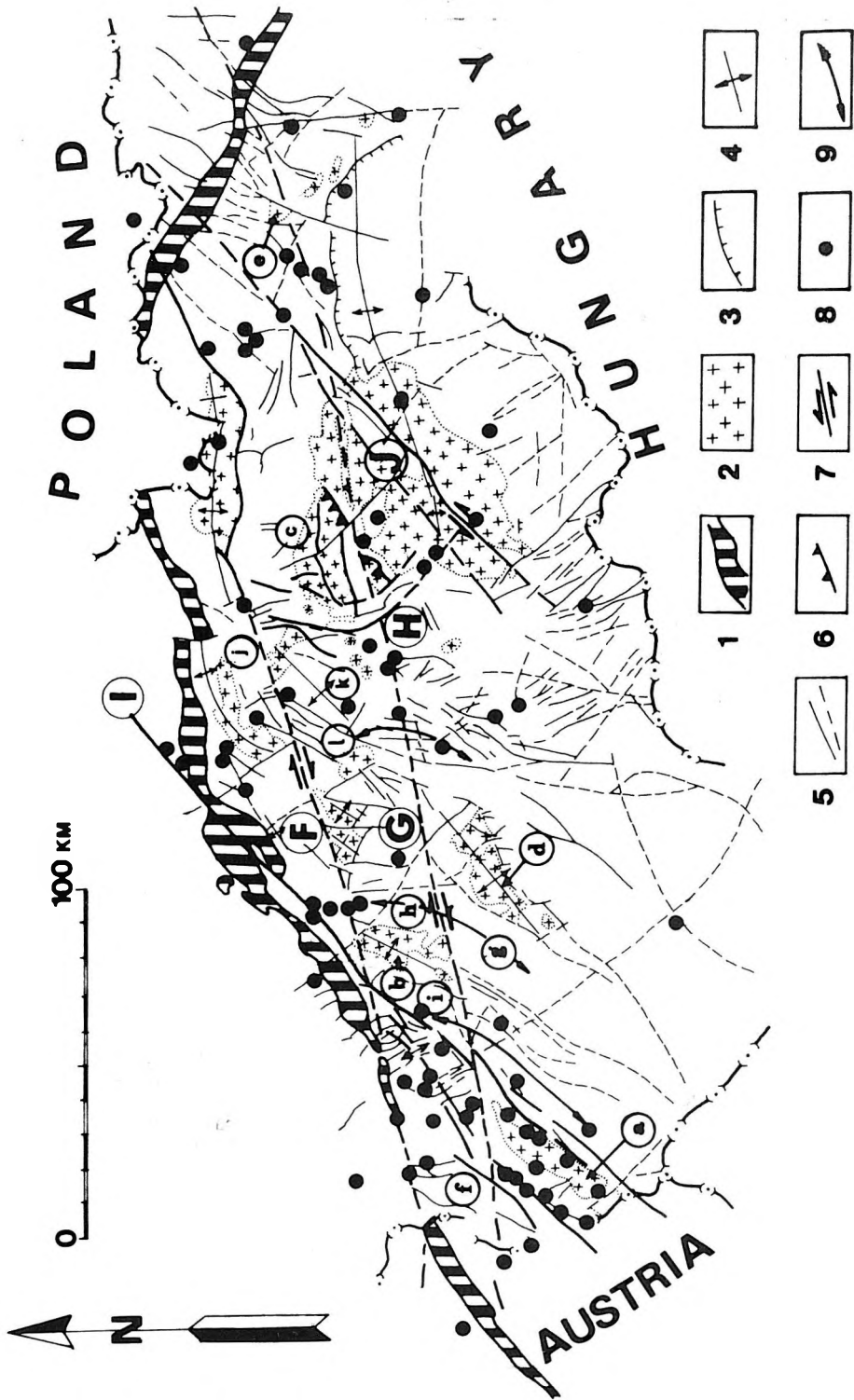
- 1 — crystalline complexes; 2 — Palaeozoic sediments; 3 — Mesozoic complexes;
 4 — Central Carpathian Paleogene; 5 — Neogene sediments and volcanites;
 6 — vertical density contact; 7 — fault; 8 — earthquake epicentre; *HT* — High Tatras;
LT — Low Tatras; *GF* — Great Fatras; *CHv* — Choč Mts.; *LD* — Liptov depression;
Lm — Lubochňa crystalline block; *Td* — Turiec depression; *SHv* — Staré Hory tectonic window;
K — Križná nappe; *F* — Myjava-subTatra linement; *G* — Hron lineament

4. ábra. A Revúca tektonikai rendszer

- 1 — kristályos összletek; 2 — paleozoos üledékek; 3 — mezozoos összletek;
 4 — belső-kárpáti paleogén üledékek; 5 — neogén üledékek és vulkanitok; 6 — függőleges sűrűséghatár;
 7 — törés; 8 — földrengés epicentrum; *HT* — Magas-Tátra; *LT* — Alacsony Tátra; *GF* — Nagy Fáttra;
CHv — Liptói Magura; *Ld* — Liptói süllyedék; *Lm* — Lubochňa kristályos tömb;
Td — Turóczi süllyedék; *SHv* — óhegyi tektonikus ablak; *K* — Krizsna takaró;
F — Míava-szubTátra lineamens; *G* — Garam lineamens

Рис. 4. Ревуцкая тектоническая система.

- 1 — кристаллические комплексы; 2 — палеозойские отложения; 3 — мезозойские толщи;
 4 — центрально-карпатские палеогеновые отложения; 5 — неогеновые отложения и вулканиты; 6 — вертикальные плотностные границы; 7 — разломы; 8 — эпицентры землетрясений; *HT* — Высокие Татры; *LT* — Низкие Татры; *GF* — Великие Фатры; *CHv* — Горы „Хоч“; *Ld* — Липтовская впадина; *Lm* — Любохнинский кристаллический массив;
Td — Турецкая впадина; *SHv* — Тектоническое окно „Старе Хори“; *K* — покров Крижня; *F* — Миявско-Подтатранский линеамент; *G* — Хронский линеамент



position cannot be determined with sufficient accuracy, however. Its location was most probably in the broader neighbourhood of Banská Bystrica [KÁRNÍK et al. 1984]. The depth of this earthquake is estimated to be at 25 km. Its origin could be bound to the Hron tectonic zone, since some other earthquakes (1855, 1862) of an intensity of $6^{\circ} - 6.5^{\circ}$ MSK are also found on this zone between Banská Bystrica and Lubietova. The focal depths of the earthquakes of this region vary within a range of 4 – 12 km.

The earthquake occurrences (Figs. 4, 5 and 6) can be associated with the weakened points of the Hron and Myjava–subTatra tectonic zones, especially where the Revúca fault system crosses them. Even though we know of 18 earthquake shocks in the area under investigation, the lack of direct recordings did not allow us to determine the fault plane solution for any of them. Nevertheless, the available seismological material did enable us to determine the directions of decreased seismic energy (Fig. 6). Use was made of the isoseismal maps known for some of the mentioned shocks, all of them being in the southern part of the area investigated. The analysis shows that in the valley of the Hron river, E-W or actually ENE-WSW directions prevail. Their coincidence with the direction of the Hron tectonic zone is very good [POSPÍŠIL et al. 1986].

4.3 Seismotectonic and geodynamic analyses

In addition to the data on earthquake occurrence, we utilized the results of gravity and magnetic measurements of this area [OBERNAUER 1980], and the correlation of seismological data with lineations determined from satellite images

Fig. 5. Earthquakes and tectonic blocks in the Western Carpathians

1 — Pieniny klippen belt; 2 — crystalline complexes;

3 — overthrust; 4 — axes of the post-Palaeogene anticlines [MAHEL' 1974]; 5 — fault;

6 — gravity nappe; 7 — strike-slip fault; 8 — earthquake epicentres; 9 — axis of gravity low;

F — Myjava–subTatra lineament; G — Hron lineament; H — Revúca fault zone;

I — Verona–Semmering–Váh tectonic zone; J — Mýto–Tisovec fault zone;

a — Little Carpathians; b — Povážský Inovec; c — Low Tatra; d — Tribeč Mts.; e — Branisko Mts.;

f — Vienna basin; g — Topolčány bay; h — Bánovce depression; i — Piešťany bay; j — Little Fatra;

k — Krížna nappe; l — Bacúrov depression

5. ábra. Földrendések és tektonikai tömbök a Nyugati-Kárpátokban 1 — Pieniny szirtöv;

2 — kristályos összlet; 3 — feltolódás; 4 — poszt-paleogén antiklinálisok tengelyei [MAHEL' 1974]

5 — eltolódás; 6 — gravitációs takaró; 7 — eltolódás; 8 — földrendés epicentrum;

9 — gravitációs minimum tengelye; F — Miava–szubTátra lineamens; G — Garam lineamens;

H — Revúca vetőzóna; I — Verona–Semmering–Vág tektonikai zóna; J — Tiszolc–Vámos lineamens;

a — Kis-Kárpátok; b — Inovec; c — Ajacsny Táttra; d — Nagy-Tribečs; e — Branyiszko hegység;

f — Bécsi medence; g — Topolcsányi öböl; h — Bán süllyedék; i — Postényi öböl; j — Kis-Fáttra;

k — Krizsna takaró; l — Turóci süllyedék

Рис. 5. Землетрясения и тектонические блоки Западных Карпат.

1 — зона Пьенинских утесов; 2 — кристаллические комплексы; 3 — взбросы; 4 — оси

последепалеогеновых антиклиналей [МАHEL' 1974]; 5 — разломы; 6 — гравитационные

минимумов; 7 — сдвиги; 8 — эпицентры землетрясений; 9 — оси гравитационных

минимумов; F — Миявско-Подтатранский линеамент; G — Хронский линеамент; H —

Ревуцкая зона разломов; I — тектоническая зона Верона–Земмеринг–Вах; J —

Мито–Тисовецкая зона разломов; a — Малые Карпаты; b — Иновец; c — Низкие Татры;

d — Трибеч; e — горы Браниско f — Венский бассейн; g — Топольчанский залив; h —

Бановцевская впадина; i — Пештянский залив; j — Малые Фатры; k — покров Крижня;

l — Бацуровская впадина

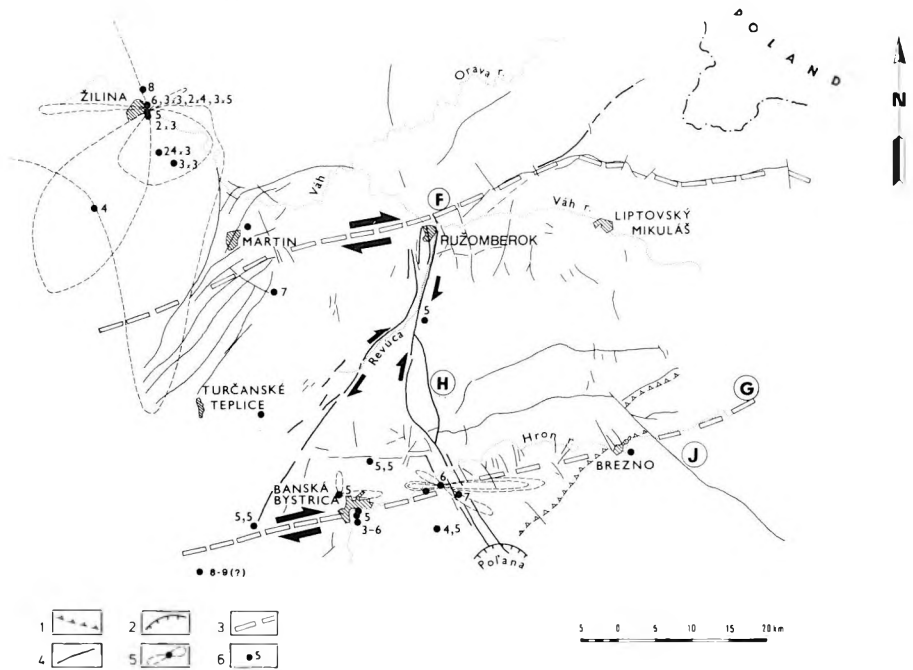


Fig. 6. Dynamics of the Revúca fault system

- 1 — gravity nappe [KLÍNEC et al. 1985]; 2 — central zone of Pol'ana volcanoes;
 3 — wrench fault of the 1st-order; 4 — faults; 5 — direction of the 1st-order seismic energy attenuation;
 6 — earthquake epicentres; for other symbols see Fig. 5

6. ábra. A Revúca vetőrendszer dinamikája. 1 — gravitációs takaró [KLÍNEC et al. 1985];
 2 — a polyánai vulkánok központja; 3 — elsőrendű eltolódás; 4 — vető;
 5 — csökkent szeizmikus csillapítási irányok; 6 — földrengés epicentrum; egyéb jelöléseket lásd az 5. ábrán

Рис. 6. Динамика Ревуцкой зоны разломов.

- 1 — гравитационные покровы [KLÍNEC et al. 1985]; 2 — центральная зона Полянскогo
 вулкана; 3 — главные сдвиги; 4 — разломы; 5 — направления минимального
 сейсмического затухания; 6 — эпицентры землетрясений; прочие обозначения см. на
 рис. 5

[POSPÍŠIL et al. 1985.]. It appears that contrary to previous interpretations, we can include in the dextral transcurrent system even its broader surroundings, i.e. even the tectonic zone that bounds the crystalline basement of the Great Fatra on the east side. According to gravity data the zone continues to the southwest as far as the western margin of the Staré Hory tectonic window [ANDRUSOV 1965]. All the interpreted tectonic elements manifest themselves in the gravity field by sharp gradients.

It is understandable that an analysis of the tectonic history cannot account for the entire development in time and space of the study area. The character of faults, however, suggests the probable stress conditions that must have existed in a given area. A palaeogeographic analysis of the Tertiary development of the area revealed the uplift of the Low Tatra region with respect to its surroundings until the Pliocene Age [KLÍNEC et al. 1985]. In the last period, this uplift accelerated as a consequence

of the horizontal movements of the Carpathian blocks along the faults of ENE-WSW direction [JANKŮ et al. 1984, POSPÍŠIL et al. 1985]. These faults are buried and seated under Tertiary sediments in the crystalline basement. On the surface, only fragments of these faults can be detected (e.g. Strážovské vrchy Mts., High Tatra, Vienna basin etc.).

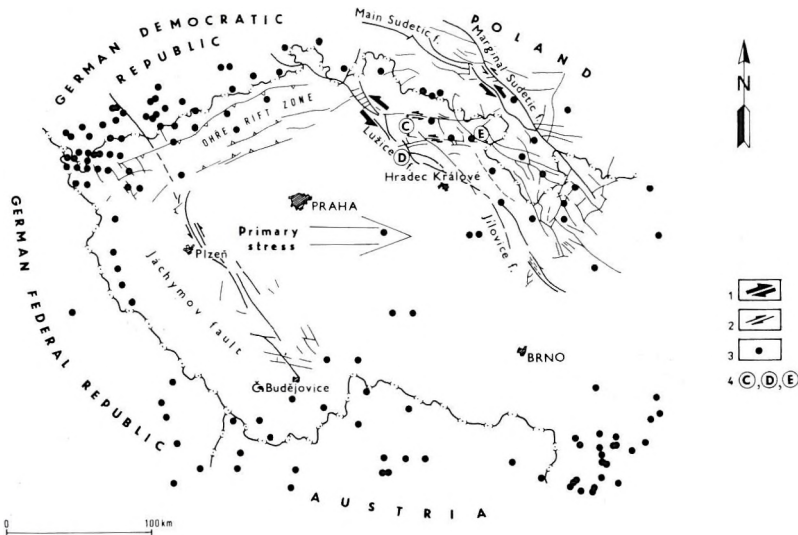


Fig. 7. Dynamics of Recent tectonic movements of the central part of the Bohemian Massif
 1 — 1st-order wrench fault; 2 — 2nd order wrench fault; 3 — earthquake epicentres;
 4 — tectonic zones (for symbols see fig. 2)

7. ábra. A recens tektonika dinamikája a Cseh-masszívum középső részén
 1 — elsőrendű eltolódás; 2 — másodrendű eltolódás; 3 — földrengés epicentrum;
 4 — tektonikai zóna; egyéb jelöléseket lásd a 2. ábrán

Рис. 7. Динамика современной тектоники в центральной части Чешского массива.
 1 — главные сдвиги; 2 — второстепенные сдвиги; 3 — эпицентры землетрясений; 4 — тектонические зоны; прочие обозначения см. на рис. 2

5. Discussion

The seismotectonic and geodynamical analyses of the investigated areas of the Bohemian Massif and the Western Carpathians are based on the following presumptions:

- a) the existence of a Central European rift system [KOPECKÝ 1979], which originated due to mass movement on the lithosphere–asthenosphere boundary;
- b) the rift system played a decisive role in the neotectonic development of the Bohemian Massif and partly of the Western Carpathians [POSPÍŠIL and VASS 1984, Fig. 7];
- c) individual parts of the rift system are limited by deep-seated fault zones; in the case of the Ohře rift these are the Odra and Danube lineaments [POSPÍŠIL and VASS 1984].

According to these presumptions, the main direction of block movement in Bohemia during the Neogene Age was E-W (Fig. 7). Its origin is attributed to opening up of a branch of the Central European rift system — the Ohře rift. Since at that time in the Bohemian Massif Variscan tectonic zones already existed — the Main Sudetic and the Lužice-Jílovice fault systems — extensive vertical as well as horizontal movements occurred along rejuvenated faults that balanced the accumulating stress in the Earth's crust during the Upper Tertiary and Quaternary Ages. The movement of the Bohemian Massif towards the east brought about, in the near-surface parts of the Earth's crust, the action of tensile forces. The orientation of these forces in the marginal belts of the moving block does not substantially differ from the direction of the pressure forces acting at its front.

In the Neogen Age this movement affected the geodynamics of the Western Carpathians. Thus the origin of some of the main transcurrent fault zones in the Western Carpathians can be explained by the Ohře rift. But while in the marginal parts of the Bohemian Massif sinistral movements may be observed (Main Sudetic fault, Lužice-Jílovice fault), in the western part of the Carpathians transcurrent lineaments with dextral movements can be found (Myjava-subTatra tectonic zone, Hron tectonic zone). The evidence of these movements can be traced in the palaeogeographical maps of the Neogene — orientation of basins, sediment types [SENEŠ 1982] — and in palaeomagnetic data [MUŠKA and VOZÁR 1984].

It is characteristic of both regions under investigation that pairs of transcurrent faults originated that controlled and strongly affected the dynamics of the adjoining blocks. The pairs of parallel 1st-order faults with similar movement regularly give rise to 2nd-order faults. Thus the space between the 1st-order faults is segmented into a number of blocks. The character of movements on the 2nd-order faults is then the resultant of the difference of the movements along the 1st-order faults. The 2nd-order faults balance the movement differences on the 1st-order faults, which often leads to a rotation of the blocks between the 1st-order faults. In both regions these features can be observed in the form of intensive uplifts and extensive overthrusts. Gravity and magnetic data support these conclusions.

REFERENCES

- ANDERSON E. M. 1951: The dynamics of faulting. Edinburgh Oliver and Boyd, 206 p.
- ANDRUSOV D. 1965: Geology of the Czechoslovak Carpathians (in Slovak). Slovak Acad. Sci., Bratislava 392 p.
- BALATKA B., ROTH Z., SLÁDEK J., ZEMAN A. 1983: The Bohemian Massif: Discussion on its Delineation and Tectonic Division (in Czech). Věst. Ústf. Úst. Geol., Prague, **58**, pp. 369–387
- BILLINGS M.P. 1954: Structural geology. 2nd edn. New York, Prentice-Hall, 514 p.
- BROUČEK I. 1987: Earthquake Catalogue of Slovakia. Geoph. Inst. Slovak Acad. Sci., Bratislava, unpublished
- BUDAY T., POSPÍŠIL L., ŠŤORA A. 1986: Geological Meaning of Some Boundaries in Western Slovakia and Eastern Moravia Interpreted from Satellite Images, Mineralia Slov., Bratislava, **18**, 6, pp. 481–499
- BUJNOVSKÝ A. 1979: Geological Profile and Structure Elements of Nappes in the NW Part of the Low Tatra and Revúca Fault Zone. In: Mahel'M (ed) Tectonic Profiles through the West Carpathians. Geolog. Inst. Dionýza Štúra, Bratislava, pp. 85–89
- DOKTÓR S. and GRANICZNY M. 1982: Geological Interpretation of Satellite and Radar Images of the Eastern Part of the Western Carpathians (in Polish). Kwartalnik Geologiczny, Warsaw, **26**, 1, pp. 231–245

- FUSAN O., BIELY A., IBRMAJER J., PLANČAR J., ROZLOŽNÍK L. 1987: Basement of the Tertiary of the Inner Western Carpathians, Geol. Inst. Dionýza štúra, Bratislava, 123 p.
- FUSAN O., IBRMAJER J., PLANČAR J., SLAVÍK J., SMÍSEK M. 1971: Geological Framework of the Pre-Neogene Basement of the Southern Part of the Inner Carpathians. *Zb. geolog. vied, rad ZK, Bratislava*, zv. 15, 173 p.
- HAFNER W. 1951: Stress Distribution and Faulting. *Geol. Soc. Am. Bull.*, **62**, pp. 373–398
- HUBBERT M. K. 1951: Mechanical Basis for Certain Familiar Geologic Structures, *Geol. Soc. Am. Bull.* **62**, pp. 355–372
- IBRMAJER J. 1964: The Gravity Map of Czechoslovakia. Scale 1:500,000 Geol. Inst., Prague
- JANKŮ J., POSPÍŠIL L., VASS D. 1984: Contribution of Remote Sensing to Knowledge of the Western Carpathian Structure (in Slovak). *Mineralia slovacica*, **16**, 2, pp 121–137
- JIRÍČEK R. 1978: Paleogeography of the Lower Miocene in the Western Carpathians (in Czech), *Zemní plyn a nafta*, **23**, pp 21–38
- KÁRNÍK V., SCHENKOVÁ Z., SCHENK V. 1984: Earthquake Activity in the Bohémian Massif and in the Western Carpathians. *Travaux Inst. Geophys. Acad. Tehecosl. Sci. Academia Praha* **29**, pp. 9–33
- KENNEDEY W. A. 1946: The Great Glen Fault *Geol. Soc. London Quart. J.*, **102**, 41 p.
- KLINEC A., POSPÍŠIL L., PULEC M., FERANEC J., STANKOVIANSKÝ M. 1985: Identification of a Gravity Nappe in the Low Tatras by Satellite Images (in Slovak). *Mineralia Slovacica*, **17**, 6, pp. 485–499
- KOČÁK A., MAYER S., NĚMEC F. 1973: Report on Reflexion Seismic Measurements in the Vienna basin during 1971–72 Years (in Slovak). *Geofond Bratislava*, manuscript, 148 p.
- KOPECKÝ L. 1979: Magmatism of the Ohře Rift in the Bohemian Massif. Its relationship to the Deep Fault Tectonics and to the Geologic Evolution and Its Ore Mineralization In: Mahel' M. (ed) *Proc. Conf. Czechosl. Geology and Global Tectonics*. Veda Bratislava, pp. 167–181
- KUBÍNY D. 1962: Geological Position of the Staré Hory Crystalline Complex (in Slovak). *Geologické práce, zošit 62*, Geol. Inst. Dionýza Štúra, Bratislava, pp. 26–38
- KVÍTKOVIČ J. and VANKO J. 1980: Recent Vertical Movements of the Earth's Crust in the West Carpathians, *Geografický časopis*, **32**, 2–3, pp. 171–179
- LINSSE H. 1967: Investigations of Tectonics by Gravity Detailing. *Geophy. Prospecting*, **15**, 3, pp. 480–515
- MAHEL' M. (ed) 1974: Tectonics of the Carpathian-Balkan Regions: Explanations to the Tectonic Map of the Carpathian-Balkan Regions and their Forelands. *Geol. úst. Dionýza Štúra, Bratislava*, 453 p.
- MALKOVSKÝ M., BENEŠOVA Z., ČADEK J., HOLUB V., CHALOUPSKÝ J., JETEL J., MÜLLER V., MASÍN J., TÁSLER R. 1974: Geology of the Bohemian Cretaceous Basin and Its Basement (in Czech). *Geol. Inst., Prague, Académia*, 262 p.
- MÍŠAR Z., DUDEK A., HAVLENA V., WEISS J., 1983: Geology of the ČSSR – I. Bohémian Massif (in Czech). *Statní pedagogické naklad.*, Prague 333p.
- MOODY J. D. and HILL M. J. 1956: Wrench-Fault Tectonics. *Geol. Soc. Am. Bull.*, **67**, pp. 1207–1246
- MUSKA P. and VOZÁR J. 1984: Various Directions of Remanent Magnetic Polarization of Crystalline Complexes of the Western Carpathians (in Czech). *Jednota c. matematiků a fyziků, mimořádné číslo*, **1**, Prague, pp. 10–114
- OBERC J. 1972: Geological Structures of Poland. *Tectonics III part – Sudetes and surrounding areas*. *Wyd. Geol.*, pp. 464–475
- OBERNAUER D. 1980: Geophysical Research of the Western part of the Slovenské rudohorie Mts. and the Eastern part of the Low Tatras (in Slovak). *Faculty of Natural Science, Bratislava*, PhD Thesis, 115 p.
- POSPÍŠIL L., NEMČOK J., GRANICZNY M. and DOKTOR S. 1986: Contribution of Remote Sensing to the Identification of the Strike-slip Faults in the Western Carpathians (in Slovak). *Mineralia Slovacica*, **18**, 5, pp. 385–402
- POSPÍŠIL L., SCHENK V. and SCHENKOVÁ Z. 1985: Relation between seismoactive zones and remote sensing data in the West Carpathians. *Proc. 3rd Intern. Symp. Analysis of Seismicity and Seismic Risk, Liblice, Vol. 1*, Prague, pp. 256–263
- POSPÍŠIL L. and VASS D. 1984: Influence of the Structure of the Lithosphere on the Formation and Development of Intramontane and Back Molasse Basins of the Carpathian Mts. *Geophys. Transactions*, **30**, 4, pp. 355–371
- PROCHÁZKOVÁ D. and KÁRNÍK V. (eds) 1978: Atlas of Isoseismal Maps for Central and Eastern Europe. *Geoph. Inst., Czechosl. Acad. Sci., Prague*, 134 p.
- SCHENK V., SCHENKOVÁ Z., POSPÍŠIL L., ZEMAN A. 1985: Seismotectonic Model of the Upper Part of the Earth's Crust of Czechoslovakia. *Studia geoph. et geod.*, **30**, pp. 321–330

- SCHENKOVÁ Z., and KÁRNÍK V. (eds) 1988: Catalogue of Earthquakes for Central and Eastern Europe, Geophys. Inst. Czechosl. Acad. Sci., Prague, (unpublished)
- SCHENKOVÁ Z., KÁRNÍK V., SCHENK V. 1979: Earthquake Epicentres, in Central and Eastern Europe. *Studia geoph. et. geod.* 23, 2, pp. 197–199, 204a,b
- SENES J. 1982: Paleogeography of the Neogene. In: MAZUR E. (ed) Atlas of SSR. Veda, Bratislava
- SUESS E. 1885: Face of the Earth (in German), English Edit. (1904–1925), New York, Oxford Univ. Press, 5 p.
- TÁSLER R. (ed.) 1983: Geology of the Bohemian Part of the Intra-Sudetic Depression (in Czech). Geolog. Inst., Academia, Prague. 292 p.
- ZEMAN A., VYSKOCIL P., BALATKA B., BATIK P., DORNIČ J., LYSENKO V., SLÁDEK J. 1983: Comprehensive Study of the Tectonic and Block Relations of the Bohemian Massif in Respect of the Nuclear Power Plant Siting (in Czech). Ústr. Úst. Geol., Prague, manuscript.

VETŐRENDSZEREK DINAMIKÁJA ÉS A SZEIZMICITÁS ÖSSZEFÜGGÉSE – PÉLDÁK A CSEH MASSZIVUM ÉS A NYUGATI KÁRPÁTOK TERÜLETÉRŐL

Vladimir SCHENK, Zdeňka SCHENKOVÁ
és Lubomil POSPÍŠIL

Két vetőrendszert vizsgáltunk hosszú és rövid időtávon ható mozgásuk szempontjából. A következő jelenségeket tanulmányoztuk: a vetőrendszerek késő harmad- és a negyedidőszaki földtani fejlődésének jellege: szerkezeti blokkok vízszintes és függőleges mozgásainak földtani bizonyítékai; kéregmozgások; távérzékelési adatok (műhold felvételekkel meghatározott lineamentumok); a szeizmikus aktivitás adatai; gravitációs és mágneses anomáliák. A jelenségek mind azt támasztották alá, hogy vízszintes elmozdulások zajlottak le a vizsgált lineamentumok mentén, amelyek irányát és helyzetét is meghatároztuk.

ВЗАИМОСВЯЗЬ МЕЖДУ ДИНАМИКОЙ СИСТЕМ РАЗРЫВОВ И СЕЙСМИЧНОСТЬЮ – ПРИМЕРЫ ИЗ ЧЕШСКОГО МАССИВА И ЗАПАДНЫХ КАРПАТ

Владимир ШЕНК, Зденка ШЕНКОВА и Любомил ПОСПИШИЛ

Две системы разрывных нарушений были изучены с точки зрения движений по ним за короткий и длинный промежутки времени. Изучались следующие явления: характер геологического развития систем разрывных нарушений в позднегерценовое и четвертичное время; геологические доказательства горизонтальных и вертикальных смещений структурных блоков; коровые движения; данные дистанционных наблюдений (линеамента, выявленные по космическим снимкам); гравитационные и магнитные аномалии. Всеми этими явлениями подтверждается, что вдоль рассматриваемых линеаментов имели место горизонтальные смещения, направленность и приуроченность которых также были установлены.

A COMPILATION OF PALEOMAGNETIC RESULTS FROM HUNGARY

Emő MÁRTON* and Péter MÁRTON**

To facilitate access to and promote the use of palaeomagnetic results that have originated in Hungary over the last two decades, a comprehensive list is presented of those palaeomagnetic results obtained on fully oriented field samples. The results are listed — wherever possible — for localities in order to demonstrate the degree of consistency, both in space and time, of the tabulated palaeomagnetic directions.

Keywords: Palaeomagnetism, Hungary, Mesozoic, Palaeozoic, Tertiary

Introduction

A fair amount of palaeomagnetic results have originated from Hungary during the last two decades. A good part of the data has been published in international journals which are easily accessible to the scientific community whereas some are available in journals only of local or regional circulation. In addition, a further amount of data can be traced only with difficulty in various unpublished reports of the Eötvös Loránd Geophysical Institute of Hungary and the Eötvös University, Budapest.

To facilitate access to and promote the use of all these palaeomagnetic data we present a comprehensive list of all palaeomagnetic results which have hitherto been obtained on fully oriented field samples from Hungary. The aim, however, is not only one of convenience. In presenting these results we should also like to demonstrate the consistency, both in space and time, of our data. To achieve this, we list the results for localities rather than sites.

As regards a locality we follow TARLING [1983] who suggests that this term be used when the palaeomagnetic result represents a time average of the ancient geomagnetic field. If the time average covers a sufficiently long interval then all kinds of short-term variations of the Earth's magnetic field are eliminated. A single lava flow, a thin dyke, or a sedimentary layer are commonly regarded as point readings of the geomagnetic field of the past. These are called sites and a minimum of three is required to give a locality. Site means are tabulated, however, when the above conditions for locality are not fulfilled. These are the rhyolite at Sárszentmiklós and the monchiquite at Pákozd (*Fig. 1*).

* Eötvös Loránd Geophysical Institute of Hungary, POB 35. Budapest, H-1440

**Geophysics Department, Eötvös University, Kun Béla tér 2. Budapest, H-1083

Manuscript received (revised version): 14 March, 1988

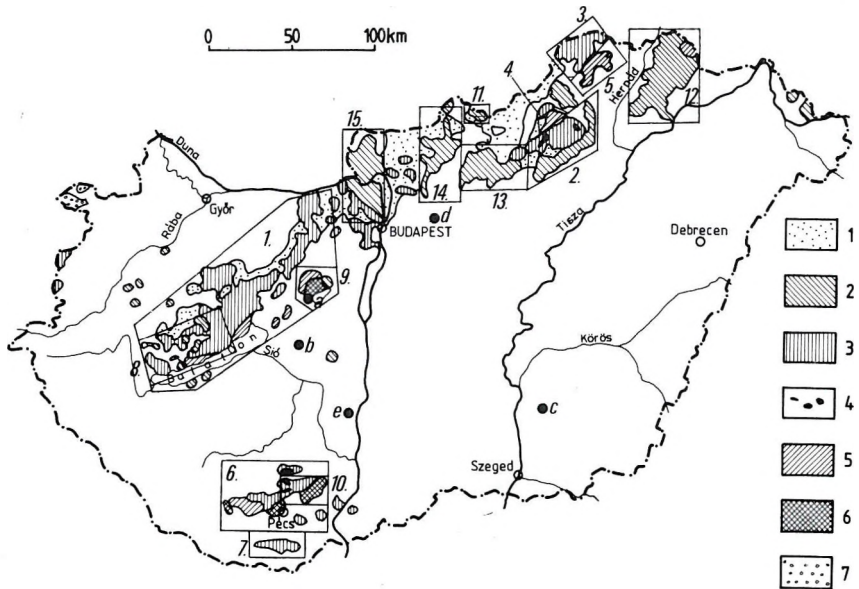


Fig. 1. Geological sketch of Hungary. Numbering of regions in accordance with tabulated data: 1. Transdanubian Central Range, 2. Bükk Mountains, 3. Aggtelek–Rudabánya region, 4. Uppony Hills, 5. Szendrő Hills, 6. Mecsek Mountains, 7. Villány Hills. Within each region, the results are arranged in order of geological age, starting from the Palaeozoic. The results from the Tertiary volcanics are compiled separately: 8. Balaton Highlands, 9. Velence Hills, 10. Mecsek Mountains, 11. Nógrád Hills, 12. Zemplén Mountains, 13. Mátra Mountains, 14. Cserhát Hills, 15. Borszöny–Dunazug Mountains. Site means for Tertiary volcanics and localities in loess are marked by letters: *a* — Pákozd, monchiquite; *b* — Sárszentmiklós, rhyolite; *c* — Hódmezővásárhely, loess; *d* — Mende, loess; *e* — Paks, loess. Legend for outcrops: 1 — Palaeogene sedimentary rocks; 2 — Tertiary volcanics; 3 — Mesozoic sedimentary rocks; 4 — Mesozoic eruptive rocks; 5 — Palaeozoic sedimentary rocks; 6 — Palaeozoic granite; 7 — gneiss, crystalline schist

1. ábra. Magyarország földtani vázlata

A területek számozása a táblázat sorrendjét követi, egy területen belül a paleozoikummal kezdődően a földtani kor a rendező elv. A harmadkori vulkanitok külön szerepelnek. Harmadkori vulkanitok és löszminták helyi átlagait betűkkel jelöltük: *a* — Pákozd, moncsikit; *b* — Sárszentmiklós, riolit; *c* — Hódmezővásárhely, lösz; *d* — Mende, lösz; *e* — Paks, lösz. A földtani térkép jelmagyarázata: 1 — paleogén üledékes kőzetek; 2 — harmadkori vulkanitok; 3 — mezozoos üledékes kőzetek; 4 — mezozoos kiömlési kőzetek; 5 — paleozoos üledékes kőzetek; 6 — paleozoos gránit; 7 — gneisz, kristályos pala

Рис. 1. Геологическая схема Венгрии.

Нумерация регионов соответствует последовательности таблиц. Внутри регионов данные приведены по геологическому возрасту. Третичные вулканиты нанесены отдельно. Усредненные значения третичных вулканитов и лёсов обозначены буквами: *a* — Пáкозд, мончикит; *b* — Шарсентмиклош, риолит; *c* — Ходмезёвашархей лёс; *d* — Менде, лёс; *e* — Пакш, лёс.

Обозначения на геологической карте:

1 — осадочные породы палеогенового возраста; 2 — третичные вулканиты; 3 — осадочные породы мезозойского возраста; 4 — вулканиты мезозойского возраста; 5 — палеозойские осадочные породы; 6 — палеозойский гранит; 7 — гнейс, кристаллический сланец.

Explanatory notes to the palaeomagnetic data list (Table I.)

Column 1 gives the geographical name of the sampling locality and its geographical coordinates, latitude and longitude, to two decimal figures. The mean position of geographically distributed sites is given by one-decimal figures (e.g. Velence Hills, andesites; Balaton Highlands, basalts).

Column 2 gives the type of rock and the isotope or geological age, the latter being abbreviated according to the Cambridge geologic time scale, 1982.

Column 3 contains the number of collecting site(*S*) and the number of samples(*N*) on which results are based. Where a dash is put in the place of *S*, it means that the sample was taken from a single site.

Columns 4 and 5 contain an estimate of the mean direction of magnetization before and after tectonic correction. Of the two pairs of data, usually the tectonically corrected values are compiled. Nevertheless, showing both pairs side by side seems to be useful.

The palaeomagnetic direction before tectonic correction gives an idea of the stability in time of the natural remanence. A magnetization significantly different in direction from that of the present geomagnetic field at the sampling place must be an ancient remanence though not necessarily a primary one. A comparison between uncorrected and corrected means shows the effect of the tilt correction on the coeval directions, i.e. from our list the improvement or increase of the scatter on restoring the rocks to the horizontal position can be deduced.

Tectonic correction is not always applied; it is tacitly assumed that it is not needed or its application is meaningless (e.g. one of the secondary components in Salföld Permian siltstone)

Columns 6 and 7 give Fisher's precision parameters, *k* and *A95*, the circle of confidence at the 95 % level [FISHER 1953]. The statistical parameters are computed using the number of independently oriented samples, except when the number of sites is indicated in column 3. In this case the statistics is based on the latter.

Of the two commonly calculated parameters it is *A95* which is widely used to estimate the reliability of a palaeomagnetic observation. We particularly wish to call attention to *k*, the precision parameter. However large the scatter of the directions may be, *A95* can be made very small by enlarging the data base. Improving *k*, on the other hand, requires thorough cleaning of the characteristic remanence of all secondary components; this being an important requirement if we wish to trace fast and relatively small tectonic changes — as is the case in the Mediterranean area.

It is obvious, however, that the best cleaning procedure is powerless to produce large *k* when the intensity of the natural remanence is close to the noise level of the best measuring instruments. An example cited from our list is the Albian Limestone from the Transdanubian Central Range.

Columns 8 and 9 give the latitude and the longitude of the pole corresponding to one pair of directions in columns 4 and 5. When tectonic correction is not needed, the palaeomagnetic pole is of course calculated from the remanence direction in the present geomagnetic coordinates; when the tilt correction is meaningless, for the rock was obviously remagnetized in the Earth's present magnetic field, no pole is listed. Some poles in the list are based on uncorrected palaeomagnetic declina-

tion–inclination in spite of the obvious and measurable tilts at the sampling location. This is to indicate that we interpret the remanence as secondary in relation to the deformation responsible for the tilts.

Column 10 shows whether the result was obtained by thermal (Th) or alternating field (AF) cleaning, and at what temperature (Centigrade) or peak field (Tesla). Some directions are not the measured vectors but the subtracted ones during cleaning. These are marked by *sv*.

Column 11 contains the references and, occasionally, remarks concerning the age or the polarity of the magnetization. For reasons of simplicity and brevity, reference to work by the first author is made as E. Márton despite the originals that may give this author's name differently.

Table I: List of palaeomagnetic results

S — number of sites; N — number of samples; k — precision parameter; A95 — radius of the circle of confidence at the 95 per cent probability level; D — declination; cD — declination, corrected; I — inclination; cI — inclination, corrected; sv — subtracted vector. For age abbreviations see HARLAND et al. [1982]



I. táblázat. Magyarországi paleomágneses eredmények

S — mintavételi helyek száma; N — minták száma; k — pontossági paraméter; A95 — konfidencia kör sugara 95 %-os valószínűségi szinten; D — deklináció; cD — deklináció dőléskorrekció után; I — inklináció; cI — inklináció dőléskorrekció után; sv — különbség vektor. Kor rövidítéseket lásd HARLAND et al. [1982]



Таблица 1. Венгерские палеомагнитные результаты.

S — число мест наблюдений; N — число образцов; k — параметр точности; A95 — окружность конфиденции на уровне вероятности 95%; D — деклинация; cD — деклинация после коррекции падения; I — инклинация; cI — инклинация после коррекции падения; sv — вектор вычитанный.
Обозначения возрастных единиц см. HARLAND et al. [1982].



1	2	3	4	5	6	7	8	9	10
Locality geogr. coord. Nlat. Elon.	rock type age	S/N	D cD	I cI	k k	A95 A95	Pole Nlat Elon	Clean	Ref. Remark
Transdanubian Central Range(1), Palaeozoic									
Folgárdi 47.05 18.27	limestone grey,D	4/22	112 -	-36 -	18 -	22.3 -	29 287	Th300- 550	Márton E. unpublished; metamorphic, Mesozoic magnetization ?
Sukoró 47.23 18.53	granite grey,C2	-/9	152 -	35 -	10 -	16.9 -	19 226	Th525- 550	Márton E. 1984,1986a
Sukoró 47.25 18.57	granite pink,C2	-/13	140 -	31 -	9 -	15.9 -	18 236	Th525- 550	Márton E. 1984,1986a
Sukoró 47.23 18.55	granite grey,C2	-/5	153 -	29 -	33 -	14.3 -	23 227	Th525- 550	Márton E. 1984,1986a
Fákozd 47.22 18.55	granite pink,C2	-/7	140 -	39 -	11 -	19.0 -	12 236	Th525- 550	Márton E. 1984,1986a
Sukoró 47.24 18.57	granite grey,C2	-/8	132 -	16 -	6 -	25.9 -	20 250	Th525- 550	Márton E. 1984,1986a
Sukoró 47.24 18.57	granite dyke,C2	-/13	158 -	-30 -	59 -	5.4 -	54 236	Th>500	Márton E. 1984,1986a; remagnetized,30 Ma ?
Sukoró 47.24 18.58	granite aplite,C2	-/7	155 -	-69 -	94 -	6.9 -	73 316	Th>500	Márton E. 1984,1986a; remagnetized,30 Ma ?
Sukoró 47.24 18.58	granite red,C2	-/5	168 -	-65 -	27 -	14.9 -	82 291	Th>550	Márton E. 1984,1986a; remagnetized,30 Ma ?
Sukoró 47.24 18.58	diabase C?	-/6	148 -	-60 -	6 -	24.6 -	66 285	AF0.18	Márton E. 1984,1986a; remagnetized,30 Ma ?
Sukoró 47.25 18.55	granite dyke,red,C2	-/4	144 -	-24 -	14 -	25.3 -	44 252	Th>525	Márton E. 1984,1986a; remagnetized,30 Ma ?
Kisfaludpuszta 47.20 18.45	granite dyke,red,C2	-/5	316 -	26 -	34 -	13.3 -	40 261	Th>500	Márton E. 1984,1986a; remagnetized,30 Ma ?
Kisfaludpuszta 47.20 18.45	granite aplite,C2	-/5	299 -	29 -	17 -	19.0 -	31 278	AF0.03- 0.05	Márton E. 1984,1986a; remagnetized,30 Ma ?
Sági major 47.25 18.51	granite C2	-/7	144 -	-44 -	26 -	12.9 -	54 264	AF0.03	Márton E. 1984,1986a; remagnetized,30 Ma ?
Szabadbattyán 47.14 18.34	sandstone grey,C2	-/4	47 17	48 60	450 450	4.3 4.3		Th575- 600	Márton E. 1985 unpublished
Szabadbattyán 47.14 18.34	sandstone grey,C2	-/4	10 22	51 24	82 82	10.2 10.2		Th350- 600	Márton E. 1985 unpublished

1	2	3	4	5	6	7	8	9	10
Transdanubian Central Range, Palaeozoic cont.									
Badacsonyörs 46.80 17.47	siltstone red, P1	-/6	81 24 79 -11	24 13.9- 24 13.9				Th700 3 119	Márton E. & Elston in press
		-/11	302 47 347 52	34 7.9 34 7.9				Th150- 650sv	
Salföld 46.80 17.57	siltstone red, P2	-/9	336 64 342 46	124 4.7 123 4.7				Th300- 475	Márton E. & Elston in press, secondary rem. ?
		-/9	323 60 332 43	125 4.6 125 4.6				Th300- 575sv	
		-/9	7 62 - -	46 7.7 - -				Th575	
Balatonalmádi 47.15 18.02	siltstone red, P2	-/20	323 49 319 9	21 7.8 21 7.8				Th500	Márton E. & Elston 1985; secondary rem. ?
Balatonarács 46.96 17.87	siltstone red, P2	-/29	322 53 307 18	25 5.7 25 5.7				ThNRM- 525sv	Márton E. & Elston 1985, sec. rem. ?
Balatonfüred 46.95 17.83	siltstone red, P2	-/9	301 24 293 -8	53 7.1 53 7.1				Th400- 500sv	Márton E. & Elston 1985, sec. rem. ?
Kövágóörs 46.83 17.62	siltstone red, P2	-/8	309 47 310 24	113 4.9 113 4.9				Th400- 500sv	Márton E. & Elston 1985, sec. rem. ?
Transdanubian Central Range, Triassic									
Balatonfüred 46.97 17.83	marl, grey Tr1	-/12	320 34 315 38	80 5.0 80 5.0			46 269	Th500	Márton & Márton 1981, 1983
Csopak I. 46.95 17.90	marl, grey Lad-Crn	-/9	328 66 314 33	165 4.0 165 4.0			42 266	Th500	Márton & Márton 1981, 1983
Csopak II. 46.95 17.90	marl, grey Lad-Crn	-/5	302 50 303 35	12 24.0 12 24.0			35 303	Th200	Márton & Márton 1981, 1983
Felsőörs 47.08 17.93	limestone grey, Ans	-/33	306 62 304 41	13 7.2 13 7.2			40 280	Th400- 500	Márton & Márton 1983
Felsőörs 47.08 17.93	limestone grey, Lad	-/5	310 58 291 35	30 14.3 30 14.3			28 287	Th400- 500	Márton & Márton 1983
Transdanubian Central Range, Jurassic									
Bakony- csernye I. 47.30 18.17	limestone red, P1b	-/51	281 57 299 55	- 2.6 - 2.6			44 297	Th450	Márton et al. 1980, Márton & Márton 1983
Bakony- csernye II. 47.30 18.10	limestone red, P1b	-/7	291 56 302 48	47 8.9 47 8.9			42 286	Th450	Márton et al. 1980, Márton & Márton 1983

1	2	3	4	5	6	7	8	9	10
Transdanubian Central Range, Jurassic cont.									
Tardos 47.65 18.47	limestone red, P1b	-/6	312 310	58 57	40 40	10.7 10.7	52 291	Th400	Márton & Márton 1981, 1983
Tata 47.63 18.32	limestone red, J1	-/10	317 332	57 58	72 72	5.7 5.7	68 275	Th500	Márton & Márton 1981, 1983
Lókút 47.20 17.87	limestone red, J1	-/21	279 288	53 47	18 18	8.0 8.0	32 296	Th450	Márton & Márton 1981, 1983
Bakonycsernye 47.30 18.10	limestone red, Toa	-/15	279 295	53 52	-	5.8 5.8	39 296	Th450	Márton et al. 1980, Márton & Márton 1983
Labatian 47.71 18.56	limestone red, Toa-Baj	-/53	308 293	46 44	-	4.0 4.0	34 291	Th450	Márton & Márton 1982 unpublished
Úrkút 47.08 17.65	limestone grey, Baj	-/10	300 314	40 37	3 8	33.4 17.4	44 269	Th400- 500	Márton & Márton 1983
Hárskút 47.15 17.80	limestone red, Baj-Bth	-/30	304 307	48 39	-	9.0 9.0	41 276	Th500- 600	Márton & Márton 1983
Városlőd 47.13 17.65	limestone grey, J3	-/6	91 256	42 52	72 76	8.0 7.7	16 320	Th520- 550	Márton & Márton 1983; corr. overturned pos.
Tardos 47.65 18.45	limestone grey, Tth	-/11	267 278	17 42	-	7 7	23 300	Th560	Márton & Márton 1983
Lókút 47.21 17.83	limestone grey, Tth	-/14	249 264	37 38	95 95	4.1 4.1	12 308	Th500	Márton & Márton 1981, 1983
Sümeğ 46.97 17.30	limestone grey, Tth	-/42	329 260	36 32	8 8	7.9 7.9	8 297	Th545	Márton, E. 1982 Márton & Márton 1983
Sümeğ 46.97 17.30	limestone grey, Tth	-/39	272 270	33 36	7 7	9.2 9.2	14 301	Th500	Márton E. 1985b
Hárskút 47.16 17.79	limestone grey, Tth	-/106	262 254	51 40	29 29	2.6 2.6	7 312	Th400- 500	Márton, E. 1986b
Borzavár 47.27 17.82	limestone grey, Tth	-/63	269 262	46 39	30 30	3.3 3.3	10 308	Th400- 500	Márton, E. 1986b
Transdanubian Central Range, Cretaceous									
Sümeğ 46.96 17.26	limestone grey, Ber	-/56	312 277	42 31	6 6	13.7 13.7	17 294	Th500	Márton, E. 1982 Márton & Márton 1983
Labatian 47.73 18.50	limestone Vlg-Hau	-/10	299 290	45 39	25 25	9.9 9.9	29 290	Th400- 500	Márton & Márton 1983
Borzavár 47.27 17.83	limestone grey, Vlg-Hau	-/8	258 263	40 42	42 42	8.8 8.8	13 310	Th525- 625	Márton & Márton 1983

1	2	3	4	5	6	7	8	9	10
Transdanubian Central Range, Cretaceous cont.									
Borzavár I. 47.27 17.83	limestone grey, Apt	-/6	271 275	42 43	52 52	9.4 9.4	21 302	Th500- 550	Márton & Márton 1981, 1983
Borzavár II. 47.27 17.83	limestone grey, Apt	-/11	290 294	42 47	39 39	7.4 7.4	36 292	Th500	Márton & Márton 1983
Vértessomlyó 47.50 18.37	limestone grey, Apt	-/7	289 285	27 47	- 35	16.0 10.3	30 299	Th500	Márton & Márton 1981, 1983
Úrkút 47.10 17.65	limestone grey, Alb	-/8	309 308	60 30	13 13	15.8 15.8	38 269	Th400- 500	Márton & Márton 1983
Olaszfalva 47.23 17.90	limestone grey, Alb	-/9	297 300	25 44	12 12	15.8 15.8	39 285	Th250- 350	Márton & Márton 1983
Jásd 47.28 18.03	limestone grey, Alb	-/22	284 292	47 40	12 12	11.5 11.5	32 289	Th300- 500	Márton & Márton 1983
Halimba 47.05 17.55	marl, red Cmp-Maa	-/10	305 312	58 50	- -	11.0 11.0	50 281	Th500	Márton & Márton 1983
Magyarcsanak 47.18 17.56	marl, grey Cmp-Maa	-/5	314 320	72 52	- 75	14.0 8.9	56 277	Th500	Márton & Márton 1983
Bakonyjákó 47.22 17.58	marl, grey Cmp-Maa	2/8	347 330	59 57	29 22	10.4 12.1	66 275	Th150- 200	Márton & Márton 1983
Tapolcai 47.27 17.53	marl, grey Cmp-Maa	2/11	145 133	-57 -54	31 31	8.4 8.4	52 285	Th150- 300	Márton & Márton 1983
Transdanubian Central Range, Paleogene									
Gánt 47.40 18.36	marl, grey Eo2	4/14	312 312	50 50	24 24	9.6 9.6	50 281	AF0.02 Th400	Márton, E. 1987
Bükk Mts (2)									
Nagyvisnyó 48.13 20.45	schist grey, C	-/4	255 -	41 -	7 -	36.5 -		AF0.01- 0.02	Márton, E. 1978
Nagyvisnyó 48.14 20.45	limestone grey, C	-/4	75 -	74 -	239 -	8.0 -		AF0.02	Márton, E. 1978
Tarófd 48.12 20.45	limestone grey, C	-/6	295 -	61 -	38 -	11.0 -		AF0.01- 0.025	Márton, E. 1978
Nagyvisnyó 48.12 20.44	limestone grey, C	-/8	103 129	50 62	9 9	19.2 19.2		Th300	Márton, E. 1979
Nagyvisnyó 48.12 20.44	limestone grey, C	-/5	129 164	59 60	15 15	20.2 20.2		Th300	Márton, E. 1979

1	2	3	4	5	6	7	8	9	10
Bükk Mts, cont.									
Nagyvisnyó 48.11 20.48	limestone grey,C	-/7	303 294	32 22	6 6	30.0 30.0		Th300- 450	Márton,E. 1979
Nagyvisnyó 48.13 20.42	limestone G2	-/5	304 323	20 25	6 6	33.9 33.9		Th450- 500	Márton,E. 1979
Nagyvisnyó 48.13 20.42	sandstone red,P2	-/10	317 327	52 47	23 23	10.3 10.3		Th250- 475	Márton,E. 1984 unpublished
Nagyvisnyó 48.13 20.42	limestone black,P2	-/13	321 180 26	62 79 74	18 38 38	9.9 6.8 6.8		NRM Th350 AF0.05	Márton,E. 1979, unstable from 350 C and 0.05T on!
Nagyvisnyó 48.11 20.48	schist variegated P	-/6	264 -	67 -	8 -	24.4 -		Th200	Márton,E. 1979; negative fold test!
Mályinka 48.13 20.50	limestone grey,C	-/6	254 - 194 218	66 - 73 5	14 - 9 9	18.3 - 27.4 27.4		AF0.01 Th100- 400	Márton,E. 1978 Márton,E. 1979
Mályinka 48.12 20.52	limestone grey,C	-/4	151 191	68 59	21 21	20.4 20.4		AF0.01	Márton,E. 1979
Mályinka 48.12 20.51	limestone grey,C	-/9	48 285	72 85	8 8	18.3 18.3		Th350- 500	Márton,E. 1979
Mályinka 48.12 20.52	limestone grey,C	-/3	154 180	56 50	21 21	27.3 27.3		Th450	Márton,E. 1979
Gerennavár 48.09 20.43	limestone olihhic, Tr?	-/5	16 6	32 36	36 36	20.8 20.8		Th450	Márton,E. 1979
Hollókő 48.09 20.44	dolomite Tr?	-/9	332 324	26 17	15 15	13.6 13.6		Th400- 500	Márton,E. 1979
Rónabükk 48.08 20.43	limestone cherty,Tr?	-/9	282 282	17 3	5 5	39.0 39.0		Th450	Márton,E. 1979
Omassa 48.10 20.54	limestone P	-/6	316 329	43 30	32 32	12.1 12.1		AF0.05- 0.1	Márton,E. 1978
Omassa 48.10 20.54	schist dolomite Tr1	-/6	343 340	- -12	123 123	8.3 8.3		Th300- 500	Márton,E. 1979
Omassa 48.11 20.57	dolomite Tr	-/7	340 340	14 8	19 19	14.2 14.2		Th300- 450	Márton,E. 1979
Eger, Wind 47.88 20.38	sandstone late Oligo- early Mio- cene	-/75	110 105	-24 -48	20 20	3.7 3.7		AF0.04- 0.05	Márton,P. 1983

1	2	3	4	5	6	7	8	9	10
Aggtelek-Rudabánya area (3)									
Silice nappe									
Ferkupa 48.47 20.69	sandstone red,Tr1	-/6	105 103	-20 -14	19 19	17.6 17.6		Th670- 680	Márton et al. in preparation
Szin 48.50 20.67	marl grey,Tr1	-/6	256 255	+20 +10	49 32	9.7 12.0		Th525- 600	Márton et al. in preparation
Ferkupa 48.47 20.69	marl, variegated Tr1	-/6	304 292	+54 +31	24 26	16.9 13.4		Th500- 525	Márton et al. in preparation
Jósvafő 48.48 20.56	limestone grey,Tr1	-/8	309 308	+78 +27	28 38	10.6 9.0		Th500- 525	Márton et al. in preparation
Jósvafő 48.48 20.56	dolomite, grey,Ans	-/5	284 269	+58 +49	55 55	10.4 10.4		Th250- 500	Márton et al. in preparation
Jósvafő 48.48 20.56	dolomite, grey,Ans	-/7	291 277	+24 +22	37 37	10.0 10.0		Th350	Márton et al. in preparation
Jósvafő 48.48 20.56	dolomite grey,Ans	-/4	119 81	-44 -46	49 49	13.2 13.2		Th450- 500	Márton et al. in preparation
Jósvafő 48.48 20.56	limestone white,Ans	-/6	300 282	+40 +43	15 15	18.2 18.2		Th400- 500	Márton et al. in preparation
Derenk 48.62 20.67	limestone red,Nor	5/32	259 284	+39 +61	25 40	15.5 12.2		Th250- 450	Márton et al. in preparation
Bódva nappe									
Martonyi 48.50 20.78	dolomite grey,Ans	-/8	305 317	+31 +28	59 59	7.3 7.3		Th300- 400	Márton et al. in preparation
Telekesvölgy 48.43 20.70	limestone red,Lad	-/12	136 278	+81 +33	55 55	5.9 5.9		Th400	Márton et al. in preparation
Szárhegy 48.47 20.72	dolomite Ans	-/6	25 277	+31 +61	47 47	9.9 9.9		Th400	Márton et al. in preparation
Tornaszent- andrás 48.53 20.79	dolomite grey,Ans	-/6	301 309	+47 +10	93 93	7.0 7.0		Th150- 250	Márton et al. in preparation
Bedellabánya 48.44 20.64	limestone grey,Lad	-/8	265 302	+62 +35	38 38	9.1 9.1		Th250- 500	Márton et al. in preparation
Lászipusztá 48.44 20.64	limestone variegated Nor	-/10	35 39	+83 +58	41 41	7.6 7.6		Th525	Márton et al. in preparation
Bódvalenke 48.54 20.81	limestone variegated Lad-Crn	-/21	147 47	+47 +50	27 27	6.2 6.2		Th300	Márton et al. in preparation

1	2	3	4	5	6	7	8	9	10
Aggtelek-Rudabánya area cont.									
Martonyi nappe									
Nagyrednek									
völgy	limestone	-/5	4	-4	44	11.7		Th350-	Márton et al.
48.47	20.77	grey, Lad-Črn	49	-15	44	11.7	19 148	450	in preparation
Torna-									
szentandrás	limestone	-/11	303	+29	157	3.7		Th250	Márton et al.
48.51	20.79	grey, Črn	305	-17	157	3.7	15 258		in preparation
Rakaca-									
Becskeháza	limestone	-/7	138	+66	58	8.0		Th400-	Márton et al.
48.53	20.84	grey, Nor	106	+62	58	8.0	22 70	515	in preparation
Bódvarákó paraautochthon									
Bódvarákó									
48.51	20.78	limestone olistolith, Ans-Lad	2	+76	427	3.2		Th300	Márton et al.
			47	+56	427	3.2	54 112		in preparation
Bódvarákó									
48.51	20.78	tuff & shilt, Lad	312	+8	28	10.7		Th400	Márton et al.
			315	+20	28	10.7	37 261		in preparation
Bódvarákó									
48.51	20.78	dolomite Ans-Lad	333	+80	26	7.7		Th400	Márton et al.
			9	+58	26	7.7	78 164		in preparation
Uppony Hills (4) Devonian									
Dédestapolcsány schist									
48.18	20.47	-/3	326	67	55	16.7		AF0.03	Márton, E. 1978
			208	62	55	16.7			
Uppony									
48.21	20.40	limestone grey	284	52	58	8.9		AF0.1	Márton, E. 1978
			233	40	58	8.9			
Uppony									
48.21	20.40	schist	245	22	58	12.1		AF0.0B	Márton, E. 1978
		-/4	227	22	58	12.1		Th300	
Uppony									
48.21	20.40	limestone with diabase tuff	273	25	18	18.8		AF0.0B	Márton, E. 1978
		-/5	254	43	18	18.8			
Szendrő Hills (5) Devonian									
Szendrő									
48.38	20.75	schist, black	152	50	11	21.0		AF0.02	Márton, E. 1978
		-/6	153	8	11	21.0			
Szendrő, Castle hill									
48.40	20.73	cryst. limestone	202	37	37	9.2		AF0.1	Márton, E. 1979
		-/8	180	36	37	9.2			degree of anisotropy 10-20 %

1	2	3	4	5	6	7	8	9	10	
Szendrő Hills cont.										
Rakacaszend 48.45 20.85	schist with limestone lenses	-/4	222 158	83 45	18 18	22.0 22.0		Th300	Márton, E. 1978	
Rakacaszend 48.46 20.87	schist with limestone lenses	-/4	179 143	60 35	21 21	20.4 20.4		AF0.025 Th350	Márton, E. 1978	
Rakacaszend 48.46 20.85	cryst. limestone	-/6	128 138	49 18	45 45	10.1 10.1		AF0.01 Th200	Márton, E. 1978	
Csákánykút	sandy schist	-/3	253 310	72 50	23 23	16.5 16.5		Th400	Márton, E. 1979	
Rakaca 48.45 20.90	cryst limestone	-/4	106 132	54 22	18 18	22.6 22.6		AF0.005	Márton, E. 1978	
Mecsek Mountains (b), Palaeozoic										
Mórág 46.22 18.63	granite 365Ma, U/Pb	-/11	182 -	14 -	28 -	8.8 -	37 196	Th300- 500	Márton E. 1980, 1986a	
Üveghuta 46.21 18.57	granite 365Ma, U/Pb	-/7	188 -	15 -	26 -	12.1 -	36 189	Th450	Márton E. 1980, 1986a	
Lochmalom 46.12 18.47	granite 365Ma, U/Pb	-/4	190 -	30 -	12 -	27.2 -	27 188	Th300- 550	Márton E. 1980, 1986a	
Erdősaecske 46.18 18.50	granite 365Ma, U/Pb	-/5	199 -	20 -	8 -	25.8 -	31 177	Th300	Márton E. 1980, 1986a	
Kismórág 46.23 18.63	granite 365Ma, U/Pb	-/5	194 -	-2 -	14 -	21.0 -	43 179	Th300- 550	Márton E. 1980, 1986a	
Ófalu 46.22 18.49	serpent- inite, Pz	-/8	183 -	31 -	11 -	21.5 -	27 195	Th400	Márton E. 1986a	
Kismórág 46.24 18.62	aplite 280Ma, Rb/Sr	-/5	99 -	40 -	19 -	18.3 -	10 86	Th400- 600	Márton E. 1980, 1986a; remagnetized in Cretaceous	
Kismórág 46.24 18.62	aplite 280Ma, Rb/Sr	-/5	92 -	51 -	25 -	15.8 -	21 84	Th400	Márton E. 1980, 1986a; remagnetized in Cretaceous	
Egédpuszta 46.10 18.00	siltstone red, P1	-/48	- 187	- -18	- 14	- 5.8	- 53	188	Th150	Kotasek et al., 1969
Egédpuszta 46.10 18.00	siltstone red, P1	-/11	167 185	-20 -10	35 35	6.1 6.1	- 49	190	Th525	Márton E. & Elston, 1985

1	2	3	4	5	6	7	8	9	10
Mecsek Mountains, Palaeozoic cont.									
Boda 46.10 18.00	siltstone red,P1	-/17	188 170	-31 0	25 25	9.8 9.8	43 212	Th500	Márton E. & Elston, 1985
Mecsek Mountains, Mesozoic									
Abaliget 46.14 18.11	limestone grey,T1	-/4	240 194	-66 -22	32 32	16.4 16.4	53 175	Th500	Márton E. 1986a
Magyaregregy 46.21 18.31	limestone grey, Tth-Ber	-/6	28 348	53 39	8 5	24.6 33.0	64 224	Th500	Márton E. 1986a
Magyaregregy 46.25 18.31	limestone grey, Tth-Ber	-/7	98 32	48 68	7 7	24.5 24.5	68 84	Th500- 575	Márton E. 1986a
Magyaregregy 46.21 18.31	limestone grey, Tth-Ber	-/3	27 17	13 22	19 19	29.1 29.1	52 170	Th500	Márton E. 1986a
Zobák 46.18 18.30	limestone grey, Tth-Ber	-/9	5 13	2 37	5 5	25.9 25.9	62 171	Th400- 500	Márton E. 1986a
Mórág area 46.2 18.3	alkali- volcanics, K1	10/41	94 -	57 -	28 -	9.3 -	24 77	Th300- 600	Márton E. 1984; includes 2 aplite magnetized in Cretaceous
Eastern Mecsek 46.2 18.3	alkali- volcanics, K1	6/50	79 47	54 56	7 5	27.2 33.6	54 107	AF300- 500	Márton and Márton 1970, Márton, E. 1984, 1986a
Eastern Mecsek 46.2 18.3	alkali- volcanics, K1	11/?	43 334	79 47	11 7	14.6 18.7	56 62 46 256	AF	Dagley & Ade-Hall, 1971
Villány Hills (7), Mesozoic									
Villány 45.87 18.45	limestone variegated Tr3	-/8	- 25	- 64	- 109	- 5.3	72 100	Th500	Márton, E. 1981
Máriagyűd 45.87 18.25	dolomite grey, Tr3	-/5	- 356	- 26	- 29	- 14.3	58 205	Th525	Márton, E. 1981
Máriagyűd 45.87 18.25	limestone red, J3	-/6	6 19	36 58	91 91	7.0 7.0	75 128	AF, Th525	Márton & Márton 1978
Harkány 45.87 18.23	limestone pink, J3	-/5	3 10	27 57	64 64	9.6 9.6	78 154	Th525 AF	Márton & Márton 1978

1	2	3	4	5	6	7	8	9	10
Villány Hills cont									
Hársány 45.86 18.40	limestone grey, J3	-/5	11 0 34 69	31 14.0 31 14.0	14.0	67	80	AF, Th525	Márton & Márton 1978
Beremend 45.79 18.40	limestone grey, K1	-/5	23 52 15 53	55 10.4 55 10.4	10.4	74	150	AF	Márton & Márton 1978
Tertiary volcanics									
Transdanubian Central Range (8)									
Balaton Highlands									
46.9 17.4	basalt 3.0-2.5Ma, K/Ar	10/-	10 63 - -	78 6.9 - -	83 123			AF Th	Márton, E. 1985a normal polarity only
46.9 17.4	basalt 5.0-3.0Ma, K/Ar	11/-	175 -59 - -	32 6.9 - -	82 226			AF Th	Márton, E. 1985a reversed polarity only
46.9 17.4	basalt Plio- Pleistocene	8/-	183 -65 - -	22 12.0 - -	88 91			AF	Dagley & Ade-Hall 1970; reversed polarity only
46.9 17.4	basalt Plio- Pleistocene	5/-	15 52 - -	238 5.0 - -	153 72			AF	Dagley & Ade-Hall 1970; normal polarity
Velence Hills (9)									
47.2 18.5	andesites 30 Ma, K/Ar	8/40	153 -45 - -	28 10.6 - -	60 254			AF 0.04 Th525	Márton, E. 1986a
Necsek Mountains (10)									
46.19 18.27	andesite 21 Ma, K/Ar	3/33	59 65 - -	32 22.2 - -	51 84			AF	Márton & Márton, 1969, 1970 Márton, E. 1986a Dagley & Ade-Hall, 1971
Nógrád Hills (11)									
48.2 19.9	basalt Pliocene	3/-	180 -62 - -	16 32.0 - -	85 202			AF	Márton & Márton, 1970
Zemplén Mountains (12)									
48.4 21.5	andesite rhyolite, mid-Miocene	20/-	339 69 - -	25 6.6 - -	76 316			AF	Márton & Márton, 1972
48.4 21.5	andesite rhyolite mid-Miocene	10/-	352 66 - -	10 9.6 - -	85 299			AF	Dagley & Ade-Hall 1971

1	2	3	4	5	6	7	8	9	10
Mátra Mountains (13) 47.8 20.0	andesite rhyolite mid-Miocene	16/-	2 50	29	6.9	74	194	AF	Márton & Márton, 1970 Márton, E., 1981
Cserhat Mountains (14) 48.0 19.5	andesite mid-Miocene	5/-	182 -60	45	4.1	84	188	AF	Márton & Márton, 1970; reversed polarity only
Börzsöny- Dunazug Mts (15) 48.0 19.0	andesite dacite rhyolite mid-Miocene	84/-	1 60	20	3.5	82	195	AF Th	Márton & Márton, 1971 Ando et al., 1977 Baila & Márton, E. 1980
Fákozd (a) 47.22 18.55	monchiquite 60 Ma, K/Ar	-/10	334 43	33	8.5			Th500	Márton, E. 1986a
Sárszent- miklós (b) 48.87 18.63	ignimbrite 16 Ma, K/Ar	-/12	315 55	43	6.7			AF0.03- 0.05	Márton, E. 1982 unpublished
Loess									
Hódmező- vásárhely (c) 46.38 20.33	infusion loess Ple(i)	-/40	348 55	13	6.9			AF0.03	Márton, P. et al. 1979
Mende (d) 47.43 19.42	loess & fossil soil, P(i)	5/41	350 60	25	4.6			AF0.04	Marton, P. 1979a
Faks (e) 46.62 18.87	loess & fossil soil, P(m-1)	11/42	4 63	52	6.4			AF0.04	Marton, P. 1979b

REFERENCES

- ANDÓ J., KIS K., MÁRTON E., MÁRTON P. 1977: Palaeomagnetism of the Börzsöny Mountains, Hungary. *Pure Appl. Geophys.* **115**, 4, pp. 979–987
- BALLA Z., MÁRTON-SZALAY E., 1978: The paleomagnetic sequence in the Börzsöny volcanic area (in Hungarian). *Magyar Geofizika*, **19**, 2, pp. 51–59, **19**, 3, pp. 114–120
- DAGLEY P., ADE-HALL J. M. 1970: Cretaceous, Tertiary and Quaternary palaeomagnetic results from Hungary. *Geophys. J. Roy. Astr. Soc.*, **20**, 1, pp. 65–87
- FISHER R. A. 1953: Dispersion on a sphere. *Proc. Roy. Soc. London, Ser. A*, **217**, pp. 295–305
- HARLAND W. B., COX A. V., LLEWELLYN P. G., PICKTON C. A. G., SMITH A. G., WALTERS R. 1982: A geologic time scale. Cambridge Univ. Press. 131 p.
- KOTASEK J., KRS M., JÁMBOR Á. 1969: Palaeomagnetic study on the Permian rocks of the Pannonian Basin (in German). *Geophys. Trans.*, **18**, 1–2, pp. 43–56
- MÁRTON E. 1980: Multicomponent remanent magnetization of migmatites, Mórágý area, SW Hungary. *Earth and Plan. Sci. Lett.*, **47**, 1, pp. 102–112
- MÁRTON E. 1981: Tectonic implications of paleomagnetic data for the Carpatho-Pannonian region. *Earth Evolution Sciences*, **1**, 3–4, pp. 257–264
- MÁRTON E. 1982: Late Jurassic–early Cretaceous magnetic stratigraphy from the Sümeg section, Hungary. *Earth and Plan. Sci. Lett.*, **57**, 1, pp. 182–190
- MÁRTON E. 1984a: Palaeomagnetism of Paleozoic granitoids and connected metamorphic rocks in Hungary. *IGCP5 Newsletter* 6. Barcelona, pp. 65–71
- MÁRTON-SZALAY E. 1984b: Paleomagnetism of the igneous rocks from the Velence Hills (in Hungarian). *Magyar Geofizika*, **25**, 2–3, pp. 48–56
- MÁRTON E. 1985a: Tying the basalts from the Transdanubian Central Mountains to the standard polarity time scale. Problems of the Neogene and Quaternary. Eds. Kretzoi M., Pécsi M. *Akadémiai Kiadó*, pp. 99–108
- MÁRTON-SZALAY E. 1985b: Palaeomagnetic study of geological basic sections (in Hungarian). Report of the Eötvös L. Geophysical Institute of Hungary
- MÁRTON E. 1986a: Palaeomagnetism of igneous rocks from the Velence Hills and Mecsek Mountains. *Geophys. Trans.*, **32**, 2, pp. 83–145
- MÁRTON E. 1986b: The problems of correction between magnetozones and Calpionellid zones in late Jurassic–early Cretaceous sections. *Acta Geologica Hungarica* **29**, 1–2, pp. 125–131
- MÁRTON E. 1987: Palaeomagnetism and tectonics in the Mediterranean region. *J. of Geodynamics*, **7**, 1–2 pp. 33–57
- MÁRTON E., ELSTON D. P. 1985: Structural rotations from paleomagnetic directions of some Permo-Triassic red beds, Hungary. *Geophys. Trans.*, **31**, 1–3, pp. 217–230
- MÁRTON E., ELSTON D. P. 1987: Tectonic rotations south of the Bohemian Massif from paleomagnetic directions of Permian red beds in Hungary. *Tectonophysics*, **139**, 1–2, pp. 43–51
- MÁRTON-SZALAY E., MÁRTON P. 1978: On the difference between the palaeomagnetic poles from the Transdanubian Central Mountains and the Villány Mountains, respectively (in Hungarian). *Magyar Geofizika*, **19**, 4, pp. 129–136
- MÁRTON E., MÁRTON P. 1981: Mesozoic paleomagnetism of the Transdanubian Central Mountains and its tectonic implications. *Tectonophysics*, **72**, 1–2, pp. 129–140
- MÁRTON E., MÁRTON P. 1983: A refined apparent polar wander curve for the Transdanubian Central Mountains and its bearing on the Mediterranean tectonic history. *Tectonophysics*, **98**, 1–2, pp. 43–57
- MÁRTON E., MÁRTON P., HELLER F. 1980: Remanent magnetization of a Pliensbachian limestone sequence at Bakonycsérnye, Hungary. *Earth and Plan. Sci. Lett.*, **48**, 1, pp. 218–226
- MÁRTON E., MÁRTON P., LESS GY. 1987: Post-Triassic rotations in the Aggtelek–Rudabánya Mountains indicated by palaeomagnetic directions (in Hungarian). *Magyar Geofizika*, **28**, 1, pp. 1–19
- MÁRTON P. 1979a: Palaeomagnetism of the Mende brickyard exposure. *Acta Geologica Hungarica* **22**, 1–4 pp. 403–407
- MÁRTON P. 1979b: Palaeomagnetism of the Paks brickyard exposure. *Acta Geologica Hungarica* **22**, 1–4 pp. 443–449
- MÁRTON P. 1983: Palaeomagnetic investigation of Oligocene formations of the northern part of Hungary (in Hungarian). Report of ELTE Geophysical Department, Budapest
- MÁRTON P., MÁRTON-SZALAY E. 1969: Palaeomagnetic investigation of magmatic rocks from the Mecsek Mountains, Southern Hungary. *Ann. Univ. Sec. Geol.*, **12**, pp. 67–80

- MÁRTON P. 1983: Palaeomagnetic investigation of Oligocene formations of the northern part of Hungary (in Hungarian). Report of ELTE Geophysical Department, Budapest
- MÁRTON P. MÁRTON-SZALAY E. 1969: Palaeomagnetic investigation of magmatic rocks from the Mecsek Mountains, Southern Hungary. *Ann. Univ. Sec. Geol.*, **12**, pp. 67–80
- MÁRTON P. MÁRTON-SZALAY E. 1970: Secular changes, polarity epoch and tectonic movements as indicated by paleomagnetic studies of Hungarian rock samples. *Pure Appl. Geophys.*, **79**, 2, pp./ 151–161
- MÁRTON P., MÁRTON-SZALAY E. 1971: Palaeomagnetic studies in the Börzsöny Mountains (in Hungarian). *Magyar Geofizika* **12**, 2–3, pp. 77–83
- MÁRTON P., MÁRTON-SZALAY E. 1972: Palaeomagnetic studies in the Tokaj area (in Hungarian). *Magyar Geofizika*, **13**, 6, pp. 219–226
- MÁRTON P., PÉCSI M., SZEKENYI E., WAGNER M. 1979: Alluvial loess (infusion loess) on the Great Hungarian Plain. *Acta Geologica Hungarica* **22**, 1–4, pp. 539–555
- TARLING D. H. 1983: *Palaeomagnetism. Principles and applications in geology, geophysics and archeology.* Chapman and Hall, London, New York, 379 p.

MAGYARORSZÁGI PALEOMÁGNESES MÉRÉSEK EREDMÉNYEI

MÁRTON Emő és MÁRTON Péter

Az elmúlt két évtized alatt magyarországi kőzeteken meghatározott paleomágneses irányok elérhetőségét és felhasználását megkönnyítendő, listát készítettünk, amely összefoglalja a teljesen orientált mintákon kapott paleomágneses megfigyeléseket. Az irányokat — ahol csak lehetett — mintavételi pontokra adtuk meg azért, hogy a paleomágneses meghatározások időbeli és térbeli egyezőségét szemlélthessük.

РЕЗУЛЬТАТЫ ПАЛЕОМАГНИТНЫХ ИЗМЕРЕНИЙ В ВЕНГРИИ

Эмő МАРТОН и Петер МАРТОН

В целях облегчения доступности и использования данных о палеомагнитных направлениях, определенных в последние два десятилетия на пробах пород с венгерской территории составлен список, содержащий данные измерений, полученных по полностью ориентированным образцам. Направления — по возможности — указаны по дискретным точкам, с целью выявления пространственного и временного совпадения палеомагнитных определений.

FILTERED GRAVITY ANOMALY MAP OF HUNGARY

Zoltán SZABÓ*

The gravity survey of Hungary started in 1901 with Eötvös's torsion balance measurements. The regional gravity survey of the country (appr. 1.2 station/ km²) was completed in 1979, and its data system is stored in a gravity database. For filtering, a data system of Bouguer anomalies corrected by $\sigma=2.4 \text{ t/m}^3$ was used. The resulting map is of the derivative type, suitable for structural analysis. As a possible interpretation we present a gravity lineament map. The pattern and the directions of the lineaments make it possible to delineate structural units.

Keywords: gravity anomalies, regional anomalies, base network, gravity surveys, filtering, numerical filters, tectonic units, Hungary

1. Introduction

The gravity survey of Hungary was begun in the winter of 1901, when Loránd Eötvös carried out torsion balance measurements on the frozen Lake Balaton. Till 1950 torsion balance measurements were still widespread although gravity meter surveys had already begun in 1937, but their accuracy did not match today's demands. FACSINAY, in order to connect surveys of different areas, established a network of gravity bases of 168 base stations covering Transdanubia.

The gravimeter surveys providing acceptable accuracy started in 1950, when two Heiland GSC-3 gravity meters of $\pm 0.03 \text{ mGal}$ accuracy were purchased by ELGI. The only problem with them was that because of the size of the instrument and weight of its accompanying battery, a special car was needed for transportation. This disadvantage greatly affected the station-distribution of the reconnaissance survey, since the observation lines had to be placed along motorable roads.

As soon as modern gravity meters were put to work in 1950, planning and field work of the first- and second-order gravity base networks began. The establishment of these networks had two aims: to obtain a regional gravity map of the country within a short time, and to make it possible to insert all local maps into a unified system.

To fulfill the first aim, the base stations were placed far from inhabited areas in order to avoid the effect of the surrounding buildings. As it turned out later, this decision was not so successful, because the base stations, lacking suitable protection, decayed within 20-30 years.

*Eötvös Loránd Geophysical Institute of Hungary, POB 35, Budapest H-1440
Manuscript received: 19 June, 1989

The first order gravity network comprised 16 stations. The gravity meters were transported by aeroplane. The distribution of the base stations was governed by the reading range of the instruments (max. 120 mGal) and the airports at our disposal. The base station at Budapest-Ferihegy airport — with its gravity value determined in the Potsdam system — was the reference point for the measurements.

The second-order base network was set up along roads and contained 493 stations; the distance between the stations was 10–20 km [FACSINAY – SZILÁRD 1956]. Field work on the second-order base network with the Heiland GSC–3 No. 40 gravity meter finished in 1955. The preliminary processing was completed in 1956, the final adjustment finished off in 1959 [SZILÁRD 1959, RENNER 1959] with a mean error of ± 0.029 mGal. After the repeated survey of the first-order base network in 1970, it transpired that because of the non-linearity of the instrument the network has a 1 mGal distortion. Simultaneously with the base networks, the reconnaissance survey of the whole country was started. This work was completed in 1978.

2. Construction of the regional Bouguer anomaly map

The intensive prospecting for raw materials in the 60s necessitated a regional gravity map of the country. The base networks set up in the 50s served as bases for the construction of the map. The map was constructed to a scale of 1:50,000 and the data of the torsion balance surveys collected since the turn of the century were also used for its construction. Calculating the Δg isolines from horizontal gradients, a linear interpolation was used. The characteristics of the map were the followings: Potsdam system; the normal value of gravity was calculated on the ground of Cassinis' formula of 1930; for the Bouguer correction $\sigma=2.0$ t/m³ density was used. The topographic effect was computed within a circle of 22 km radius. The contour interval was 1.0 mGal.

On the basis of the above described maps, F. Kovács (Geophysical Exploration Company) was the first to attempt to construct a residual anomaly map of the country to a scale of 1:200,000. Bouguer anomalies were read in a regular 1 km grid and filtered with Meskó's band-pass filter of $\kappa=7-4$ [MESKÓ 1965, 1966]. These parameters were successfully used in practice for local surveys.

As computers became wide-spread it proved expedient to store data on punched cards and to establish a gravity database. As soon as the reconnaissance survey was finished in 1979, all data belonging to it (120,000 stations) were input into a gravity database.

With this gravity database it became possible to construct a unified Bouguer anomaly map. Our starting point in the construction of the map was the Potsdam system corrected by -14 mGal; the theoretical value of gravity was determined on the basis of Helmert's formula of 1901. The Bouguer and cartographic corrections were calculated with $\sigma=2.4$ t/m³. This choice was made because of the following reasons:

- a) Density determinations on areas of Tertiary stratovolcanos gave a $\sigma = 2.4$ t/m³ average.
- b) On plains σ is less than 2.4 t/m³ but because of the small difference in elevation, the application of a density bigger than the real one does not cause any considerable distortion.

c) Rocks on the surface with σ bigger than 2.4 t/m^3 (limestone, dolomite, granite) represent the basin floor, so the Bouguer anomalies, though distorted, reflect the effect of the basement.

For constructing the filtered gravity map, first the Bouguer anomalies were calculated in the irregular grid as described above. Then data were interpolated to a regular grid of $s=800 \text{ m}$ grid interval by a spline interpolation method. For filtering the data set we again used Meskó's $\kappa=7-4$ filter matrix.

The isoanomaly map (*Enclosure 1*) was also constructed by computer from the filtered data system. The results were plotted to two scales: 1:100,000 and 1:500,000.

3. Methodological considerations

To study the character of the filtered map we set up the histogram of the anomalies. It had been found previously [PINTÉR-STOMFAI 1979] that changing the parameters of filtering results in maps of different types: residual, derivative or intermediate. Residual anomaly maps give a flat histogram, while derivative-type maps have sharp frequency maximum in the vicinity of 0 anomaly. The anomaly frequency distribution of our map indicates its derivative type (*Fig. 1*).

While in basin areas Bouguer anomaly maps regularly contain depth information, maps of the derivative type primarily comprise structural information. To enhance this information, lines of maximum gradient, which we called gravity lineaments, were also computed. On the deepest parts of the basin the gradients of the

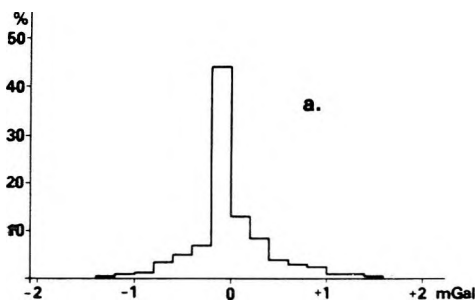


Fig. 1. Characteristic histograms of filtered anomalies
a) on highlands
b) on lowlands

1. ábra. A szűrt anomáliák jellegzetes eloszlási görbéi
a) dombvidéken
b) síkvidéken

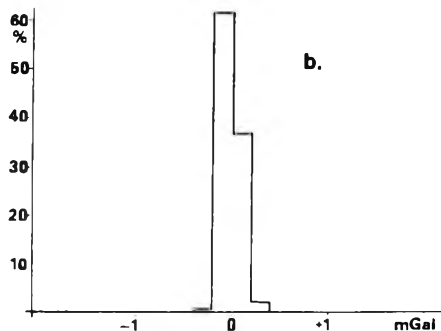


Рис. 1. Характерные кривые распределений
фильтрованных аномалий
а) на холмистом районе
б) на низменности



c) Rocks on the surface with σ bigger than 2.4 t/m^3 (limestone, dolomite, granite) represent the basin floor, so the Bouguer anomalies, though distorted, reflect the effect of the basement.

For constructing the filtered gravity map, first the Bouguer anomalies were calculated in the irregular grid as described above. Then data were interpolated to a regular grid of $s=800 \text{ m}$ grid interval by a spline interpolation method. For filtering the data set we again used Meskó's $\kappa=7-4$ filter matrix.

The isoanomaly map (*Enclosure 1*) was also constructed by computer from the filtered data system. The results were plotted to two scales: 1:100,000 and 1:500,000.

3. Methodological considerations

To study the character of the filtered map we set up the histogram of the anomalies. It had been found previously [PINTÉR-STOMFAI 1979] that changing the parameters of filtering results in maps of different types: residual, derivative or intermediate. Residual anomaly maps give a flat histogram, while derivative-type maps have sharp frequency maximum in the vicinity of 0 anomaly. The anomaly frequency distribution of our map indicates its derivative type (*Fig. 1*).

While in basin areas Bouguer anomaly maps regularly contain depth information, maps of the derivative type primarily comprise structural information. To enhance this information, lines of maximum gradient, which we called gravity lineaments, were also computed. On the deepest parts of the basin the gradients of the

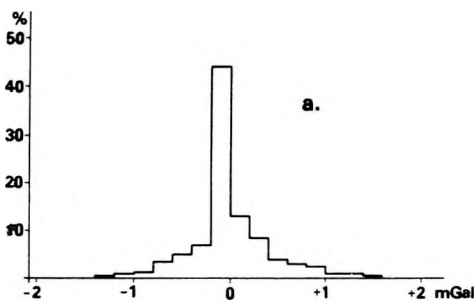


Fig. 1. Characteristic histograms of filtered anomalies
a) on highlands
b) on lowlands

1. ábra. A szűrt anomáliák jellegzetes eloszlási görbéi
a) dombvidéken
b) síkvidéken

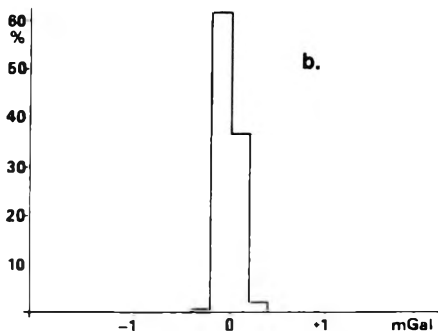


Рис. 1. Характерные кривые распределений
фильтрованных аномалий
а) на холмистом районе
б) на низменности



gravity field are so small, that in such parts we had to complete our map with manually constructed lineaments, based on the steady direction of the isolines. When interpreting the gravity lineaments as structural lines, the following criteria must be kept in mind:

- 1) The map from which we start out is of a derivative type.
- 2) The sites of sharp vertical density contrasts are at the same time structural lines.
- 3) There are no sharp horizontal density contrasts within the basin fill.

The reliability of the structural interpretation of the gravity lineament map depends on whether the above criteria are fulfilled or not. In our case we think that these conditions are met with acceptable approximation.

Comparing the gravity lineament map (*Fig. 2*) with the pre-Tertiary basement contour map [KILÉNYI–RUMPLER 1987], one can see that in the areas of outcrops and where depths to basement do not exceed 2000 m, strikingly sharp structural lines exist; in the areas of deeper basins, where the gravitational effect of the basement is masked by the overlying sediments, the tracing of the structural directions is less reliable. We must mention, however, that different structural directions do not necessarily indicate different geological formations.

4. Structural interpretation

On the grounds of lineament directions we tried to delineate structural units (*Fig. 3*). Characterization of patterns is extremely difficult and highly subjective, as in forming a pattern, many different effects take part, like basement topography, tectonization of the basement, volcanism, erosional forms in areas of outcrops etc. Therefore in geologically similar conditions differing patterns may occur, because of the different dominating effects. The best example is provided by the comparison of young Miocene volcanic areas.

The Zemplén–Tokaj area of NE Hungary (6) is characterized by a disordered (random) distribution of weak, short gradients, reflecting most probably the erosional forms of the volcanic mountains and hills. Somewhat similar pattern can be recognized in the Börzsöny–Dunazúg Mts (2), but there a dominating radial pattern is superimposed on the weak volcanic texture. Conspicuously different is the pattern of the Mátra Mts. (4), which is also built up from Miocene volcanics. There the circular and radial pattern originating from the volcanic processes dominates.

The most impressive feature is the WSW–ENE oriented, elongated zone (7) cutting the area of Hungary into two halves. In the NE part its northern boundary is rather ambiguous. It is therefore marked by dashed line. In the structural maps of Hungary constructed in the near past, this zone (or rather its southern border) is

Fig. 2. Gravity lineaments with dip directions

1 — first-order, 2 — second-order, 3 — third-order lineament

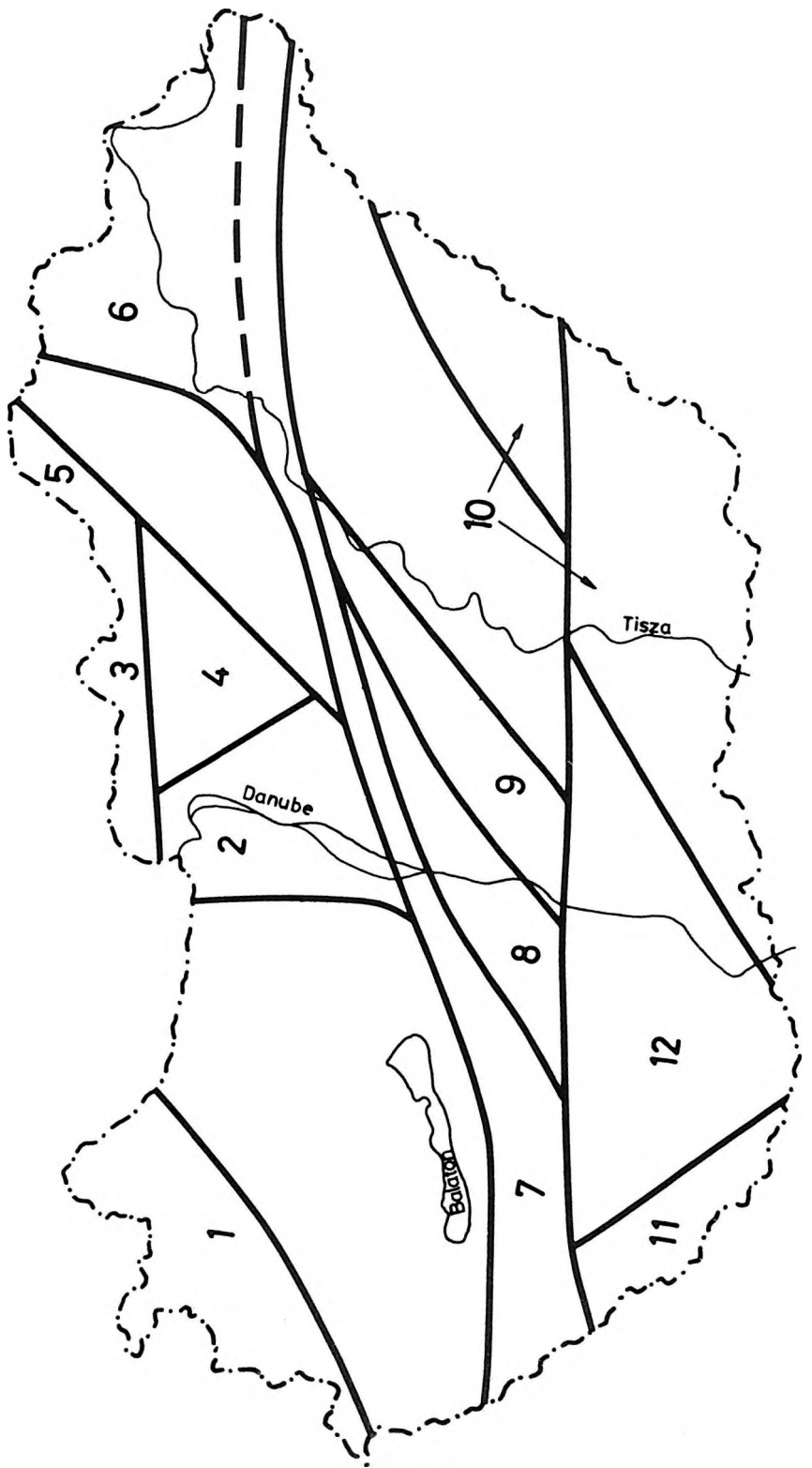
2. ábra. Gravitációs lineamensek a „dőlési” irány feltüntetésével

1 — elsőrendű, 2 — másodrendű, 3 — harmadrendű lineamensek

Рис. 2. Гравитационные линеаменты.

Нанесены направления „подстиля”.

Линеаменты: 1 – первого, 2 – второго, 3 – третьего разряда



called the Mid-Hungarian Megatectonic Line. In determining this line the filtered gravity anomaly map played an important role, but several other pieces of geological evidence also prove the conclusions concerning the difference between the northern and southern halves. As to the character of the tectonic movement along this zone, it is already supported by seismic profiles, that horizontal displacement of considerable distance took place in the Upper Cretaceous to Late Miocene time span.

No wonder that some of the most widely known structural lines clearly appear in this map, viz., the Rába line (1), the Darnó zone (5), or the Diósjenő dislocation zone (3), as some sort of earlier gravity maps contributed to their recognition.

In the southern half, some units of strikingly different pattern can be recognized. The pattern characterizing the Mecsek Mts. and Villány Hills (12) with the Mecsek's Mesozoic volcanics, extends the hilly area deep into the Danube–Tisza interfluvium. The Dráva Basin (11) appears with sharp contrast and similarly, the deep basins of the Great Hungarian Plain (10). The most problematic is the central part, the two wedges next to the Mid-Hungarian zone (8 and 9). Their gravity lineament pattern is different from each other and from the neighbouring areas, but we do not want to take a stand on any interpretation possibility regarding the meaning of this phenomenon in the structural sense.

Our aims with this paper were nothing else but to draw attention to the filtered gravity anomaly map and its manifold application possibilities.

Acknowledgments

The filtered gravity map could not have been accomplished without the contribution of those many people who took part in the setting up of the gravity database and in the planning and carrying out the different stages of gravity surveys in the last three decades. Thanks are due to all of them, particularly to Attila Sárhidai who did the computer work of processing and map construction.




Fig. 3. Structural units delineated by gravity lineaments

3. ábra. A gravitációs lineamensek alapján elkülöníthető szerkezeti egységek

Рис. 3. Структурные единицы определяемые на основе гравитационных линеаментов

REFERENCES

- FACSINAY L. – SZILÁRD J. 1956: The Hungarian network of gravity bases (in Hungarian with English abstract). *Geofizikai Közl.* **5**, 2, pp. 3–49
- KILÉNYI E. – RUMPLER J. 1985: Pre-Tertiary basement relief map of Hungary. *Geophys. Trans.* **30**, 4, pp. 425–428
- MESKÓ A. 1965: Some notes concerning the frequency analysis for gravity interpretation. *Geophys. Prosp.* **13**, 3, pp. 475–488
- MESKÓ A. 1966: Two-dimensional filtering and the second derivative method. *Geophysics*, **31**, 3, pp. 606–617
- PINTÉR A. – STOMFAI R. 1979: Gravitational model calculation. *Geophys. Trans.* **25**, pp. 5–29
- RENNER J. 1959. Final elaboration of the measurements of the national Hungarian network of gravity bases (in Hungarian with English abstract). *Geofizikai Közl.* **8**, 3, pp. 105–141
- SZILÁRD J. 1959: Some problems of the national gravitational base network (in Hungarian with English abstract). *Geofizikai Közl.* **8**, 3, pp. 97–104

MAGYARORSZÁG SZÜRT GRAVITÁCIÓS ANOMÁLIA TÉRKÉPE

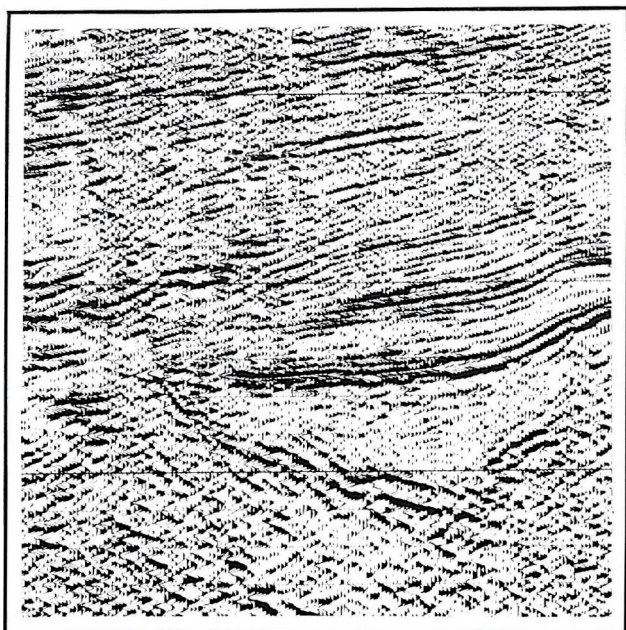
SZABÓ Zoltán

Magyarország gravitációs felmérése 1901-ben Eötvös torziós-inga méréseivel vette kezdetét, és a regionális felmérés (kb. 1,2 állomás/km²) 1979-ben fejeződött be. A mérési adatokat gravitációs adatbankban tároltuk. A szűrés alapjául a $s = 2,4 \text{ t/m}^3$ sűrűségértékkel korrigált Bouguer-anomália adatrendszer szolgált. A szűrés eredményeként derivált jellegű térképet kaptunk, amely elsősorban szerkezeti értelmezésre alkalmas. Ennek érdekében a szűrt térkép alapján elkészítettük a gravitációs lineáris térképet. A lineárisok eltérő irányítottága nagyszerkezeti egységek elkülönítését teszi lehetővé.

КАРТА ОТФИЛЬТРОВАННЫХ ГРАВИТАЦИОННЫХ АНОМАЛИЙ ВЕНГРИИ

Золтан САБО

Гравиразведочные съемки в Венгрии начались в 1901 году с измерениями, проведенными Л. Этвеш торзионным маятником. Региональные гравиразведочные исследования закончились в 1979 году (с приблизительной густотой станций 1,2 на км²). Данные измерения хранятся в банке гравитационных данных. Основой фильтрации служила система данных аномалий Буге, полученных с плотностью 2,4 т/м³. В результате фильтрации была получена карта производного характера, которая может служить в первую очередь, основой структурной интерпретации. На основе карты отфильтрованных аномалий была составлена карта гравитационных линейментов. Разная направленность линейментов позволяет выделить глобальные структурные единицы.



Land data example courtesy of OKGT

GECO is in the forefront of exploration technology with worldwide experience in:-

DATA ACQUISITION
 DATA PROCESSING
 INTERPRETATION
 MAPPING
 SEISMIC SOFTWARE
 GEOCHEMICAL ANALYSIS
 WORKSTATIONS

GECO OFFERS THE FULL RANGE OF GEOPHYSICAL SERVICES FROM SURVEY PLANNING TO BASIN EVALUATION

DATA ACQUISITION:

Our land crews operate with telemetry systems to ensure high productivity 2D and 3D surveys.

WORKSTATIONS:

GECO's CHARISMA work stations are acknowledged to be the finest in the industry providing unrivalled performance and functionality.

DATA PROCESSING:

Advanced algorithms coupled with high performance Vector Processors allow rapid delivery of quality data.

SEISMIC SOFTWARE:

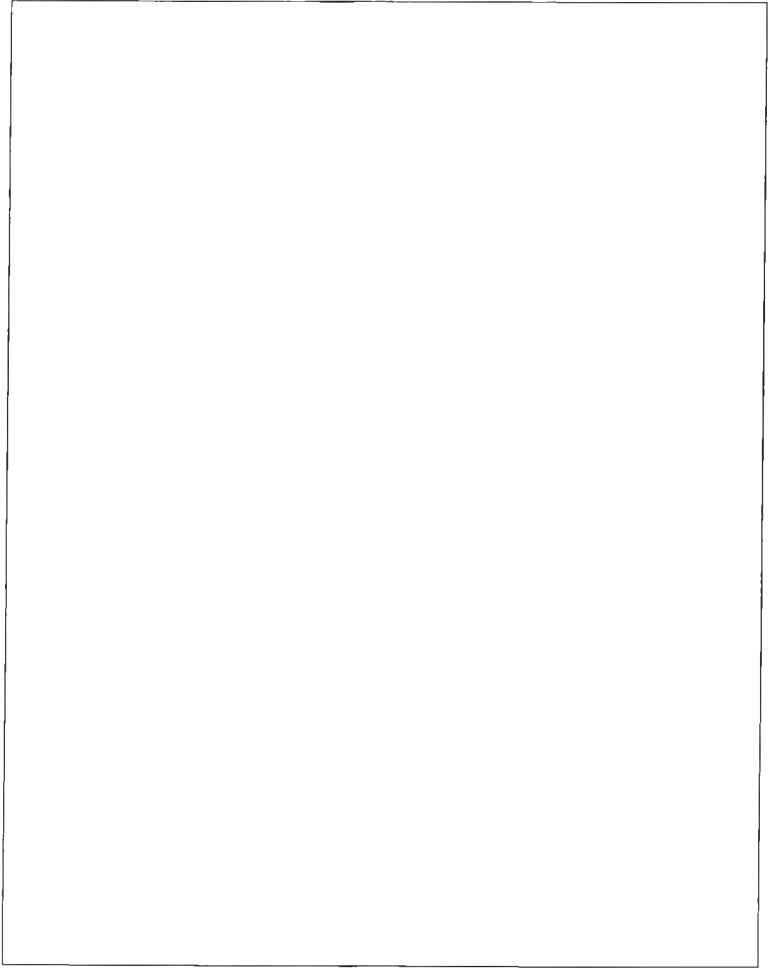
GECO's portable package, STARPAK, runs on micros, minis, mainframes and supercomputers for 2D and 3D processing.

For further information please contact Chris Walker in England or John Christensen in Norway

HEAD OFFICE
 GECO A.S
 Kjorbokollen
 N-1300 Sandvika NORWAY
 Telephone: 47 (0) 2 47 55 00
 Telefax: 47 (0) 2 47 55 55
 Telex: 78623 geco n

EUROPE-AFRICA-MIDDLE EAST
 GECO Geophysical Company Ltd.
 The GECO Centre
 Knoll Rise, Orpington
 Kent BR6 0XG
 UNITED KINGDOM
 Telephone: 44 (0) 689 32133
 Telefax: 44 (0) 689 22650
 Telex: 895 4894 geco g





This page is waiting for you!